Quantifying food web interactions and limitations for native salmonids in Ross Lake, WA and implications for the introduction of anadromous salmonids

Rachelle Carina Johnson

A dissertation
submitted in partial fulfillment of the
requirements for the degree of

Doctor of Philosophy

University of Washington
2023

Reading Committee:
Julian D. Olden, Co-chair
David A. Beauchamp, Co-chair
Thomas P. Quinn

Program Authorized to Offer Degree:
School of Aquatic and Fishery Sciences

University of Washington

Abstract

Quantifying food web interactions and limitations for native salmonids in Ross Lake, WA and implications for the introduction of anadromous salmonids

Rachelle Carina Johnson

Co-chairs of the Supervisory Committee:
Julian D. Olden
David A. Beauchamp

School of Aquatic and Fishery Sciences

Food web function influences ecosystem productivity and plays a critical role in ecosystem services and conservation of species of concern. In reservoirs, existing and future changes to these ecosystems (e.g., invasive species, climate change, water operations) may alter their capacity to support native species. As introducing anadromous fish upstream of migration barriers is gaining traction as a conservation strategy, these food web dynamics can also influence the success or failure of such programs. In this dissertation, I explore these ideas using Ross Lake, a hydropower reservoir in the Upper Skagit River, Washington, USA, as a case study. I used a bioenergetics-based approach to quantify food web interactions to identify potential limitations (e.g., prey supply, predation, temperature) to growth and production of native species and proposed introductions of anadromous salmonids in the lake and examined these processes within the context of seasonal thermal constraints on habitat use and prey

availability. In Ross Lake, the proliferation of an unauthorized introduction of redside shiner *Richardsoniu balteatus* approximately 20 years ago has fundamentally altered food web interactions by providing a novel prey source for piscivorous fishes and becoming the dominant zooplanktivore/invertivore. A bioenergetics model did not exist for this species; therefore, my first objective was to parameterize and evaluate this model using controlled laboratory experiments (Chapter 1). With this model in our toolbelt, I then quantified food web interactions to identify the relative roles of direct competition with redside shiner (Chapter 2) versus predation (Chapter 3) in limiting growth and production of native salmonids in Ross Lake. This baseline assessment of the bottom-up and top-down limitations in the Ross Lake food web provided the foundation to then examine these food web dynamics in the reservoir as limitations to the feasibility of introducing anadromous salmonids above the Upper Skagit River dams (Chapter 4). Collectively, this dissertation provides a framework for assessing the food web constraints to native species conservation in regulated river systems, including important considerations for future feasibility studies in Ross Lake and other regulated rivers where anadromous salmonid introduction programs are considered.

TABLE OF CONTENTS

ACKNOWLEDGMENTS

There are many people without which this project would not have been possible, and many additional people that helped me succeed in my journey through grad school. First and foremost, I am grateful for my fearless leader, Dave Beauchamp, and his unwavering support and confidence in me. To the rest of my all-star committee, Julian Olden, Tom Quinn, and Aaron Wirsing, thank you for the many ideas, invaluable feedback on these manuscripts, and genuinely enjoyable conversations along the way.

As you will discover in this dissertation, these studies required a massive amount of field and lab work, none of which would have been possible without the hard work and dedication of my fabulous colleagues at Western Fisheries Research Center. Thank you to Tessa Code, Marshal Hoy, Ben Jensen, Karl Stenberg, and Jon Mclean for the heavy lifting on much of this work. There is no road to Ross Lake – getting there requires either hiking down around 1,000ft of elevation from the highway, or barging across Diablo Lake and then driving or hiking from there up to Ross Lake. This required incredibly complex logistics for our many field missions that were successfully led by Marshal, Tessa, and Ben. I would also like to thank Seattle City Light for funding and support – particularly Jeff Fisher, Erin Lowery, and Ed Conner for their knowledge of the ecosystem and support in the field, and the Diablo Lake boathouse crew for assistance with logistics. I am also grateful for Ross Lake Resort and their generosity with accommodations, and Tom Barnett in particular for his support, angling efforts, and deep knowledge of and concern for the Ross Lake fishery.

They say it takes a village, and that was certainly true for my journey through grad school. Thank you to my many other colleagues at WFRC for your support and encouragement. I'm especially grateful for Jeff Duda – the mentorship and opportunities you have provided over the past 7+ years have played a key role in my development as a scientist. I also had a wonderful support system at SAFS – from my cohort, the Olden Lab, and other friends made along the way. None of this have been possible without the constant support and encouragement from my parents, and for that I am eternally grateful. To the rest of my friends and family in Seattle (and beyond) and my sister Kelsey, I am thankful for the many fun ski trips, concerts, camping trips, and casual hangouts that provided much needed breaks and relaxation. And last but not least, I want to thank my partner Greg for his dedication and patience throughout the last 4 years in this incredibly challenging (but *so* rewarding) adventure.

Introduction

Food web function influences ecosystem productivity and plays a critical role in ecosystem services and conservation of species of concern (McCann 2007). In lentic ecosystems, food web structure and function are influenced by a combination of biotic and abiotic factors, both natural and anthropogenic, including thermal structure, invasive species, climate change, and altered flow regimes. Increasing water demand and changing land use exacerbate impacts to native species through direct and indirect effects that propagate through food webs. Much progress has been made in studying how aquatic ecosystems are restructuring and adapting in response to both climatic and non-climatic stressors (McCann and Rooney 2009), but owing to complex interactions among stressors, the function of many ecosystems under future change remains highly uncertain (Staudinger et al. 2021). With increasing focus on managing for such ecosystem transformations (Lynch et al. 2021), additional research is needed to understand the complex dynamics that drive food web structure and adaptive capacity in lentic systems to best conserve ecosystem function, services, and species of concern under global change (McMeans et al. 2016).

Climate change alters thermal regimes and habitat accessibility in lakes and reservoirs worldwide (Woolway and Merchant 2019; Miranda et al. 2020). Seasonal thermal stratification in lakes is influenced by climatic factors such as regional air temperatures, the timing, location, temperature, and magnitude of inflows, and wind-driven mixing. For ectotherms living in lakes or reservoirs (e.g., fish, invertebrates), temperature constrains habitat use by influencing metabolic rates, growth potential, and physiological stress (Magnuson et al. 1979). As climate change shifts the timing and increases the duration and magnitude of thermal stratification

(O'Reilly et al. 2015; Richardson et al. 2017; Woolway et al. 2020, 2021), habitat availability for native cold-water species like trout and other salmonids will likely decrease (Ficke et al. 2007). Additionally, shifts in the timing of stratification can cause mismatches between predator and prey resources (Winder and Schindler 2004). In Germany's Bautzen reservoir, for example, shifts in thermal structure during a critical growing season caused decreased *Daphnia* densities due to overexploitation of phytoplankton and increased predation by small perch (Wagner and Benndorf 2007). Thermal stratification also affects fishes through prey availability and access when the majority of prey production occurs in the warmer, shallow depths of the offshore (pelagic) and nearshore or bottom-oriented (benthic) habitats (e.g., Tunney et al. 2012; Sorel et al. 2016b; Trottier et al. 2019). In cold water systems, increased surface temperatures coupled with increased duration of stratification could thermally exclude cold-water consumers from access to prey in the productive surface and littoral zones during critical periods of the growing season (Cyterski and Ney 2005; Dolson et al. 2009; Hansen et al. 2013; Plumb et al. 2014).

The effects of thermal exclusion and habitat limitations are further exacerbated by introductions of nonnative species (Cucherousset and Olden 2011). Species introductions in freshwater can alter food webs in a variety of ways, by creating novel trophic links, or by otherwise disrupting or reducing existing links (Jackson et al. 2017). In temperate North American lakes and reservoirs, cold-water invasive species like lake trout *Salvelinus namaycush* and mysid shrimp have heavily disrupted native salmonid communities in western North America (Martinez 2009; Ellis et al. 2011). Because these invasive species share similar thermal ranges, they experience more direct interactions, and as suitable thermal habitat shrinks, they are concentrated together in high densities that can result in increased direct or indirect competitive or predatory interactions; however, the relative strength of these interactions is mediated by lake depth and temperature (Schoen et al. 2015). But even when thermal requirements of the invader do not match that of the native species, competitive interactions could still exist depending on the food web and thermal structure. For example, lake trout were susceptible to direct resource competition for littoral prey fish following invasion of warm water predators (and associated decrease in growth rates) when pelagic prey fish are not present in a lake (Vander Zanden et al. 2004). Thus, stratification patterns that restrict native species to deeper waters could favor production of invasive species due to higher habitat availability and access to prey.

To further amplify these issues, climate-induced drought can impose additional stressors on freshwater ecosystems confronted with a projected 20-30% increase in global water demands from the present to 2050 (Boretti and Rosa 2019) and an increased reliance on freshwater reservoirs to meet these demands. In these ecosystems, the effects of dam operations such as timing, magnitude, and depth of water withdrawals represent significant additional influences on food web structure through ecological impacts of de-watering (Carmignani and Roy 2017) and driving thermal structure (Duka et al. 2021). The extent of winter drawdown of reservoirs has been associated with declining biomass of macroinvertebrates (Trottier et al. 2019) and implicated in trophic compression of the benthic energy pathway in fish food webs (Hansen et al. 2018). While lakes have inherent adaptive capacity in food web structure, large scale anthropogenic alterations (e.g., loss in benthic production due to drawdowns) could limit the ability of these ecosystems to adapt to other stressors (McMeans et al. 2016).

Water management strategies can also play an important role in mitigating stressors on reservoir ecosystems. For example, rapid and severe reservoir drawdowns have been associated with decreased abundance in invasive species and release of native fish from predation pressure

(Murphy et al. 2019), and lake de-stratification has been posed as a method of eradicating warm-water invasive species in cold-water food webs (Gaeta et al. 2012). Water operations, climate change, and invasive species can interact in complex ways to shape lentic food webs, but we have limited understanding of how lake and reservoir ecosystems will respond to these complex dynamics and the associated impacts on native species of concern.

The goal of my research was to quantify species interactions and identify limits to native salmonid growth and production within the context of an invasive species and potential introductions of anadromous salmonids in a hydropower reservoir in Washington State. The knowledge gained from this project informs the management of native and introduced fish populations and future water management strategies given the emerging threat of climate change. Our assessment of the thermal and food web constraints to the growth and potential mortality for salmonids will help managers decide if introducing anadromous salmonids into this system is justified and likely to succeed. Additionally, by understanding how thermal structure drives species interactions in these reservoirs, ecologically-based water management strategies can be employed to manipulate the thermal structure to support ecosystem balance and function in the reservoirs.

Ross and Diablo lakes are the upper two of three reservoirs impounded by hydroelectric projects in the Upper Skagit River, WA. While Gorge Lake is the lower reservoir in the project, it is smaller, more run-of-river than Ross or Diablo, and does not thermally stratify, thus I did not evaluate it in this project. Both Ross and Diablo lakes have simple fish communities characterized by native and nonnative species. Native species include rainbow trout *Oncorhynchus mykiss*, bull trout *S. confluentus*, and Dolly Varden *S. malma* and nonnative species include eastern brook trout *S. fontinalis* (introduced in early 1900s), cutthroat trout *O. clarkii* (introduced in early or mid-1900s), and redside shiner *Richardonius balteatus* (introduced ca. 2000). In addition, hybridization has been documented between rainbow trout and cutthroat trout, Dolly Varden and bull trout, and Dolly Varden and brook trout. Redside shiners spread to Diablo Lake after their introduction to Ross, but the population has not proliferated in Diablo as it has in Ross. Ross Lake is characterized by strong thermal stratification from around June to October when the thermocline deepens and begins to destratify, with peak summer surface temperatures between 19-22ºC. In addition, Ross Lake is drawn down between 16-25 m (50-75ft) every year during the winter, although drawdowns in recent years have reached 40 m (125 ft). Diablo Lake is colder, weakly stratified, and lake level fluctuates within ± 1.5 m throughout the year. While my dissertation focuses primarily on Ross Lake, the more limited information collected in Diablo Lake is presented as Supplementary Materials for each chapter.

Managers' concerns for the native salmonid populations stem from historical trends in the population size and fish growth over the last 30 years, including recent trends of declining recruitment of juvenile salmonids, on top of additional stressors from climate change, invasive species, and hydropower management. The rainbow trout population in Ross Lake was first studied extensively for three years in the early 1970s, when data were collected on the physical environment, growth, diets, prey availability, spawning, population size, and mortality of rainbow trout in Ross Lake and the Upper Skagit River (Seattle City Light 1974; Woodin 1974). Additional monitoring has occurred periodically since the late 1980s, during which there was concern about the fishery negatively impacting the size and number of rainbow trout in the lake (Johnston 1989; Loof 1995). Contemporary monitoring found fluctuating trends in the size and growth of rainbow trout, decreasing from 2004 to 2006, but then maximum size, maximum age, and size at age for fish age-2 and older all increased between from 2006 to 2012 (Downen 2014; Hugh Anthony, unpublished data). Despite increases in age and growth, catch rates of rainbow trout continued to decline through 2012, mirroring similar trends observed in Ross Lake spawning surveys (Hugh Anthony, unpublished data) and snorkel surveys in the Canadian reaches of the Upper Skagit River (Foster 2020). I hypothesized that these trends were related to adult rainbow trout accessing a new resource of redside shiner in the lake while the juveniles remained limited by competition with redside shiners for food. Unlike rainbow trout, the bull trout and Dolly Varden populations were not historically monitored in this system to the same extent. Thus, long-term trends in growth and abundance of the native char populations are unknown. However, snorkel surveys in the Canadian portion of the Skagit River conducted periodically since 1998 show a dramatic increase in the adult population peaking in 2011 and slowly declining in the following years.

While these monitoring data allow a glimpse of recent bull trout and rainbow trout population dynamics, food web data in Ross and Diablo lakes are necessary to understand the mechanisms driving changes in growth and production of native fish. For this system, however, these data are extremely limited or nonexistent. Seattle City Light conducted a diet study for rainbow trout in the lake from 1971-1974, but food web data in Diablo Lake do not exist. Climate warming and the invasion of redside shiners have shifted food web dynamics, underscoring the need for a contemporary study. By quantifying the species interactions in these lakes, we have identified limitations within the food web to growth and production of native fish populations and highlighted vulnerabilities to mounting impacts of climate, invasive species, and dam operations.

Bioenergetics models provide a valuable tool in fisheries management as they allow for quantifying trophic interactions and evaluating biotic and abiotic limitations to fish growth (Deslauriers et al. 2017). These models are based on energy-balance equations that partition total energy intake (i.e., food consumed) into three basic components: 1) waste losses, 2) metabolism, and 3) growth. As such, these models can be used to estimate growth from consumption or vice versa, while accounting for size- and temperature-dependent effects on these physiological processes. This provides insights into how bioenergetic requirements change as individuals grow, experience different thermal conditions (i.e., seasons), and have access to variable amounts and quality of food, allowing for the examination of key limiting factors during critical life stages (Beauchamp 2009). Applications of these models range widely (see Deslauriers et al. 2017 for review) but can include quantitative assessments of predation mortality (Lowery and Beauchamp 2015; Sorel et al. 2016b) or consumption demand and carrying capacity (Sorel et al. 2016a; Taylor et al. 2020), estimating habitat quantity/quality and growth potential (Weber et al. 2014; Carmichael et al. 2020), or evaluating possible distributional (Lawrence et al. 2015) or trophic shifts due to climate change (Breeggemann et al. 2016).

Despite these valuable applications of bioenergetics models, their implementation is limited by the species of interest, as reliable model results are dependent upon accurate species-specific parameterizations (Ney 1993). For application in the Upper Skagit system, these models exist for the primary salmonids of interest (rainbow trout: Rand et al. 1993; eastern brook trout: Hartman and Cox 2008; bull trout/Dolly Varden: Mesa et al. 2013), but a model for redside shiner did not exist. Therefore, in Chapter 1 of my dissertation I addressed this knowledge gap. Using controlled laboratory experiments, I developed and evaluated performance of a bioenergetics model for redside shiner. In Chapter 2, I then applied this model in Ross Lake to quantify seasonal and annual food consumption by the invasive redside shiner to evaluate scope for competition with juvenile native rainbow trout. Once I evaluated bottom-up limitations in this food web, my focus in Chapter 3 shifted to looking at top-down limitations, by quantifying consumption rates of piscivores and evaluating the impacts of predation mortality on the population dynamics of invasive redside shiner and native juvenile salmonids. Using the baseline food web data acquired in Chapters 2 and 3, I was then able to evaluate potential food web limitations in the reservoir for the proposed introduction of anadromous salmonids above the dams in Chapter 4. This evaluation included quantifying the carrying capacity of the reservoirs for introduced reservoir-rearing species after accounting for temporal consumption demand by the existing planktivore community, and quantifying predation mortality on juvenile salmonids rearing in and migrating through the reservoirs. Combined with companion studies looking at spawning and rearing potential in the tributary habitats above the dams, this work provides a broader understanding of the feasibility of introducing anadromous salmonids above these dams. The Upper Skagit River reservoirs are facing numerous emerging challenges that will affect food web dynamics and native fish populations, including persistence of a warm-water invasive species, possible introductions of anadromous salmonid populations, and climate change induced shifts to thermal structure and water operations. This research contributes valuable information on current food web dynamics as they relate to species introductions and thermal structure that can guide resource management and water operations in the Upper Skagit River reservoirs, in addition to providing context for other regulated river systems facing similar challenges.

References

Beauchamp, D. A. 2009. Bioenergetic ontogeny: Linking climate and mass-specific feeding to life-cycle growth and survival of salmon. American Fisheries Society Symposium 70:1–19.

Boretti, A., and L. Rosa. 2019. Reassessing the projections of the World Water Development Report. npj Clean Water 2:15.

Breeggemann, J. J., M. A. Kaemingk, T. J. DeBates, C. P. Paukert, J. R. Krause, A. P. Letvin, T. M. Stevens, D. W. Willis, and S. R. Chipps. 2016. Potential direct and indirect effects of climate change on a shallow natural lake fish assemblage. Ecology of Freshwater Fish 25:487–499.

Carmichael, R. A., D. Tonina, E. R. Keeley, R. M. Benjankar, and K. E. See. 2020. Some like it slow: A bioenergetic evaluation of habitat quality for juvenile chinook salmon in the lemhi river, Idaho. Canadian Journal of Fisheries and Aquatic Sciences 77:1221–1232.

Carmignani, J. R., and A. H. Roy. 2017. Ecological impacts of winter water level drawdowns on lake littoral zones: A review. Aquatic Sciences 79:803–824.

Cucherousset, J., and J. D. Olden. 2011. Ecological impacts of non-native freshwater fishes. Fisheries 36:215–230.

Cyterski, M. J., and J. J. Ney. 2005. Availability of clupeid prey to primary piscivores in Smith Mountain Lake, Virginia. Transactions of the American Fisheries Society 134:1410–1421.

Deslauriers, D., S. R. Chipps, J. E. Breck, J. A. Rice, and C. P. Madenjian. 2017. Fish Bioenergetics 4.0: An R-based modeling application. Fisheries 42:586–596.

Dolson, R., K. McCann, N. Rooney, and M. Ridgway. 2009. Lake morphometry predicts the degree of habitat coupling by a mobile predator. Oikos 118:1230–1238.

Downen, M. R. 2014. Final report: Ross Lake rainbow broodstock program, Upper Skagit reservoir fish community surveys and management plan (FPT 14-09). Washington Department of Fish & Wildlife.

Duka, M. A., T. Shintani, and K. Yokoyama. 2021. Thermal stratification responses of a monomictic reservoir under different seasons and operation schemes. Science of the Total Environment 767:144423.

Ellis, B. K., J. A. Stanford, D. Goodman, C. P. Stafford, D. L. Gustafson, D. A. Beauchamp, D. W. Chess, J. A. Craft, M. A. Deleray, and B. S. Hansen. 2011. Long-term effects of a trophic cascade in a large lake ecosystem. Proceedings of the National Academy of Sciences of the United States of America 108:1070–1075.

Ficke, A. D., C. A. Myrick, and L. J. Hansen. 2007. Potential impacts of global climate change on freshwater fisheries. Reviews in Fish Biology and Fisheries 17:581–613.

Foster, J. 2020. 2020 Skagit River snorkel survey report. Triton Environmental Consultants Ltd.

Gaeta, J. W., J. S. Read, J. F. Kitchell, and S. R. Carpenter. 2012. Eradication via destratification: Whole-lake mixing to selectively remove rainbow smelt, a cold-water invasive species. Ecological Applications 22:817–827.

Hansen, A. G., D. A. Beauchamp, and C. M. Baldwin. 2013. Environmental constraints on piscivory: Insights from linking ultrasonic telemetry to a visual foraging model for cutthroat trout. Transactions of the American Fisheries Society 142:300–316.

Hansen, A. G., J. R. Gardner, K. A. Connelly, M. Polacek, and D. A. Beauchamp. 2018. Trophic compression of lake food webs under hydrologic disturbance. Ecosphere 9:1–11.

Hartman, K. J., and M. K. Cox. 2008. Refinement and testing of a brook trout bioenergetics model. Transactions of the American Fisheries Society 137:357–363.

Jackson, M. C., R. J. Wasserman, J. Grey, A. Ricciardi, J. T. A. Dick, and M. E. Alexander. 2017. Novel and disrupted trophic links following invasion in freshwater ecosystems. Pages 55–97 *in* D. Bohan, A. Dumbrell, and F. Massol, editors. Networks of Invasion: Empirical Evidence and Case Studies. Academic Press.

Johnston, J. M. 1989. Ross Lake: The fish and fisheries (Report No. 89-6). Washington Department of Wildlife.

Lawrence, D. J., D. A. Beauchamp, and J. D. Olden. 2015. Life-stage-specific physiology defines invasion extent of a riverine fish. Journal of Animal Ecology 84:879–888.

Loof, A. C. 1995. Ross Lake rainbow trout study: 1994-95 final report (SEEC Report No. 94-08). Washington Department of Fish & Wildlife.

Lowery, E. D., and D. A. Beauchamp. 2015. Trophic ontogeny of fluvial bull trout and seasonal predation on Pacific salmon in a riverine food web. Transactions of the American Fisheries Society 144:724–741.

Lynch, A. J., L. M. Thompson, E. A. Beever, D. N. Cole, A. C. Engman, C. H. Hoffman, S. T. Jackson, T. J. Krabbenhoft, D. J. Lawrence, D. Limpinsel, R. T. Magill, T. A. Melvin, J. M. Morton, R. A. Newman, J. O. Peterson, M. T. Porath, F. J. Rahel, G. W. Schuurman, S. A. Sethi, and J. L. Wilkening. 2021. Managing for RADical ecosystem change: Applying the Resist-Accept-Direct (RAD) framework. Frontiers in Ecology and the Environment 19:461–469.

Magnuson, J. J., L. B. Crowder, and P. A. Medvick. 1979. Temperature as an ecological resource. Integrative and Comparative Biology 19:331–343.

Martinez, P. 2009. Introduced species: Western lake trout woes. Fisheries 34:424–442.

McCann, K. 2007. Protecting biostructure. Nature 446:29.

McCann, K. S., and N. Rooney. 2009. The more food webs change, the more they stay the same. Philosophical Transactions of the Royal Society B: Biological Sciences 364:1789–1801.

McMeans, B. C., K. S. McCann, T. D. Tunney, A. T. Fisk, A. M. Muir, N. Lester, B. Shuter, and N. Rooney. 2016. The adaptive capacity of lake food webs: From individuals to ecosystems. Ecological Monographs 86:4–19.

Mesa, M. G., L. K. Weiland, H. E. Christiansen, S. T. Sauter, and D. A. Beauchamp. 2013. Development and evaluation of a bioenergetics model for bull trout. Transactions of the American Fisheries Society 142:41–49.

Miranda, L. E., G. Coppola, and J. Boxrucker. 2020. Reservoir fish habitats: A perspective on coping with climate change. Reviews in Fisheries Science and Aquaculture 28:478–498.

Murphy, C. A., G. Taylor, T. Pierce, I. Arismendi, and S. L. Johnson. 2019. Short-term reservoir draining to streambed for juvenile salmon passage and non-native fish removal. Ecohydrology 12:1–9.

Ney, J. J. 1993. Bioenergetics modeling today: Growing pains on the cutting edge. Transactions of the American Fisheries Society 122:736–748.

O’Reilly, C. M., S. Sharma, D. K. Gray, S. E. Hampton, J. S. Read, R. J. Rowley, P. Schneider, J. D. Lenters, P. B. McIntyre, B. M. Kraemer, G. A. Weyhenmeyer, D. Straile, B. Dong, R. Adrian, M. G. Allan, O. Anneville, L. Arvola, J. Austin, J. L. Bailey, J. S. Baron, J. D. Brookes, E. Eyto, M. T. Dokulil, D. P. Hamilton, K. Havens, A. L. Hetherington, S. N. Higgins, S. Hook, L. R. Izmest’eva, K. D. Joehnk, K. Kangur, P. Kasprzak, M. Kumagai, E. Kuusisto, G. Leshkevich, D. M. Livingstone, S. MacIntyre, L. May, J. M. Melack, D. C. Mueller-Navarra, M. Naumenko, P. Noges, T. Noges, R. P. North, P. Plisnier, A. Rigosi, A. Rimmer, M. Rogora, L. G. Rudstam, J. A. Rusak, N. Salmaso, N. R. Samal, D. E. Schindler, S. G. Schladow, M. Schmid, S. R. Schmidt, E. Silow, M. E. Soylu, K. Teubner, P. Verburg, A. Voutilainen, A. Watkinson, C. E. Williamson, and G. Zhang. 2015. Rapid and highly variable warming of lake surface waters around the globe. Geophysical Research Letters 42:1–9.

Plumb, J. M., P. J. Blanchfield, and M. V. Abrahams. 2014. A dynamic-bioenergetics model to assess depth selection and reproductive growth by lake trout (*Salvelinus namaycush*). Oecologia 175:549–563.

Rand, P. S., D. J. Stewart, P. W. Seelbach, M. L. Jones, and L. R. Wedge. 1993. Modeling steelhead population energetics in Lakes Michigan and Ontario. Transactions of the American Fisheries Society 122:977–1001.

Richardson, D., S. Melles, R. Pilla, A. Hetherington, L. Knoll, C. Williamson, B. Kraemer, J. Jackson, E. Long, K. Moore, L. Rudstam, J. Rusak, J. Saros, S. Sharma, K. Strock, K. Weathers, and C. Wigdahl-Perry. 2017. Transparency, geomorphology and mixing regime explain variability in trends in lake temperature and stratification across Northeastern North America (1975–2014). Water 9:442.

Schoen, E. R., D. A. Beauchamp, A. R. Buettner, and N. C. Overman. 2015. Temperature and depth mediate resource competition and apparent competition between *Mysis diluviana* and kokanee. Ecological Applications 25:1962–1975.

Seattle City Light. 1974. The aquatic environment, fishes and fishery: Ross Lake and the Canadian Skagit River (Interim report No. 3 Volume 1). City of Seattle.

Sorel, M. H., A. G. Hansen, K. A. Connelly, and D. A. Beauchamp. 2016a. Trophic feasibility of reintroducing anadromous salmonids in three reservoirs on the North Fork Lewis River, Washington: Prey supply and consumption demand of resident fishes. Transactions of the American Fisheries Society 145:1331–1347.

Sorel, M. H., A. G. Hansen, K. A. Connelly, A. C. Wilson, E. D. Lowery, and D. A. Beauchamp. 2016b. Predation by northern pikeminnow and tiger muskellunge on juvenile salmonids in a high-head reservoir: Implications for anadromous fish reintroductions. Transactions of the American Fisheries Society 145:521–536.

Staudinger, M. D., A. J. Lynch, S. K. Gaichas, M. G. Fox, D. Gibson-Reinemer, J. A. Langan, A. K. Teffer, S. J. Thackeray, and I. J. Winfield. 2021. How does climate change affect emergent properties of aquatic ecosystems? Fisheries 46:423–441.

Taylor, T. N., B. K. Cross, and B. C. Moore. 2020. Modeling brook trout carrying capacity in Owhi Lake, Washington, using bioenergetics. North American Journal of Fisheries Management 40:84–104.

Trottier, G., H. Embke, K. Turgeon, C. Solomon, C. Nozais, and I. Gregory-Eaves. 2019. Macroinvertebrate abundance is lower in temperate reservoirs with higher winter drawdown. Hydrobiologia 834:199–211.

Tunney, T. D., K. S. McCann, N. P. Lester, and B. J. Shuter. 2012. Food web expansion and contraction in response to changing environmental conditions. Nature Communications 3:1–9.

Vander Zanden, M. J., J. D. Olden, J. H. Thorne, and N. E. Mandrak. 2004. Predicting occurrences and impacts of smallmouth bass introductions in north temperate lakes. Ecological Applications 14:132–148.

Wagner, A., and J. Benndorf. 2007. Climate-driven warming during spring destabilises a *Daphnia* population: A mechanistic food web approach. Oecologia 151:351–364.

Weber, N., N. Bouwes, and C. E. Jordan. 2014. Estimation of salmonid habitat growth potential through measurements of invertebrate food abundance and temperature. Canadian Journal of Fisheries and Aquatic Sciences 71:1158–1170.

Winder, M., and D. E. Schindler. 2004. Climate change uncouples trophic interactions in an aquatic ecosystem. Ecology 85:2100–2106.

Woodin, R. M. 1974. Age, growth, and mortality of rainbow trout (*Salmo gairdneri*, Richardson) from Ross Lake drainage. Master's thesis, University or Washington. 119 pages.

Woolway, R. I., B. M. Kraemer, J. D. Lenters, C. J. Merchant, C. M. O'Reilly, and S. Sharma. 2020. Global lake responses to climate change. Nature Reviews Earth and Environment 1:388–403.

Woolway, R. I., and C. J. Merchant. 2019. Worldwide alteration of lake mixing regimes in response to climate change. Nature Geoscience 12:271–276.

Woolway, R. I., S. Sharma, G. A. Weyhenmeyer, A. Debolskiy, M. Golub, D. Mercado-Bettín, M. Perroud, V. Stepanenko, Z. Tan, L. Grant, R. Ladwig, J. Mesman, T. N. Moore, T. Shatwell, I. Vanderkelen, J. A. Austin, C. L. DeGasperi, M. Dokulil, S. L. Fuente, E. B. Mackay, S. G. Schladow, S. Watanabe, R. Marcé, D. C. Pierson, W. Thiery, and E. Jennings. 2021. Phenological shifts in lake stratification under climate change. Nature Communications 12:1–11.

Chapter 1: Bioenergetics model for the nonnative Redside Shiner

Authors: R.C. Johnson, D.A. Beauchamp, J.D. Olden

Published in *Transactions of the American Fisheries Society*, 2023, 152:94-113. Copyright Wiley, with permission to use for dissertation purposes.

Abstract

Redside Shiner (*Richardsonius balteatus*) has expanded from its native range in the Pacific Northwest region of North America to establish populations in six other western states. This expansion has fueled concerns regarding competition between Redside Shiner and native species, including salmonids. We developed a bioenergetic model for Redside Shiner, providing a powerful tool to quantify its trophic role in invaded ecosystems and evaluate potential impacts on native species. Mass- and temperature-dependent functions for consumption and respiration were fit based on controlled laboratory experiments of maximum consumption (C_{max}) rates and routine metabolic rates using intermittent-flow respirometry, across a range of fish sizes (0.6–27.3 g) and temperatures (5–31° C). Initial bioenergetic simulations of long-term growth experiments indicated large model error for predicted consumption and growth, and deviations from observed responses varied systematically as a function of daily consumption rate ($J \cdot g^{-1} \cdot d^{-1}$) and water temperature. A growth rate error (GRE) correction function was developed and included in the bioenergetics model framework on a daily timestep, resulting in decreased absolute model error in all experimental groups. Predicted values from the corrected model were highly correlated with observed values (R^2; consumption = 0.97, final weight = 0.99) and unbiased. These results show that the optimal temperature for Redside Shiner growth (18° C) exceeds that of

Oncorhynchus spp. By 2–6° C under a scenario of high food availability and moderate food quality. Consequently, increases in water temperature associated with climate change may favor growth and expansion of Redside Shiner populations while negatively affecting some salmonids. The bioenergetics model presented here provides the necessary first step in quantifying trophic impacts in sensitive ecosystems where Redside Shiner have invaded or in ecosystems where anadromous salmonid re-introductions are being considered.

Introduction

Freshwater biodiversity is declining at rates that outpace both terrestrial and marine systems due to numerous emerging and intensifying threats (Reid et al. 2019). The severity of this conservation crisis in freshwater environments has been increasingly recognized, alongside the need to adopt an emergency recovery plan to scale up conservation efforts (Tickner et al. 2020). Of particular concern are threats associated with aquatic invasive species, including severe ecological effects ranging from declining population abundances to the complete re-structuring of freshwater food webs (Gallardo et al. 2016). Food web structure plays an important role in the adaptive capacity and stability of freshwater ecosystems in the face of ongoing environmental change, and thus could be integrated into programs for more effective monitoring and management of invasive fish species (Cucherousset and Olden 2011).

Bioenergetics models provide a valuable tool in fisheries management by quantifying trophic interactions and evaluating biotic and abiotic limitations to fish growth. These models are based on simple energy-balance equations which partition total energy intake (i.e., food consumed) into three basic components: 1) waste losses, 2) metabolism, and 3) growth. As such, these models can be used to estimate growth from consumption or vice versa, while accounting for size- and temperature-dependent effects on these physiological processes. Applications of these models range widely (see Deslauriers et al. 2017 for review) but can include quantitative assessments of predation mortality (Lowery and Beauchamp 2015; Sorel et al. 2016b) or consumption demand and carrying capacity (Sorel et al. 2016a; Taylor et al. 2020), estimating habitat quantity and growth potential (Weber et al. 2014; Carmichael et al. 2020), or evaluating possible distributional (Lawrence et al. 2015) or trophic shifts due to climate change (Breeggemann et al. 2016).

This ability to quantify trophic interactions and habitat-dependent growth potential makes bioenergetics modeling particularly suited to understand the potential ecological effects of invasive species. For example, they have been used to assess invader impacts like predation rates on sensitive native species (Muhlfeld et al. 2008), consumption demand and the associated changes to habitat (van der Lee et al. 2017) or competitive interactions with native species (Schoen et al. 2015; Kinlock et al. 2020), and the emergence of new energy pathways in a food web (Johnson et al. 2005). The bioenergetics framework can also be used to assess the potential for invader range expansion based on thermal habitat suitability (Lawrence et al. 2015; Thomas et al. 2016) or resource availability (Cooke and Hill 2010). Management actions for dealing with species invasions can also be informed by bioenergetics modeling, for example by evaluating feasibility of novel eradication methods (Gaeta et al. 2012), quantifying the benefits of suppression efforts (Courtney et al. 2018), or guiding adaptive management for invasive species in the face of changing climate (Cline et al. 2014). Despite these valuable applications of bioenergetics models, their implementation is limited by the species of interest, as reliable model results are dependent upon accurate species-specific parameterizations (Ney 1993) which exist for well-studied species but are rare for novel invaders.

There is no parameterized bioenergetics model for the Redside Shiner (*Richardsonius balteatus*), but it would be a valuable tool to explore the role of this species in lake and reservoir food webs across its native and introduced range. The Redside Shiner has established nonnative populations in 34 subbasins (USGS hydrologic unit code 8) across Arizona, Colorado, Montana, Utah, Washington, and Wyoming (Nico and Fuller 2020) in addition to lakes in British Columbia (Larkin and Smith 1954). These introductions have caused concern over potential ecological impacts to native fish. Negative impacts of Redside Shiner introduction on growth and production of Rainbow Trout (*Oncorhynchus mykiss*) have been extensively studied in some British Columbian lakes (Lindsey 1950; Larkin and Smith 1954; Johannes and Larkin 1961), and a laboratory study with the closely related Lahontan Redside (*Richardonius egregius*) suggested competitive advantages over Lahontan Cutthroat Trout (*O. clarki henshawi*) for food resources in turbid waters in Nevada (Vinyard and Yuan 1996). More recently, an unauthorized introduction of Redside Shiner in Ross Lake, Washington in the early 2000s sparked concern over possible competition with juvenile trout, given their diet overlap (Welch 2012). Rapid population growth following introductions in other high mountain lakes have accompanied declines in trout growth rates, leading to management actions seeking eradication (Messner and Schoby 2019; Smith et al. 2021). In these situations, quantifying consumption demand of Redside Shiner on shared resources, particularly as it relates to thermal environment (Reeves et al. 1987) and species distribution, would aid in evaluating the scope for competition with native fish.

The goal of this study was to parameterize a Wisconsin-style bioenergetics model for the Redside Shiner to be integrated into the Fish Bioenergetics 4.0 program (FB4, Deslauriers et al. 2017) and evaluate its performance for individuals from two large high-elevation reservoirs in Washington, United States. Specifically, the objectives were to: 1) estimate the temperature-dependent and allometric relationships for daily maximum consumption (C_{max}) and routine metabolic rate (RMR) of Redside Shiner using controlled laboratory experiments representing ecologically relevant ranges for temperature and fish sizes, 2) use the resulting data to parameterize a bioenergetics model for Redside Shiner, and 3) conduct controlled long-term growth studies to evaluate model performance and prediction error. This model provides a method for attaining temperature- and size-dependent growth and consumption estimates for the Redside Shiner, which can be used to assess its trophic role across native or invaded ecosystems under variable environmental conditions.

Methods

Fish collection and handling

In June 2019, approximately 350 Redside Shiners (size range: ca. 50–80 mm FL) were collected from Ross Lake (48.739°N, –121.058°W) using minnow traps. Approximately 100 additional fish were collected from Diablo Lake (48.716°N, –121.100°W) and Ross Lake in July 2020 to obtain fish < 50 mm FL and > 80 mm FL. Fish were transported to the U.S. Geological Survey–Western Fisheries Research Center in Seattle, WA in large coolers supplied with oxygen and monitored for oxygen levels and temperature periodically. Fish were held in 120-L circular tanks supplied with temperature-controlled, filtered, and UV-treated water from Lake Washington (47.672°N, –122.247°W) and were fed pelleted trout food (Skretting, Classic Fry sinking 1-mm) on a maintenance ration. Experimental temperatures up to 18° C were controlled through the system and higher temperatures required submersible heaters. All fish were gradually introduced to new temperatures at a rate ≤ 2° C/d and were acclimated at the experimental temperature for at least 5 d prior to the onset of experiments. Light regimes mimicked the natural photoperiod, with lights on 1-h before sunrise and off 1-h after sunset. Data generated as a part of this study described in the methods below can be found online in the U.S. Geological Survey ScienceBase (Johnson and Beauchamp 2022).

Consumption

Temperature dependence of C_{max}

We conducted a series of experiments to determine the temperature(s) associated with the maximum daily consumption rate (C_{max}) and the effect of environmentally relevant temperatures on C_{max}. These experiments were conducted on fish of the most available size (n=62; 55–65 mm FL; 1.3–4.5 g) from July to November in 2019 and 2020, with the exception of 7° C trials which were conducted in March 2021.

All C_{max} experiments were conducted over 4 consecutive days because we identified biases created by binge feeding on the first day of feeding trials during pilot trials in 2019, which have been reported for other species (e.g., Bull Trout: Mesa et al. 2013). Fish were deprived of food for at least 24-h and acclimated individually in small static test arenas (volume = 8-L containers with 5 L water). Fish were fed a pre-weighed *ad libitum* ration of pellets (Skretting, Classic Fry sinking 1-mm) offered 3–5 times over a 24-h period. Remaining food was collected after each 24-h period, oven-dried for 48-h, and weighed to maintain an accurate accounting for food eaten each day. Subsamples of pellets from each batch of food were weighed, dried for 48 h, and then weighed again to determine initial water content of the dry pellets (94.5–96.9% dry weight). Percent dry weight was then used to convert the weight of oven-dried leftover food to the initial pellet weight. Specific consumption per day ($g \cdot g^{-1} \cdot d^{-1}$) was calculated for each fish by dividing the total weight of food consumed each day by the initial weight of the fish at the beginning of the 4-d trials. C_{max} was calculated for each fish as the mean specific daily consumption rate for days 2–4. In the FB4 framework, the temperature dependence functions estimate C_{max} as a unitless proportion, so we transformed C_{max} data as a proportion of the mean consumption rate at 23° C, the temperature of maximum consumption, prior to model fitting.

We fit a number of thermal performance functions to the C_{max} data using non-linear least squares regression with the 'nls.mulstart' (Padfield and Matheson 2020) and 'rTPC' (Padfield and O'Sullivan 2021) packages in R version 4.0.4 (R Core Team 2021). We fit 12 functions in the 'rTPC' package (all of which we selected only if the response variable was restricted to ≥ 0) in addition to functions presented in Kitchell et al. (1977) and Thornton and Lessem (1978), which are integrated in the FB4 framework as default options (models 2 and 3, respectively: Deslauriers et al. 2017). Confidence intervals (95%) on the predictions and parameters were computed on the best performing model with bootstrapping using the 'car' package (Fox and Weisberg 2019) to assess model performance and fit of the data.

Mass dependence of C_{max}

The C_{max} experiments were repeated for body weights ranging from 0.6 to 27.3 g at 23°C (the temperature of maximum consumption). Consumption rates for the dry pellets were adjusted to the wet weight of the pellets after soaking in the water for 20 minutes (dry : soaked weight = 50%), as fish did not consume the pellets immediately in these trials. We measured pellet hydration to ensure that the modeled C_{max} rates accurately reflect maximum consumption ability due to stomach fullness. The model calculates consumption rate (C, in $g \cdot g^{-1} \cdot d^{-1}$) according to:

$$C = C_{max} \times p \times f(T) \qquad (1)$$

where C_{max} is the weight-dependent maximum specific consumption rate ($g \cdot g^{-1} \cdot d^{-1}$), p is the proportion of C_{max}, and $f(T)$ is the temperature dependence function. C_{max} is dependent on fish weight and determined at the temperature of maximum consumption (23° C) according to:

$$C_{max} = CA \times W^{CB} \qquad (2)$$

where CA and CB are the intercept and slope of the weight-dependent power function for C_{max}, fit with the $\log_e$-transformed linear regression. We chose the temperature dependence function ($f(T)$) by the best model fit as described above.

Routine metabolic rate

Data collection

Routine metabolic rate (RMR) was estimated across a range of temperatures (5–29° C) and fish sizes (0.9–26.8 g) using intermittent-flow respirometry following Svendsen et al. (2016). This method is considered the most suitable for accurate respirometry measurements as experiments can be conducted over extended periods, preventing data quality issues associated with spontaneous movements (Clark et al. 2013). This was advantageous in our study because we sought to estimate the average metabolic activity across the whole 24-h period to best capture RMR. Experiments were conducted between April and August 2021, with the coldest temperature trials conducted during the spring and warmest trials during the summer. We made respirometers from airtight plastic containers in a variety of sizes (range: 0.39–5.52 L) to accommodate the range of fish sizes. Respirometers were placed in pairs in 120-L fiberglass tanks partially filled with fresh water at the appropriate temperature. Each respirometer was connected to two submersible pumps (150 L/h, Eheim): one for recirculating and mixing the water (Rodgers et al. 2016) and the other for flushing the respirometer with fresh water from the water bath (Fig. 1). Flow rates from the pumps were reduced to minimize fish stress, depending on respirometer and fish size, by reducing tubing diameter on the pump outflow. Oxygen data were collected using a fiber-optic oxygen meter and oxygen probes with optical isolation (FireStingO2 4-channel meter [FSO2-4] and 3-mm Robust Oxygen Probes [OXROB3]) which were inserted into the respirometers using a watertight cable gland that was sealed to the lid of the respirometer. Temperature data were also recorded by the oxygen meter using the associated teflon-coated temperature probe. Oxygen meters were calibrated in fully saturated water according to manufacturer instructions prior to each trial.

Pilot trials indicated that fish placed individually in respirometers demonstrated atypical swimming behavior. Consequently, we placed three or four similarly sized fish together in a respirometer in order to obtain estimates of RMR (Appendix Table A.1). Trials were run for 24 h, as we discovered diel changes in metabolic rates associated with crepuscular periods during pilot trials. Food was withheld from the fish for at least 24–48 h prior to respiration trials (72–96 h for 5° C and 8° C trials). Fish were anesthetized with buffered tricaine methanesulfonate (80 mg/L MS-222) and weighed (0.1 g) before placing in respirometers with pumps on. We chose respirometer size to allow fish just enough room to swim freely while minimizing the respirometer : fish volume ratio, targeting a ratio between 50–150 (Svendsen et al. 2016). Once respirometers were closed, they were monitored over the next 30 min for the accumulation of air bubbles, which were then released by briefly opening the lids underwater to ensure no bubbles remained. Lids were placed on top of the water bath tanks to minimize disturbances and fish were allowed to acclimate for a minimum of another 30 min before oxygen data were recorded. During the acclimation time, flush pumps were manually turned off and on, and oxygen content was monitored to determine the appropriate cycle timing for measurement and flush periods in order to record measurable oxygen consumption while preventing saturation from declining to < 80% (Svendsen et al. 2016). Recirculation pumps operated continuously throughout the trial and flush pumps were controlled by a short period cycle timer (BN-LINK). Following each trial, fish were removed, flush pumps turned off and oxygen was measured in the empty respirometers for 0.3–48.0 h (depending on temperature and microbial activity) to calculate background respiration rates due to microbial activity in the respirometers. Respirometers were disinfected in an iodine bath (Argentyne) prior to each trial to limit/eliminate microbial activity.

Data processing

Oxygen concentration data from respirometry trials were processed and analyzed using the ‘rMR’ package (Moulton 2018) in R. Because the cycle timer controlling the flush pump did not use precise timing, the measurement periods were identified and extracted from the full oxygen data by smoothing the data and applying a peak-finding algorithm to identify the end of each measurement period when flush pumps were turned back on. Linear regressions relating oxygen content (mg/L) to time (s) were computed for each measurement period in each trial and visualized to ensure the data showed a linear trend with no obvious leaking in the respirometer. We determined regressions represented accurate estimates of respiration rates due to their high R^2 values (>0.74) and heterogeneous distribution of residuals. A single background rate was calculated for each respirometer in each trial by fitting a linear regression to oxygen content (mg/L) over time (s) in the closed, empty respirometer. Background rate was subtracted from the rate of each measurement period to correct for background microbial respiration, although background rates were negligible (range: 0–1.1e-04 mg O_2/s). This corrected rate was then converted to RMRs (mg $O_2 \cdot g^{-1} \cdot s^{-1}$) according to (Svendsen et al. 2016):

$$V_{RE} = V_{RT} - 0.001 \times W_o \rho_o^{-1} \qquad (3)$$

$$RO_{2B} = V_{RT} \times \frac{\delta O_2}{\delta t} \qquad (4)$$

$$RO_{2A} = V_{RE} \times \frac{\delta O_2}{\delta t} \qquad (5)$$

$$RO_{2cor} = RO_{2A} - RO_{2B} \qquad (6)$$

$$MO_{2cor} = RO_{2cor} \times W_o^{-1} \qquad (7)$$

where V_{RE} is the effective respirometer volume (L) with fish inside, V_{RT} is the total respirometer volume (L) including the recirculation loop, W_o is the total weight of all fish in the respirometer (g), ρ_o is the density of the organisms (assumed to be neutrally buoyant, 1.0 kg/L), RO_{2B} is the background respiration rate (mg O_2/s), RO_{2A} is the total respiration rate of all animals in the respirometer plus background respiration (mg O_2/s), $\frac{\delta O_2}{\delta t}$ is the slope of the linear regression of oxygen content (mg O_2/L) over time (s), RO_{2cor} is the total respiration rate of all animals in the respirometer after correcting for background respiration, and MO_{2cor} is the corrected weight-specific oxygen consumption rate of all animals in the respirometer (mg $O_2 \cdot g^{-1} \cdot s^{-1}$). A final RMR value for each group of fish was calculated as the mean of all MO_{2cor} rates throughout each trial, which was converted to g $O_2 \cdot g^{-1} \cdot d^{-1}$.

The relationship between body weight (averaged across all fish in a single respirometer), temperature, and RMR was determined by fitting a multiple linear regression of $\log_e$(RMR) as a function of $\log_e(\overline{W}_o)$ and temperature. The regression of RMR as a function of body weight and temperature was used to fit the basic form of the respiration function according to Model 1 in Deslauriers et al. (2017):

$$RMR = RA \times W^{RB} \times e^{RQ \times T} \qquad (8)$$

where RMR is the respiration rate (g $O_2 \cdot g^{-1} \cdot d^{-1}$), RA and RB are the intercept and slope of the allometric weight function, and RQ is the exponential coefficient for the temperature dependence function, and T is water temperature (° C).

Waste losses and specific dynamic action

The bioenergetics model also requires estimates of waste losses (egestion and excretion) and specific dynamic action (SDA). Waste losses are often reported as a constant proportion to consumption (Kitchell et al. 1977) and have been relatively insensitive in bioenergetics simulations (Ney 1993). Experiments with the European Minnow (*Phoxinus phoxinus*) also found SDA and excretion parameters to be equally insensitive to bioenergetics simulation predictions; simplifying egestion and excretion parameters to model them as a constant fraction of consumption had little effect on model predictions (Cui and Wootton 1989). Thus, we borrowed values for these parameters from the literature for Cyprinidae species.

Model corroboration and correction

Laboratory evaluation of the model

We evaluated model performance using laboratory growth and consumption experiments that lasted for 35–71 d. Two sets of experiments were conducted: experiment 1 used high energy trout pellets (Skretting, Classic Fry 1-mm sinking; mean energy density: 21,200 J/g dry pellet or 10,600 J/g wet weight after soaking) and experiment 2 used frozen *Mysis* pieces (mean energy density: 3,220 J/g wet weight) to mimic the energy density of their natural prey, which in Ross Lake is a mixture of zooplankton, benthos, and insects (Welch 2012). Within each experiment, two ration level treatments were employed. The high daily ration treatment was fed at an estimated 80% C_{max} (p-value = 0.8), and the low ration treatment was fed at an estimated 25% C_{max}. Fish were anesthetized and weighed (0.1 g) and placed individually into 8-L containers at the beginning of each experiment. For the duration of the experiments water temperature was monitored with temperature loggers (HOBO pendant, Onset Electronics, Onset, Massachusetts) and daily food rations were measured to the nearest 0.001 g (dry weight for pellets and blotted wet weight for frozen *Mysis*). Any food not consumed was collected from containers and weighed (0.001 g) to obtain an accurate accounting of the total food consumed by each individual. Fish were weighed periodically throughout the experiments to record growth or weight loss.

Energy densities

Energy densities (J/g wet weight) were measured for a random selection of stock fish (initial energy density) and for each fish at the end of the long-term growth experiments (final energy density, averaged for each food type and ration). Fish were euthanized, weighed, and dried at 60° C for a minimum of seven days or until dry weight stabilized before homogenizing with a mortar and pestle. Percent dry weights (pDW, %) were computed for each fish, and energy densities (ED) were measured on the dried homogenized tissue using bomb calorimetry (Parr 6725 Semi-Micro Calorimeter) or estimated based on pDW using an established regression between pDW and wet weight energy density for laboratory-reared and wild Redside Shiners ($ED = -4096.17 + 384.26 \times pDW$; $R^2 = 0.95$; $P < 0.001$; Appendix Fig. A.1). Energy density of each food item was measured using bomb calorimetry.

Estimating model error

Data from the long-term growth experiments were used as bioenergetic model simulation inputs to 1) estimate total consumption (g) based on observed final weight (g), and 2) estimate final weight based on observed total consumption for each individual fish. Simulations were conducted for two distinct subperiods of experiment 1 and a single period for experiment 2 to ensure that model error was calculated across stable temperatures and consumption rates. We did not have measured energy densities at the end of the first subperiod (because it requires lethal sampling), so energy densities across the entirety of experiment 1 were linearly interpolated. We classified each simulation by mean temperature groups in order to evaluate any differences in error based on temperature: high (18–19° C), mid (15° C), and low (8° C). A growth rate prediction error (GRE; $J \cdot g^{-1} \cdot d^{-1}$) value was calculated for each fish in each simulation according to:

$$GRE = \frac{(P_f - O_f)}{n\overline{O}} \times ED \qquad (9)$$

where P_f and O_f are the predicted and observed final weight at the end of each simulation, n is the number of days in the simulation, $\overline{O}$ is the mean observed weight of the fish during the simulation, and ED is the mean energy density of the fish throughout the simulation (J/g).

Correcting for model error

Following the methods of Bajer et al. (2004a), we used the three main inputs for bioenergetic models—consumption ($J \cdot g^{-1} \cdot d^{-1}$), temperature (° C), and fish weight (g)—as predictor variables in various combinations with model error (GRE) using linear regression. We selected the best model based on BIC scores and R^2_{adj}, and then subsequently incorporated it into the bioenergetics model simulation to correct growth estimates on a daily timestep. To do this, we modified the FB4 code to include an additional sub-equation to calculate GRE on a daily timestep within the 'grow' function. Corrected daily growth was calculated by subtracting the GRE from the original growth estimate. The corrected model was evaluated for improvement by comparing changes in prediction error to the uncorrected model across treatment groups. Percent error was calculated as:

$$Error(\%) = \frac{(P_f - O_f)}{O_f} \times 100 \qquad (10)$$

where $Error(\%)$ is the total consumption error (CE) or growth error (GE), and O_f and P_f are the observed and predicted consumption or final weight, respectively.

Temperature-dependent growth potential

To gain insights into thermal drivers of trophic interactions with sympatric salmonid species, we estimated temperature-dependent growth potential for Redside Shiner using the parameterized model (with correction factor) and compared to that of three salmonid species. Model parameters in FB4 were used for Sockeye Salmon (*Oncorhynchus nerka*: Beauchamp et al. 1989), Chinook Salmon (*O. tshawytscha*: Stewart and Ibarra 1991; as modified by Plumb and Moffitt 2015), and steelhead (*O. mykiss*: Rand et al. 1993)—three species that use various degrees of lentic habitat in their early life history (Arostegui and Quinn 2019). Daily growth was simulated for a 2-g fish of each species at a range of temperatures (1–30° C) assuming an average prey energy density of 3,500 J/g wet weight at their respective C_{max} (p-value = 1). Fish energy densities (J/g wet weight) were estimated using their equation in FB4 for Sockeye Salmon (5256), Chinook Salmon (5766), and steelhead (5766), and using measured energy densities of

Redside Shiner < 10 g from Ross Lake (n = 8, mean = 4911, SE = 378). Daily growth (g/g) for each species was transformed as a relative proportion of the maximum growth rate estimated.

Results

Consumption and metabolic rate

Consumption rates increased with temperature, peaked at 23° C, and then declined until 31° C, when experiments were stopped due to high (> 50%) mortality rates (Fig. 2). The Kitchell model for $F(T)$ (Model 2 in FB4) was chosen as the best model as it performed well with the other top two performing models based on ΔAIC, ΔAIC_c, and ΔBIC (Table 1), and it has the benefit of already existing in the FB4 framework (Table 2; full equation available in the Appendix).

Functions for effects of weight on C_{max} and for both weight and temperature on RMR were parameterized by fitting to experimental data (coefficients and 95% confidence intervals in Table 2). Maximum specific consumption rates decreased exponentially with fish body weight (Fig. 2, $R^2 = 0.66$, $F_{1,18} = 35.24$, $P < 0.001$):

$$C_{max} = 0.0883 \times W^{-0.468} \qquad (11)$$

Routine metabolic rates (RMR, g $O_2 \cdot g^{-1} \cdot d^{-1}$) decreased with fish body weight (g) and increased with temperature (Fig. 3, $R^2_{adj} = 0.88$, $F_{2,45} = 173.67$, $P < 0.001$):

$$RMR = 0.00177 \times W^{-0.249} \times e^{(T \times 0.0659)} \qquad (12)$$

Energy density

Energy densities (J/g wet weight) varied considerably among laboratory fish (4,466–8,450 J/g) but were unrelated to fish wet weight ($R^2 = 0.112$, P = 0.022). Therefore, the linear energy density function was not used for the laboratory simulations and initial and final energy densities were entered manually, using linear interpolation to derive daily energy densities. Initial energy densities were set as the mean value from a random selection of stock fish at the beginning of the experiments (n = 17, mean = 6369 J/g, SE = 263). Final energy densities were measured for each of the fish used in the long-term growth experiments and then averaged at the end of each experiment for the two ration types as follows: experiment 1 high ration (n = 10, mean = 7,113 J/g, SE = 312) experiment 1 low ration (n = 6, mean = 5,986 J/g, SE = 458), experiment 2 high ration (n = 8, mean = 6,172 J/g, SE = 225), and experiment 2 low ration (n = 6, mean = 5,696 J/g, SE = 147).

Model corroboration and correction

Laboratory evaluation of the model

The uncorrected Redside Shiner bioenergetics model parameterized in this paper tended to overestimate consumption and underestimate growth, though this response varied among fish in the long-term experiments (Fig. 4). Model error was greater for consumption estimates than for growth estimates. The regression for predicted versus observed consumption was significant ($R^2 = 0.85$, P < 0.001), and the intercept was not significantly different from zero (95% CI: -0.21 to 0.62); however, the slope was significantly larger than 1 (95% CI: 1.25 to 1.62). The regression for predicted versus observed final weight was also significant ($R^2 = 0.91$, P < 0.001), and the slope was not significantly different from one (95% CI: 0.92 to 1.11); however, the intercept was significantly less than zero (95% CI: -0.79 to -0.02).

Estimating model error

We explored potential sources of model prediction errors and biases by evaluating differences in model error between treatment groups. Error in model predictions varied substantially across treatment groups (mean $\text{Error}_{\text{cons}}$: -17.8 to 334.7%; mean Error_{wt}: -25.8 to 10.1%), indicating possible influences of temperature, ration, or food type on model error. A multiple regression model containing mean daily consumption, in terms of energy (C, $\text{J}\cdot\text{g}^{-1}\cdot\text{d}^{-1}$), temperature ($T$, °C), and consumption interacting with temperature ($C \cdot T$), was determined to be the best model to predict GRE (Table 3, $R^2_{\text{adj}} = 0.82$, $F_{3,41} = 66.93$, $P < 0.001$). The following equation was then used to estimate and correct for GRE on a daily timestep in the model:

$$GRE = -7.00 + -0.300C + -1.20T + 0.029(C \cdot T) \qquad (13)$$

When the GRE correction was incorporated into model simulations, absolute error (%) decreased in every treatment group for both estimates of final weight while fitting to observed consumption (Table 4) and estimates of consumption while fitting to final weight (Table 5). The corrected model improved the significance of the relationship between predicted and observed values across all experimental fish for total consumption ($R^2 = 0.97$, $P < 0.001$) and final weight ($R^2 = 0.99$, $P < 0.001$; Fig. 4). The regression intercept for consumption did not differ significantly from 0 (95% CI: -0.13 to 0.12), and while the slope was significantly greater than 1 (95% CI: 1.01 to 1.12), it was by a margin less than the typical measurable precision in the field, indicating that the corrected equation is not significantly biased in consumption estimates. The intercept for final weight did not differ significantly from 0 (95% CI: -0.19 to 0.1), nor did the slope differ significantly from 1 (95% CI: 0.97 to 1.04), indicating that the corrected equation is not significantly biased in growth estimates. While the corrected model performed very well for fish in the mid and high temperature groups (absolute error range; consumption: 2.05 to 24.89%; final weight: 0.1 to 3.41%), error rates were still high for fish at the coldest temperatures (absolute error range; consumption: 55.27 to 68.28%; final weight: 2.29 to 4.39%; Tables 4 and 5).

Temperature-dependent growth potential

Under the modeled conditions, the temperature of maximum growth potential was higher for Redside Shiner (18° C) than it was for steelhead (16° C), Chinook Salmon (13° C), or Sockeye Salmon (12° C; Fig. 5). For Redside Shiner, the temperature range over which growth potential was greater than 90% (16–20° C) only slightly overlapped with that of Sockeye Salmon (7–18° C) and Chinook Salmon (10–17° C), suggesting that similar sized individuals of these two species would inhabit distinct thermal habitats when those optimum temperatures are available. For steelhead, the temperature range over which growth potential was greater than 90% (12–20°C) was warmer than for the other salmonids and overlapped completely with that of Redside Shiner, suggesting that under these modeled conditions, similar sized individuals of these two species would likely overlap in their thermal habitat.

Discussion

This work represents the first bioenergetics model parameterized for Redside Shiner—an invasive species of concern, given its competitive interactions with native salmonids (Lindsey 1950; Larkin and Smith 1954; Johannes and Larkin 1961; Vinyard and Yuan 1996; Smith et al. 2021). Parameters were developed within the Wisconsin-style framework and thus can be easily applied using the FB4 software. Though we observed considerable error in the original parameterization when applied to laboratory growth data, we accounted for it by applying a correction factor to the daily timestep (Bajer et al. 2004a; Whitledge et al. 2006). For the Redside Shiner, this model should be particularly useful for exploring its trophic role as a forage fish, consequences of invasions into native fish communities (particularly scope for competition), and for predicting the implications of thermal structure (mediated by climate change or water use operations) for population dynamics and possible range expansion. We believe the model will be widely applicable and have reasonable predictive capability given our use of wild fish, parameterization experiments that spanned nearly the full range of body sizes and temperatures currently experienced by this species, and the variety of conditions under which model performance was assessed.

We confronted the challenges that small-bodied, slow growing fishes present in experiments relying on detectable and accurate measures of growth (or weight loss), especially at temperatures where growth performance or consumption would be low. Such constraints leave little scope for reasonably detecting those dynamics; many of our experimental groups showed weight differences that did not statistically differ from zero. However, this observation could indicate generally low metabolic performance under these conditions which is informative when considering the species' role in freshwater food webs. Further, our simulations of growth potential indicate that Redside Shiner may have a narrow range in temperatures and prey availability under which they can express significant growth and activity. These constraints could have important implications for understanding the role of Redside Shiner as a competitor with juvenile salmonids and forage fish for piscivores, as well as for assessing risks for invasion and range expansion by this species.

The limited thermal range for growth of Redside Shiner suggests there is a relatively narrow environmental window under which it may pose a significant risk for invasion. In ecosystems where cold water persists through the majority of the year, salmonids (and likely other native cold-water species) are better suited as they have a wider range of temperatures under which positive growth can be attained, even below 5° C. This relationship could aid in population control of the species where the infrastructure exists to de-stratify the water column or otherwise reduce water temperatures (*a la* Gaeta et al. 2012). However, as climate change shifts the timing and increases the duration and magnitude of thermal stratification in lake and reservoir habitats (Livingstone 2003), more ecosystems may be at risk for invasion by Redside Shiner or population expansion.

This species is native in many waterbodies, where it coexists with cold- and cool-water piscivores, and these possible climate change-induced alterations to the thermal structure will shift seasonal habitat use and resource access based on species-specific thermal optima. Our simulations and other studies suggest that some salmonid species may be more affected by warming surface waters than others (Wenger et al. 2011; Crozier et al. 2019). The higher thermal optima of the Redside Shiner may allow it to dominate the warm productive surface waters during stratified periods, limiting resource access for Sockeye Salmon and possibly Chinook Salmon when most prey production occurs in the warmer, shallow depths of the pelagic and littoral habitats (e.g., Tunney et al. 2012; Sorel et al. 2016a). Under such scenarios of high prey productivity and thus high consumption rates, steelhead appear to have a similar thermal tolerance to Redside Shiner on the warm end of the spectrum, suggesting they may have comparable access to prey resources. However, previous experiments have shown significant decreases in production of juvenile steelhead in the presence of Redside Shiner in warm water

(19–22° C) compared to production in the absence of Redside Shiner, suggesting a variety of competitive forces at play (Reeves et al. 1987).

Accuracy of bioenergetic models due to the internal parameters can be compromised by unknown activity costs, extrapolations of allometric functions, or borrowing parameters from ill-chosen species (Ney 1993). Because we fit the respiration function using routine metabolic rates (as opposed to standard metabolic rates), we eliminated the need to use additional parameters to account for activity levels, assuming that the routine rates we observed reflected an "average" metabolic rate experienced for wild fish. We observed similar activity rates by fish in holding tanks and in the wild, characterized by constant movement punctuated by occasional swimming bursts. Though we were unable to quantify them, similar movement patterns were observed in respirometers when at least three fish were held together, thus allowing us to estimate metabolic rates that more closely account for routine metabolism. Additionally, the use of intermittent-flow respirometry enabled the calculation of average metabolic rates computed across a 24-h period to account for the inherent diel and random variation in oxygen consumption throughout the day. We tested a wide range of fish sizes, representative of that observed in Ross Lake, except for early post-larval fry (< 0.5 g), as well as fish sizes found across their distributional range (Wydoski and Whitney 2003). Additionally, the wide range of temperatures under which parameters were developed encompassed those likely experienced by these fish throughout the year across most of their distribution, except in some northern or high elevation locations where winter water temperatures can reach below 5° C (e.g., Ross Lake, WA). Experimental limitations required us to borrow waste and SDA parameters from related species, thus our model is likely unable to accurately model those bioenergetic components, and we caution users when interpreting those outputs. However, we believe our model correction factor reasonably accounted for this when predicting fish growth or consumption.

The consumption-dependent error that we observed in our uncorrected model is widely observed in other bioenergetics models (e.g., Bajer et al. 2004b; Chipps and Wahl 2008). For our model, it is likely that part of this consumption-dependent error is due to the waste loss functions (egestion and excretion), which were informed by other species and model waste losses as a fixed proportion of energy consumed. Although waste is modeled this way for most fish species currently in FB4, some authors have argued that egestion, excretion, and SDA (the metabolic costs associated with digestion) should be modeled instead as a function of ration size rather than fixed proportion, as conversion efficiency may decline at high ration levels (Elliott 1976; Chipps et al. 2000). We found a strong relationship between daily consumption and consumption error when standardized by energy intake ($J \cdot g^{-1} \cdot d^{-1}$) as opposed to daily ration in terms of weight, consistent with data from Bajer et al. (2004a) and Whitledge et al. (2006). This accounted for the large differences in food energy density between the trout pellets and the frozen *Mysis*, suggesting that consumption-dependent error was related to energy intake rather than ration by weight. Though respiration rate is not a consumption-dependent function, SDA is modeled as a constant proportion of consumption (in terms of J/g in FB4, and g/g in previous versions), and some of this consumption-dependent error could also be due to changes in metabolism driven by consumption rate. Supporting this hypothesis, Ranney (2008) found that the feeding history of largemouth bass had a significant impact on metabolic rate, with fish that were fed maintenance rations exhibiting metabolic rates nearly half of those fed *ad libitum*. Given this, it may be more appropriate to model SDA as a dynamic function of consumption to better account for metabolism-related consumption-dependent error, and future experimental studies in this area could be beneficial to model development. Identifying the underlying cause of these consumption-dependent errors was outside the scope of this paper; however, our error correction procedure circumvents this requirement when using the bioenergetics model to predict consumption or growth. Thus, we caution users while interpreting the model outputs beyond consumption and growth in future applications of the Redside Shiner model.

Our model correction regression performed well, explaining 82% of the variation in growth rate error in the uncorrected model. However, due to low sample size across treatments groups and time requirements for the long-term growth experiments, cross-validation of the error correction procedure was not possible. Thus, we expect that true errors of model performance using the corrected model will be higher than what we report here. The corrected model performed well predicting growth for fish, with absolute percent error below 5% for all experimental groups. Comparatively, Chipps and Wahl (2008) reported all 9 laboratory experiments they reviewed had growth errors exceeding 5%. Consumption errors were generally higher than for growth and the corrected model performed reasonably well for most experimental groups, with absolute error below 25% for all but the two cold temperature experimental groups, exceeding the predictive performance of many models for other species (Chipps and Wahl 2008). The higher errors in the cold temperature trial could have been caused by inaccurate estimates of final energy density of the consumers, if energy densities did not change linearly across the entire experiment 1 as we assumed, but we were unable to measure final energy densities after subperiod 1 of experiment 1 without lethally sampling the fish.

Bioenergetics simulations are sensitive to predator energy density and inaccurate estimates can result in biased consumption or growth estimates (Johnson et al. 2017). We are confident that the mean energy density values at the conclusion of both experiments are representative because they followed expected trends – fish fed the high energy pellets at the high ration had the highest mean energy density, and fish fed the lower energy frozen *Mysis* at the low ration had the lowest mean energy density. The high level of individual variation in energy densities presented a challenge for accurately characterizing changes in energy density throughout the simulation, however we believe we accounted for this by using mean energy densities. Importantly, when applying these bioenergetics models to field data, we are reliant upon using population means, so we believe this approach best represents how this model would be used with field data.

Though we expect this corrected model to perform well for this population of Redside Shiner in Ross and Diablo Lakes, users of this model should be aware that parameters can vary within a species across their environmental and geographical range (see e.g., Munch and Conover 2002; Galarowicz and Wahl 2003). This population is not in an unusual climate or elevation for this species, thus we expect it to perform well for many populations. However, future research comparing growth performance and consumption of select populations from different environments could improve the robustness and applicability of this model.

In presenting a framework for bioenergetic model development and application, Chipps and Wahl (2008) offered three main recommendations to reduce the uncertainty in model applications: 1) models should be evaluated under a broad range of conditions, 2) parameters should be tested using hypothesis-based methods, and 3) enhanced communication between model developers and users to improve information sharing. In this paper, we believe we have adequately addressed the first two recommendations. In the spirit of the final recommendation, we have released and archived our data in a publicly available repository (Johnson and Beauchamp 2022) and encourage the application and thorough inspection of our model. When applying this model to field data, accuracy of model predictions will depend on the accuracy of model inputs such as growth rates, prey energy densities, and predator energy densities. Additionally, we caution users in applying this current model in extreme/untested environmental conditions (e.g., low dissolved oxygen, extreme temperatures outside of the range tested here), but we encourage future experiments targeting these current uncertainties in model parameters and performance.

Acknowledgments

Funding for this study was provided by Seattle City Light. We are grateful for Marshal Hoy and Tessa Code for planning field operations and ensuring the safe collection and transportation of experimental fish. We also thank Karl Stenberg, Ben Jensen, Jon Mclean, and Ella Wagner for assistance with animal care and the many consumption experiments, and Tom Quinn and three anonymous reviewers for valuable editorial comments that improved the quality of this manuscript. Handling of vertebrates was conducted under the auspices of the Institutional Animal Care and Use Committee of the U.S. Geological Survey, Western Fisheries Research Center IACUC protocols #2008-57 and #2008-64. Any use of trade, firm, or product names is for descriptive purposes only and does not imply endorsement by the U.S. Government.

References

Arostegui, M. C., and T. P. Quinn. 2019. Reliance on lakes by salmon, trout and charr (*Oncorhynchus*, *Salmo* and *Salvelinus*): an evaluation of spawning habitats, rearing strategies and trophic polymorphisms. Fish and Fisheries 20:775–794.

Bajer, P. G., R. S. Hayward, G. W. Whitledge, and R. D. Zweifel. 2004a. Simultaneous identification and correction of systematic error in bioenergetics models: demonstration with a White Crappie (*Pomoxis annularis*) model. Canadian Journal of Fisheries and Aquatic Sciences 61:2168–2182.

Bajer, P. G., G. W. Whitledge, and R. S. Hayward. 2004b. Widespread consumption-dependent systematic error in fish bioenergetics models and its implications. Canadian Journal of Fisheries and Aquatic Sciences 61:2158–2167.

Beauchamp, D. A., D. J. Stewart, and G. L. Thomas. 1989. Corroboration of a bioenergetics model for Sockeye Salmon. Transactions of the American Fisheries Society 118:597–607.

Breeggemann, J. J., M. A. Kaemingk, T. J. DeBates, C. P. Paukert, J. R. Krause, A. P. Letvin, T. M. Stevens, D. W. Willis, and S. R. Chipps. 2016. Potential direct and indirect effects of climate change on a shallow natural lake fish assemblage. Ecology of Freshwater Fish 25:487–499.

Carmichael, R. A., D. Tonina, E. R. Keeley, R. M. Benjankar, and K. E. See. 2020. Some like it slow: a bioenergetic evaluation of habitat quality for juvenile Chinook Salmon in the Lemhi River, Idaho. Canadian Journal of Fisheries and Aquatic Sciences 77:1221–1232.

Chipps, S. R., L. M. Einfalt, and D. H. Wahl. 2000. Growth and food consumption by tiger muskellunge: effects of temperature and ration level on bioenergetic model predictions. Transactions of the American Fisheries Society 129:186–193.

Chipps, S. R., and D. H. Wahl. 2008. Bioenergetics modeling in the 21st century: reviewing new insights and revisiting old constraints. Transactions of the American Fisheries Society 137:298–313.

Clark, T. D., E. Sandblom, and F. Jutfelt. 2013. Aerobic scope measurements of fishes in an era of climate change: respirometry, relevance and recommendations. Journal of Experimental Biology 216:2771–2782.

Cline, T. J., J. F. Kitchell, V. Bennington, G. A. McKinley, E. K. Moody, and B. C. Weidel. 2014. Climate impacts on landlocked Sea Lamprey: implications for host-parasite interactions and invasive species management. Ecosphere 5(6):1–13.

Cooke, S. L., and W. R. Hill. 2010. Can filter-feeding Asian carp invade the Laurentian Great Lakes? A bioenergetic modelling exercise. Freshwater Biology 55:2138–2152.

Courtney, M. B., E. R. Schoen, A. Wizik, and P. A. H. Westley. 2018. Quantifying the net benefits of suppression: truncated size structure and consumption of native salmonids by invasive Northern Pike in an Alaska lake. North American Journal of Fisheries Management 38:1306–1315.

Crozier, L. G., M. M. McClure, T. Beechie, S. J. Bograd, D. A. Boughton, M. Carr, T. D. Cooney, J. B. Dunham, C. M. Greene, M. A. Haltuch, E. L. Hazen, D. M. Holzer, D. D. Huff, R. C. Johnson, C. E. Jordan, I. C. Kaplan, S. T. Lindley, N. J. Mantua, P. B. Moyle, J. M. Myers, M. W. Nelson, B. C. Spence, L. A. Weitkamp, T. H. Williams, and E. Willis-Norton. 2019. Climate vulnerability assessment for Pacific salmon and steelhead in the California Current Large Marine Ecosystem. PLoS ONE 14(7):1–49.

Cucherousset, J., and J. D. Olden. 2011. Ecological impacts of non-native freshwater fishes. Fisheries 36:215–230.

Cui, Y., and R. J. Wootton. 1989. Bioenergetics of growth of a cyprinid, *Phoxinus phoxinus* (L.): development and testing of a growth model. Journal of Fish Biology 34:47–64.

Deslauriers, D., S. R. Chipps, J. E. Breck, J. A. Rice, and C. P. Madenjian. 2017. Fish Bioenergetics 4.0: an R-based modeling application. Fisheries 42:586–596.

Elliott, J. M. 1976. Energy losses in the waste products of Brown Trout (*Salmo trutta* L.). The Journal of Animal Ecology 45:561–580.

Fox, J., and S. Weisberg. 2019. An R companion to applied regression, 3rd edition. Sage, Thousand Oaks CA.

Gaeta, J. W., J. S. Read, J. F. Kitchell, and S. R. Carpenter. 2012. Eradication via destratification: whole-lake mixing to selectively remove Rainbow Smelt, a cold-water invasive species. Ecological Applications 22:817–827.

Galarowicz, T. L., and D. H. Wahl. 2003. Differences in growth, consumption, and metabolism among Walleyes from different latitudes. Transactions of the American Fisheries Society 132:425–437.

Gallardo, B., M. Clavero, M. I. Sánchez, and M. Vilà. 2016. Global ecological impacts of invasive species in aquatic ecosystems. Global Change Biology 22:151–163.

Johannes, R. E., and P. A. Larkin. 1961. Competition for food between Redside Shiners (*Richardsonius balteatus*) and Rainbow Trout (*Salmo gairdneri*) in two British Columbia lakes. Journal of the Fisheries Research Board of Canada 18:203–220.

Johnson, T. B., D. B. Bunnell, and C. T. Knight. 2005. A potential new energy pathway in Central Lake Erie: the Round Goby connection. Journal of Great Lakes Research 31:238–251.

Johnson, B. M., W. M. Pate, and A. G. Hansen. 2017. Energy density and dry matter content in fish: new observations and an evaluation of some empirical models. Transactions of the American Fisheries Society 146:1262–1278.

Johnson, R.C., and D. A. Beauchamp. 2022. Data used to parameterize and evaluate a bioenergetics model for Redside Shiner (*Richardsonius balteatus*): U.S. Geological Survey data release, https://doi.org/10.5066/P9NAIACL.

Kinlock, N. L., A. J. Laybourn, C. E. Murphy, J. J. Hoover, and N. A. Friedenberg. 2020. Modelling bioenergetic and population-level impacts of invasive Bigheaded Carps (*Hypophthalmichthys* spp.) on native Paddlefish (*Polyodon spathula*) in backwaters of the lower Mississippi River. Freshwater Biology 65:1086–1100.

Kitchell, J. F., D. J. Stewart, and D. Weininger. 1977. Applications of a bioenergetics model to Yellow Perch (*Perca flavescens*) and Walleye (*Stizostedion vitreum vitreum*). Journal of the Fisheries Research Board of Canada 34:1922–1935.

Larkin, P. A., and S. B. Smith. 1954. Some effects of introduction of the Redside Shiner on the Kamloops Trout in Paul Lake, British Columbia. Transactions of the American Fisheries Society 83:161–175.

Lawrence, D. J., D. A. Beauchamp, and J. D. Olden. 2015. Life-stage-specific physiology defines invasion extent of a riverine fish. Journal of Animal Ecology 84:879–888.

Lindsey, C. C. 1950. The relation of the Redside Shiner to production of trout in British Columbia. B.C. Game Commission, Scientific Report.

Livingstone, D. M. 2003. Impact of secular climate change on the thermal structure of a large temperate central European lake. Climatic Change 57:205–225.

Lowery, E. D., and D. A. Beauchamp. 2015. Trophic ontogeny of fluvial Bull Trout and seasonal predation on Pacific salmon in a riverine food web. Transactions of the American Fisheries Society 144:724–741.

Mesa, M. G., L. K. Weiland, H. E. Christiansen, S. T. Sauter, and D. A. Beauchamp. 2013. Development and evaluation of a bioenergetics model for Bull Trout. Transactions of the American Fisheries Society 142:41–49.

Messner, J., and G. Schoby. 2019. Fisheries management Annual Report: Salmon Region 2017. Idaho Department of Fish; Game, 19-102.

Moulton, T. L. 2018. rMR: Importing data from Loligo Systems software, calculating metabolic rates and critical tensions. R package version 1.1.0.

Muhlfeld, C. C., D. H. Bennett, R. K. Steinhorst, B. Marotz, and M. Boyer. 2008. Using bioenergetics modeling to estimate consumption of native juvenile salmonids by nonnative Northern Pike in the upper Flathead River system, Montana. North American Journal of Fisheries Management 28:636–648.

Munch, S. B., and D. O. Conover. 2002. Accounting for local physiological adaptation in bioenergetic models: testing hypotheses for growth rate evolution by virtual transplant experiments. Canadian Journal of Fisheries and Aquatic Sciences 59:393–403.

Ney, J. J. 1993. Bioenergetics modeling today: growing pains on the cutting edge. Transactions of the American Fisheries Society 122:736–748.

Nico, L., and P. Fuller. 2020. *Richardsonius balteatus* (Richardson, 1836): U.S. Geological Survey, Nonindigenous Aquatic Species Database. Available: https://nas.er.usgs.gov/queries/FactSheet.aspx?SpeciesID=644.

Padfield, D., and G. Matheson. 2020. Nls.multstart: Robust non-linear regression using AIC scores. R package version 1.2.0.

Padfield, D., and H. O’Sullivan. 2021. rTPC: Functions for fitting thermal performance curves. R package version 1.0.0.

Plumb, J. M., and C. M. Moffitt. 2015. Re-estimating temperature-dependent consumption parameters in bioenergetics models for juvenile Chinook Salmon. Transactions of the American Fisheries Society 144:323–330.

R Core Team. 2021. R: A language and environment for statistical computing. R Foundation for Statistical Computing, Vienna, Austria.

Rand, P. S., D. J. Stewart, P. W. Seelbach, M. L. Jones, and L. R. Wedge. 1993. Modeling steelhead population energetics in Lakes Michigan and Ontario. Transactions of the American Fisheries Society 122:977–1001.

Ranney, S. H. 2008. Influence of feeding history on metabolic rates in fishes: evidence for metabolic compensation in Largemouth Bass (*Micropterus salmoides*). Master’s thesis. South Dakota State University, Brookings.

Reeves, G. H., F. H. Everest, and J. D. Hall. 1987. Interactions between the Redside Shiner (*Richardsonius balteatus*) and the steelhead trout (*Salmo gairdneri*) in western Oregon: the influence of water temperature. Canadian Journal of Fisheries and Aquatic Sciences 44:1603–1613.

Reid, A. J., A. K. Carlson, I. F. Creed, E. J. Eliason, P. A. Gell, P. T. J. Johnson, K. A. Kidd, T. J. MacCormack, J. D. Olden, S. J. Ormerod, J. P. Smol, W. W. Taylor, K. Tockner, J. C. Vermaire, D. Dudgeon, and S. J. Cooke. 2019. Emerging threats and persistent conservation challenges for freshwater biodiversity. Biological Reviews 94:849–873.

Rodgers, G. G., P. Tenzing, and T. D. Clark. 2016. Experimental methods in aquatic respirometry: the importance of mixing devices and accounting for background respiration. Journal of Fish Biology 88:65–80.

Schoen, E. R., D. A. Beauchamp, A. R. Buettner, and N. C. Overman. 2015. Temperature and depth mediate resource competition and apparent competition between *Mysis diluviana* and kokanee. Ecological Applications 25:1962–1975.

Smith, T. W., B. W. Liermann, and L. A. Eby. 2021. Ecological assessment and evaluation of potential eradication approaches for introduced Redside Shiners in a montane lake. North American Journal of Fisheries Management 41:1473–1489.

Sorel, M. H., A. G. Hansen, K. A. Connelly, and D. A. Beauchamp. 2016a. Trophic feasibility of reintroducing anadromous salmonids in three reservoirs on the North Fork Lewis River, Washington: prey supply and consumption demand of resident fishes. Transactions of the American Fisheries Society 145:1331–1347.

Sorel, M. H., A. G. Hansen, K. A. Connelly, A. C. Wilson, E. D. Lowery, and D. A. Beauchamp. 2016b. Predation by Northern Pikeminnow and tiger muskellunge on juvenile salmonids in a high-head reservoir: implications for anadromous fish reintroductions. Transactions of the American Fisheries Society 145:521–536.

Stewart, D. J., and M. Ibarra. 1991. Predation and production by salmonine fishes in Lake Michigan 1978-88. Canadian Journal of Fisheries and Aquatic Sciences 48:909–922.

Svendsen, M. B. S., P. G. Bushnell, and J. F. Steffensen. 2016. Design and setup of intermittent-flow respirometry system for aquatic organisms. Journal of Fish Biology 88:26–50.

Taylor, T. N., B. K. Cross, and B. C. Moore. 2020. Modeling Brook Trout carrying capacity in Owhi Lake, Washington, using bioenergetics. North American Journal of Fisheries Management 40:84–104.

Thomas, Y., S. Pouvreau, M. Alunno-Bruscia, L. Barillé, F. Gohin, P. Bryère, and P. Gernez. 2016. Global change and climate-driven invasion of the Pacific oyster (*Crassostrea gigas*) along European coasts: a bioenergetics modelling approach. Journal of Biogeography 43:568–579.

Thornton, K. W., and A. S. Lessem. 1978. A temperature algorithm for modifying biological rates. Transactions of the American Fisheries Society 107:284–287.

Tickner, D., J. J. Opperman, R. Abell, M. Acreman, A. H. Arthington, S. E. Bunn, S. J. Cooke, J. Dalton, W. Darwall, G. Edwards, I. Harrison, K. Hughes, T. Jones, D. Leclère, A. J. Lynch, P. Leonard, M. E. McClain, D. Muruven, J. D. Olden, S. J. Ormerod, J. Robinson, R. E. Tharme, M. Thieme, K. Tockner, M. Wright, and L. Young. 2020. Bending the curve of global freshwater biodiversity loss: an emergency recovery plan. BioScience 70:330–342.

Tunney, T. D., K. S. McCann, N. P. Lester, and B. J. Shuter. 2012. Food web expansion and contraction in response to changing environmental conditions. Nature Communications 3(1105):1–9.

van der Lee, A. S., T. B. Johnson, and M. A. Koops. 2017. Bioenergetics modelling of Grass Carp: estimated individual consumption and population impacts in Great Lakes wetlands. Journal of Great Lakes Research 43:308–318.

Vinyard, G. L., and A. C. Yuan. 1996. Effects of turbidity on feeding rates of Lahontan Cutthroat Trout (*Oncorhynchus clarki henshawi*) and Lahontan Redside Shiner (*Richardsonius egregius*). The Great Basin Naturalist 56:157–161.

Weber, N., N. Bouwes, and C. E. Jordan. 2014. Estimation of salmonid habitat growth potential through measurements of invertebrate food abundance and temperature. Canadian Journal of Fisheries and Aquatic Sciences 71:1158–1170.

Welch, C. A. 2012. Seasonal and age-based aspects of diet of the introduced Redside Shiner (*Richardsonius balteatus*) in Ross Lake, Washington. Master's thesis. Western Washington University, Bellingham.

Wenger, S. J., D. J. Isaak, C. H. Luce, H. M. Neville, K. D. Fausch, J. B. Dunham, D. C. Dauwalter, M. K. Young, M. M. Elsner, B. E. Rieman, A. F. Hamlet, and J. E. Williams. 2011. Flow regime, temperature, and biotic interactions drive differential declines of trout species under climate change. Proceedings of the National Academy of Sciences of the United States of America 108:14175–14180.

Whitledge, G. W., P. G. Bajer, and R. S. Hayward. 2006. Improvement of bioenergetics model predictions for fish undergoing compensatory growth. Transactions of the American Fisheries Society 135:49–54.

Wydoski, R. S., and R. R. Whitney. 2003. Inland fishes of Washington, 2nd edition. University of Washington Press, Seattle.

Tables

Table 1. Non-linear least squares regression results for a selection of the top performing temperature function models defining the relationship for maximum consumption rate (C_{max}) as a function of temperature for Redside Shiner (*Richardsonius balteatus*). For the definition of the 'kitchell' and 'thornton' models see the documentation for Fish Bioenergetics 4.0 (Deslauriers et al. 2017). For the definition of all other models, see the 'rTPC' package (Padfield and O'Sullivan 2021). AICc: Akaike information criterion corrected for small sample sizes, BIC: Bayesian information criterion.

Model name	# Parameters	AICc	ΔAICc	BIC	ΔBIC
gaussian	3	-34.808	0.000	-27.079	0.000
pawar	4	-34.704	0.104	-25.241	1.838
kitchell	3	-33.114	1.694	-25.385	1.694
modifiedgaussian	4	-32.431	2.377	-22.968	4.111
oneill	4	-32.347	2.461	-22.883	4.195
weibull	4	-32.041	2.767	-22.577	4.501
boatman	5	-31.494	3.314	-20.385	6.694
ratkowsky	4	-30.101	4.707	-20.637	6.441
delong	5	-30.052	4.756	-18.943	8.136
beta	5	-30.011	4.797	-18.901	8.178
flinn	3	-29.910	4.898	-22.181	4.898
thornton	6	-25.628	9.180	-12.965	14.114

Table 2. Parameters for the Redside Shiner (*Richardsonius balteatus*) bioenergetics model and bootstrapped 95% confidence intervals (CI). Parameters for SDA, FA, and UA were borrowed from other Cyprinidae sp. and parameter definitions were modified from the FB4 user manual (Deslauriers et al. 2017).

Parameter	Definition	Value	Lower 95% CI	Upper 95% CI	Units
	Consumption				
CA	Intercept: weight-dependent power function of maximum consumption (C_{max}; equivalent to the C_{max} of a 1-g fish at CTO)	0.0883	0.0696	0.118	$g \cdot g^{-1} \cdot d^{-1}$
CB	Slope: weight-dependent power function of C_{max}	-0.468	-0.646	-0.315	
CTO	Optimal temperature for consumption	23.7	22.5	25.3	°C
CTM	Maximum temperature above which consumption ceases	191.7*	37.5	2628.4	°C
CQ	The rate at which consumption increases over relatively low water temperatures	3.97	3.10	5.17	
	Metabolism				
RA	Intercept: weight-dependent power function of MO_2 (equivalent to specific oxygen consumption by a 1-g fish at 0°C)	0.00177	0.00145	0.00217	$g\ O_2 \cdot g^{-1} \cdot d^{-1}$
RB	Slope: weight-dependent power function of MO_2	-0.249	-0.324	-0.181	
RQ	Slope: temperature-dependence	0.0659	0.0582	0.0764	°C
SDA	Specific dynamic action, as a proportion of assimilated energy (J/g)	0.172			
	Waste				
FA	Proportion of consumption (J/g) lost to egestion	0.2			
UA	Proportion of assimilated energy (J/g) lost to excretion	0.1			

*Note: this extremely high value for CTM is the correct parameter value for the Kitchell version of the consumption model in order to adequately fit the thermal response of RSS over the natural range of temperatures. This function has a long asymptotic region that forces the CTM value into such high values. In this situation, the traditional definition of CTM described here is not applicable for this parameter.

Table 3. Multiple regression results for the response of growth rate error (GRE, J· g^{-1} · d^{-1}) to mean values of consumption (C, J· g^{-1} · d^{-1}), fish weight (W, g), and temperature (T, °C) in each simulation. AIC: Akaike information criterion, BIC: Bayesian information criterion.

Predictor variables	df	df_{res}	P	F	R^2_{adj}	AIC	ΔAIC	BIC	ΔBIC
C+T+C:T	3	41	< 0.001	66.93	0.82	295.85	0.00	304.89	0.00
C+T+W+C:T	4	40	< 0.001	49.14	0.81	297.73	1.88	308.57	3.68
C	1	43	< 0.001	123.30	0.74	310.84	14.99	316.26	11.37
C+T	2	42	< 0.001	62.91	0.74	311.37	15.52	318.59	13.70
C*T*W	7	37	< 0.001	26.73	0.80	302.66	6.81	318.92	14.03

Table 4. Mean initial weights (IW, g), observed final weights (FW_{obs}, g) and mean predicted final weights (FW_p, g) for the uncorrected and corrected models, along with the mean error (%) for each experiment and treatment group. Treatment groups were defined by the food ration and type (HR: high ration (~80% C_{max}), LR: low ration (~25% C_{max}), HE: high energy pellets, N: natural prey proxy (frozen *Mysis*), and the experimental temperature (low: mean of 8°C, mid: mean of 14-15°C, high: mean of 18-19°C). Symbols in the 'Growth' column indicate whether the treatment group exhibited weight loss (-), zero weight change (0), or positive growth (+) during the trial. SE values are given in parentheses.

							Uncorrected		Corrected	
Experiment	Food	Growth	Temp	N	IW	FW_{obs}	FW_p	%Error	FW_p	%Error
Exp 1-1	HR-HE	(-)	cold	5	3.82 (0.63)	3.68 (0.58)	3.14 (0.52)	-14.93 (0.84)	3.53 (0.59)	-4.39 (0.95)
Exp 1-2	HR-HE	(+)	high	5	4.20 (0.54)	5.14 (0.64)	5.60 (0.59)	10.11 (3.79)	5.25 (0.60)	2.76 (3.28)
Exp 1-1	HR-HE	(+)	mid	5	3.48 (0.51)	4.20 (0.54)	3.96 (0.50)	-5.64 (1.07)	4.14 (0.55)	-1.70 (1.18)
Exp 1-2	HR-HE	(+)	mid	5	3.68 (0.58)	3.90 (0.60)	3.66 (0.54)	-5.93 (1.07)	3.93 (0.59)	0.81 (1.12)
Exp 2-1	HR-N	(0)	high	3	3.33 (0.17)	3.40 (0.10)	2.99 (0.14)	-12.16 (1.52)	3.29 (0.17)	-3.41 (2.15)
Exp 2-1	HR-N	(0)	mid	4	3.62 (1.06)	3.72 (1.13)	3.06 (0.88)	-16.83 (1.46)	3.75 (1.13)	0.86 (1.19)
Exp 1-1	LR-HE	(-)	cold	3	3.13 (0.49)	2.93 (0.49)	2.64 (0.43)	-9.77 (0.39)	3.00 (0.49)	2.29 (0.44)
Exp 1-2	LR-HE	(0)	high	3	3.50 (0.17)	3.67 (0.24)	3.35 (0.15)	-8.37 (3.06)	3.57 (0.17)	-2.23 (2.84)
Exp 1-1	LR-HE	(0)	mid	3	3.40 (0.23)	3.50 (0.17)	3.00 (0.21)	-14.46 (1.76)	3.42 (0.24)	-2.49 (2.11)
Exp 1-2	LR-HE	(0)	mid	3	2.93 (0.49)	2.90 (0.50)	2.57 (0.44)	-11.30 (1.41)	2.90 (0.50)	-0.10 (1.53)
Exp 2-1	LR-N	(-)	high	3	3.50 (0.15)	3.07 (0.20)	2.27 (0.11)	-25.83 (1.71)	2.97 (0.15)	-3.06 (2.06)
Exp 2-1	LR-N	(-)	mid	3	3.23 (0.42)	3.00 (0.40)	2.25 (0.32)	-24.99 (0.87)	2.98 (0.42)	-1.01 (1.31)

Table 5. Mean observed cumulative consumption (CC_{obs}, g) and mean predicted cumulative consumption (CC_p, g) for the uncorrected and corrected models, along with the mean error (%) for each experiment and treatment group. Treatment groups were defined by the food ration and type (HR: high ration (~80% C_{max}), LR: low ration (~25% C_{max}), HE: high energy pellets, N: natural prey proxy (frozen *Mysis*), and the experimental temperature (low: mean of 8°C, mid: mean of 14-15°C, high: mean of 18-19°C). Symbols in the 'Growth' column indicate whether the treatment group exhibited weight loss (-), zero weight change (0), or positive growth (+) during the trial. SE values are given in parentheses.

						Uncorrected		Corrected	
Experiment	Food	Growth	Temp	N	CC_{obs}	CC_p	%Error	CC_p	%Error
Exp 1-1	HR-HE	(-)	cold	5	0.15 (0.01)	0.46 (0.05)	208.71 (11.50)	0.23 (0.02)	55.27 (10.50)
Exp 1-2	HR-HE	(+)	high	5	1.70 (0.11)	1.41 (0.16)	-17.80 (5.90)	1.60 (0.18)	-6.34 (8.20)
Exp 1-1	HR-HE	(+)	mid	5	1.01 (0.08)	1.16 (0.10)	14.24 (2.88)	1.06 (0.07)	5.05 (3.50)
Exp 1-2	HR-HE	(+)	mid	5	0.56 (0.04)	0.71 (0.08)	25.61 (5.54)	0.54 (0.05)	-3.66 (4.95)
Exp 2-1	HR-N	(0)	high	3	6.20 (0.17)	7.90 (0.01)	27.71 (3.45)	6.86 (0.24)	11.12 (7.04)
Exp 2-1	HR-N	(0)	mid	4	3.89 (0.60)	6.48 (1.53)	61.44 (12.03)	3.79 (0.62)	-2.82 (4.21)
Exp 1-1	LR-HE	(-)	cold	3	0.05 (0.00)	0.20 (0.03)	334.70 (50.84)	0.01 (0.00)	-68.28 (6.70)
Exp 1-2	LR-HE	(0)	high	3	0.48 (0.01)	0.65 (0.06)	37.20 (14.73)	0.55 (0.08)	15.93 (17.75)
Exp 1-1	LR-HE	(0)	mid	3	0.31 (0.02)	0.59 (0.01)	90.80 (11.04)	0.37 (0.03)	18.75 (15.93)
Exp 1-2	LR-HE	(0)	mid	3	0.17 (0.02)	0.34 (0.05)	103.85 (17.17)	0.17 (0.03)	2.05 (14.52)
Exp 2-1	LR-N	(-)	high	3	2.19 (0.06)	5.34 (0.44)	143.37 (15.39)	2.74 (0.43)	24.89 (17.50)
Exp 2-1	LR-N	(-)	mid	3	1.25 (0.10)	4.03 (0.42)	221.69 (11.09)	1.34 (0.12)	8.98 (12.22)

Figures

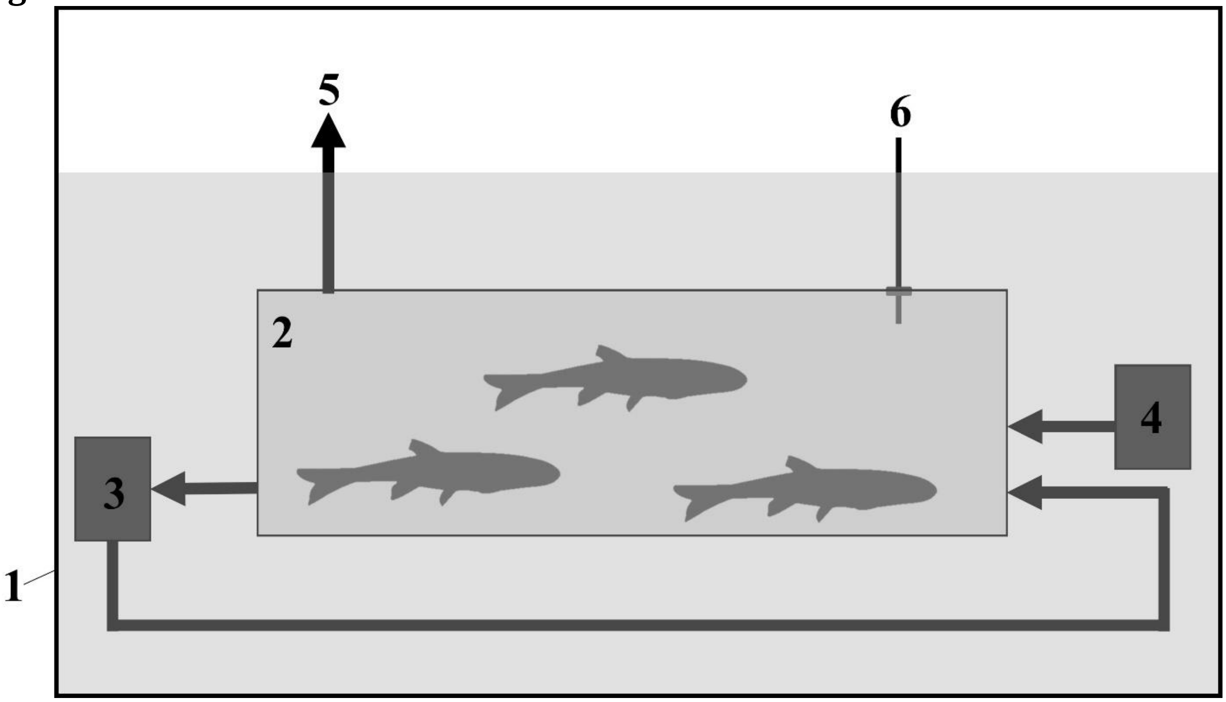

Figure 1. Respirometer design used in this study. Numbers correspond to (1) water bath tank, (2) sealed respirometer chamber, (3) recirculation pump that is running continuously, (4) flush pump that is activated using a cycle timer (water exits at 5), (5) water overflow pipe, which extends above the water surface, and (6) oxygen probe seated in the respirometer with a watertight cable gland. Gray shading depicts water.

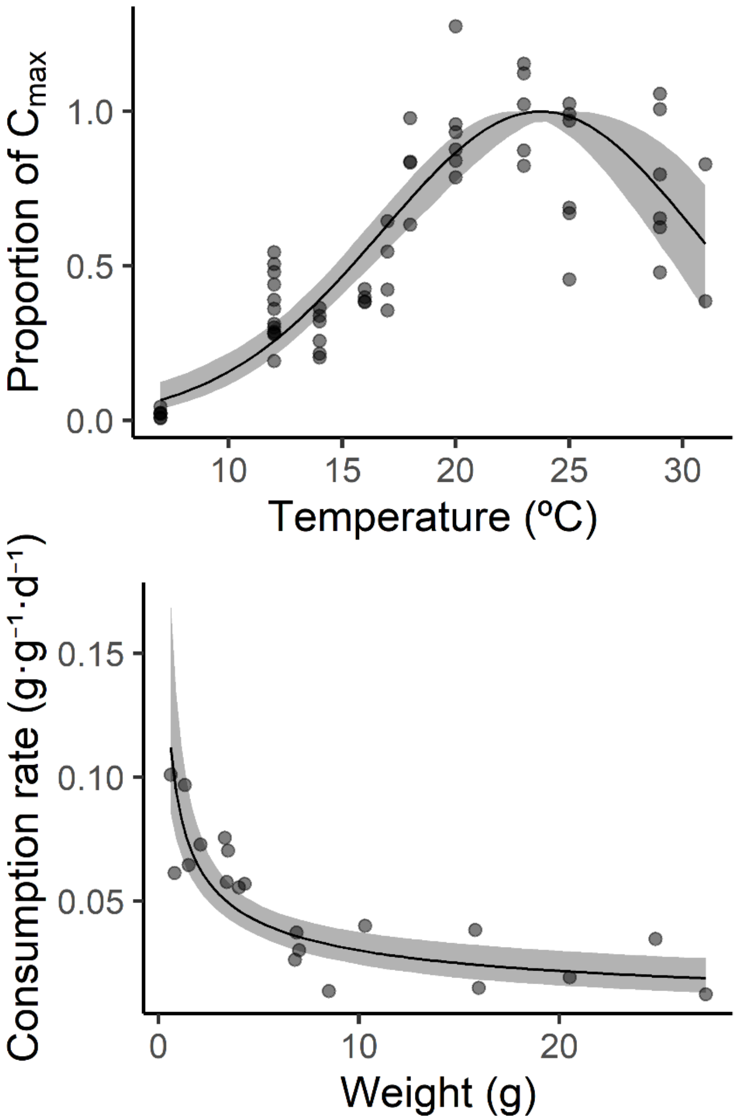

Figure 2. The response of weight- specific maximum consumption rate (C_{max}) to temperature (upper panel) and fish weight (lower panel). Each point represents an individual fish. Response to fish weight (lower panel) was tested at 23°C, the temperature at maximum consumption. The C_{max} experiments were stopped at 31°C due to high mortality rates (> 50%).

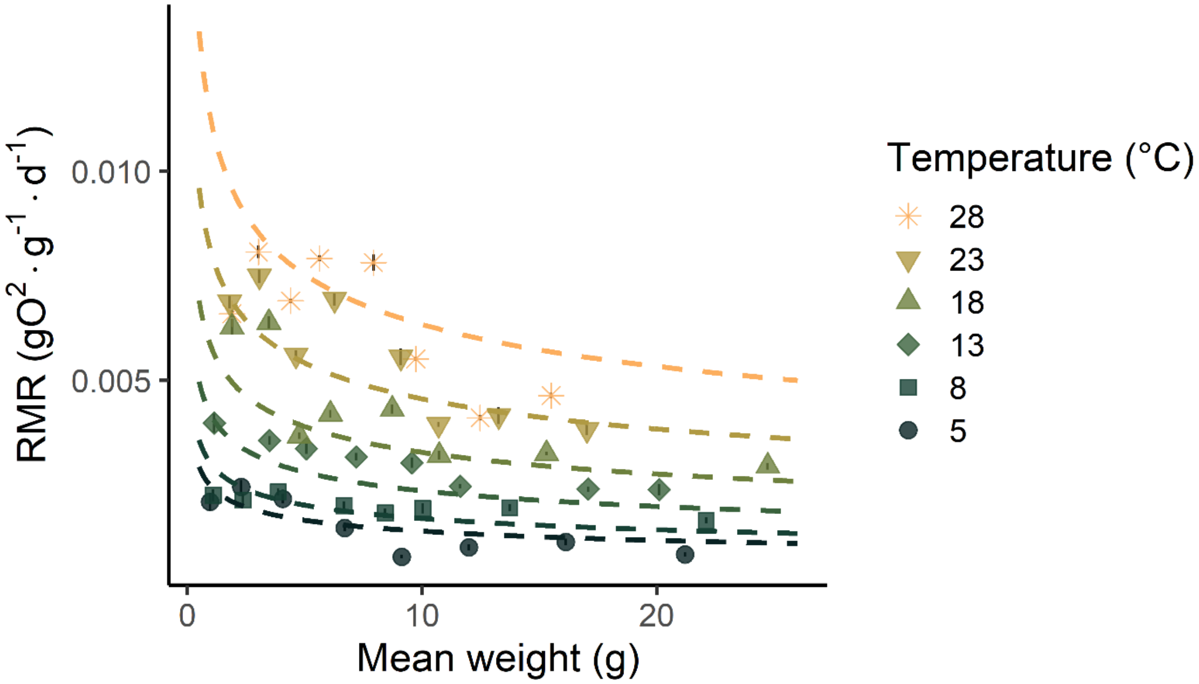

Figure 3. The response of routine metabolic rate (RMR) to temperature and fish weight. Each data point represents the average oxygen consumption across a group of three to four fish in a single respirometer and the mean weight of those fish.

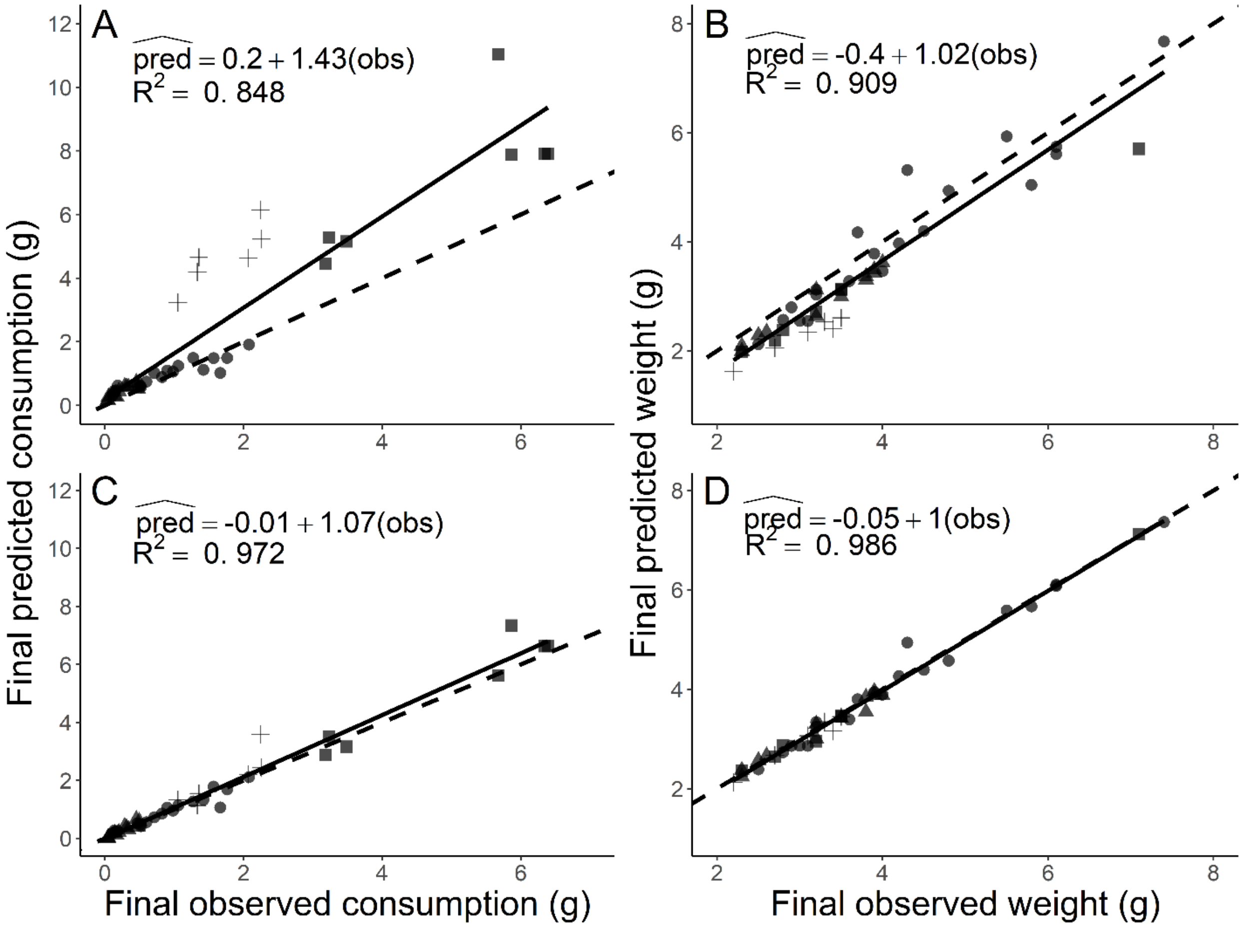

Figure 4. Predicted versus observed values for (A) uncorrected consumption, (B) uncorrected growth, (C) corrected consumption, and (D) corrected growth. Each point represents a single fish in each experimental treatment: pellet food with high ration (circles), pellet food with low ration (triangles), frozen *Mysis* with high ration (squares), and frozen *Mysis* with low ration (plus signs). In each panel, the solid line represents the linear regression and the dotted line represents the 1:1 line of correspondence between the observed and predicted values.

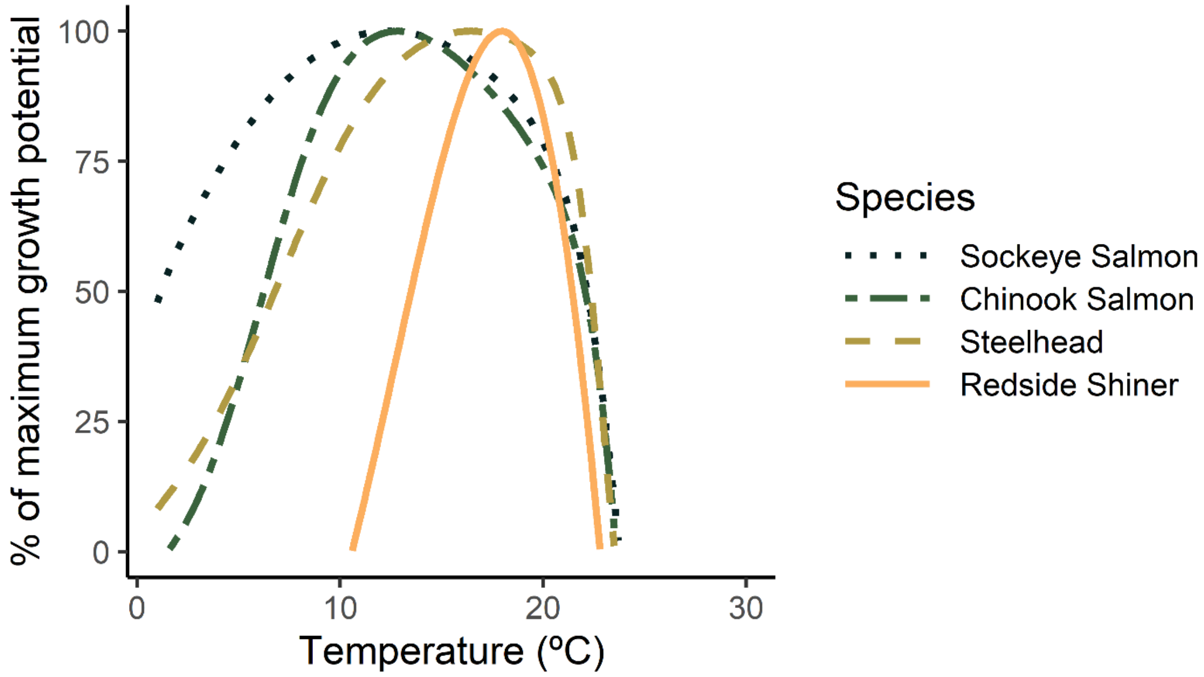

Figure 5. Relative growth potential as a function of temperature for Redside Shiner compared with Sockeye Salmon, Chinook Salmon, and steelhead. Bioenergetic simulations were modeled for 2- g fish of each species, assuming $\%C_{max}$ = 1 and a mean prey energy density of 3,500 J/g wet weight.

Appendix

Temperature-dependence function for consumption

The parameterized temperature-dependence function ($F(T)$) for Redside Shiner (*Richardsonius balteatus*) consumption based on Kitchell et al. (1977), which corresponds to model 2 in Fish Bioenergetics 4.0 (Deslauriers et al. 2017):

$$F(T) = V^{X} \times e^{X(1-V)} \qquad (A.1)$$

where:

$$V = \frac{191.7 - T}{191.7 - 23.7}$$

$$X = \frac{\{Z^{2} \times \left[\, 1 + \left(1 + \frac{40}{Y}\right)^{0.5} \right] \ {}^{2}\}}{400}$$

$$Y = log_{e}(3.97) \times (191.7 - 23.7 + 2)$$

$$Z = log_{e}(3.97) \times (191.7 - 23.7)$$

Routine Metabolic Rate (RMR) trial data

Table A.1. Total, mean, and standard deviation of Redside Shiner (*Richardsonius balteatus*) weights in each respirometer for the routine metabolic rate experiments.

Trial	Channel	Respirometer ID	Respirometer Volume (L)	Mean Temp (°C)	No. of Fish	Total Weight Fish (g)	Mean Weight Fish (g)	Std Dev
apr14	ch1	C	0.765	5.1	3	12.2	4.1	0.2
apr14	ch2	A	0.393	5.1	3	2.9	1.0	0.1
apr14	ch3	B	0.395	5.1	3	6.9	2.3	0.4
apr14	ch4	D	0.768	5.1	3	20.1	6.7	0.4
aug3	ch1	G	2.623	28.2	3	37.4	12.5	1.2
aug3	ch2	F	1.145	28.2	3	29.2	9.7	0.6
aug3	ch3	H	5.522	28.2	3	46.5	15.5	0.3
aug3	ch4	E	1.143	28.2	3	23.8	7.9	0.1
aug5	ch1	D	0.768	28.4	3	16.9	5.6	0.2
aug5	ch2	B	0.395	28.4	3	9.1	3.0	0.4
aug5	ch3	A	0.393	28.4	3	5.7	1.9	0.4
aug5	ch4	C	0.765	28.4	3	13.2	4.4	0.2
jul2	ch1	F	1.145	18.8	3	26.2	8.7	0.5
jul2	ch2	G	2.623	18.8	3	45.9	15.3	1.3
jul2	ch3	E	1.143	18.8	3	32.2	10.7	0.3
jul2	ch4	H	5.522	18.8	3	74.2	24.7	1.8
jun14	ch1	F	1.145	13.3	3	34.9	11.6	0.8
jun14	ch2	G	2.623	13.3	3	51.2	17.1	0.6
jun14	ch3	E	1.143	13.3	3	28.7	9.6	0.3
jun14	ch4	H	5.522	13.3	3	60.3	20.1	1.3
jun16	ch1	B	0.395	13.2	3	10.5	3.5	0.1
jun16	ch2	D	0.768	13.2	3	21.6	7.2	0.2
jun16	ch3	A	0.393	13.2	4	4.6	1.1	0.2

Trial	Channel	Respirometer ID	Respirometer Volume (L)	Mean Temp (°C)	No. of Fish	Total Weight Fish (g)	Mean Weight Fish (g)	Std Dev
jun16	ch4	C	0.765	13.2	3	15.2	5.1	0.2
jun22	ch1	B	0.395	23.0	3	9.2	3.1	0.3
jun22	ch2	D	0.768	23.0	3	18.8	6.3	0.1
jun22	ch3	A	0.393	23.0	3	5.4	1.8	0.4
jun22	ch4	C	0.765	23.0	3	13.9	4.6	0.2
jun24	ch1	F	1.145	23.1	3	32.1	10.7	0.8
jun24	ch2	G	2.623	23.1	3	39.8	13.3	1.6
jun24	ch3	E	1.143	23.1	3	27.3	9.1	0.0
jun24	ch4	H	5.522	23.1	3	51.1	17.0	0.6
jun9	ch1	B	0.395	18.2	3	10.4	3.5	0.2
jun9	ch2	D	0.768	18.2	3	18.3	6.1	0.2
jun9	ch3	A	0.393	18.2	3	5.7	1.9	0.3
jun9	ch4	C	0.765	18.2	3	14.3	4.8	0.3
may21	ch1	A	0.393	8.3	3	3.3	1.1	0.2
may21	ch2	C	0.765	8.3	3	11.6	3.9	0.2
may21	ch3	D	0.768	8.3	3	20.0	6.7	0.2
may21	ch4	B	0.395	8.3	3	7.1	2.4	0.1
may24	ch1	H	5.522	8.6	3	66.3	22.1	3.0
may24	ch2	E	1.143	8.6	3	25.3	8.4	0.2
may24	ch3	G	2.623	8.6	3	41.2	13.7	0.3
may24	ch4	F	1.145	8.6	3	30.1	10.0	0.7
may4	ch1	H	5.522	5.3	3	63.6	21.2	4.1
may4	ch2	E	1.143	5.3	3	27.4	9.1	0.6
may4	ch3	G	2.623	5.3	3	48.4	16.1	0.2
may4	ch4	F	1.145	5.3	3	36.0	12.0	1.4

Energy density and percent dry weight

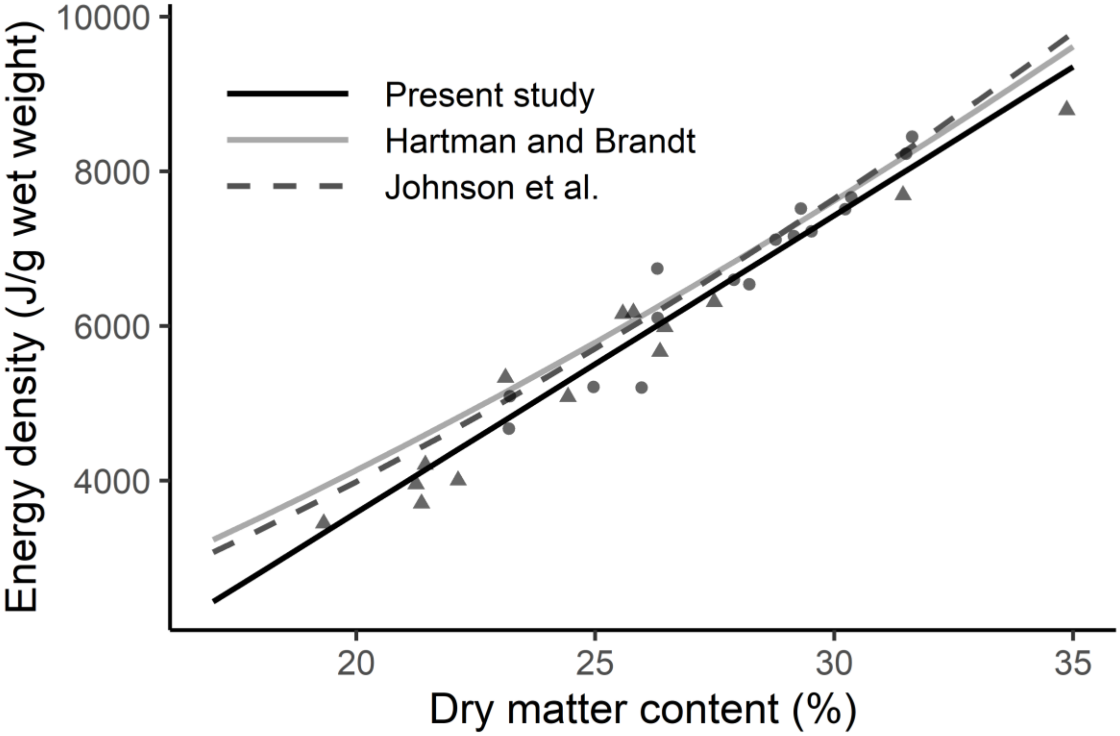

Figure A.1. Relationship between energy density (ED; J/g wet weight) and dry matter content (PDW; %) for wild Redside Shiner (*Richardsonius balteatus*) collected from Ross Lake, WA (triangles) and lab-reared Redside Shiner that originated from Ross Lake, WA (circles). Regression lines from the present study (ED = -4096.17 + 384.26 × PDW) are compared to the multi-species models developed in Hartman and Brandt (1995) ($ED = 45.29 \times PDW^{1.507}$), and Johnson et al. (2017) ($ED = 32.678 \times PDW^{1.604}$).

References

Deslauriers, D., S. R. Chipps, J. E. Breck, J. A. Rice, and C. P. Madenjian. 2017. Fish Bioenergetics 4.0: an R-based modeling application. Fisheries 42:586–596.

Hartman, K. J., and S. B. Brandt. 1995. Estimating energy density of fish. Transactions of the American Fisheries Society 124:347–355.

Johnson, B. M., W. M. Pate, and A. G. Hansen. 2017. Energy density and dry matter content in fish: new observations and an evaluation of some empirical models. Transactions of the American Fisheries Society 146:1262–1278.

Kitchell, J. F., D. J. Stewart, and D. Weininger. 1977. Applications of a bioenergetics model to Yellow Perch (*Perca flavescens*) and Walleye (*Stizostedion vitreum vitreum*). Journal of the Fisheries Research Board of Canada 34:1922–1935.

Chapter 2: Change in growth and prey utilization for a native salmonid following invasion by an omnivorous minnow in an oligotrophic reservoir

Abstract

Aquatic invasive species can affect food web structure and native fish growth and production, depending on the traits of the invasive species and the pre-invasion conditions of the ecosystem. An unauthorized introduction of redside shiner (*Richardsonius balteatus*) into reservoirs in the Upper Skagit River, Washington caused concern by managers that potential competition might decrease production and recruitment of rainbow trout (*Oncorhynchus mykiss*). We sought to quantify food web structure and function in Ross Lake, the largest of these reservoirs, to evaluate the growth environment and carrying capacity for native rainbow trout and determine the trophic role of the invasive fish. Bioenergetics modeling and stable isotope analysis were combined with field data to quantify consumption demand of native and invasive planktivores and relate consumption to the availability of key prey. We found low per capita consumption on *Daphnia* by redside shiner; however, they were the dominant consumers in Ross Lake due to their high density. Although monthly consumption demand by the planktivorous fish community was less than 50% of the monthly production and biomass of *Daphnia* in Ross Lake, the current *Daphnia* densities and growth of rainbow trout were considerably lower than during 1971-1974. These reductions correspond to lower annual consumption of *Daphnia*. Our study provides insight on mechanisms driving and constraining food web impacts of an invasive planktivore in cold water reservoirs. Climate change, water operations, and introductions of anadromous fishes into this system could act to amplify or otherwise modify the effects of redside shiner on shared prey, and our study provides necessary information to support related

management decisions and supplies important context for approaching similar issues in other regulated systems.

Introduction

Freshwater ecosystems are threatened globally and suffering from disproportionate biodiversity loss as they are subjected to many processes that degrade them and reduce their functionality and ecosystem services (Reid et al. 2019). Reservoir ecosystems are particularly vulnerable to impacts of climate change (Miranda et al. 2020), invasive species (Johnson et al. 2008), and increasing water demand and scarcity (Boretti and Rosa 2019). Reservoir ecosystems are artificial but can provide critical water storage and cold-water refuge for cool- and cold-water fish species under a warming climate. These systems often pose special management challenges associated with “hybrid” food webs, highlighting the need to incorporate food web research into management decisions in order to identify and maintain productive and resilient ecosystems (Naiman et al. 2012).

Aquatic invasive species can disrupt native food webs and trophic structure through a variety of direct and indirect pathways (Jackson et al. 2017). These impacts are often context-dependent, varying by characteristics such as the invader’s taxon and the ecosystem’s food web structure and resources (Thomsen et al. 2011). Quantitative studies are needed to understand the mechanisms by which these invader-driven food web alterations may affect native species at the individual level to give context to resulting changes observed at the population and community level. This knowledge is critical to choosing appropriate management actions for invasive species control, mitigation, or other restoration actions. For example, trophic overlap or separation can indicate different mechanisms at play: overlap could indicate exploitative competition in resource-poor environments or it can also be a result of abundant resources; similarly, trophic segregation can result from competitive exclusion from a preferred prey or adaptive. The impact of such trophic shifts on individuals thus depends on timing of availability and access to preferred and alternative prey. Knowledge of this trophic structure is needed within the context of resource availability, consumption demand, and observed growth to understand the resulting effects of invasive species on growth and survival of native species and the corresponding population-level effects.

Lakes and reservoirs experience different effects of invasive species compared to riverine habitats because thermal structure often drives fish habitat use in response to physiological constraints such as metabolism, stress, and growth potential (Magnuson et al. 1979). Thermal stratification can thus constrain suitable habitat availability (and access to prey) for cold- and cool-water species during the growing season. By contrast, invasive species with higher thermal optima benefit from greater access to abundant prey resources in the epilimnion (Tunney et al. 2012) or refuge from cool- and cold-water predatory fish in thermally-stratified waterbodies. Further, changes to seasonal thermal structure due to a warming climate (Woolway et al. 2021) is altering spatial and temporal habitat availability which could lead to cascading effects throughout the food web by modifying habitat overlap and species interactions (Ficke et al. 2007). For reservoirs in particular, it is important to evaluate these thermally-driven interactions within the context of how climate conditions and water operations, both present and future, may interact to influence the timing, magnitude, and vertical structure of thermal stratification (Moreno-Ostos et al. 2008; Feldbauer et al. 2020).

Redside shiner (*Richardsonius balteatus*), a small-bodied minnow, have invaded numerous mid- and high-elevation lakes and reservoirs and have been associated with declines in salmonid growth rates, inspiring some managers to seek eradication methods (Messner and Schoby 2019; Smith et al. 2021). Negative interactions between redside shiner and rainbow trout (*Oncorhynchus mykiss*) have been well studied in a series of Canadian lakes, with declines in growth and production of rainbow trout following introductions of redside shiner (Lindsey 1950; Larkin and Smith 1954; Johannes and Larkin 1961). Additionally, redside shiner have a higher thermal optimum than salmonid species – a potential advantage under warming conditions (Johnson et al. 2023). However, effects of redside shiner invasions on prey resources have been varied (Johannes and Larkin 1961) and this species coexists naturally in salmonid-dominated systems throughout the western United States, leaving in question the mechanisms by which this species can affect native salmonids in invaded systems and the conditions which allow it. In Washington's North Cascades, an unauthorized (likely through baitfish, Rahel and Smith 2018) introduction of redside shiner in Ross Lake in the early 2000s quickly flourished and spread to downstream Diablo Lake, concerning managers about potential impacts to native juvenile salmonids that may be competing for resources in these reservoirs. Although analysis of redside shiner stomach contents in Ross Lake have shown potential diet overlap with native juvenile salmonids in this system (Welch 2012), it is unknown whether redside shiner limit growth and survival of juvenile salmonids through resource competition or other means.

The goal of our study is to understand the role an invasive omnivore plays in driving prey supply and the growth environment for a native species in a mid-elevation reservoir ecosystem. Using Ross and Diablo Lakes as a study system, our specific objectives were to 1) quantify seasonal prey availability and seasonal consumption by native (rainbow trout) and nonnative (redside shiner) planktivores in the reservoir, and 2) compare seasonal prey availability and consumption demand to evaluate whether prey supply is a limiting factor for rainbow trout in the reservoirs. We leveraged historical growth and diet data for rainbow trout in the reservoir collected in the 1970s (pre-invasion) to compare annual energy budgets and evaluate any changes to rainbow trout growth and energy acquisition between the two studies. These processes were examined within the context of seasonal thermal stratification and the associated constraints on habitat access and availability within the reservoirs.

Methods

Study system

Ross Lake is the largest and deepest of the three reservoirs impounded by hydroelectric projects in the upper Skagit River, WA (elevation at full pool = 489 m above sea level, storage at full pool = 1.78 km^3, max depth = 116 m, mean depth = 37 m), extending northward from Ross Dam for approximately 37 km, just beyond the border with British Columbia at full pool (Fig. 1). Ross Lake is ultraoligotrophic (TDP < 2 µg/L), generally clear (Turbidity < 1.0 NTU) and shows strong thermal stratification from around June until October when the thermocline deepens and begins to destratify. Peak summer surface temperatures are 18-22 °C, depending on the year and region of the lake (Fig. 2). In addition to the seasonal thermal changes, Ross Lake is drawn down between 16-25 m every year during the fall and winter before refilling in the spring, and drawdowns in recent years have reached 40 m for maintenance purposes (Fig. S1). Native fish species include rainbow trout *Oncorhynchus mykiss*, bull trout *Salvelinus confluentus*, and Dolly Varden *S. malma*. Nonnative species include eastern brook trout *S. fontinalis* (introduced in early 1900s), cutthroat trout *O. clarkii* (introduced in early or mid-1900s), and redside shiner *Richardonius balteatus* (introduced ca. 2000). Rainbow trout spawn in tributaries in the spring

(May-June), emerge in the late summer, and most recruit to Ross Lake around age 2-3. Char spawn in streams during fall and also recruit to the reservoir at ages 2 and older, whereas redside shiner spawn during summer and complete their life cycle within the lake.

Fish collection

From 2019-2021, fish were collected in spring, summer, and fall using sinking multi-mesh gill nets set in three approximate depth strata corresponding to the epilimnion (0-10 m), metalimnion (10-20 m), and hypolimnion (20-30 m; Beauchamp et al. 2007a). Limitations to fish sampling in 2019 and 2020 due to limited-take permitting for threatened species and COVID-19 restrictions resulted in low sample sizes or missing samples for some species/size class/season combinations, so data were pooled across all years. Angling was conducted opportunistically to increase sample sizes and minimize mortality risk to bull trout, which are listed as threatened under the Endangered Species Act.

Fish to be released were held in a live well with aerators, anesthetized with buffered MS-222 prior to processing, allowed to recover in the live well, and released. All fish were measured for fork length (mm), weight (0.1 g), and tissues were collected: fin tissue (for stable isotopes), and scale samples (plus otoliths from mortalities). Stomach contents from fish were collected using gastric lavage, with contents filtered into a 500-ug sieve and immediately placed on ice.

Size structure, abundance, mortality

We used hydroacoustic surveys of the nearshore and slope zones in October 2021 to estimate a total abundance of approximately 12 million redside shiner > 40 mm FL in Ross Lake (Table S1; details provided in the Supplementary Methods). Population abundances of the salmonid species are not well studied in this system and not conducive to hydroacoustic techniques, thus we analyzed dietary consumption in Ross Lake based on size structured unit populations of 1,000 fish > 200 mm FL (the modal size for recruitment of adfluvial salmonids to the reservoir was approximated at 200 mm FL) as well as an estimated population of 3,000 bull trout. This estimated population size was generated from recent snorkel survey counts in the upper Skagit River in British Columbia assuming that the surveyed area represented 40% of the high quality spawning habitat accessible from Ross Lake (Seattle City Light 2012; Foster 2020). This approach allows managers to easily scale the resulting consumption estimates up or down to evaluate different predation scenarios based on alternative population estimates and uncertainty (Beauchamp et al. 2007b). From the unit population of bull trout, we used relative catch frequencies from the gill net sampling in 2018-2021 to estimate the relative abundance of the other salmonid species indexed to bull trout (Table 1).

We created age-structured populations for each species using annual survival rates (S) to allocate these total population abundances to each age-class for each species. We used previously reported S for redside shiner in Ross Lake (Welch 2012), and used weighted catch curve analysis on gillnet monitoring data from 2006-2018 (collected and maintained by North Cascades National Park) to estimate S for the salmonids. We used these data to estimate annual instantaneous mortality rates (Z) and annual survival rates (S) for each species (Table 1; Miranda and Bettoli 2007). We then created estimates of daily age-class abundance for an annual cycle by applying the daily instantaneous mortality rate (Z/365) to the initial age-class abundance estimate.

Prey availability

We conducted vertical zooplankton tows (net: 30 cm diameter, 90 cm length, 150 µm mesh) seasonally in 2019 (June, July, October) and monthly during 2021 (May-October) at two stations in Ross Lake (Fig. 1) to assess pelagic prey availability. Tows sampled two depth bins, 20-0 m and 10-0 m depth intervals, with two replicate tows for each depth interval. These depth bins were selected to correspond to the epilimnion and metalimnion so that we could quantify depth-specific prey availability and compare to depth-distribution of planktivores during thermal stratification (e.g., Sorel et al. 2016a). After rinsing from the net and cod end, zooplankton were stored in ethanol. Additional horizontal tows were conducted to collect zooplankton samples for stable isotope analysis.

In the lab, zooplankton samples were concentrated, and crustacean taxa and eggs were enumerated in 3-5 individual 5-mL aliquots for each sample. Cladocerans were identified to genus and all others identified to order. Preservation methods tend to expel eggs from cladoceran carapaces, making it challenging to identify loose eggs and obtain accurate egg counts when multiple taxa coexist in a sample. To address this issue, we proportionally applied loose cladoceran eggs to *Daphnia* based on relative frequency of adult cladoceran taxa in the sample. The first 50 *Daphnia* encountered in each sample were measured using Image Pro Premier digital image-analysis software (version 10; Media Cybernetics) for body length (BL; mm) from the top of the helmet to the base of the tail spine. BL was converted to wet weight (W; µg) with the following equations which estimates dry weight (DW; µg) from pooled *Daphnia* species (Dumont et al. 1975), and then converted from dry weight using a percent dry weight value of 10% (Luecke and Brandt 1993):

$$DW_{\mu g} = 1.5 \times 10^{-5} \times BL^{2.84} \qquad (1)$$

$$W_{\mu g} = DW_{\mu g} \times 10 \qquad (2)$$

Daphnia density (individuals/L) was calculated as an average between replicate samples for each sampling date, depth strata, and site. Areal density for each site and date (individuals/m^2) was also calculated from volumetric density sampled in the 0-20 m depth strata, assuming that negligible densities of exploitable zooplankton were present below 20 m depth, to compare to historical estimates of zooplankton density (1971-1973, Seattle City Light 1974). Standing stock biomass was estimated for each sampling date by multiplying the mean individual wet weight by densities. Production rates were estimated with the egg-ratio method (Paloheimo 1974; details available in the Supplemental Methods).

Pelagic volume was used to expand biomass and production to total lake-wide estimates. Pelagic volume was estimated in Ross Lake using surface area estimates at 1 ft (0.3 m) contours derived from the 2018 drawdown DEM (provided by Seattle City Light). For each lake surface elevation specific to the date of sampling, we estimated volume of the pelagic epilimnion by multiplying the surface area of the 10 m (33 ft) depth contour by 10, and volume of the metalimnion as the surface area of the 20 m (66 ft) depth contour by 10. For each sampling date, whole-lake biomass and production were estimated for each depth range sampled (0-10 m and 0-20 m), averaged between the two sites, and estimates for the metalimnion (10-20 m) were calculated by subtracting lake-wide estimates for 0-10 m from those of 0-20 m.

Stable isotope analysis

Stable isotope analysis was conducted on fish fin tissue and whole bodies of zooplankton and assorted benthic invertebrates (tissue removed from shells) to map the lake's food web and to complement stomach content analysis. We aimed to analyze fin tissue from 5-10 fish of each species in each size class (100 mm FL increments for salmonids, 50 mm FL for redside shiners) during the summer; however, samples from other years and seasons were combined if sample sizes were not sufficient. Most fish and zooplankton samples were collected in 2019, whereas all other invertebrate samples were collected in the fall of 2021. Other invertebrate herbivores and omnivores were collected for stable isotope analysis to provide representative samples for primary pelagic and benthic consumers in the food web.

All the fish consumer and invertebrate samples were measured for δ^{15}N and δ^{13}C by the University of Washington IsoLab using a ThermoFinnigan MAT253 isotope ratio mass spectrometer and Costech elemental analyzer or by the University of Washington Facility for Compound-Specific Isotope Analysis of Environmental Samples using a Thermo Scientific Delta V isotope ratio mass spectrometer and a CE elemental analyzer. Both labs referenced samples to 2 glutamic acid standards and Bristol Bay sockeye salmon. Stable isotope ratios are reported using delta (δ) notation in permil units (‰) compared to Vienna Pee Dee Belemite for C and air for N. Isotopic values of fish consumers were compared among size classes within each lake using nonparametric Kruskal-Wallis and Dunn's multiple comparison test to evaluate ontogenetic differences in diet and guide how we pooled isotope and diet data across size classes within a species.

We implemented Bayesian stable isotope mixing models (SIMMs) using the MixSIAR package in R (Stock et al. 2018) to estimate diet proportions from stable isotope signatures (details available in the Supplemental Methods). These estimates of diet proportions integrate over longer periods and thus complement the finer-scale taxonomic resolution and short-term (e.g., within the previous ~24 h) diet proportions estimated from stomach content analysis. In each season, species were pooled within size classes according to multiple comparison test results described above. Most tissue samples analyzed were collected in the summer (most during gillnet surveys in late July), with some also collected in the fall (early October). Enough data existed to model SIMMs with season as a fixed factor for rainbow trout 300-399 mm FL and redside shiner 100+. Support for a seasonal model to describe diet proportions was evaluated using leave-one-out cross-validation (LOO).

Bioenergetic model inputs

Bioenergetics models are energy-balance equations that partition energy intake (i.e., food) into waste, metabolism, and growth, while accounting for their relationships with temperature and body size. Thus, using measurements of observed growth, these models can be used to predict total consumption on a daily timestep in addition to an estimate of feeding rate (as a proportion of maximum consumption, C_{max}). The required inputs for these models, described in detail below, include observed growth (initial and final weights) and energy density of the consumer, spawning losses, thermal experience, seasonal diet composition, and prey energy density.

Depth-use and thermal experience

Vertical temperature profiles were conducted monthly at two stations in Ross Lake (Fig. 1) to measure the thermal structure from spring through fall. These data were supplemented by Seattle City Light temperature loggers in Ross Lake forebays for winter and early spring, and profiles collected by the National Park Service from 2010-2018 to generate estimates of average temperatures across this time span. Temperatures from discrete dates and depths were linearly interpolated in both dimensions to generate a symmetric grid of temperatures for computing mean temperatures across layers (epi-, meta-, and hypolimnion) and through time. For simplicity in bioenergetics simulations, we only used temperature data from the southern of the two limnological sites to estimate thermal experience.

Thermal experience was determined using patterns in depth distribution observed from gillnet catch data (rainbow trout) and hydroacoustic surveys (redside shiner). Due to permitting restrictions on gill netting effort, depth distribution of rainbow trout was evaluated at 2 sites in Ross Lake only during 2021, when the southern region was sampled seasonally but the northern site was only sampled during summer. Thermal experience for rainbow trout was assigned by temperature-based rules developed from these depth distribution patterns (Fig. S2) and general knowledge about the species thermal requirements. If the mean temperature in the epilimnion was ≤ 18 °C, rainbow trout were assumed to be entirely within this layer, and the average epilimnion temperature was used. If the mean temperature in the epilimnion was > 18 °C, we applied a weighted average temperature assuming that 75% of rainbow trout were in the metalimnion and 25% in the epilimnion. We assumed that 80% of redside shiner occupied the epilimnion and 20% occupied the metalimnion during the growing season (Fig. S3). Daily temperatures were averaged across each layer and weighted-average temperatures calculated based on proportion of fish assumed to occupy each depth layer (Table S4).

Diet composition and prey energy density

We analyzed diets from rainbow trout but relied on previously published diet information for redside shiner in Ross Lake (Welch 2012) supplemented by stable isotope analysis. Stomach contents were identified using a dissecting microscope and sorted into functional taxonomic groups. Blotted wet weights (0.0001 g) were recorded for each taxonomic group identified and pooled across key functional groups of prey. Wet weights were converted into proportions, which were then averaged within species, size-class, and season sampling blocks. Diet data were pooled across size-classes where stable isotope values were not significantly different. Prey energy densities were estimated using bomb calorimetry for fish prey and taken from the literature for all other prey groups (Table S5).

Diet proportions evaluated from Bayesian stable isotope mixing models (SIMMs) were compared to diet proportions from stomach content analysis assuming that stable isotope signatures from fin tissue incorporated diets from approximately the previous 1-3 months. This approximation was used for simplicity and loosely guided by isotopic half-life predictions ranging from 38 days for a 5 g fish to 73 days for a 100 g fish (Eq. 2 in Vander Zanden et al. 2015). Thus, SIMMs from summer collected samples were compared to spring stomach contents, and SIMMs from fall collected samples were compared to summer stomach contents. Details on how SIMMs (Figs. S4-S8) were incorporated with stomach content analysis (Tables S6-S7), ecological assumptions made to fill in seasonal diets where data did not exist, and the final diet inputs used in the bioenergetics simulations (Table S8) can be found in the Supplemental Methods.

Age, growth, and energy density

For each species, scales were imaged, measuring circuli and annuli using Image Pro Premier software. When necessary and available, we corroborated scale-based ages and annuli markings with otoliths. Geometric mean regression (GMR) was used to evaluate the relationship between fish fork length (FL) and scale radius (SR) to avoid biased estimates from either of the ordinary regressions of FL~SR or SR~FL (Ricker 1992). Scale data were pooled across sites within each species. The Fraser-Lee proportional method (Isley and Grabowski 2007) was used to back-calculate fish FL at each annulus using the following equation:

$$FL_i = \frac{SR_i}{SR_{cap}} \times \left(FL_{cap} - a\right) + a \qquad (3)$$

where FL_i is the back-calculated fork length (mm) at a given annulus, SR_i is the scale radius at that annulus, SR_{cap} is the scale radius (mm) at capture, FL_{cap} is the fork length (mm) at capture, and a is the intercept from the GMR lines (rainbow trout: $FL = 42.894 + 155.501 \times SR$, R^2=0.774; redside shiner: $FL = 10.599 + 68.114 \times SR$, R^2=0.884). Back-calculated FLs were converted to wet weight using wet weight-FL regressions (rainbow trout: $WT = 1.27 \times 10^{-5} \times FL^{2.961}$, N = 1917, R^2= 0.996; redside shiner: $WT = 7.48 \times 10^{-6} \times FL^{3.119}$, N = 90, R^2= 0.973).

Energy density (J/g wet weight) of consumers was estimated using bomb calorimetry (Parr model 6725 semi-micro bomb calorimeter) for a subset of whole bodies collected across seasons in Ross Lake (rainbow trout: N = 27, FL = 148-492 mm, W = 33-989 g; redside shiners: N = 46, FL = 37-125 mm, W = 0.4-29.1 g). We evaluated the relationship between energy density and body weight of the consumers within each species and set energy density inputs for the bioenergetics simulations depending on the initial and final weights for each age-class (Table 2).

In the simulations, spawning was represented as a loss in weight occurring on a single day. We assumed that redside shiner lost approximately 11% body weight during spawning, which was based on samples collected in Ross Lake in June. We assumed that the mean spawning time occurred on July 1 (day 61 of the simulation), that this species matures at age 2, and spawns every year (Smith et al. 2021). For rainbow trout, we assumed that fish ≥ age 3 lost 8% body weight during spawning (Juncos et al. 2013) which occurred in mid-June (day 45 of the simulation).

Consumption demand and carrying capacity

Fish Bioenergetics 4.0 (Deslauriers et al. 2017) was used to run the simulations parameterized for rainbow trout (Rand et al. 1993) and redside shiner (Johnson et al. 2023) to estimate daily, seasonal, and annual consumption demand (g of each prey category). We fit the model to annual growth starting at the beginning of the growing season, May 1 (Woodin 1974), using average back-calculated weight at annulus as the initial and final weights (g). Per capita consumption for each age-class of each consumer was expanded to the population level by multiplying individual consumption by the daily age-class abundance. *Daphnia* weigh about 50% less and contain about 50% less water in diet samples than they do fresh (Luecke and Brandt 1993; Stockwell et al. 1999); therefore, simulated consumption of *Daphnia* (g) was multiplied by

2 to estimate the fresh weight consumed for direct comparison to biomass and production estimates.

Historical data from rainbow trout were used to run comparable simulations using the same methods described above to evaluate any changes in the growth environment and energy budgets, using back-calculated size at age in 1970-1972 (Woodin 1974), vertical temperature profiles from a site near Devil’s Creek (approximately 6 km upstream of the southern limnological station) from Jun 1970-Sep 1974 (Seattle City Light unpublished data), and monthly size-based diet composition from May-Oct 1970 (Seattle City Light 1972). Historical back-calculated size at age was adjusted by adding 1 year to each annulus to appropriately compare to our back-calculation data. Sampling of tributary fish and scales during this study led us to conclude that the size at age 1 reported in Woodin (1974) was too large, and we believe that the first annulus was not counted in these data.

Monthly consumption demand was compared to *Daphnia* production and standing stock biomass to evaluate the carrying capacity of the reservoirs and food limitation. *Daphnia* were the dominant zooplankton in rainbow trout diets and were thus determined to be the primary driver of food limitation for rainbow trout in the reservoirs. Previous work in other reservoir systems have shown that rainbow trout consumption (% C_{max}) was directly related to *Daphnia* biomass (Tabor et al. 1996), further supporting our use of this metric to evaluate feeding conditions. We evaluated consumption demand versus *Daphnia* availability for the whole water column (0-20 m depth) in addition to a depth-use scenario to determine whether thermally driven behavior may be limiting access to food supplies. For this depth-use scenario, we estimated consumption demand versus prey availability separately for the epilimnion (0-10 m) and the metalimnion (10-20 m) in

Ross Lake, assuming that salmonids would be restricted to the metalimnion during peak stratification. We divided redside shiner consumption evenly between the two layers and restricted all rainbow trout consumption to the metalimnion during the growing season to estimate depth-specific consumption demand versus *Daphnia* production.

Results

Stable isotope analysis (and food web structure)

Ross Lake rainbow trout exhibited ontogenetic shifts in stable isotope signature and trophic position (Fig. 3; Supplement Tables S9 and S10). Smaller rainbow trout (100-199 mm FL) began at a moderate position along the benthic-pelagic axis and a low trophic position (N = 5; mean ± SE: $\delta^{15}N$ = 7.2 ± 0.1, $\delta^{13}C$ =-26.7 ± 0.8) and then shifted to more pelagic prey as they increased to 200-299 mm FL (N = 10; mean ± SE: $\delta^{15}N$ = 7.7 ± 0.2, $\delta^{13}C$ =-28.0 ± 0.3). They increased trophic position in the transition size of 300-399 mm FL (N = 26; mean ± SE: $\delta^{15}N$ = 9.2 ± 0.1, $\delta^{13}C$ =-27.1 ± 0.2) before stabilizing at a top trophic position upon reaching 400+ mm FL (N = 9; mean ± SE: $\delta^{15}N$ = 9.8 ± 0.2, $\delta^{13}C$ =-25.9 ± 0.3). Redside shiner in Ross Lake exhibited stable isotope signatures similar to smaller rainbow trout (N = 23; mean ± SE: $\delta^{15}N$ = 7.2 ± 0.1, $\delta^{13}C$ =-25.7 ± 0.4), without significant differences in isotopic signature between size classes.

Diet composition

Diet proportions estimated from SIMMs tended to estimate higher contributions of fish prey for smaller rainbow trout (<300 mm FL) and all redside shiner in Ross Lake compared to stomach contents (Table S7). Due to gape limitations and prey access, we attributed this to predation on redside shiner eggs and larvae, which would have a much higher rate of digestion and thus a lower probability of detection in stomach contents (Legler et al. 2010), especially for fish collected in gill nets and minnow traps that were set for an extended amount of time. Alternatively, predation on eggs and larvae could be episodic, corresponding with spawn and emergence timing, making it difficult to detect in stomach contents. Therefore, we relied on SIMMs to inform the contribution of fish prey for these groups for the spring-summer interval and adjusted the other prey groups accordingly for bioenergetics simulations.

Diet proportions estimated from SIMMs generally aligned well for rainbow trout ≥ 300 mm FL in Ross Lake, except for the allocation between benthos/insects and zooplankton in spring for 300-399 mm FL fish (Table S7). Diet proportions in spring for this size class showed heavy reliance on immature insects (Table S6), and the benthic production fueling these insects could have been pelagically-derived due to a combination of steep-walled bathymetry of the lake and interruptions to spring benthic production due to winter drawdowns via hydroelectric operations. We were unable to collect immature insects in the spring preventing us from evaluating potential seasonal differences in their stable isotope signatures. Therefore, we relied on stomach contents to inform the diet inputs used in the bioenergetics simulation for this season and size class.

***Daphnia* availability**

Monthly zooplankton samples were only collected during 2021, thus our ability to statistically compare *Daphnia* densities across years was limited. However, densities and seasonal trends seemed similar among years, characterized by low availability of edible-sized *Daphnia* ≥ 1 mm BL (< 1 individual/L; Fig. 4). *Daphnia* densities peaked in the spring (May or June) at the south site, while densities in the north site were highest in October 2021. Densities were generally lower in the metalimnion (10-20 m) than in the epilimnion, though this was not always the case. Areal densities (individuals/m^2) recorded during the current study are lower than observed in 1971-1973 in most months (Fig. S9). Mean *Daphnia* body lengths were ≥ 1 mm in all months (Fig. S10).

Rainbow trout growth

Rainbow trout in Ross Lake grew at the highest rate between annuli 2-3 and 3-4, corresponding to lake recruitment (Fig. 5). Rainbow trout in our study grew slower than fish sampled in 1971-73 at ages 2-4, but then began outgrowing fish from the earlier period, especially in terms of weight and body condition, at age 5 (mean initial FL: 338 mm), when fish became the dominant prey source (Fig. 5B).

Consumption demand versus prey availability

Rainbow trout in Ross Lake fed at low rates and generally exhibited low growth efficiency (31-36 %C_{max}; 4-10% GE; Table 2). Rainbow trout consumption was highest in the spring and summer (Apr-Jun, Jul-Sep) and lowest in the winter (Fig. S11). In Ross Lake, zooplankton was most important as prey during the growing season for rainbow trout 200-299 mm FL. Rainbow trout smaller than this (100-199 mm FL) consumed more insects and benthos during the spring and summer, potentially indicating differing habitat usage. Rainbow trout in the larger size classes progressively increased their reliance on fish prey, primarily identified in the diet samples as redside shiner. Trout 300-399 mm FL represented this transitional size, as evidenced in the stable isotope data (Fig. 3), and fish > 400 mm FL were consistently piscivorous.

Redside shiner fed at high rates but also experienced poor growth efficiency (112-122 %C_{max}; 8-10%; Table 2). Consumption peaked in the summer and was 4x higher than spring and nearly 3x higher than fall consumption (Fig. S11). Summer was the primary growing season for redside shiner in this system due to their higher and relatively narrow band of optimal growth temperatures (Johnson et al. 2023). Redside shiner consumed a mix of zooplankton, insects, and benthos across all seasons and fish (eggs/larvae) in the spring/summer. While zooplankton represented the highest proportion of their diets in the fall, total biomass of zooplankton consumed was highest in the summer.

Rainbow trout ate more *Daphnia* than did redside shiner on a per capita basis (Table 2); however, due to large differences in population size, the redside shiner population consumed the vast majority of *Daphnia* in Ross Lake. With an estimated population of around 12 million redside shiner > 40 mm FL, monthly population consumption of *Daphnia* by redside shiner ranged from 78-96% of the population consumption by salmonid and redside shiner combined.

Lake-wide *Daphnia* production and biomass in Ross Lake was lowest in May and peaked in August before a large decline in September (Fig. 6). Combined population consumption followed a similar trend, though consumption rates peaked in September before slightly declining in October. Consumption demand accounted for less than half of the lake-wide *Daphnia* production in all months except September, when *Daphnia* was most limited and consumption accounted for 48% of production, and 28% of total production + biomass. When evaluating depth-specific *Daphnia* supply versus demand, prey resources in the metalimnion were most limited in June and September, when consumption demand accounted for 49% and 43% of *Daphnia* production, respectively.

Comparisons of historical energy budgets to those in this current study suggest that rainbow trout are not feeding as effectively as they did in 1971-73. Rainbow trout in the current study were smaller at annuli 2-5 and these lower growth rates were accompanied by lower total annual energy budgets compared to rainbow trout sampled in the 1970s (Fig. 7). The annual energy budget declined for nearly all prey categories, though this decline was largest for *Daphnia*. Lower contribution of *Daphnia* in the energy budgets of rainbow trout also coincided with lower *Daphnia* abundance (density per m2) measured in the current study compared to the 1970s (Fig. S9). Despite the addition of redside shiner to the energy budget for larger rainbow trout in the current study, the energetic contribution of this new prey source was not great enough to overcome the decline in the other prey categories.

Discussion

Our quantitative food web analysis highlighted the dominant role that the invasive redside shiner play as a zooplankton consumer in Ross Lake. Although the planktivorous fish community consumed less than 50% of the monthly production and biomass of *Daphnia*, the current densities of *Daphnia* were considerably lower than during 1971-1974. Rainbow trout in the current study experienced lower contributions of *Daphnia* to their annual energy budget and lower growth rates compared to the 1970s.These comparisons suggest that foraging success by rainbow trout has declined, especially for smaller rainbow trout feeding on *Daphnia*. Thus, for rainbow trout, growth and foraging performance may be more sensitive to reduced prey density than could be inferred simply by cruder measures of available prey supply. These findings support hypotheses regarding the role of redside shiner as a resource competitor limiting growth of rainbow trout (Larkin and Smith 1954; Johannes and Larkin 1961).

Areal densities of *Daphnia* (#/m^2) were substantially higher in 1971-1973 than in 2019-2021 in multiple regions of the lake throughout the summer, supporting the hypothesis that density is currently too low for rainbow trout to feed as effectively. However, differences in sample collection depths between the studies confound this comparison of densities across time. We only collected zooplankton from 20 m to the surface, and we assumed zero individuals below 20 m; thus, if habitat occupancy extended below 20 m depth, our reported areal densities would be underestimated and the reported difference between the two studies would be inflated. However, even if we extend our observed densities down to 50 m depth (rather than the 20 m we sampled), this still results in lower areal densities than observed in 1971-1973 summers; therefore, it is probable that *Daphnia* densities are lower now than they were historically, though the true magnitude of the difference is unknown.

This trend in *Daphnia* density could be the result of individual or combined effects from numerous environmental factors. One hypothesis is that increased consumption demand by redside shiner following their introduction could be suppressing population growth of *Daphnia* and maintaining them at a lower abundance. Alternatively, decreased *Daphnia* abundance could be due to nutrient limitation and decreases in productivity as the reservoir has aged; however, the largest productivity decline would likely have occurred in the first decade following inundation during the 1950s (Ney 1996).

Comparison of thermal structure in current years compared to the 1971-73 (Fig. S12) indicates that rainbow trout may be thermally excluded from the epilimnion for more of the growing season under current conditions, which could also be limiting their access to *Daphnia*. Densities in the metalimnion (10-20 m depth) were similar to or greater than in the epilimnion (0-

10 m depth) in July and September at the northern site, and in June, August, and September at the southern site, thus thermal exclusion is unlikely to limit rainbow trout consumption during these months. However, lower *Daphnia* densities in the metalimnion could exacerbate the existing limitation of low lake-wide *Daphnia* densities during July in the south and during August in the north.

Decreased *Daphnia* consumption by rainbow trout in Ross Lake could also result from predator-induced changes to habitat selection and behavior of the trout. Predation pressure on juvenile rainbow trout may be higher now compared to the 1970s, as bull trout abundance in the upper Skagit River in British Columbia, and presumably in Ross Lake as well, has increased since the introduction of redside shiner (Foster 2020), and larger rainbow trout are now piscivorous. Small rainbow trout in lakes and reservoirs commonly seek predation refuge in nearshore habitats, which would limit their access to *Daphnia*, which are concentrated in the pelagic zone (Tabor and Wurtsbaugh 1991). Supporting this hypothesis, we found that benthos contributed to a larger fraction of the energy budget for age 2 fish and this decreased with age in the current study, while in the 1970s, benthos contributed the least to age 2 energy budgets then increased with age.

Rainbow trout growth and consumption in other reservoirs has been tightly linked with Daphnia biomass per unit volume (Tabor et al. 1996), aligning with our findings in Ross Lake. These pelagic resources play a particularly important role in reservoirs compared to natural lakes as reservoir water level fluctuations can disrupt benthic productivity depending on the timing and extent of water drawdown (Hansen et al. 2018; Trottier et al. 2019). Previous studies in Ross Lake have shown low standing crop of benthic invertebrates in the drawdown zone (Seattle City

Light 1972). The contributions of immature insects and other benthos to the energy budget of rainbow trout in the current study were also lower than in the 1970s indicating that these prey resources are also currently limited. Benthos and immature insects are also major components of the redside shiner diet, thus the increased consumption demand could be putting further pressure on these already limited benthic resources.

Redside shiner were apparently not food limited in Ross Lake, despite low *Daphnia* densities that affected rainbow trout feeding, thus they may be able to limit rainbow trout in resource poor systems. Part of this ability to withstand low *Daphnia* densities be result from their relatively lower metabolic activity, growth rates, and food requirements. It is also possible that they can feed more effectively than trout at low prey densities. Observations from enclosure experiments supported this hypothesis; redside shiner fed more efficiently on *Gammarus* than rainbow trout (Johannes and Larkin 1961), though these competitive interactions might also be influenced by environmental variables such as temperature (Reeves et al. 1987). Whether redside shiner are more efficient at feeding on zooplankton is uncertain. Functional response experiments could shed light on competitive advantages redside shiner may have over rainbow trout and elucidate any relationships between resource availability and impacts of invasion (Dick et al. 2014).

Limitations/Assumptions

Population abundance

Population abundance exerted the strongest influence on predicted consumption demand, therefore uncertainty around these estimates influenced our conclusions regarding consumption demand in these reservoirs. Despite considerable uncertainty regarding rainbow trout abundance in Ross Lake, the population is too small to strongly our conclusions. Our estimate of consumption by rainbow trout represented only 5-21% of the consumption demand imposed by redside shiners; therefore, the rainbow trout population would have to be manyfold larger than our current estimates in order to measurably change our conclusions about the relative consumption demand of these two species.

Redside shiner are difficult to survey with hydroacoustics due to their typical nearshore and surface-oriented shoaling behavior, but this method was more feasible than other methods of estimating population abundance (e.g., mark-recapture). We surveyed at night to leverage their typical nocturnal dispersion behavior (Crossman 1959), however we still observed higher densities nearshore, where we were unable to fully survey due to shallow depths. Their surface-orientated behavior combined with limited sample volume near the apex of the acoustic beam cone (i.e., in the shallowest depths surveyed) may also introduce bias and limit precision of our estimates, particularly for the shallow depth bins (Taylor and Maxwell 2007). Additionally, our fall surveys did not account for any declines in abundance throughout the growing season (e.g., from predation). Therefore, we may have underestimated average density (and abundance). These estimates should be viewed with caution and conclusions regarding system carrying capacity interpreted accordingly. However any bias would be directional toward underestimating the redside shiner population and the associated consumption demand on prey resources shared with salmonids.

If we underestimated redside shiner abundance, this could explain why Ross Lake zooplankton supply appears to not yet be at carrying capacity. If we use a conservative estimate of carrying capacity to be 50% of production + biomass, Ross Lake *Daphnia* supply in

September would be at carrying capacity with a redside shiner population around 1.8x our estimated size (i.e., 21.5 million), which is near the upper confidence interval of the redside shiner abundance estimate (21.4 million; Table S1). Different methods of hydroacoustics surveying (e.g., side-looking transducer, Taylor and Maxwell 2007) could be utilized to improve estimates of the redside shiner population. Additionally, hydroacoustics data could be combined with environmental variables (e.g., bathymetry, water temperature, tributary locations) and a spatially-explicit modeling design to improve the abundance estimates and help understand the factors driving distribution across the lake (e.g., Taylor et al. 2005), and support management decisions.

Daphnia production

Although the egg-ratio method for estimating production (Paloheimo 1974) is standard in such fisheries studies, it is not without flaws. First, it assumes constant birth and death rates throughout each sampling interval. In reality, these dynamics are episodic – egg ratios change considerably in short periods. A lot of variability in these metrics may be lost in longer sampling intervals, such as the monthly sampling used in this study (Brett et al. 1992), but logistical constraints in accessing field sites prevented us from collecting samples more frequently. Challenges in identifying loose cladoceran eggs add another level of uncertainty to production estimates based on egg ratios. Nevertheless, we believe that our estimates of *Daphnia* biomass and production provide a useful guide for evaluating available prey supply in these reservoirs.

Management Implications

Identifying the factors currently limiting this invasive population is critical to understanding future risks driven by a changing climate and environmental conditions as well as informing control strategies (Rahel and Olden 2008). In contrast to rainbow trout, redside shiner in Ross Lake fed at or just exceeding their theoretical $\%C_{max}$, indicating they are probably limited by factors other than prey availability. Redside shiner experience a relatively short growing season in Ross Lake, with most of their consumption occurring during June-September. Warming would increase consumption rates and likely heighten limitations they impose on shared prey supply; however, it could also increase growth and survival rates in the spring and fall, potentially facilitating further expansion into the southern region, where abundance is comparatively low. If warming was high enough, it could also constrain redside shiner distribution during the growing season, leading to overlap with native salmonids and intensifying competition for the limited zooplankton supply below the epilimnion. Bioenergetic simulations show that redside shiner growth potential is within 90% of its maximum from 16-20 °C with $\%C_{max}$ and diet energy comparable to this study (Johnson et al. 2023), suggesting behavioral thermoregulation might induce vertical habitat shifts above these temperatures.

Stable isotope mixing models detected higher levels of cannibalism by redside shiner than expected based on diet analysis, which could represent an important and previously overlooked mechanism of population control. Extent of cannibalism reported in the literature is varied (Weisel and Newman 1951; Johannes and Larkin 1961; Welch 2012), and Weisel and Newman (1951) suggested that redside shiners “are probably their own worst egg predators.” Cannibalism could indicate low resource availability or a natural response to high density (Fox 1975). Further insights into the role cannibalism plays in regulating this population could be gained by quantifying predation mortality by other predators for comparison to annual biomass and production.

High relative feeding rates (%C_{max}) exhibited by redside shiner in this system suggest that management actions to reduce abundance could decrease exploitative competition with rainbow trout in Ross Lake. This is not always the case; for example, in Lake Tahoe high consumption demand and low %C_{max} of invasive *Mysis* feeding on copepods indicated that decreases in their density could increase per capita consumption rates by *Mysis* rather than increase food available to kokanee (Hansen et al. 2023). Uncertainties in the relative roles of predation versus environmental conditions in regulating zooplankton population dynamics makes it challenging to predict the magnitude of *Daphnia* response to a partial decrease in consumption demand. Additionally, if cannibalism is a response to low food availability and/or high densities, population control could decrease rates of cannibalism and increase consumption of other prey, thus buffering potential positive effects of control.

Conclusion

Quantitative assessments of reservoir food webs, such as those presented here for Ross Lake, can provide the necessary information to manage these novel or hybrid food webs (Naiman et al. 2012). As native species re-introductions and translocations become an increasingly popular conservation tool (Seddon et al. 2007) – including current proposals to explore introducing anadromous salmonids above Ross dam – such studies can also be leveraged to evaluate whether food web capacity exists to support these often costly introductions (e.g., Sorel et al. 2016b; Hansen et al. 2023). By linking these food web processes to thermal conditions, water management strategies can be ecologically informed and optimize current and future operations to support robust ecosystems.

Acknowledgments

Funding and support for this study was provided by Seattle City Light - in particular, we thank Jeff Fisher, Erin Lowery, and the Diablo Lake boat house crew for critical support provided during our field operations. We would like to thank North Cascades National Park and Ross Lake Resort for their assistance with field sampling logistics. We also want to thank Tom Barnett in particular for his support, angling efforts, and knowledge of the Ross Lake fishery. We are grateful for Lisa Wetzel, Ella Wagner, Nancy Elder, and Jeff Duda for assistance in the field and laboratory, and Tom Quinn, Julian Olden, and Jeff Duda for providing valuable editorial comments that improved the quality of this manuscript. Handling of vertebrates was conducted under the auspices of the Institutional Animal Care and Use Committee of the U.S. Geological Survey, Western Fisheries Research Center IACUC protocols #2008-57.

References

Beauchamp, D. A., A. D. Cross, J. L. Armstrong, K. W. Myers, J. H. H. Moss, J. L. Boldt, and L. J. Haldorson. 2007a. Bioenergetic responses by Pacific salmon to climate and ecosystem variation. North Pacific Anadromous Fish Commission Bulletin 4:257–269.

Beauchamp, D. A., D. H. Wahl, and B. M. Johnson. 2007b. Predator-Prey Interactions. Pages 765–842 *in* C. S. Guy and M. R. Brown, editors. Analysis and interpretation of freshwater fisheries data. American Fisheries Society.

Boretti, A., and L. Rosa. 2019. Reassessing the projections of the World Water Development Report. npj Clean Water 2:15.

Brett, M. T., Li. Martin, and T. J. Kawecki. 1992. An experimental test of the egg-ratio method: Estimated versus observed death rates. Freshwater Biology 28:237–248.

Crossman, E. J. 1959. Distribution and movements of a predator, the rainbow trout, and its prey, the redside shiner, in Paul Lake, British Columbia. Journal of the Fisheries Research Board of Canada 16:247–267.

Deslauriers, D., S. R. Chipps, J. E. Breck, J. A. Rice, and C. P. Madenjian. 2017. Fish Bioenergetics 4.0: An R-based modeling application. Fisheries 42:586–596.

Dick, J. T. A., M. E. Alexander, J. M. Jeschke, A. Ricciardi, H. J. MacIsaac, T. B. Robinson, S. Kumschick, O. L. F. Weyl, A. M. Dunn, M. J. Hatcher, R. A. Paterson, K. D. Farnsworth, and D. M. Richardson. 2014. Advancing impact prediction and hypothesis testing in invasion ecology using a comparative functional response approach. Biological Invasions 16:735–753.

Dumont, H. J., I. V. de Velde, and S. Dumont. 1975. The dry weight estimate of biomass in a selection of Cladocera, Copepoda and Rotifera from the plankton, periphyton and benthos of continental waters. Oecologia 19:75–97.

Feldbauer, J., D. Kneis, T. Hegewald, T. U. Berendonk, and T. Petzoldt. 2020. Managing climate change in drinking water reservoirs: Potentials and limitations of dynamic withdrawal strategies. Environmental Sciences Europe 32:48.

Ficke, A. D., C. A. Myrick, and L. J. Hansen. 2007. Potential impacts of global climate change on freshwater fisheries. Reviews in Fish Biology and Fisheries 17:581–613.

Foster, J. 2020. 2020 Skagit River snorkel survey report. Triton Environmental Consultants Ltd.

Fox, L. R. 1975. Cannibalism in natural populations. Annual Review of Ecology and Systematics 6:87–106.

Hansen, A. G., J. R. Gardner, K. A. Connelly, M. Polacek, and D. A. Beauchamp. 2018. Trophic compression of lake food webs under hydrologic disturbance. Ecosphere 9:1–11.

Hansen, A. G., A. McCoy, G. P. Thiede, and D. A. Beauchamp. 2023. Pelagic food web interactions in a large invaded ecosystem: Implications for reintroducing a native top predator. Ecology of Freshwater Fish Online:1–19.

Isley, J. J., and T. B. Grabowski. 2007. Age and growth. Pages 187–228 *in* C. S. Guy and M. L. Brown, editors. Analysis and interpretation of freshwater fisheries data. American Fisheries Society.

Jackson, M. C., R. J. Wasserman, J. Grey, A. Ricciardi, J. T. A. Dick, and M. E. Alexander. 2017. Novel and disrupted trophic links following invasion in freshwater ecosystems. Pages 55–97 *in* D. Bohan, A. Dumbrell, and F. Massol, editors. Networks of Invasion: Empirical Evidence and Case Studies. Academic Press.

Johannes, R. E., and P. A. Larkin. 1961. Competition for food between redside shiners (*Richardsonius balteatus*) and rainbow trout (*Salmo gairdneri*) in two British Columbia lakes. Journal of the Fisheries Research Board of Canada 18:203–220.

Johnson, P. T. J., J. D. Olden, and M. J. V. Zanden. 2008. Dam invaders: Impoundments facilitate biological invasions into freshwaters. Frontiers in Ecology and the Environment 6:357–363.

Johnson, R. C., D. A. Beauchamp, and J. D. Olden. 2023. Bioenergetics model for the nonnative redside shiner. Transactions of the American Fisheries Society 152:94–113.

Juncos, R., D. A. Beauchamp, and P. H. Vigliano. 2013. Modeling prey consumption by native and nonnative piscivorous fishes: Implications for competition and impacts on shared prey in an ultraoligotrophic lake in Patagonia. Transactions of the American Fisheries Society 142:268–281.

Larkin, P. A., and S. B. Smith. 1954. Some effects of introduction of the redside shiner on the Kamloops trout in Paul Lake, British Columbia. Transactions of the American Fisheries Society 83:161–175.

Legler, N. D., T. B. Johnson, D. D. Heath, and S. A. Ludsin. 2010. Water temperature and prey size effects on the rate of digestion of larval and early juvenile fish. Transactions of the American Fisheries Society 139:868–875.

Lindsey, C. C. 1950. The relation of the redside shiner to production of trout in British Columbia. B.C. Game Commission, Scientific Report.

Luecke, C., and D. Brandt. 1993. Notes: Estimating the energy density of Daphnid prey for use with rainbow trout bioenergetics models. Transactions of the American Fisheries Society 122:386–389.

Magnuson, J. J., L. B. Crowder, and P. A. Medvick. 1979. Temperature as an ecological resource. Integrative and Comparative Biology 19:331–343.

Messner, J., and G. Schoby. 2019. Fisheries management Annual Report: Salmon Region 2017. Idaho Department of Fish and Game, 19-102.

Miranda, L. E., and P. W. Bettoli. 2007. Mortality. Pages 229–277 *in* C. S. Guy and M. L. Brown, editors. Analysis and interpretation of freshwater fisheries data. American Fisheries Society.

Miranda, L. E., G. Coppola, and J. Boxrucker. 2020. Reservoir fish habitats: A perspective on coping with climate change. Reviews in Fisheries Science and Aquaculture 28:478–498.

Moreno-Ostos, E., R. Marcé, J. Ordóñez, J. Dolz, and J. Armengol. 2008. Hydraulic management drives heat budgets and temperature trends in a Mediterranean reservoir. International Review of Hydrobiology 93:131–147.

Naiman, R. J., J. R. Alldredge, D. A. Beauchamp, P. A. Bisson, J. Congleton, C. J. Henny, N. Huntly, R. Lamberson, C. Levings, E. N. Merrill, W. G. Pearcy, B. E. Rieman, G. T. Ruggerone, D. Scarnecchia, P. E. Smouse, and C. C. Wood. 2012. Developing a broader scientific foundation for river restoration: Columbia River food webs. Proceedings of the National Academy of Sciences of the United States of America 109:21201–21207.

Ney, J. J. 1996. Oligotrophication and its discontents: Effects of reduced nutrient loading on reservoir fisheries. Pages 285–295 *in* L. E. Miranda and D. R. De Vries, editors. Multidimensional Approaches to Reservoir Fisheries Management. American Fisheries Society.

Paloheimo, J. E. 1974. Calculation of instantaneous birth rate. Limnology and Oceanography 19:692–694.

Rahel, F. J., and J. D. Olden. 2008. Assessing the effects of climate change on aquatic invasive species. Conservation Biology 22:521–533.

Rahel, F. J., and M. A. Smith. 2018. Pathways of unauthorized fish introductions and types of management responses. Hydrobiologia 817:41–56.

Rand, P. S., D. J. Stewart, P. W. Seelbach, M. L. Jones, and L. R. Wedge. 1993. Modeling steelhead population energetics in Lakes Michigan and Ontario. Transactions of the American Fisheries Society 122:977–1001.

Reeves, G. H., F. H. Everest, and J. D. Hall. 1987. Interactions between the redside shiner (*Richardsonius balteatus*) and the steelhead trout (*Salmo gairdneri*) in western Oregon: The influence of water temperature. Canadian Journal of Fisheries and Aquatic Sciences 44:1603–1613.

Reid, A. J., A. K. Carlson, I. F. Creed, E. J. Eliason, P. A. Gell, P. T. J. Johnson, K. A. Kidd, T. J. MacCormack, J. D. Olden, S. J. Ormerod, J. P. Smol, W. W. Taylor, K. Tockner, J. C. Vermaire, D. Dudgeon, and S. J. Cooke. 2019. Emerging threats and persistent conservation challenges for freshwater biodiversity. Biological Reviews 94:849–873.

Seattle City Light. 1972. The aquatic environment, fishes and fishery: Ross Lake and the Canadian Skagit River (Interim report No. 1 Volume 1). City of Seattle.

Seattle City Light. 1974. The aquatic environment, fishes and fishery: Ross Lake and the Canadian Skagit River (Interim report No. 3 Volume 1). City of Seattle.

Seattle City Light. 2012. Biological Evaluation - supplement: Impacts of entrainment of bull trout. Skagit River Hydroelectric Project License (FERC no. 553) amendment: addition of a second power tunnel at the Gorge Development.

Seddon, P. J., D. P. Armstrong, and R. F. Maloney. 2007. Developing the science of reintroduction biology. Conservation Biology 21:303–312.

Smith, C. D., J. M. Plumb, N. S. Adams, and G. J. Wyatt. 2021. Predator and prey events at the entrance of a surface-oriented fish collector at North Fork Dam, Oregon. Fisheries Management and Ecology 28:172–182.

Sorel, M. H., A. G. Hansen, K. A. Connelly, and D. A. Beauchamp. 2016a. Trophic feasibility of reintroducing anadromous salmonids in three reservoirs on the North Fork Lewis River, Washington: Prey supply and consumption demand of resident fishes. Transactions of the American Fisheries Society 145:1331–1347.

Sorel, M. H., A. G. Hansen, K. A. Connelly, A. C. Wilson, E. D. Lowery, and D. A. Beauchamp. 2016b. Predation by northern pikeminnow and tiger muskellunge on juvenile salmonids in a high-head reservoir: Implications for anadromous fish reintroductions. Transactions of the American Fisheries Society 145:521–536.

Stock, B. C., A. L. Jackson, E. J. Ward, A. C. Parnell, D. L. Phillips, and B. X. Semmens. 2018. Analyzing mixing systems using a new generation of Bayesian tracer mixing models. PeerJ 6:e5096.

Stockwell, J. D., K. L. Bonfantine, and B. M. Johnson. 1999. Kokanee foraging: A *Daphnia* in the stomach is worth two in the lake. Transactions of the American Fisheries Society 128:169–174.

Tabor, R. A., and W. A. Wurtsbaugh. 1991. Predation risk and the importance of cover for juvenile rainbow trout in lentic systems. Transactions of the American Fisheries Society 120:728–738.

Tabor, R., C. Luecke, and W. Wurtsbaugh. 1996. Effects of Daphnia availability on growth and food consumption of rainbow trout in two Utah reservoirs. North American Journal of Fisheries Management 16:591–599.

Taylor, J. C., and S. L. Maxwell. 2007. Hydroacoustics: Lakes and reservoirs. Pages 153–172 *in* D. Johnson, B. Shrier, J. O’Neal, J. Knutzen, X. Augerot, T. O’Neill, and T. Pearsons, editors. Salmonid field protocols handbook: techniques for assessing status and trends in salmon and trout populations. American Fisheries Society.

Taylor, J. C., J. S. Thompson, P. S. Rand, and M. Fuentes. 2005. Sampling and statistical considerations for hydroacoustic surveys used in estimating abundance of forage fishes in reservoirs. North American Journal of Fisheries Management 25:73–85.

Thomsen, M. S., T. Wernberg, J. D. Olden, J. N. Griffin, and B. R. Silliman. 2011. A framework to study the context-dependent impacts of marine invasions. Journal of Experimental Marine Biology and Ecology 400:322–327.

Trottier, G., H. Embke, K. Turgeon, C. Solomon, C. Nozais, and I. Gregory-Eaves. 2019. Macroinvertebrate abundance is lower in temperate reservoirs with higher winter drawdown. Hydrobiologia 834:199–211.

Tunney, T. D., K. S. McCann, N. P. Lester, and B. J. Shuter. 2012. Food web expansion and contraction in response to changing environmental conditions. Nature Communications 3:1–9.

Vander Zanden, M. J., M. K. Clayton, E. K. Moody, C. T. Solomon, and B. C. Weidel. 2015. Stable isotope turnover and half-life in animal tissues: A literature synthesis. PLoS ONE 10:1–16.

Weisel, G. F., and H. W. Newman. 1951. Breeding habits, development and early life history of *Richardsonius balteatus*, a Northwestern minnow. Copeia 1951:187–194.

Welch, C. A. 2012. Seasonal and age-based aspects of diet of the introduced redside shiner (*Richardsonius balteatus*) in Ross Lake, Washington. Master's thesis. Western Washington University.

Woodin, R. M. 1974. Age, growth, survival, and mortality of rainbow trout (*Salmo gairdneri gairdneri*, Richardson) from Ross Lake drainage. Master's thesis. University of Washington.

Woolway, R. I., S. Sharma, G. A. Weyhenmeyer, A. Debolskiy, M. Golub, D. Mercado-Bettín, M. Perroud, V. Stepanenko, Z. Tan, L. Grant, R. Ladwig, J. Mesman, T. N. Moore, T. Shatwell, I. Vanderkelen, J. A. Austin, C. L. DeGasperi, M. Dokulil, S. L. Fuente, E. B. Mackay, S. G. Schladow, S. Watanabe, R. Marcé, D. C. Pierson, W. Thiery, and E. Jennings. 2021. Phenological shifts in lake stratification under climate change. Nature Communications 12:1–11.

Tables

Table 1. Estimated age-structured populations and mortality rates for rainbow trout and redside shiner in Ross Lake. Age structured populations were based on on 1,000 rainbow trout ≥ 200 mm FL (age 3+) and 1,000 redside shiner ≥ 40 mm FL (age 1+). Relative species frequency of rainbow trout represents their catch rate relative to bull trout during summer gill net sampling, which was used to estimate their population abundance relative to an estimated population of 3,000 bull trout ≥ 200 mm FL. Redisde shiner population abundance was estimated from hydroacoustics surveys in October 2021 and annual survival rates were sourced from Welch (2012).

Species	Z	Annual survival (%)	Age	Abundance per 1,000 fish	Relative species frequency	Estimated population size	Age-specific abundance
Rainbow trout	1.011	36.4	2	890	2.430	7,290	6,484
			3	647			4,717
			4	236			1,720
			5	86			627
			6	31			226
Redside shiner	0.810	44.5	1	560	-	12,000,000	6,720,000
			2	249			2,988,000
			3	111			1,332,000
			4	49			588,000
			5	22			264,000
			6	10			120,000

Table 2. Bioenergetics simulation inputs and corresponding estimates of feeding rate (% C_{max}), annual per capita consumption (g), and growth efficiency (%). All simulations ran for 365 days (day 1= May 1). Energy density (ED, J/g) of the consumer was linearly interpolated during the simulation from the initial to final value reported. Sample sizes (*N*) are given for the number of individuals used in scale back-calculations for each annulus.

Species	Age	*N*	Spawn day	Spawn loss (%)	Initial FL (mm)	Initial W (g)	Final W (g)	Initial ED (J/g)	Final ED (J/g)	%C_{max}	Growth (g)	Cons (g)	GE (%)	Daphnia cons (g)
Rainbow trout	2	391		0.0	117	20.7	117.9	4,996	4,996	32	97.2	983.0	10.0	155.0
	3	355	45	8.0	210	117.9	268.5	4,996	4,996	32	150.6	1,926.0	8.0	641.0
	4	280	45	8.0	292	268.5	403.9	4,996	4,996	31	135.4	2,756.0	5.0	518.0
	5	112	45	8.0	338	403.9	554.8	4,996	6,672	36	150.9	4,197.0	4.0	796.0
	6	21	45	8.0	374	554.8	877.9	6,672	6,672	36	323.1	5,301.0	6.0	328.0
Redside shiner	1	197		0.0	34	0.5	1.4	4,911	4,911	113	1.0	10.0	10.0	4.0
	2	183	61	11.0	49	1.4	2.8	4,911	4,911	117	1.4	15.0	9.0	5.0
	3	134	61	11.0	61	2.8	4.4	4,911	4,911	113	1.6	19.0	9.0	7.0
	4	108	61	11.0	71	4.4	6.6	4,911	4,911	112	2.1	23.0	9.0	8.0
	5	86	61	11.0	80	6.6	9.1	4,911	4,911	120	2.5	30.0	8.0	11.0
	6	52	61	11.0	89	9.1	11.8	4,911	6,208	122	2.8	35.0	8.0	13.0

Figures

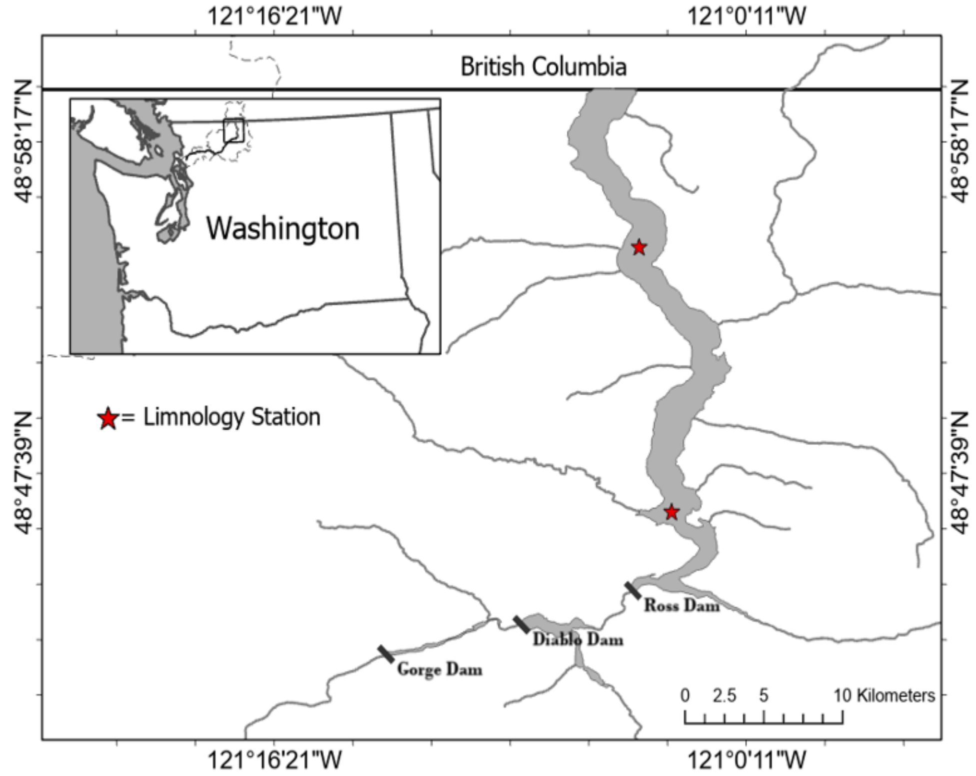

Figure 1. Map of the study system.

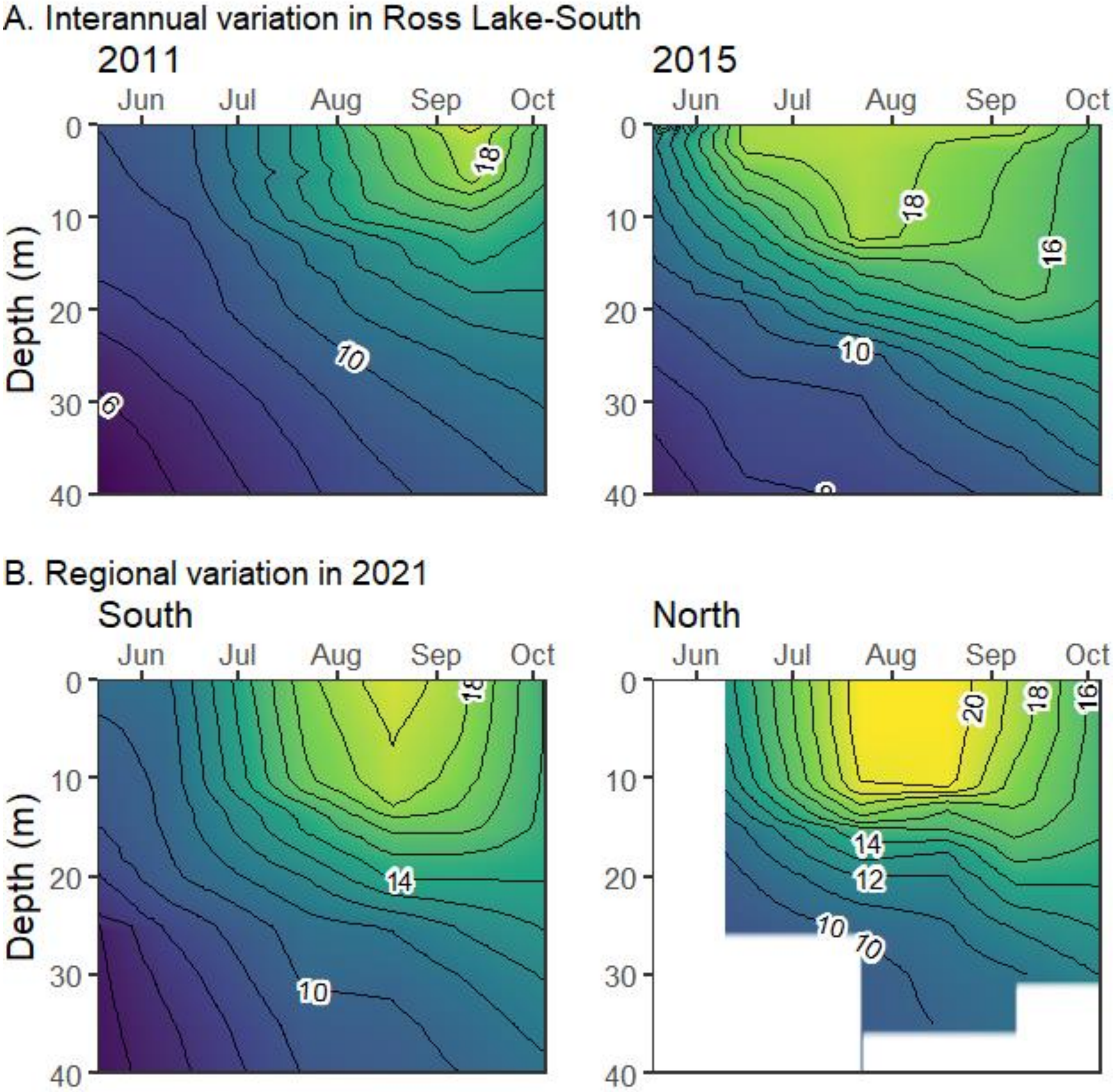

Figure 2. Isoclines for Ross Lake showing variation in thermal structure (°C) by year (A) and region (B). Data prior to 2019 was collected by the NPS. The Ross Lake South site is located mid-lake in the pelagic zone near the confluence with Big Beaver Creek, and the North site was located mid-lake in the pelagic zone near the confluence with Little Beaver Creek.

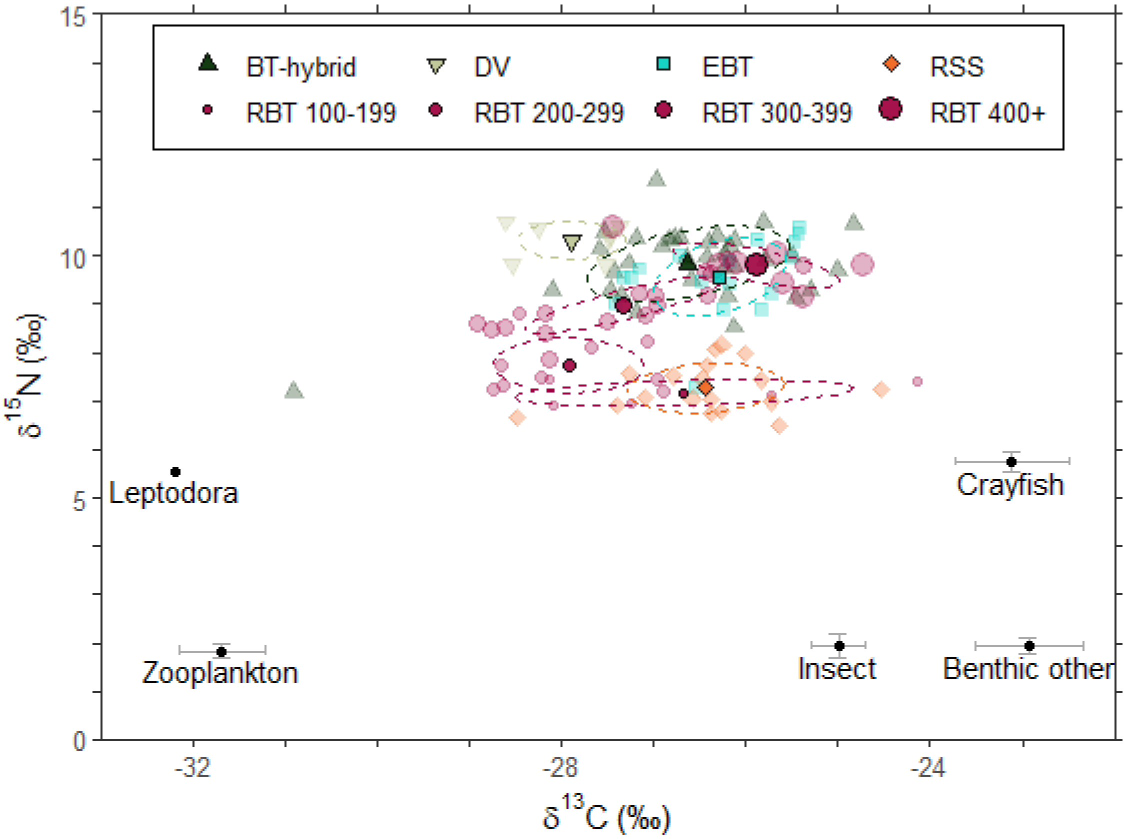

Figure 3. Stable isotope biplots of the Ross Lake food web. Consumer species were separated by size classes if significant differences in stable isotope values were observed. The darker colored symbols represent the group centroids, while the lighter shaded symbols represent individual fish. BT-hybrid: bull trout and char hybrids, DV: Dolly Varden, EBT: brook trout, RBT: rainbow trout, RSS: redside shiner. Numbers following the species code represent the group's size bin, in mm FL. Ellipses contain 40% of the data for each consumer species/size group.

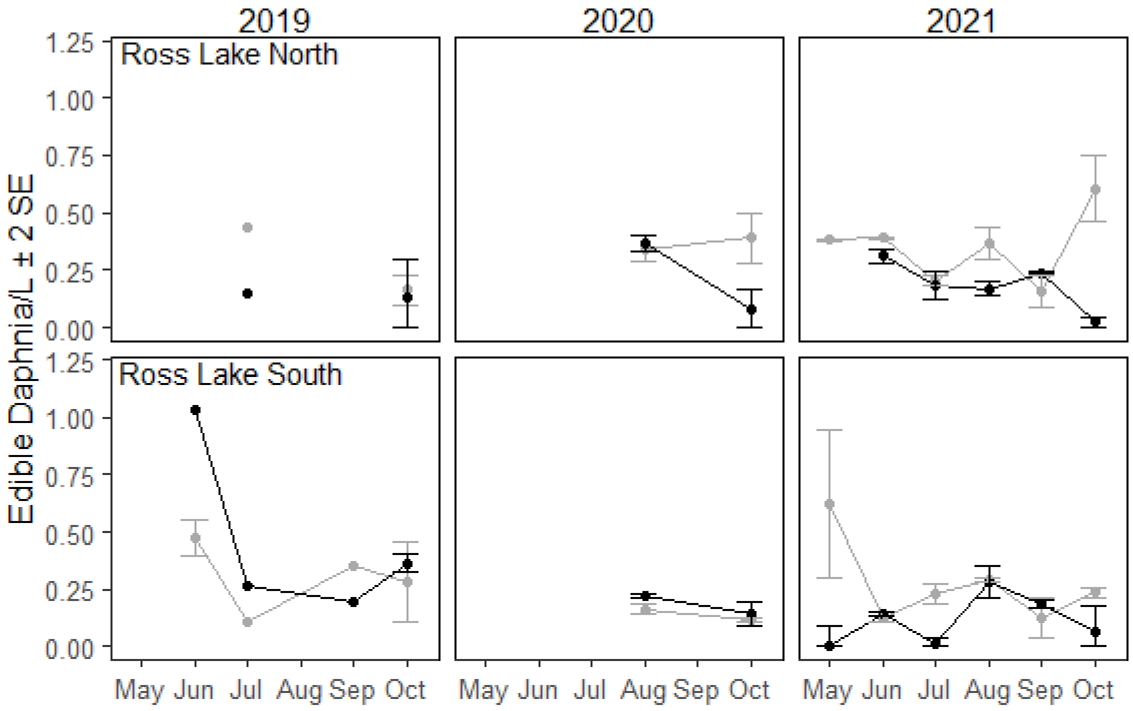

Figure 4. Average monthly densities of edible sized *Daphnia* (≥ 1 mm BL) in the epilimnion (0-10 m depth; grey symbols) and the metalimnion (10-20 m depth; black symbols) in Ross Lake 2019-2021.

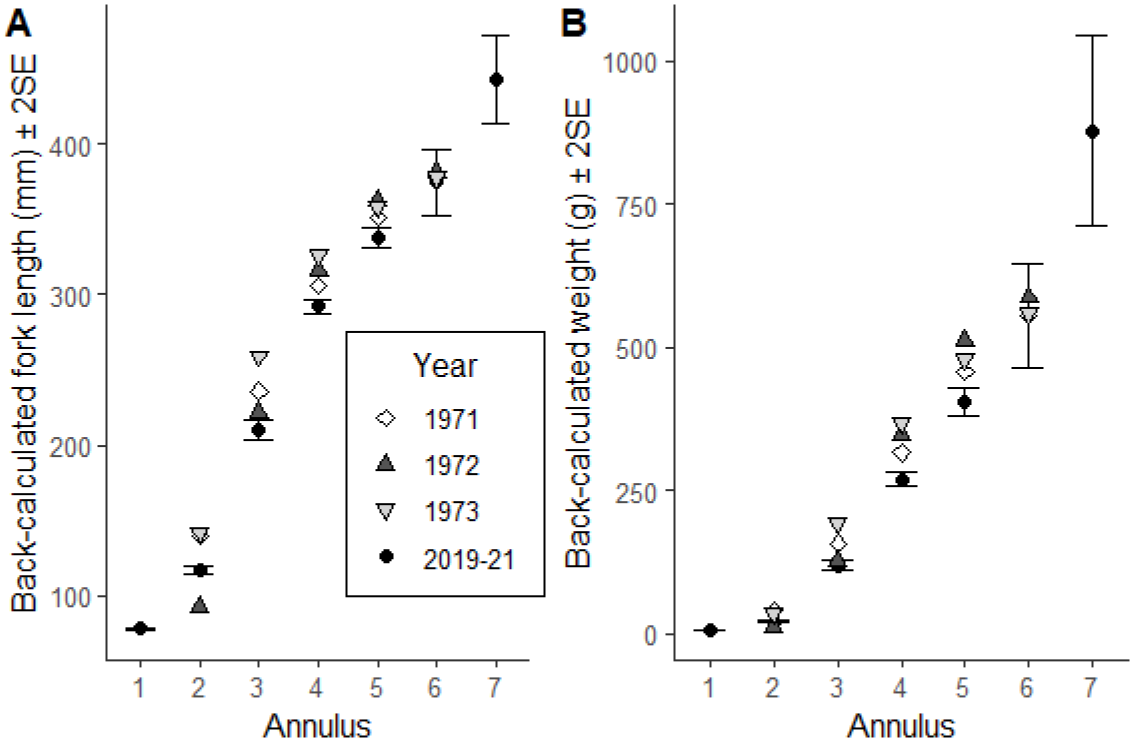

Figure 5. Ross Lake rainbow trout back-calculated fork length (A) and weight (B) at annulus. Data derived from the current study are shown by the black circles with error bars, and historical data (Woodin 1974) are shown by the grey and white symbols. Note that for the historical data, 1 year was added to each annulus to appropriately compare to our back-calculation data. Sampling of tributary fish and scales during this study led us to conclude that the size at age 1 reported in Woodin (1974) was too large, and we believe that the first annulus was not counted in this data.

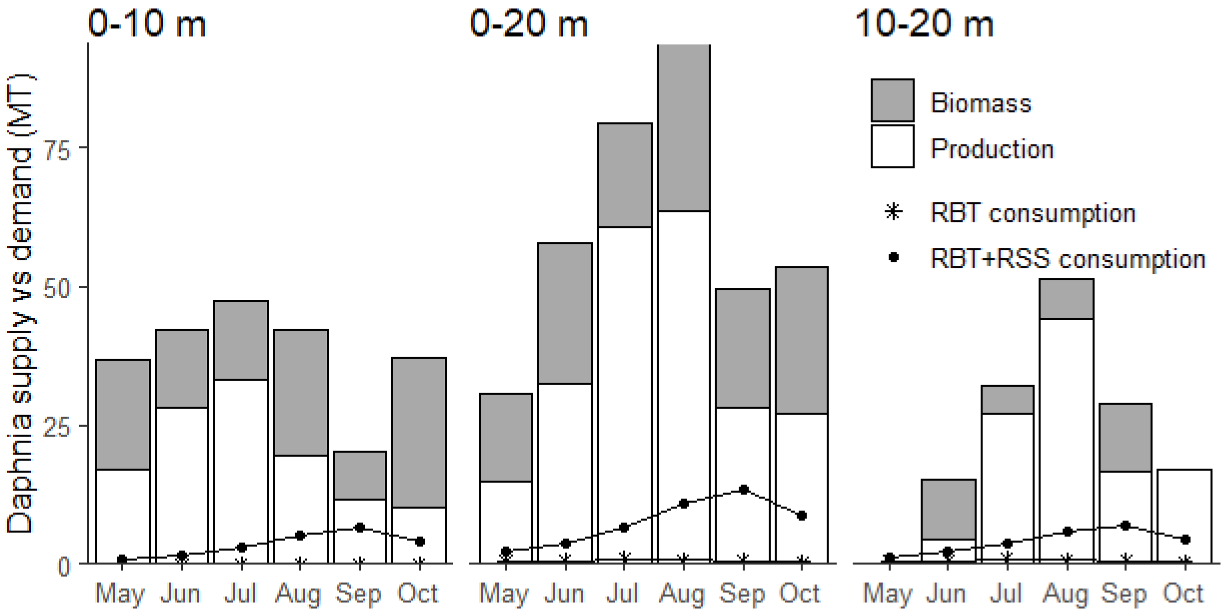

Figure 6. Mean estimates of monthly *Daphnia* production and biomass compared to population consumption demand of rainbow trout and redside shiner in Ross Lake. Consumption demand versus prey supply is shown for the combined epi- and metalimnion (0-20 m depth), the epilimnion alone (0-10 m depth), and the metalimnion alone (10-20 m depth). Refer to the methods section for a description of the depth-use scenarios used to divide consumption between the two depth layers. RBT: rainbow trout, RSS: redside shiner.

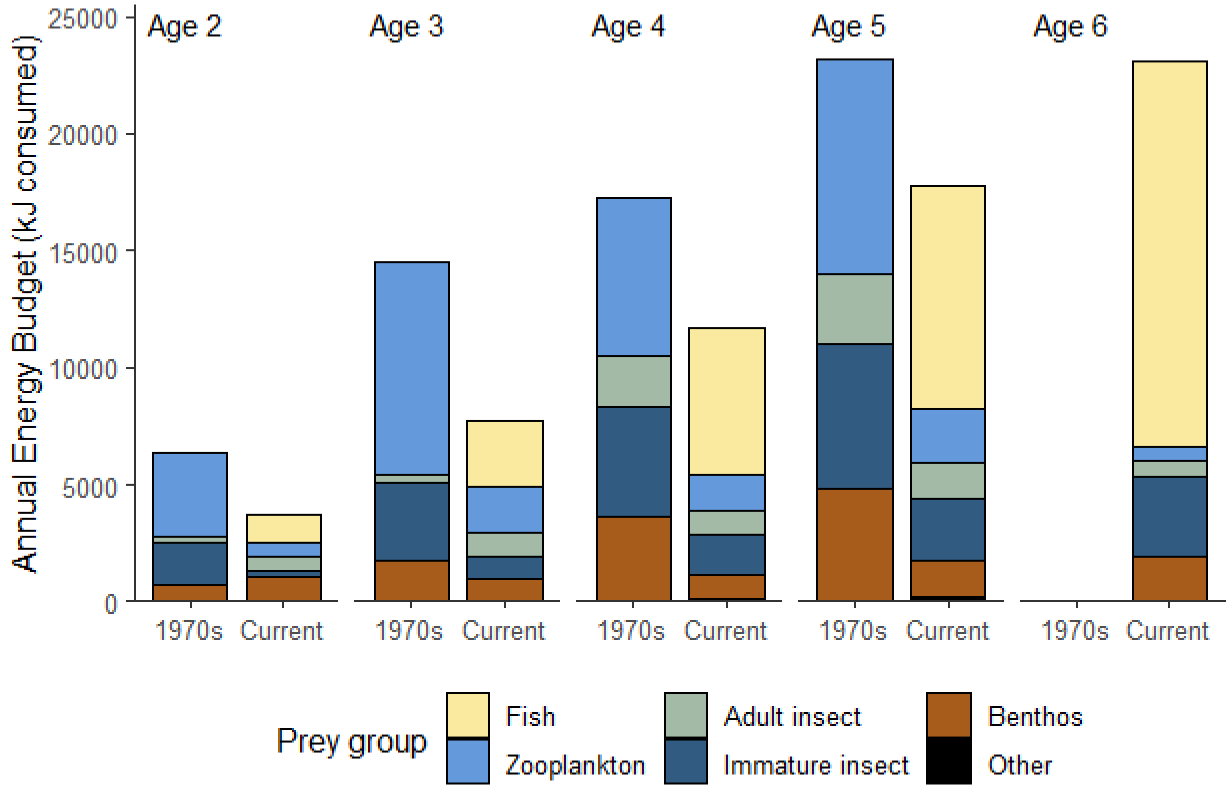

Figure 7. Comparison of annual energy budgets of rainbow trout between the historical food web study in the 1970s and the current study.

Chapter 2: Supplementary Materials - Ross Lake

Methods

Hydroacoustic surveys

We conducted hydroacoustic surveys to estimate the distribution, density, and abundance of redside shiner in Ross Lake during October 2021 using a Biosonics DT-X echo sounder with a split beam 200kHz transducer (7 degree beam angle). Pilot surveys indicated redside shiner were distributed around the perimeter of the lake rather than the entire limnetic zone and dispersed from the shallow littoral after dusk. Redside shiner exhibited shoaling behavior and occupied depths too shallow to survey during the day; therefore, all surveys were conducted at night. Due to the size of Ross Lake (approximately 96 km shoreline), transects were determined by dividing the shoreline into 500 m segments and randomly sampling these segments within region (north, mid, south), shore (east or west), and slope (steep or shallow) blocking groups (Fig. S13-15). We targeted six transects within each blocking group (n = 59), in addition to transects within 500 m of each tributary mouth (4th order or lower, n = 28). We sampled each tributary mouth as we anticipated higher densities of redside shiner at these sites and wanted to ensure adequate survey coverage. The lake was too shallow and hazardous for nighttime surveys north of the confluence with Hozomeen Creek. We conducted a transect crossing the entire lake in the region between Silver Creek and Hozomeen Creek (as far north as we could safely survey) to use to estimate redside shiner density in the north shallow region, because we found that redside shiner occupied this entire zone of the lake. We split this transect into 3 equal length sections, removing 110 m of transect length in between each section, to attain a variance estimate for this region. Acoustic targets were ground truthed by deploying a sinking multi-mesh gillnet (36-m by 1.8-m; stretched mesh panel sizes (mm): 20, 25, 37, 50, 66, 76) during one of the surveys where we identified fish targets. Minnow trap collections from 2019 were also used to determine redside shiner size structure in Ross Lake.

Due to the schooling nature of the redside shiner in Ross Lake, a combination of echo integration and single target detection was used. All data processing, filtering, and acoustics analysis was conducted in Echoview (version 13.0). The Detect Schools algorithm identified large aggregations of targets. The energy from these groups was integrated to determine the number of targets within that school. Schools classification were only accepted if shallower than 15m. Single targets were removed if within 1m from the bottom. Target strength (dB) for redside shiner across their size distribution was estimated for total length (mm, Love 1977). Density estimates were computed for every 1 m depth bin (the surface 2 m were excluded due to positioning of the transducer and nearfield acoustic noise). Density estimates from these transects were expanded to the remainder of the Ross Lake shoreline to estimate total biomass and abundance of redside shiner. Using ANOVA, trends in density from the transects were compared among the three regions (north, middle, and south), excluding the three transects in the north shallow. Mean density (fish/m2) within each region was expanded to total areal estimates of littoral regions of occupancy to estimate population size.

Redside shiner distribution was patchy and densities (individuals/m^2) were lower in the south region (mean ± SE: 0.524 ± 0.064) compared to the mid (0.896 ± 0.096) and north (0.788 ± 0.1; Tables S2-3). Due to differences in transect length/coverage and redside shiner occupancy, we analyzed the shallow north region separately from the three main regions (0.823 ± 0.648) To expand these densities to a lake-wide abundance, we multiplied each regional mean by surface area estimates of the occupied nearshore (north shallow = 5.56 km^2, north = 3.63 km^2, mid = 3.44 km^2, south = 3.02 km^2,), resulting in an estimated 12.1 million redside shiner > 30 mm TL (95% CI: 6-21.4 million; Table S1).

Daphnia production

Production rates were estimated with the egg-ratio method (Paloheimo 1974) using these equations:

$$K = \frac{65912 * (T + 6.1)^{-2.12}}{24} \qquad (1)$$

$$b = \frac{ln\left(\frac{E}{N_0} + 1\right)}{K} \qquad (2)$$

$$r = \frac{ln(N_t) - ln(N_0)}{t} \qquad (3)$$

$$\begin{aligned} B &= \\ r > 0\text{:} \quad &= \left(\frac{b}{r}\right) \times (N_t - N_0) \\ r \leq 0\text{:} \quad &= b \times \left(\frac{N_t + N_0}{2}\right) \times t \qquad (4) \end{aligned}$$

$$P = B \times \bar{W} \qquad (5)$$

$$P_d = \frac{P}{t} \qquad (6)$$

where K is egg development time (days; Cooley et al. 1986), T is the mean temperature in the depth strata throughout the interval, b is the population birth rate (individuals per day), t is the length of the interval (days), E is the number of eggs (per liter) at the start of the interval, N_0 is the number of individuals (per liter) at the beginning of the interval, N_t is the number of individuals (per liter) at the end of the interval, r is the mean instantaneous rate of population change over the interval, B is the number of new recruits in the sampling interval, $\bar{W}$ is the mean wet weight (g) of the individuals at the start of the interval, P is the total production across the interval (g wet weight), and P_d is the average daily production (g wet weight) during the interval. Average daily production in each interval (P_d) was converted to total monthly production (g/L) based on the number of days per month that fell within each interval. We extrapolated average daily production within the first and last intervals to estimate monthly production in May and October.

Stable isotope mixing models (SIMMs)

We fit the mixing models using raw source data with prey sources grouped into three broad categories (fish, zooplankton, and insects + other benthic invertebrates). Inclusion of specific prey items in the model was partially based on diet analysis and dependent on species and size class. Potential fish prey for redside shiner only included other redside shiner, as we assumed all fish consumption for this species was cannibalism on eggs and larvae due to gape limitations. We did not have stable isotope data for eggs or fish larvae and thus assumed that stable isotope signatures from the whole population would be representative. Some studies suggest that δ^{15}N and δ^{13}C of salmonid eggs are related to isotopic signatures of the maternal fish during maturation (Grey 2001). We did not identify any ontogenetic differences in stable isotope signatures among redisde shiner sizes; therefore, we determined that this assumption should not substantially bias conclusions from our stable isotope mixing models. Potential fish prey for rainbow trout 100-199 and 200-299 mm FL only included redside shiner and the smallest rainbow trout, while potential fish prey for 300+ mm FL consumers also included rainbow trout 200-299 mm. Prey sources for all consumers included all zooplankton (mixed zooplankton sample and *Leptodora*) and benthic invertebrates/insects. In the absence of species and prey-specific trophic discrimination factors (TDF), we used mean TDFs (± SD) of $\delta^{15}N = 3.4‰ \pm 1.0‰$ and $\delta^{13}C = 0.4‰ \pm 1.3‰$ (Post 2002). This is consistent with much of the literature in similar fisheries studies (e.g., Rubenson et al. 2020; Hansen et al. 2021); however, it is important to understand that TDFs can vary among species, prey items, and tissue types (Bond and Diamond 2011; Canseco et al. 2022).

Thermal experience and depth use

In the south, rainbow trout primarily occupied the epilimnion in the spring and summer (> 75% of the catch) and then were approximately evenly distributed down to 20 m depth, with few (5% of the catch) in 20-30 m, in the fall (Fig. S2). Notably, epilimnion temperatures in the south remained at or below 18 °C at the time of our summer sampling. At the north site in the summer, most rainbow trout occupied the metalimnion and only about 30% in the epilimnion, where July temperatures approached 20 °C. Redside shiner depth distribution was inferred from hydroacoustic surveys, thus limiting our ability to evaluate seasonal/thermal influences on their habitat use. Stratification in Ross Lake was degrading during the October hydroacoustics survey and the warmer surface layer (approx. 15 °C) extended down to around 15 m, below which temperatures slowly decreased (Fig. S3). The highest density of redside shiner were located between 5-10 m in all regions, though a lower proportion of fish occupied the epilimnion (0-10 m) in the south compared to the mid and north regions. These data suggest that redside shiner strongly overlap with rainbow trout distribution in the fall.

Diet inputs and seasonal consumption

Seasonal diet inputs used in the bioenergetics simulations were compiled from a combination of stomach content analysis, stable isotope mixing models, and general ecological knowledge/assumptions. We describe the specific methods we used to do this below:

For redside shiner, mixing models generally predicted a larger contribution of fish than reported from stomach content analysis (Welch 2012), therefore we adjusted diet inputs to reflect this. We assumed stable isotope signatures were incorporated over the previous 1-3 months, and thus represent average diet contribution over that entire period. Therefore, we assigned proportions from the summer sample SIMMs to be constant starting on simulation day 1 (May 1) through approximate time of summer sampling (Aug 1, Day 92). For 50-99 mm FL fish, we only had samples collected in the summer, and we tested season as a factor for 100+ mm fish. While there were some differences in stable isotope signatures between summer and fall, there was not strong support for the seasonal model implemented in MixSIAR when evaluated with LOO cross-validation. Given this, we modeled diets for all size-classes pooled and assumed that the average spring-summer diet, based on SIMMs, would linearly change from summer until beginning of fall (day 154 - Oct 1), where we used fall diet proportions from Welch (2012). From there, we assumed zooplankton would linearly decrease until the beginning of winter (day 245). This choice is based in the assumption that proportions of fish would decrease as redside spawning season is over and larvae outgrow predation risk, and zooplankton supplies decrease to an assumed winter diet of entirely benthos. This also aligns with diet data from Welch (2012) that showed lower contribution of zooplankton in fall samples. We set this winter diet to end on day 336 (Apr 1), after which zooplankton and fish proportions will linearly increase to spring time levels. We used relative proportions of benthics and insects reported in Welch (2012) to allocate this across the different category of benthos. Additionally, we assumed an approximate 50-50 split of zooplankton between *Daphnia* and other zooplankton (e.g., Bosmina, copepoda, etc).

As with the redside shiner, mixing models predicted a larger contribution of fish than stomach content analysis for small rainbow trout (100-199 and 200-299 mm), therefore we incorporated mixing model results into the spring-summer diet inputs. We assumed stable isotope signatures were incorporated over the previous 1-3 months, and therefore assigned summer SIMM proportions to be constant from simulation day 1 (May 1) to approximate timing of summer sampling (Aug 1, day 92). We did not have stable isotope samples from the fall, so we used proportions from diet analysis for both summer and fall. We assumed zero consumption of fish or zooplankton by this size class in the winter and set this winter diet to end on day 336 (Apr 1) after which it linearly increases to spring levels.

Mixing model results aligned well with stomach contents for larger rainbow trout 300+ mm (comparing stable isotope data to the previous season's stomach contents). The one exception was the predicted contribution of zooplankton versus benthos/insects in the spring for

300-399 mm fish, where the diet samples showed a heavy reliance on benthos (mainly immature insects) and the mixing model showed a reliance on zooplankton instead. We used stomach contents as the seasonal diet inputs for this size class. Due to low diet sample size, we used SIMMs proportions to inform spring-summer diets for rainbow trout 400+. Stomach contents were used for inputs for all other seasons for 300-399 and 400+ mm rainbow trout. For winter diets, we used fall stomach contents and brought zooplankton and adult insects down to zero, replacing them with benthos. As above, we set winter to end on day 336 (Apr 1) at which point diet proportions linearly change to spring levels.

References

Bond, A. L., and A. W. Diamond. 2011. Recent Bayesian stable-isotope mixing models are highly sensitive to variation in discrimination factors. Ecological Applications 21:1017–1023.

Canseco, J. A., E. J. Niklitschek, and C. Harrod. 2022. Variability in δ 13C and δ 15N trophic discrimination factors for teleost fishes: A meta-analysis of temperature and dietary effects. Reviews in Fish Biology and Fisheries 32:313–329.

Grey, J. 2001. Ontogeny and dietary specialization in brown trout (*Salmo trutta* L.) From Loch Ness, Scotland, examined using stable isotopes of carbon and nitrogen. Ecology of Freshwater Fish 10:168–176.

Hansen, A. G., J. R. Gardner, K. A. Connelly, M. Polacek, and D. A. Beauchamp. 2021. Resource use among top-level piscivores in a temperate reservoir: Implications for a threatened coldwater specialist. Ecology of Freshwater Fish:1–23.

Love, R. H. 1977. Target strength of an individual fish at any aspect. The Journal of the Acoustical Society of America 62:1397.

Paloheimo, J. E. 1974. Calculation of instantaneous birth rate. Limnology and Oceanography 19:692–694.

Post, D. M. 2002. Using stable isotopes to estimate trophic position: Models, methods, and assumptions. Ecology 83:703–718.

Rubenson, E. S., D. J. Lawrence, and J. D. Olden. 2020. Threats to rearing juvenile Chinook salmon from nonnative smallmouth bass inferred from stable isotope and fatty acid biomarkers. Transactions of the American Fisheries Society 149:350–363.

Welch, C. A. 2012. Seasonal and age-based aspects of diet of the introduced redside shiner (*Richardsonius balteatus*) in Ross Lake, Washington. Master’s thesis. Western Washington University.

Tables

Table S1. Mean redside shiner densities (individuals/m^2) and expanded abundance estimates for each sampling region from hydroacoustics surveys. *N* is the number of transects surveyed in each region, and area represents the estimated occupied littoral area in each region.

						95% confidence interval	
Region	*N*	Area (km^2)	Density	SE	Abundance	low	high
north shallow	3	5.558	0.823	0.648	4,574,735	0	11,918,927
north	28	3.627	0.788	0.100	2,859,003	2,236,440	3,660,578
mid	30	3.443	0.896	0.096	3,084,297	2,540,956	3,840,744
south	27	3.023	0.524	0.064	1,584,377	1,254,792	2,017,905
Total	**88**	**15.651**	**-**	**-**	**12,102,413**	**6,032,188**	**21,438,153**

Table S2. Results from ANOVA testing the dependence of redside shiner density (individuals/m^2) on sampling region in Ross Lake.

term	df	sumsq	meansq	statistic	p.value
region	2	2.067	1.033	4.165	0.019
Residuals	85	21.085	0.248	-	-

Table S3. Tukey HSD pairwise comparisons of density (individuals/m^2) among the regions.

Comparison	diff	lwr	upr	p.adj
North-Mid	-0.104	-0.408	0.200	0.694
South-Mid	-0.372	-0.687	-0.056	0.017
South-North	-0.267	-0.580	0.045	0.109

Table S4. Mean thermal experience for rainbow trout (RBT) and redside shiner (RSS) during each month in Ross Lake.

	Temperature °C	
Month	RBT	RSS
Jan	5.1	5.1
Feb	4.2	4.2
Mar	4.6	4.6
Apr	6.3	6.3
May	9.8	9.5
Jun	12.5	12.2
Jul	15.8	15.2
Aug	16.6	17.4
Sep	17.2	16.9
Oct	14.1	14.0
Nov	10.4	10.4
Dec	7.1	7.1

Table S5. Prey energy densities used in bioenergetics simulations. Note that the energy density for Daphnia reflects their compressed form in the gut and is approximately 2x higher in J/g than 'fresh' Daphnia.

Prey group	Energy density (J/g wet weight)	Source
RSS	5,000	this study
Salmonid	4,000	this study
Unid. Fish	5,000	this study
Amphibia	3,980	Crump 1979
Daphnia	3,860	Luecke & Brandt 1993
Leptodora	3,860	Luecke & Brandt 1993
Zooplankton other	2,260	Luecke & Brandt 1993
Amphipod	4,316	James et al. 2012
Snail	2,789	McCarthy et al. 2009
Benthic other	2,789	McCarthy et al. 2009
Immature insect	3,365	McCarthy et al. 2009
Adult insect	5,000	McCarthy et al. 2009
Other	3,500	

Table S6. Mean seasonal diet proportions (wet weight, g) for rainbow trout in Ross Lake from stomach content analysis. N: sample size of non-empty stomachs, RSS: redside shiner, Sal: salmonid, Unk-fish: unidentified fish, Daph: Daphnia, Lept: Leptodora, Zoop: other zooplankton, IM-insect: immature insect, AD-insect: adult insect.

Length	Season	N	RSS	Sal	Unk-fish	Amphibia	Daph	Lept	Zoop	Amphipod	Snail	Benthos	IM-insect	AD-insect	Other
100-199	Spring	4	0.000	0.000	0.000	0.000	0.243	0.087	0.000	0.249	0.012	0.000	0.251	0.157	0.000
	Summer	29	0.019	0.000	0.040	0.000	0.181	0.049	0.019	0.002	0.012	0.000	0.225	0.419	0.035
	Fall	2	0.000	0.000	0.500	0.000	0.000	0.000	0.273	0.000	0.000	0.000	0.031	0.196	0.000
200-299	Spring	17	0.004	0.000	0.000	0.000	0.196	0.093	0.057	0.000	0.000	0.000	0.472	0.178	0.000
	Summer	28	0.098	0.000	0.060	0.000	0.258	0.294	0.058	0.000	0.000	0.000	0.080	0.132	0.019
	Fall	13	0.077	0.035	0.190	0.000	0.225	0.033	0.002	0.000	0.000	0.000	0.162	0.268	0.008
300-399	Spring	64	0.324	0.005	0.025	0.004	0.026	0.020	0.000	0.004	0.012	0.037	0.479	0.056	0.007
	Summer	68	0.503	0.000	0.124	0.000	0.138	0.115	0.000	0.016	0.000	0.012	0.001	0.087	0.004
	Fall	77	0.346	0.006	0.043	0.000	0.185	0.039	0.001	0.000	0.017	0.007	0.191	0.150	0.016
400+	Spring	4	0.671	0.000	0.000	0.000	0.000	0.000	0.000	0.000	0.000	0.000	0.215	0.114	0.000
	Summer	12	0.894	0.000	0.083	0.000	0.005	0.001	0.000	0.004	0.000	0.006	0.001	0.001	0.005
	Fall	7	0.475	0.000	0.016	0.000	0.022	0.000	0.001	0.000	0.141	0.075	0.270	0.000	0.000

Table S7. Seasonal diet proportions (wet weight) compared to stable isotope mixing model results (SIMM, 95% credible intervals) for broad prey categories for rainbow trout and redside shiner in Ross and Diablo Lakes. Redside shiner diet data was from previously published estimates of volumetric proportions (Welch 2012). Season refers to the season that the diet sample or tissue sample was collected.

					Fish		Zooplankton		Benthos/insect/other	
Species	Length	Season	*N*: Diet	*N*: SIMM	Diet	SIMM	Diet	SIMM	Diet	SIMM
Ross Lake										
RBT	100-199	Spring	4		0.000		0.330		0.669	
		Summer	29	5	0.059	0.304 (0.111-0.496)	0.249	0.336 (0.08-0.636)	0.693	0.359 (0.088-0.607)
		Fall	2		0.500		0.273		0.227	
	200-299	Spring	17		0.004		0.346		0.650	
		Summer	28	9	0.158	0.377 (0.182-0.542)	0.610	0.434 (0.317-0.558)	0.231	0.188 (0.043-0.346)
		Fall	13		0.302		0.260		0.438	
	300-399	Spring	64		0.354		0.046		0.599	
		Summer	68	21	0.627	0.406 (0.181-0.586)	0.253	0.511 (0.3-0.75)	0.120	0.083 (0.008-0.202)
		Fall	77	10	0.395	0.607 (0.418-0.734)	0.225	0.254 (0.114-0.462)	0.381	0.138 (0.031-0.242)
	400+	Spring	4		0.671		0.000		0.329	
		Summer	12	7	0.977	0.71 (0.59-0.812)	0.006	0.076 (0.005-0.202)	0.017	0.214 (0.085-0.329)
		Fall	7		0.491		0.023		0.486	
RSS	all	Spring	95		0.005		0.566		0.429	
		Summer	95	18	0.030	0.335 (0.176-0.483)	0.511	0.302 (0.212-0.398)	0.459	0.363 (0.217-0.508)
		Fall	35		0.000		0.410		0.590	

Table S8. Rainbow trout and redside shiner seasonal diet proportions used as inputs into bioenergetics model simulations for Ross Lake. Length bins (mm FL) are reported for rainbow trout, however diets were assumed to be consistent across redside shiner body size. Sample size (N) of stomach content analysis is indicated for the seasons in which non-empty stomach contents were collected. Winter diets were set to be constant between day 245 and 336 (Jan 1- Apr 1). All diets were linearly interpolated between seasons. *Denotes seasons in which stable isotope mixing model results were used to modify these diet inputs for the bioenergetics simulations. RSS: redside shiner, Sal: salmonid, Unk-fish: unidentified fish, Daph: *Daphnia*, Lept: Leptodora, Zoop: other zooplankton, IM-insect: immature insect, AD-insect: adult insect.

				Diet proportions												
Length	Day	Season	*N*	RSS	Sal	Unk-fish	Amphibia	Daph	Lept	Zoop	Amphipod	Snail	Benthos	IM-insect	AD-insect	Other
Rainbow trout																
100-199	1	Spring*	4	0.304	0.000	0.000	0.000	0.243	0.087	0.007	0.134	0.006	0.000	0.135	0.084	0.000
	91	Summer*	-	0.304	0.000	0.000	0.000	0.243	0.087	0.007	0.134	0.006	0.000	0.135	0.084	0.000
	92	Summer	29	0.019	0.000	0.040	0.000	0.181	0.049	0.019	0.002	0.012	0.000	0.225	0.419	0.034
	154	Fall	2	0.000	0.000	0.500	0.000	0.000	0.000	0.273	0.000	0.000	0.000	0.031	0.196	0.000
	245	Winter	-	0.000	0.000	0.000	0.000	0.000	0.000	0.000	0.000	0.000	1.000	0.000	0.000	0.000
	336	Spring	-	0.000	0.000	0.000	0.000	0.000	0.000	0.000	0.000	0.000	1.000	0.000	0.000	0.000
200-299	1	Spring*	17	0.377	0.000	0.000	0.000	0.246	0.117	0.071	0.000	0.000	0.000	0.137	0.052	0.000
	91	Summer*	-	0.377	0.000	0.000	0.000	0.246	0.117	0.071	0.000	0.000	0.000	0.137	0.052	0.000
	92	Summer	28	0.098	0.000	0.060	0.000	0.258	0.294	0.058	0.000	0.000	0.000	0.080	0.132	0.020
	154	Fall	13	0.077	0.035	0.190	0.000	0.225	0.033	0.002	0.000	0.000	0.000	0.162	0.268	0.008
	245	Winter	-	0.077	0.000	0.190	0.000	0.000	0.000	0.000	0.000	0.000	0.571	0.162	0.000	0.000
	336	Spring	-	0.077	0.000	0.190	0.000	0.000	0.000	0.000	0.000	0.000	0.571	0.162	0.000	0.000
300-399	1	Spring	64	0.324	0.005	0.025	0.005	0.026	0.020	0.000	0.004	0.012	0.037	0.479	0.056	0.007
	92	Summer	68	0.503	0.000	0.124	0.000	0.138	0.115	0.000	0.016	0.000	0.012	0.001	0.087	0.004
	154	Fall	77	0.346	0.006	0.043	0.000	0.185	0.039	0.001	0.000	0.017	0.007	0.191	0.150	0.015
	245	Winter	-	0.346	0.006	0.043	0.000	0.000	0.000	0.000	0.000	0.017	0.381	0.191	0.000	0.016
	336	Spring	-	0.346	0.006	0.043	0.000	0.000	0.000	0.000	0.000	0.017	0.381	0.191	0.000	0.016
400+	1	Spring*	4	0.671	0.000	0.039	0.000	0.076	0.000	0.000	0.000	0.000	0.000	0.140	0.074	0.000
	91	Summer*	-	0.671	0.000	0.039	0.000	0.076	0.000	0.000	0.000	0.000	0.000	0.140	0.074	0.000
	92	Summer	12	0.894	0.000	0.083	0.000	0.005	0.001	0.000	0.004	0.000	0.006	0.001	0.001	0.005
	154	Fall	7	0.475	0.000	0.016	0.000	0.022	0.000	0.001	0.000	0.141	0.075	0.270	0.000	0.000
	245	Winter	-	0.475	0.000	0.016	0.000	0.000	0.000	0.000	0.000	0.141	0.098	0.270	0.000	0.000
	336	Spring	-	0.475	0.000	0.016	0.000	0.000	0.000	0.000	0.000	0.141	0.098	0.270	0.000	0.000
Redside shiner																
All	1	Spring	-	0.335	0.000	0.000	0.000	0.151	0.000	0.151	0.000	0.000	0.057	0.153	0.153	0.000
	92	Summer	-	0.335	0.000	0.000	0.000	0.151	0.000	0.151	0.000	0.000	0.057	0.153	0.153	0.000
	154	Fall	-	0.000	0.000	0.000	0.000	0.279	0.000	0.131	0.000	0.000	0.094	0.248	0.248	0.000
	245	Winter	-	0.000	0.000	0.000	0.000	0.000	0.000	0.000	0.000	0.000	0.500	0.500	0.000	0.000
	336	Spring	-	0.000	0.000	0.000	0.000	0.000	0.000	0.000	0.000	0.000	0.500	0.500	0.000	0.000

Table S9. Significance of size class as a predictor of stable isotope values for δ13C and δ15N from fish sampled in Ross Lake in the summer. Column headings represent the isotope used as a response variable and values represent p value of the nonparametric Kruskal-Wallis with size class as a predictor variable. Significant p values are reported in bold (α=0.05).

	Species	n	δ13C	δ15N
Ross Lake	RBT	37	**0.009**	**< 0.001**
	RSS	18	0.223	0.124

Table S10. Pairwise comparisons of difference in isotopic signatures between size classes from nonparametric Dunn test. Pairwise comparisons were only included for species and isotopes that were significant in the Kruskal-Wallis test. Significantly different comparisons ($p < 0.05$) are indicated in bold.

Lake	Species	Isotope	Comparison	P
Ross Lake	RBT	d13C	100-199 : 200-299	0.627
		d13C	100-199 : 300-399	1
		d13C	200-299 : 300-399	1
		d13C	100-199 : 400+	1
		d13C	**200-299 : 400+**	**0.006**
		d13C	300-399 : 400+	0.063
		d15N	100-199 : 200-299	1
		d15N	**100-199 : 300-399**	**0.005**
		d15N	**200-299 : 300-399**	**0.03**
		d15N	**100-199 : 400+**	**< 0.001**
		d15N	**200-299 : 400+**	**< 0.001**
		d15N	300-399 : 400+	0.402

Figures

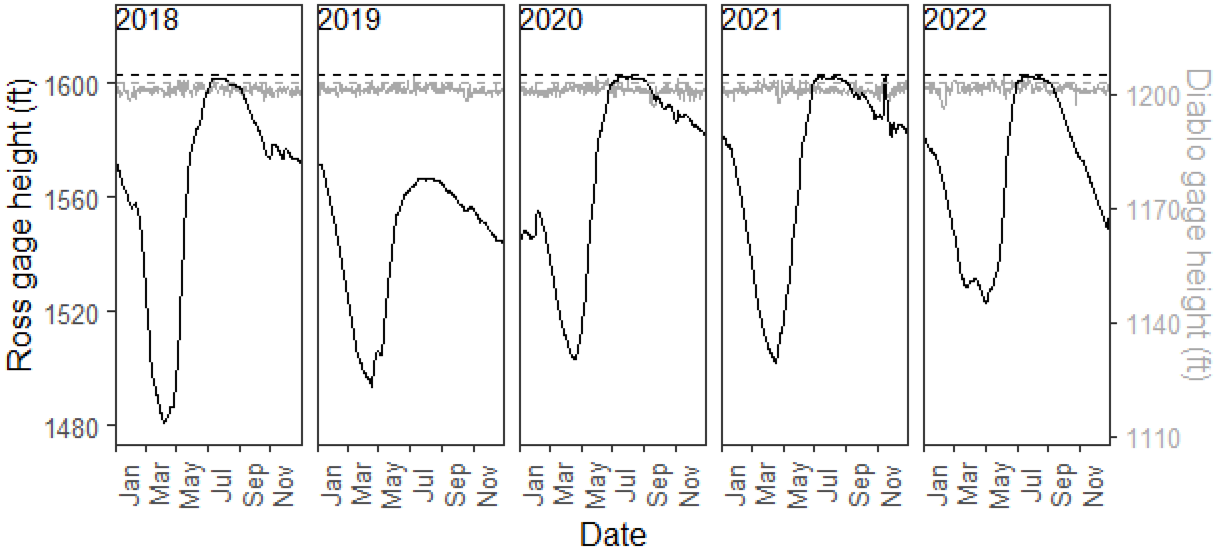

Figure S1. Reservoir surface elevation (ft) for Ross (black) and Diablo (grey) lakes in 2018-2022. Data retrieved from USGS Water Data using the 'dataRetrieval' package in R. Dotted lines represent elevation at each respective reservoirs normal 'full pool' operation.

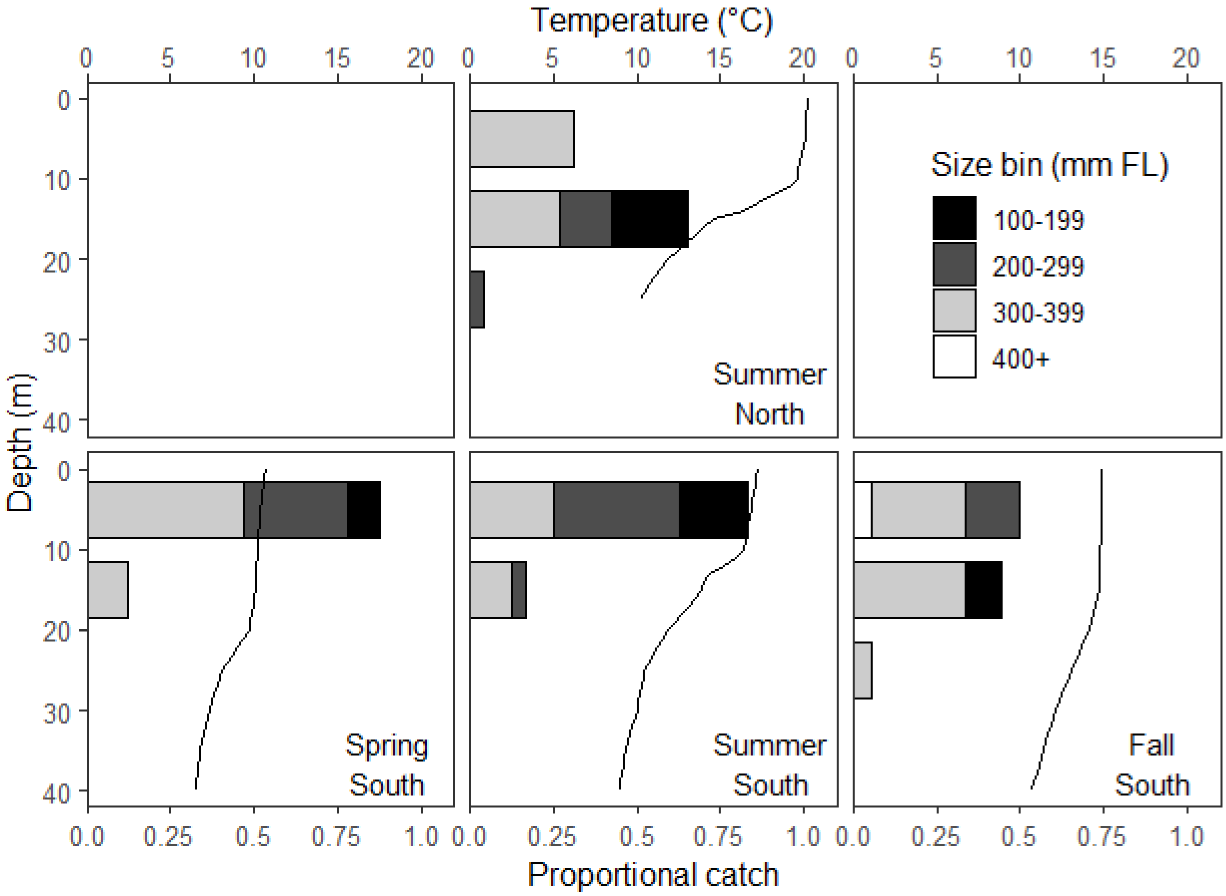

Figure S2. Depth distribution of rainbow trout as inferred through proportional catch rates in a full set of gillnet arrays in Ross Lake in 2021. Proportional catch is reported for discrete 10 m depth bins corresponding to approximate depths of gillnets, and temperature data is continuous with depth.

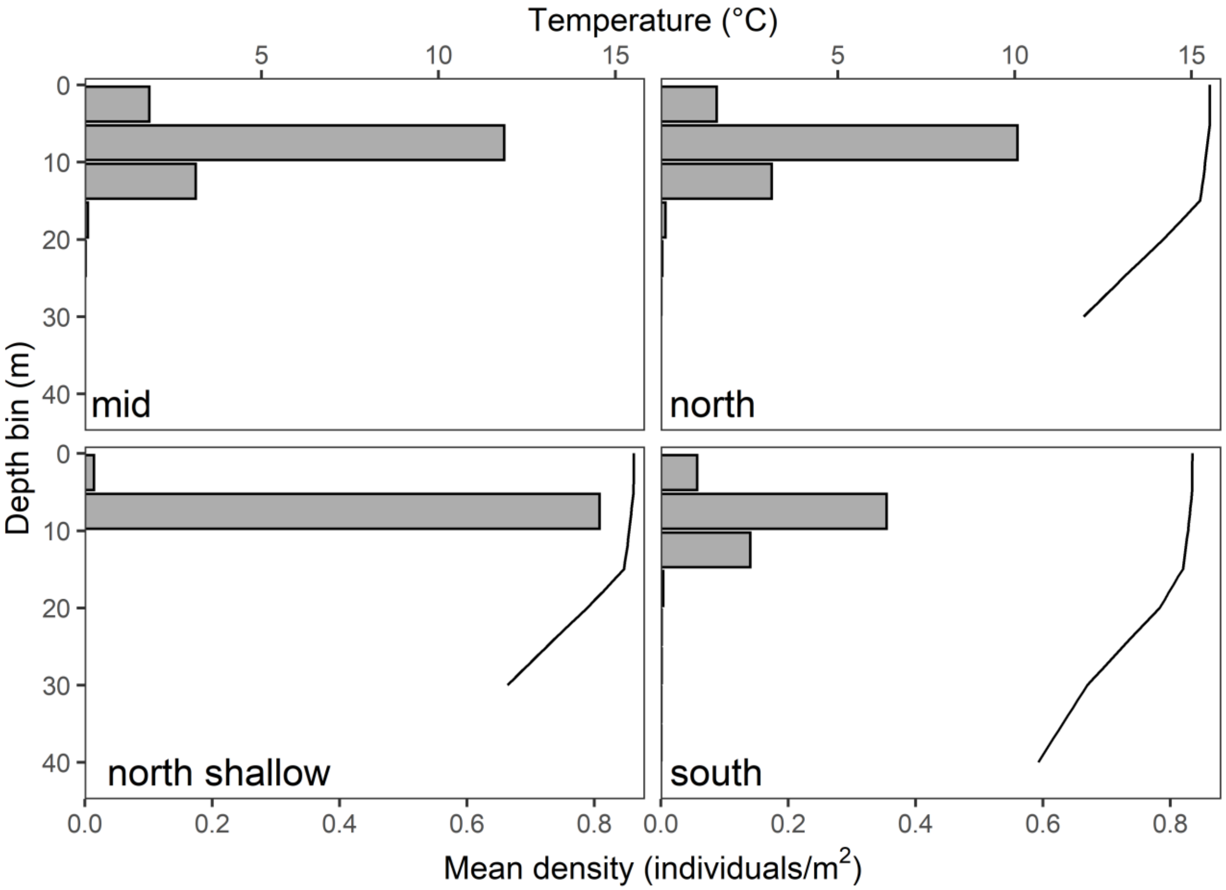

Figure S3. Depth distribution of redside shiner from hydroacoustics surveys and thermal structure in Ross Lake in early October 2021. Densities represent the region-wide average for each 5 m depth bin.

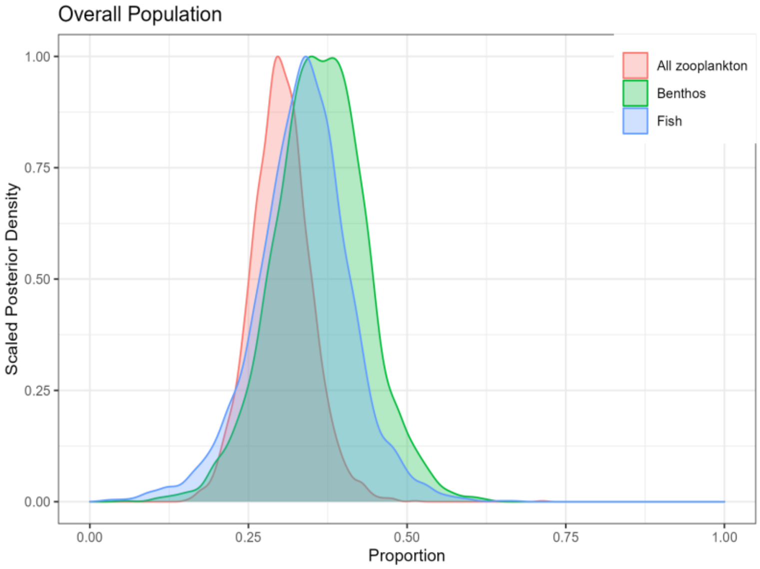

Figure S4. Stable isotope mixing model posterior densities for all redside shiner in Ross Lake sampled in the summer.

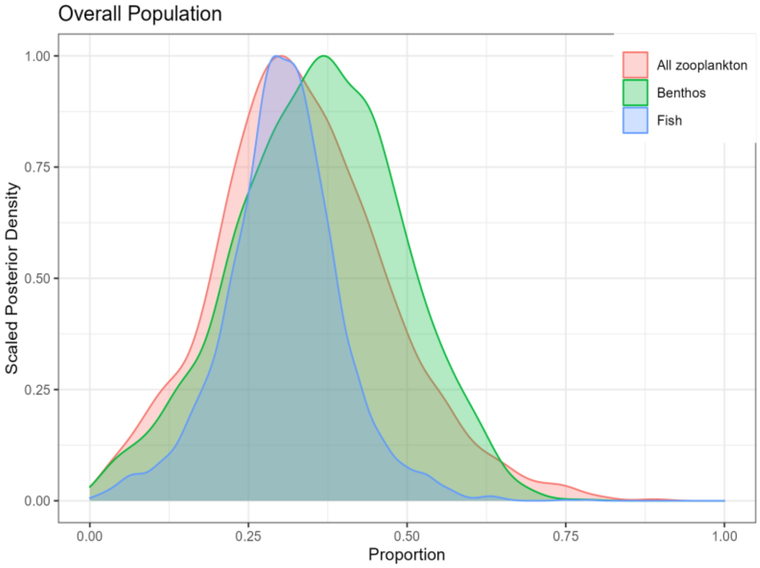

Figure S5. Stable isotope mixing model posterior densities for rainbow trout 100-199 mm FL in Ross Lake sampled in the summer.

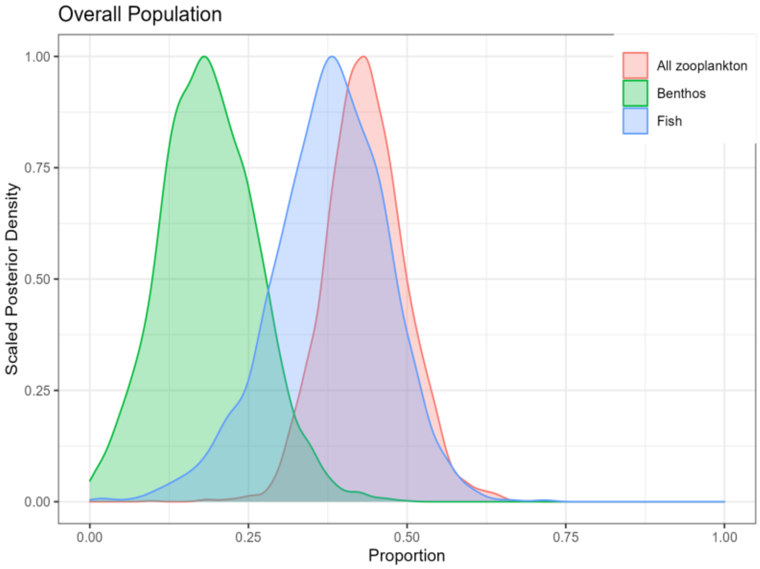

Figure S6. Stable isotope mixing model posterior densities for rainbow trout 200-299 mm FL in Ross Lake sampled in the summer.

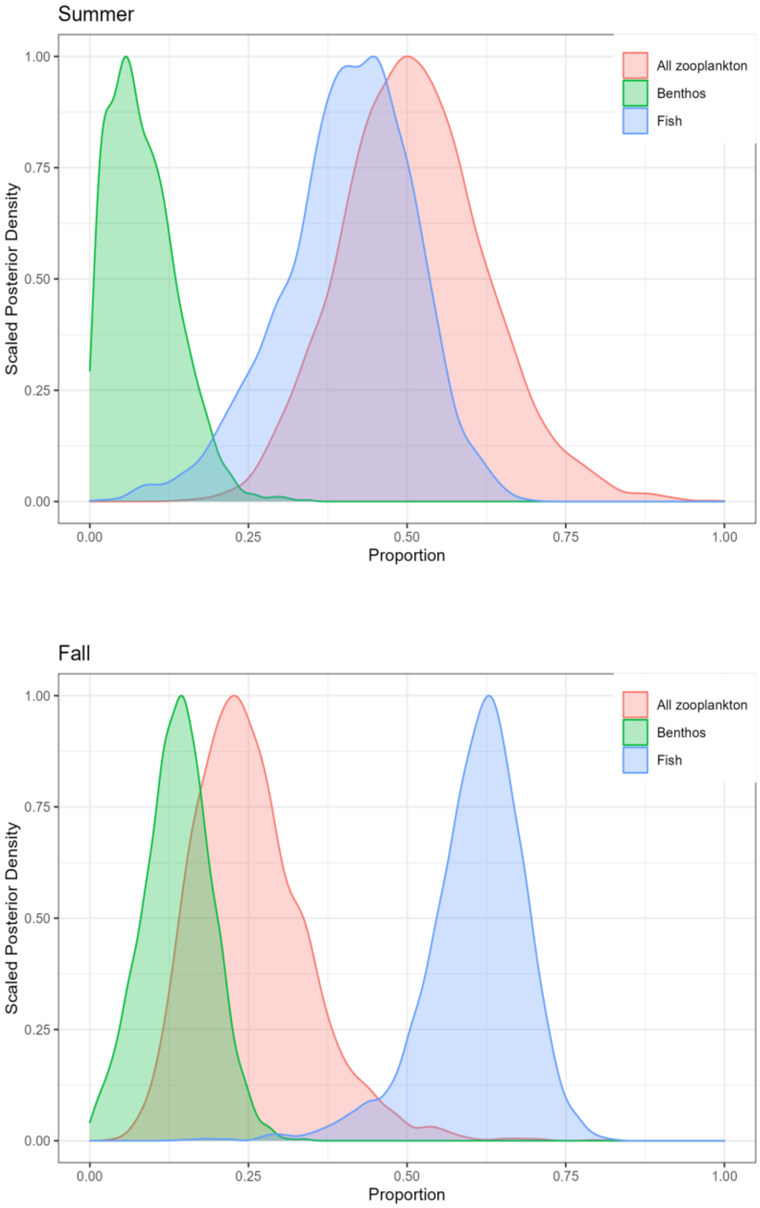

Figure S7. Stable isotope mixing model posterior densities for rainbow trout 300-399 mm FL in Ross Lake sampled in the summer and fall.

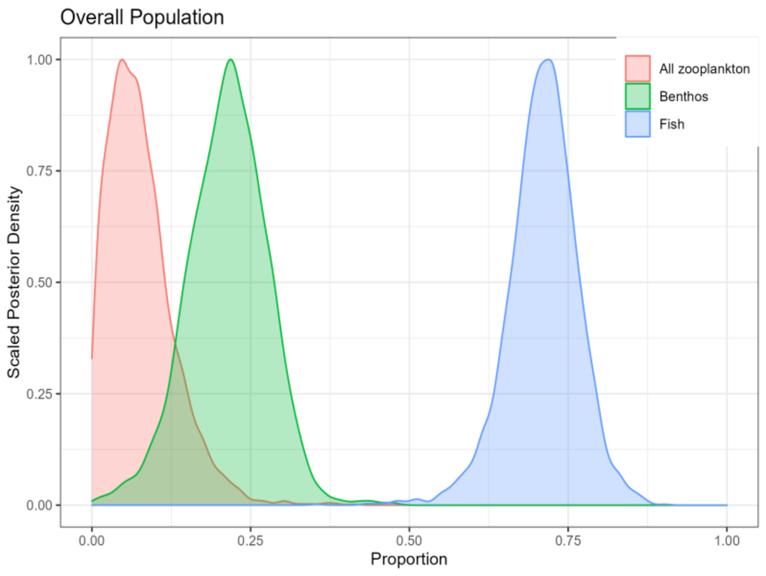

Figure S8. Stable isotope mixing model posterior densities for rainbow trout 400+ mm FL in Ross Lake sampled in the summer.

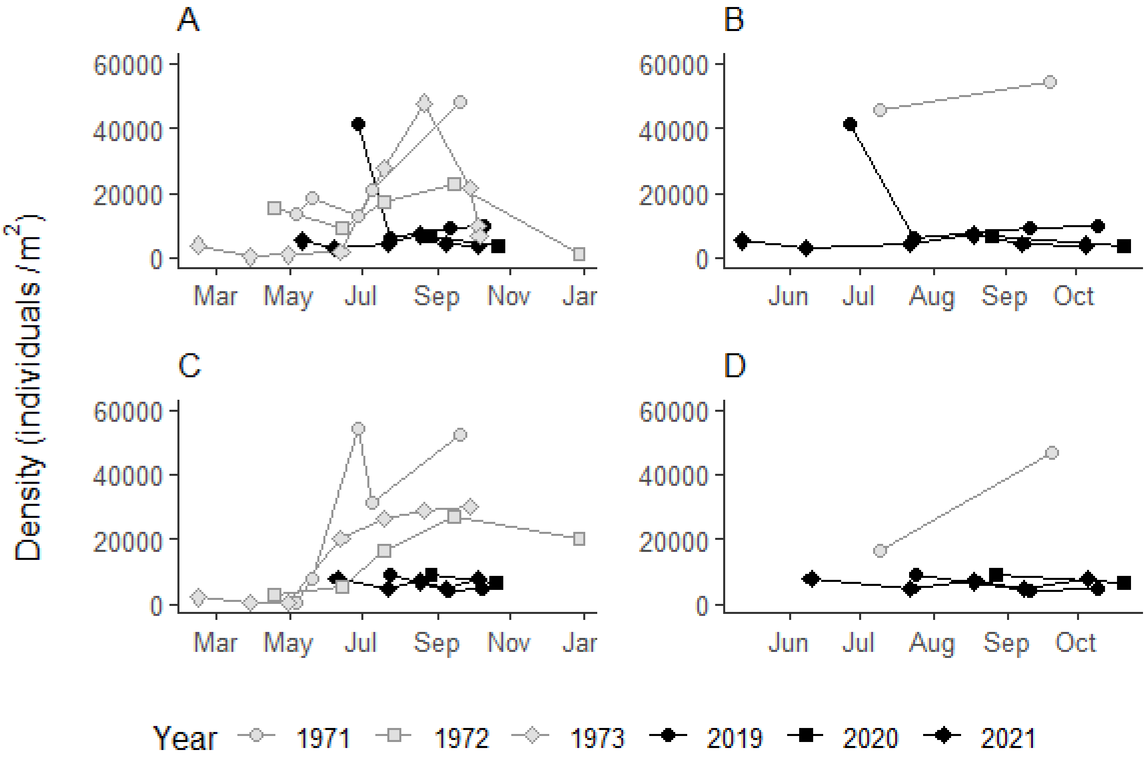

Figure S9. Comparisons of areal daphnia density from a historical study (Seattle City Light 1974) to the current study. Comparisons are made in the southern region between the current Big Beaver Creek site and the historical Station #1 near the log boom (A) and historical Station #3 near Devils Creek (B), as well as the mid/northern region between the current Little Beaver Creek site and the historical Station #5 near Lightning Creek (C) and the historical station #6 near Silver Creek (D). Note that historical zooplankton collection sampled the entire water column from the bottom depth to the surface, while zooplankton collection in the current study sampled from 20 m depth to the surface.

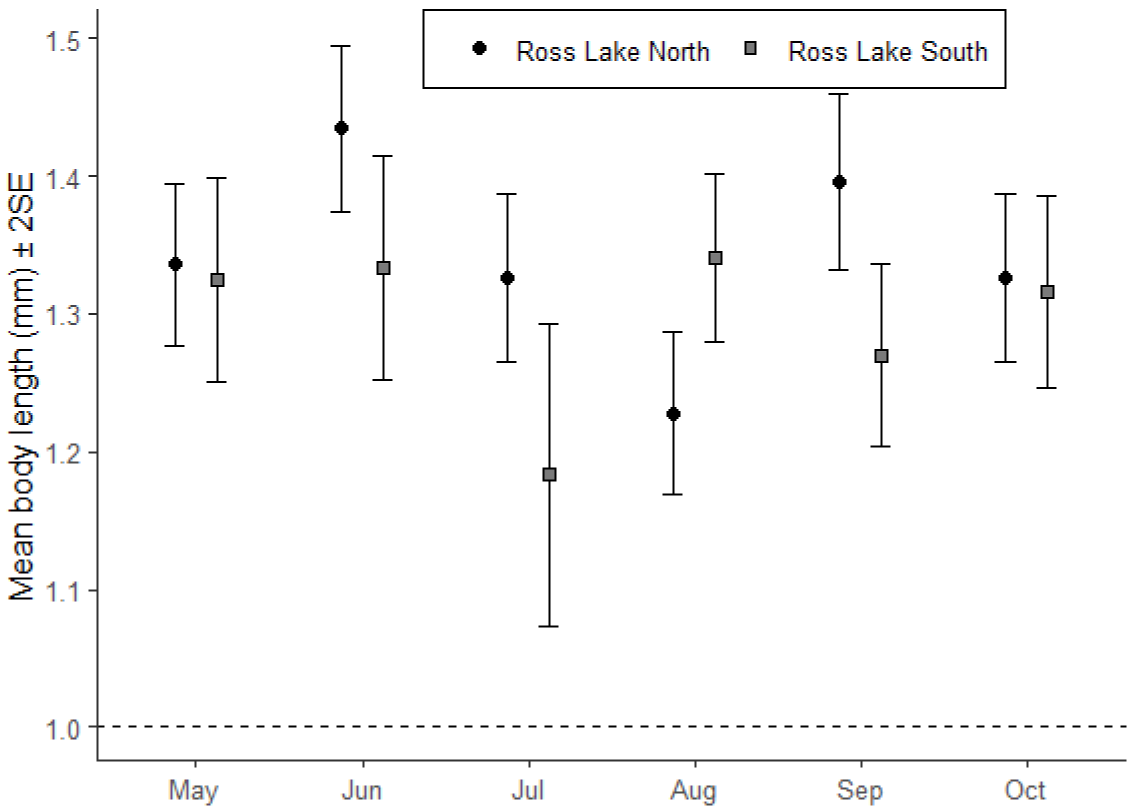

Figure S10. Monthly mean Daphnia body lengths (mm) in the 0-20 m samples at each site in 2021. Dashed line at 1-mm represents minimum edible size for salmonids.

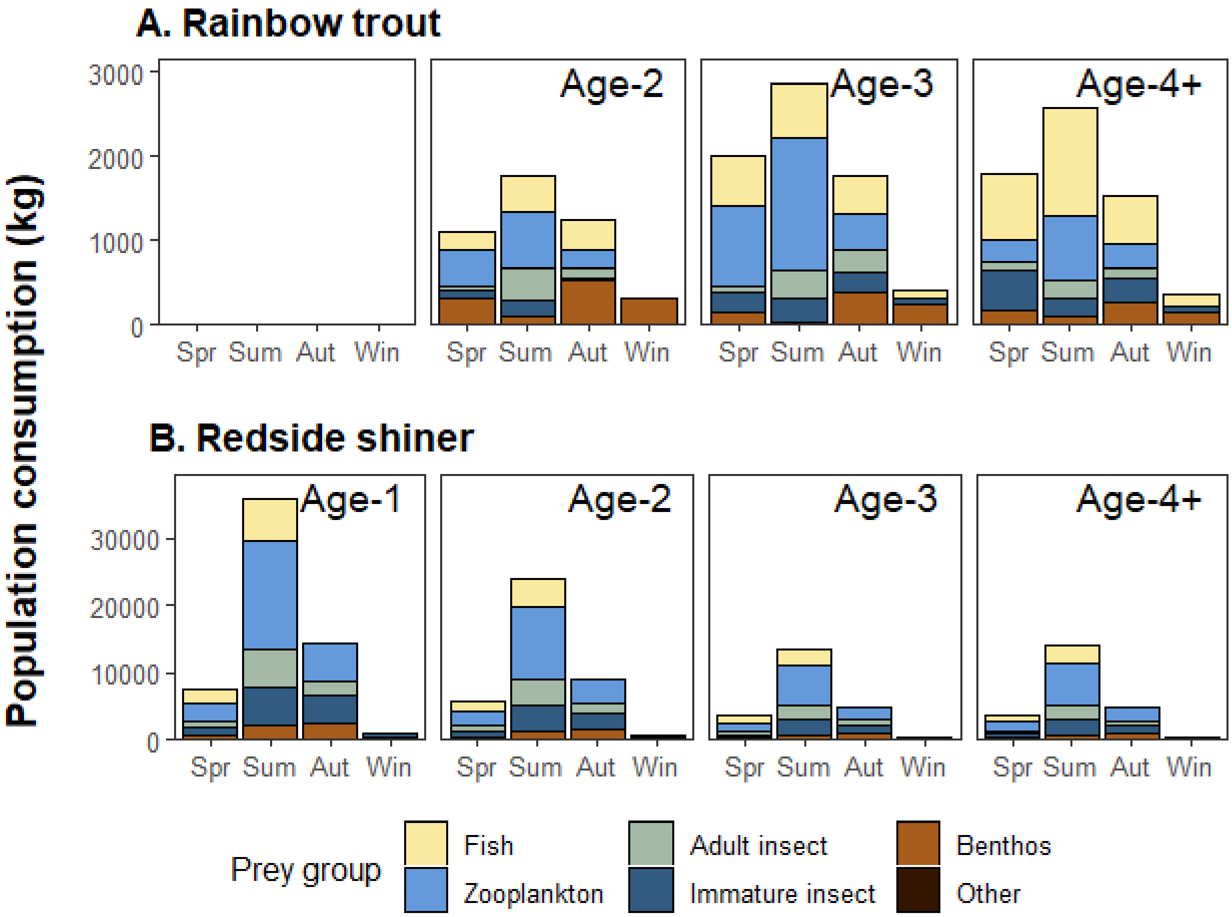

Figure S11. Seasonal population consumption in Ross Lake. Note the difference y-axis scales between A and B.

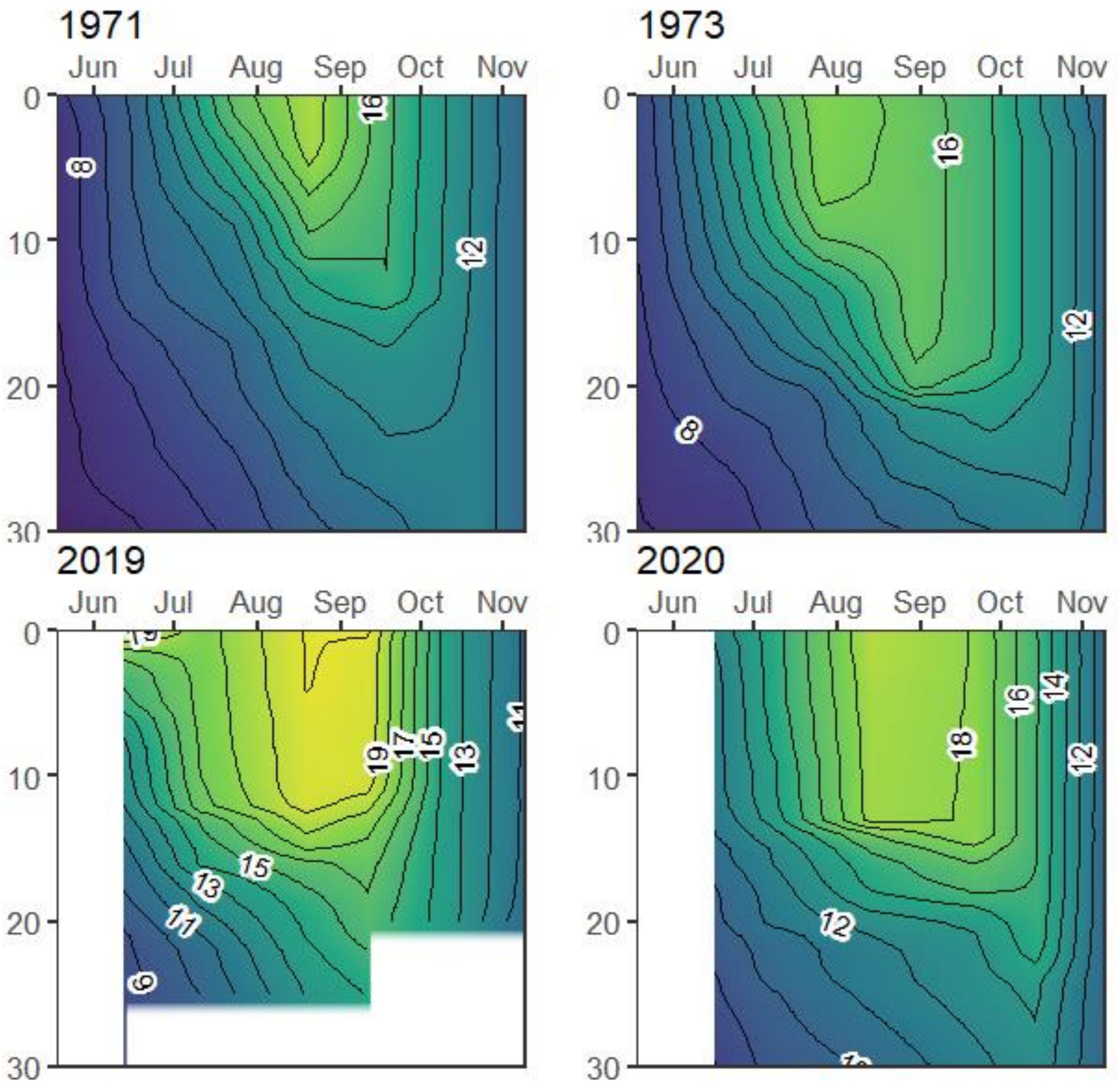

Figure S12. Historical comparison of thermal structure in Ross Lake. Data in 1971 and 1973 was taken near Devils Creek while data in 2019 and 2020 was taken off of Skymo Creek.

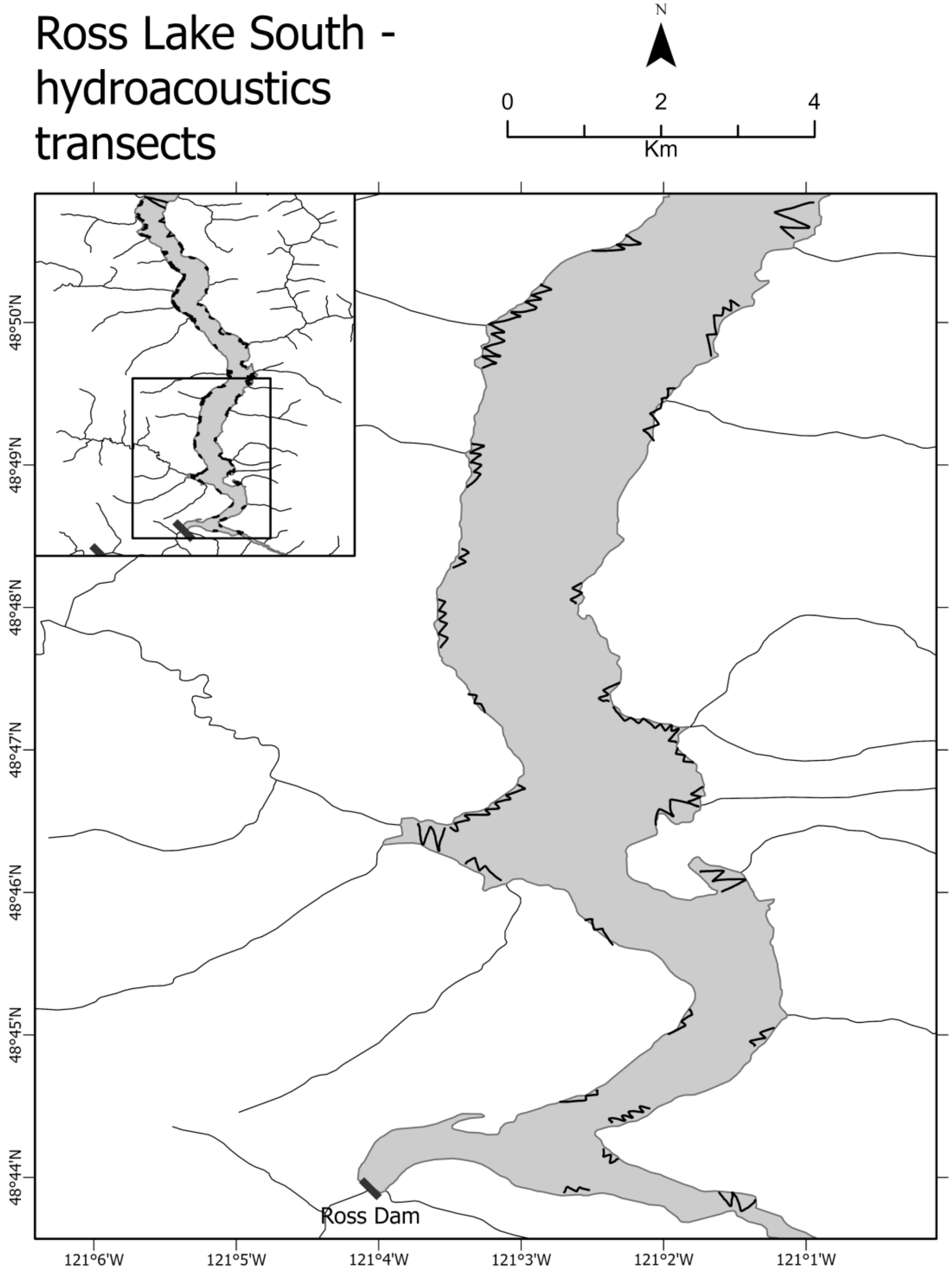

Figure S13. Map of Ross Lake hydroacoustics transects surveyed at night in the southern region in October 2021.

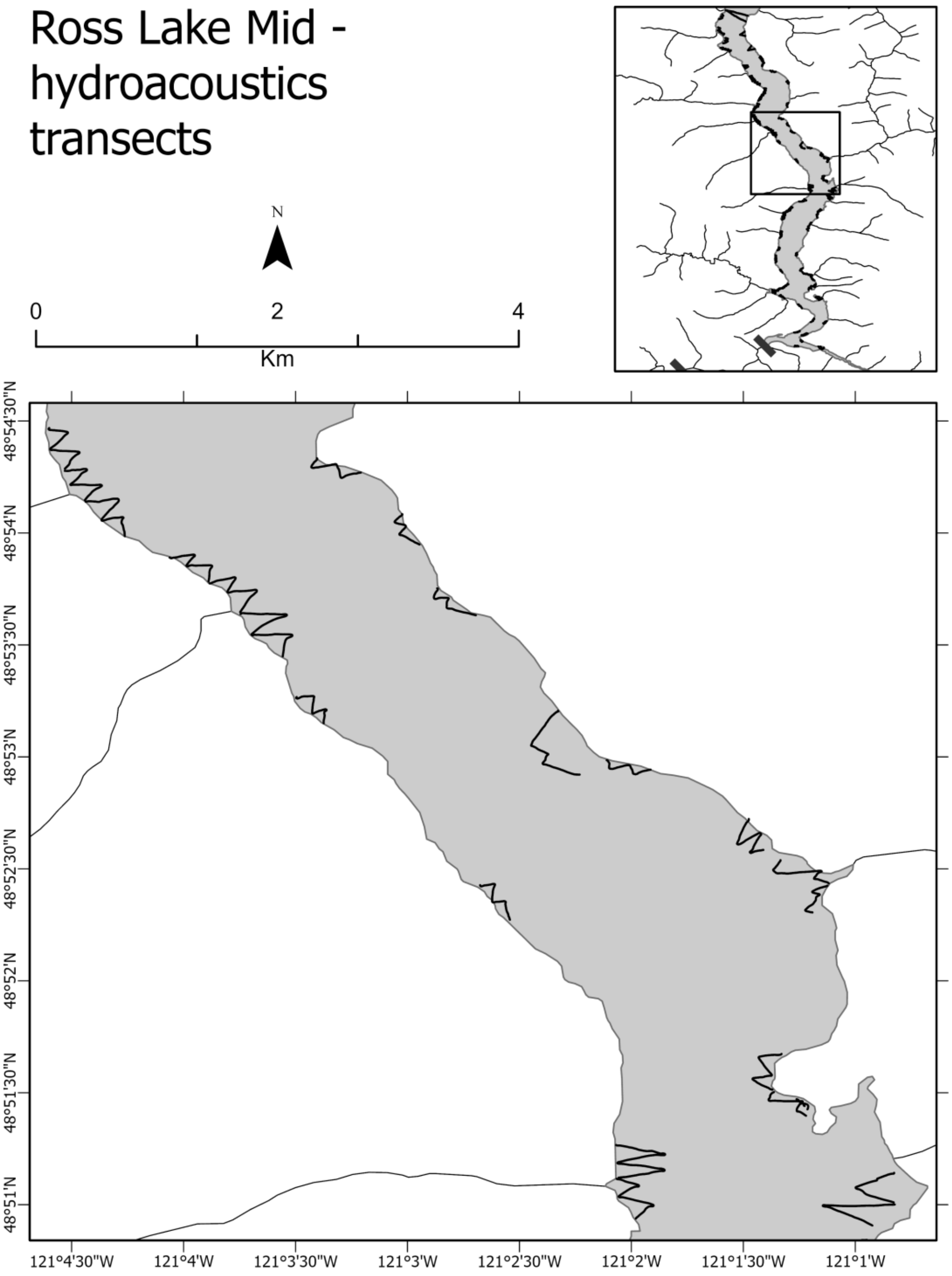

Figure S14. Map of Ross Lake hydroacoustics transects surveyed at night in the middle region in October 2021.

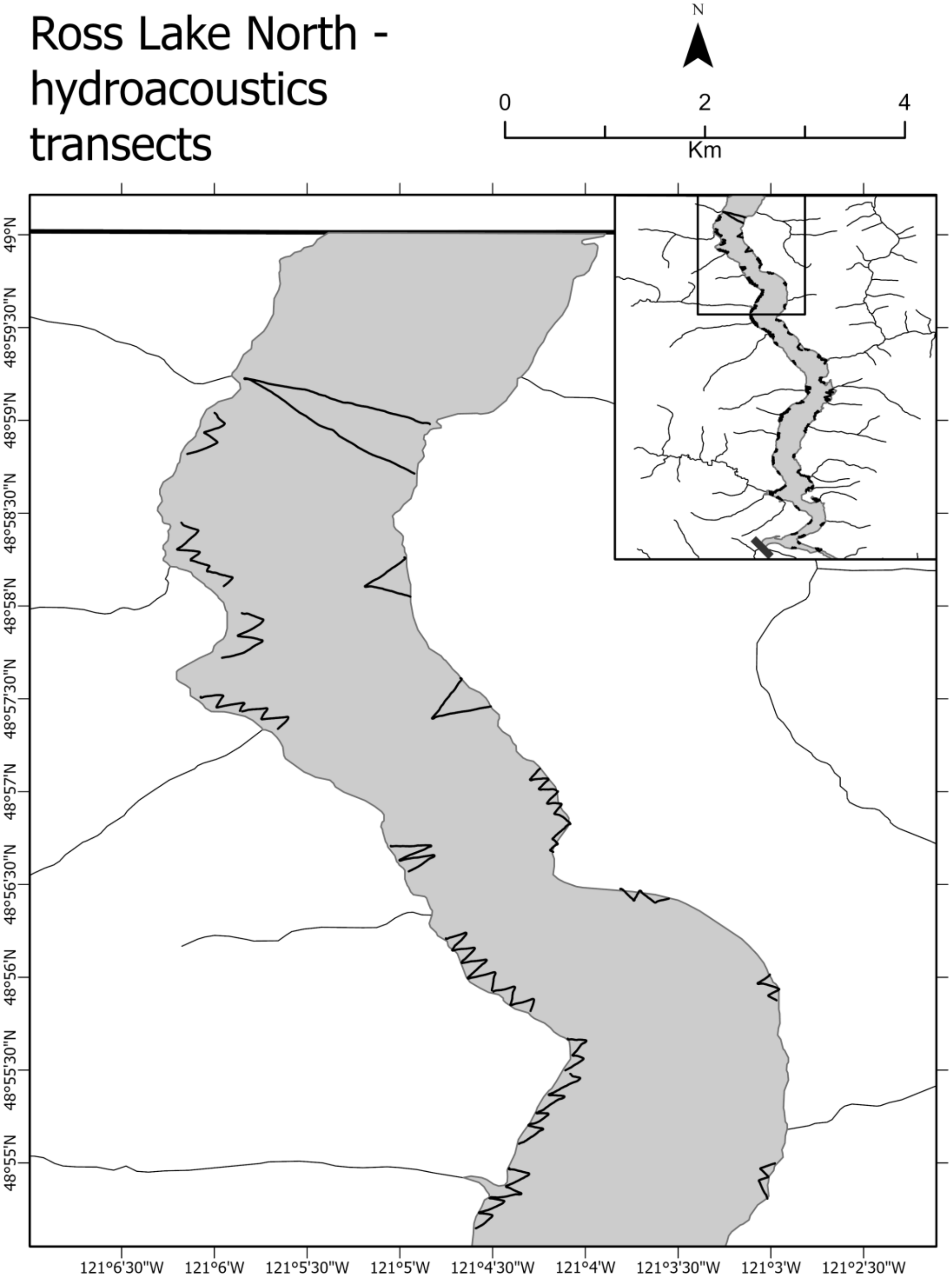

Figure S15. Map of Ross Lake hydroacoustics transects surveyed at night in the northern region in October 2021.

Chapter 2: Supplementary Materials - Diablo Lake

Methods

Study system

Diablo Lake is downstream from Ross Lake and much smaller (elevation at full pool = 368 m, storage at full pool = 0.112 km^3, max depth = 98 m, mean depth = 35 m), with lower visibility due to modest levels of glacial turbidity. Due to hypolimnetic withdrawal from Ross Lake, Diablo Lake is colder, weakly stratified, and lake level fluctuates within ± 1.5 m throughout the year (Fig. S16; Fig. S1). Native fish species assemblage is the same as Ross Lake. Redside shiner presumably spread to Diablo Lake after their introduction into Ross Lake, but the population has not yet proliferated to the same magnitude. Diablo Lake has low levels of natural fish production and is regularly stocked with rainbow trout from the Marblemount Hatchery, originated from Ross Lake broodstock (Table S11).

Fish collection

Fish collection methods were the same as described for Ross Lake. Fish sampling in Diablo Lake was particularly constrained by resource managers due to concerns about incidental lethal take of bull trout; consequently, few samples were available to analyze.

Hydroacoustics surveys

We conducted hydroacoustic surveys to estimate the distribution, density, and abundance of redside shiner in Diablo Lake during September 2021. Most of the accessible shoreline of Diablo Lake was surveyed in a single night (limited by shallow water and other hazards; Fig.

S17), supplemented with additional daytime surveys. Acoustic targets were ground truthed by deploying a sinking multi-mesh gillnet (36-m by 1.8-m; stretched mesh panel sizes (mm): 20, 25, 37, 50, 66, 76) during one of the surveys where we identified fish targets.

In Diablo Lake, echo counting was used in Echoview (version 13.0) to identify all single targets in each transect, which were filtered to include only fish from approximately 30-120 mm TL (target strength: -56.1 to -45.0 dB). Such targets were assumed to be redside shiner, based on the minimum size of salmonids captured in the ground-truth gillnet set. Transects were divided into 5-m depth intervals and 10-m distance intervals for analysis to minimize errors in volumetric density estimates due to varying nearshore bottom slope. In each transect, average density (fish per m2) was computed across all distance intervals for each 5-m depth interval and size class (30-69 mm, 70-99 mm, and 100-119 mm FL). A lake-wide average density was computed and expanded to a population estimate using an estimated occupied area of 1.96 km2, which encompasses the sampled littoral zone and all of Skagit Arm.

Size structure, abundance, mortality

We used data from the hydroacoustic surveys to estimate total abundance of redside shiner > 40 mm FL in Diablo Lake. Fish < 70 mm FL (< age 3) were not effectively sampled by hydroacoustics in Diablo Lake, thus we back-calculated age-specific abundance for ages 1 and 2. Population abundances of the salmonid species are not well studied in this system and not conducive to hydroacoustic techniques, thus we analyzed dietary consumption in Diablo Lake based on size structured unit populations of 1,000 rainbow trout > 200 mm FL. This approach allows managers to easily scale the resulting consumption estimates up or down to evaluate different predation scenarios based on alternative population estimates and uncertainty (Beauchamp et al. 2007).

We created age-structured populations for each species using annual survival rates (S) to allocate these total population abundances to each age-class for each species. To estimate S for rainbow trout, we used weighted catch curve analysis on gillnet monitoring data from 2006-2018 (collected and maintained by North Cascades National Park). For redside shiner in Diablo Lake, we estimated annual survival using size distribution data of fish > 70 mm FL observed in the hydroacoustics survey, due to limited hydroacoustic observations of smaller fish in this lake. We used these data to estimate annual instantaneous mortality rates (Z) and annual survival rates (S) for each species (Table S12; Miranda and Bettoli 2007). We then created estimates of daily age-class abundance for an annual cycle by applying the daily instantaneous mortality rate (Z/365) to the initial age-class abundance estimate.

Prey availability

Zooplankton were collected at a single site in the main basin of Diablo Lake and all collection and analysis followed the methods described for Ross Lake. In the absence of bathymetric data for Diablo Lake, pelagic volume in the epi- and metalimnion was estimated by multiplying the reported surface area of the lake (325 ha) by 10 m. Notably, this will result in an overestimate of biomass and production as it does not account for the area of shallow littoral zone.

Stable isotope analysis

Stable isotope analysis for fish sampled in Diablo Lake followed the methods described for Ross Lake. In Diablo Lake, most fish samples came from 2019 and 2017 (samples collected and maintained by North Cascades National Park) while all invertebrate samples were collected in 2019.

Bioenergetic model inputs

Bioenergetic analysis for fish in Diablo Lake followed the methods described for Ross Lake.

Thermal experience and depth – Continuous vertical temperature profiles were collected from the limnology station in the main basin of Diablo Lake (4 times/day) to measure the thermal structure of the lake. Temperatures from discrete depths were linearly interpolated to generate a symmetric grid of temperatures for computing mean temperatures across layers (epi-, meta-, and hypolimnion) and through time. Due to a lack of data in Diablo Lake, we inferred species vertical distribution based on patterns observed in Ross Lake for rainbow trout. We used the same rules reported in those methods to assign daily thermal experience for fish in Diablo Lake (Table S13).

Diet composition – Seasonal diet inputs used in the bioenergetics simulations were compiled from a combination of stomach content analysis, stable isotope mixing models (SIMMs), and general ecological knowledge/assumptions. We describe the specific methods we used to do this in the main supplement. Stomach contents were only collected for rainbow trout in Diablo Lake; therefore, we relied on stable isotope data to inform diet inputs for redside shiner in

Diablo Lake. We report mean diet proportions (by weight) from stomach content analysis (Table S14), diet proportions from SIMMs compared with stomach content analysis (Table S15), and diet proportions used as inputs for the bioenergetic simulations (Table S16).

Age, growth and energy density – Scale analysis and back-calculation was done separately for rainbow trout in Diablo Lake (scale radius-FL regression: $FL = 39.885 + 162.11 \times SR$, R^2=0.862); however, limited redside shiner collected in Diablo Lake required us to pool data across both reservoirs for the scale-radius regression and FL-weight regression (equations described in the methods for Ross Lake). Limited fish samples collected in Diablo Lake required us to use energy density values from Ross Lake.

Consumption demand and carrying capacity

Estimation of consumption demand and carrying capacity in Diablo Lake followed the methods described for Ross Lake. We did not evaluate a depth-use scenario for Diablo Lake because temperatures were low enough that thermal restriction of salmonids was not expected.

Results

Stable isotope analysis

In contrast to Ross Lake, rainbow trout isotopic signatures in Diablo Lake did not differ among size classes (Fig. S18; Kruskal-Wallis p-value > 0.05). Rainbow trout of all sizes were positioned at a low trophic level with a moderate position on the benthic-pelagic axis (N = 35; mean ± SE: δ^{15}N = 6.7 ± 0.1, δ^{13}C =-26.2 ± 0.3). Redside shiner in Diablo Lake also showed similar isotopic signatures between size classes and occupied a similar isotope space as the rainbow trout ($N = 26$; mean ± SE: $\delta^{15}N = 7.1 \pm 0.1$, $\delta^{13}C =-25.4 \pm 0.4$).

Diet composition

As in Ross Lake, diet proportions estimated from SIMMs tended to estimate higher contributions of fish prey for rainbow trout and redisde shiner in Diablo Lake compared to stomach contents (Table S15; Fig. S19-S20), and we attributed this to predation on redside shiner eggs and larvae. Therefore, we relied on SIMMs to inform the contribution of fish prey for these groups for the spring-summer interval and adjusted the other prey groups accordingly for bioenergetics simulations. We had no diet data from redside shiner in Diablo Lake, thus we relied entirely on proportions estimated from SIMMs.

Daphnia availability

Daphnia densities and seasonal trends seemed similar among years in Diablo Lake, characterized by low availability of edible-sized *Daphnia* ≥ 1 mm BL (< 1 individual/L; Fig. S21). *Daphnia* densities peaked in the spring (May or June) and were generally lower in the metalimnion (10-20 m) than in the epilimnion. Mean *Daphnia* body lengths were generally ≥ 1 mm except during August (Fig. S22).

Redside shiner abundance and distribution

Redside shiner distribution was patchy in both lakes, and density (individuals/1000 m^2) was about 100 times higher in Ross Lake compared to Diablo Lake (mean ± SD: 5 ± 18). We observed low densities of fish < 70 mm FL in Diablo Lake (15% of total estimate abundance), thus we assumed that this size class, which approximately corresponds to fish < age 3, was not effectively sampled by the hydroacoustics gear in Diablo Lake. Abundance in Diablo Lake was estimated using the lake-wide mean density estimate multiplied by 1.969 km^2 of occupied nearshore, including all of Thunder Arm and Skagit Arm, resulting in an estimated 10829 redside shiner > 70 mm. Abundance of fish < 70 mm FL (age 1-2) was back-calculated from this estimate assuming constant survival rates, for a total estimated population of approximately 22,000 fish age 1+ (Table S12).

Thermal experience and depth use

Redside shiner depth distribution was inferred from hydroacoustic surveys, thus limiting our ability to evaluate seasonal/thermal influences on their habitat use. In Diablo Lake, the September survey occurred while the lake was still weakly stratified, with a surface temperature just under 15 °C and declining to around 10 °C by 20 m (Fig. S23). Most redside shiners occupied 5-10 m in early September (74%), with fewer numbers occupying 10-25 m (18%). This pattern was true for 50-80 mm and 80-120 mm FL fish, however smaller redside shiners were most abundant in the 15-20 m depth stratum.

Consumption demand vs prey supply

Despite substantially lower redside shiner density in Diablo Lake compared to Ross Lake, the growth environment for rainbow trout is not more favorable. Rainbow trout generally fed at lower rates in Diablo Lake compared to Ross Lake but growth efficiency was roughly the same (23-33 %C_{max}; 6-10% GE; Table S17). In Diablo Lake, rainbow trout consumption was more variable than in Ross Lake (Fig. S18), with zooplankton the dominant prey during the summer and benthos contributed more during the spring and fall (Fig. S24). Per capita consumption demand on *Daphnia* increased with age and was highest in the summer (Fig. S25A). Rainbow trout in Ross Lake consumed more energy annually and fish contributed more to the energy budgets of every age class compared to those in Diablo Lake (Fig. S26). Fish were a minor contribution to energy budgets in Diablo Lake rainbow trout, and the remaining prey categories contributed similar amounts.

Daphnia production and biomass was lowest in August, when consumption per 1,000 rainbow trout 200+ mm FL (age 3+) completely exceeded both production and biomass of *Daphnia*, suggesting a bottleneck in prey supply during this month (Fig. S25). Low *Daphnia* production during this month was a result of zero eggs observed in the August zooplankton samples. Per capita consumption of *Daphnia* by redside shiner in Diablo Lake was 30-140x lower than that of rainbow trout at the same age (Table S17). Total consumption by the estimated population of approximately 20,000 redside shiner was also minimal, accounting for less consumption than 1,000 age 2 rainbow trout or the unit population of 1,000 age 3+ rainbow trout (Fig. S25B).

Bioenergetic simulations estimated that redside shiner would have to feed at higher rates in Diablo Lake compared to Ross Lake to meet observed growth (129-156 %C_{max}; Table S17). Growth efficiency of redside shiner was also higher in Diablo Lake compared to Ross Lake (11-14%). Redside shiner consumption peaked in the summer and was nearly 2.5x higher than spring or fall consumption in Diablo Lake (Fig. S24).

Discussion

Our quantitative food web analysis in in Diablo Lake highlighted the lesser role that redside shiner play as a zooplankton consumer where they are less abundant and the cooler water may suppress growth. In contrast to Ross Lake, extremely low production and biomass estimates for Diablo Lake in August suggest that *Daphnia* resource scarcity was likely limiting during this month, though this appears to depend on rainbow trout abundance (resulting from stocking rates and mortality) rather than the redside shiner population. This inference is also supported by the large decrease in *Daphnia* body length from May to August, indicating high fish predation pressure (Jeppesen et al. 2002; Iglesias et al. 2011). The contrast between the two reservoirs suggests that redside shiner have a low per capita effect on prey supply and their community level effects are driven by abundance.

Though redside shiner densities were orders of magnitude lower in Diablo Lake than in Ross Lake, rainbow trout did not exhibit faster growth. *Daphnia* densities in the two lakes were comparable, though slightly lower in Diablo in July, August, and October. Notably, around 318,000 hatchery fry were released just 10 days before our October zooplankton sample was collected, possibly contributing to the very low *Daphnia* density observed (0.015/L). Comparable contributions of benthos to annual energy budgets further indicated that resources were similarly limited in both lakes. Given relatively low redside shiner consumption in Diablo Lake, it seems most likely that any exploitative competition and food limitations during the growing season will depend on rainbow trout stocking rates.

In Diablo Lake, a lack of data on overwinter survival of hatchery fry that are planted in the fall introduced considerable uncertainty in rainbow trout population abundance. For example, in October 2020, around 250,000 rainbow trout fry (mean weight approx. 0.5 g) were released, which could result in 2,500 yearlings the following spring if survival is only 1% or 25,000 if survival was 10%. This uncertainty translates into a substantial range of estimated consumption demand and makes it challenging to assess the current capacity of Diablo Lake. Despite this uncertainty, *Daphnia* production and biomass is low enough in August to indicate that the planktivore population overwhelmed supply during this month. If survival of hatchery plants is on the higher end (> 4%), the lake could approach capacity in July as well. Data on performance and survival of hatchery plants could be used to obtain better estimates of carrying capacity in Diablo Lake.

The stark difference in redside shiner density in Diablo Lake compared to Ross Lake presents an opportunity to explore the potential factors restricting their population growth and food web impact. One hypothesis is that the colder thermal regime in Diablo is preventing adequate growth required to survive the winter. Growth based on scale back-calculations was predicted to be higher in Diablo compared to Ross, however these estimates were based on a small number of large/older individuals, which may not be representative of true growing conditions in Diablo Lake. Due to colder temperatures, the consumption rates required to reach these high growth rates are well above 100% C_{max}. It is possible that these fish spilled over from Ross Lake and thus their growth rates are representative of Ross Lake rather than Diablo. We collected no small (< 80 mm FL) redside shiner in Diablo Lake minnow traps, precluding us from obtaining a better growth estimate in this lake. Size distributions from hydroacoustics analysis also suggests that there are more fish 80-120 mm FL than in other size bins, and age 1 fish (ca. 30-50 mm FL) represent the smallest proportion – a result that differs substantially from the size structure predicted using Ross Lake survival rates. This lends support to the hypothesis that population growth in Diablo Lake is restricted by low survival rates of smaller fish. It is unclear whether this is due to low temperatures, the bottleneck in food availability during peak growing season, or a combination of the two. However, regional trends in Ross Lake densities follow temperature gradients (high densities in the warm north, lowest densities in the colder south), and we did not observe substantial regional differences in *Daphnia* availability. This suggests that temperature could play an important role in mediating impacts, consistent with the environmental matching hypothesis (Iacarella et al. 2015). The role of temperature in restricting growth and survival could be determined using laboratory experiments or by collecting seasonal growth data in the field and would be critical information to understanding the risk of population expansion due to warming climate and/or changes to water operations.

References

Beauchamp, D. A., D. H. Wahl, and B. M. Johnson. 2007. Predator-Prey Interactions. Pages 765–842 *in* C. S. Guy and M. R. Brown, editors. Analysis and interpretation of freshwater fisheries data. American Fisheries Society.

Iacarella, J. C., J. T. A. Dick, M. E. Alexander, and A. Ricciardi. 2015. Ecological impacts of invasive alien species along temperature gradients: Testing the role of environmental matching. Ecological Applications 25:706–716.

Iglesias, C., N. Mazzeo, M. Meerhoff, G. Lacerot, J. M. Clemente, F. Scasso, C. Kruk, G. Goyenola, J. García-Alonso, S. L. Amsinck, J. C. Paggi, S. J. de Paggi, and E. Jeppesen. 2011. High predation is of key importance for dominance of small-bodied zooplankton in warm shallow lakes: Evidence from lakes, fish exclosures and surface sediments. Hydrobiologia 667:133–147.

Jeppesen, E., J. P. Jensen, S. Amsinck, F. Landkildehus, T. Lauridsen, and S. F. Mitchell. 2002. Reconstructing the historical changes in Daphnia mean size and planktivorous fish abundance in lakes from the size of Daphnia ephippia in the sediment. Journal of Paleolimnology 27:133–143.

Miranda, L. E., and P. W. Bettoli. 2007. Mortality. Pages 229–277 *in* C. S. Guy and M. L. Brown, editors. Analysis and interpretation of freshwater fisheries data. American Fisheries Society.

Tables

Table S11. Recent stocking reports for rainbow trout in Diablo Lake. Data acquired from the Washington Department of Fish and Wildlife (WDFW).

Release date	Fish per pound	Number released	Mean fish weight (g)
06 Oct 2015	1,200	172,213	0.4
18 Oct 2016	1,000	172,929	0.5
28 Oct 2016	1,000	48,700	0.5
28 Apr 2017	200	84,750	2.3
21 Sep 2017	1,200	170,000	0.4
04 Apr 2018	175	85,000	2.6
08 Oct 2018	984	276,600	0.5
02 Oct 2019	713	140,229	0.6
	994	80,662	0.5
06 Oct 2020	963	249,097	0.5
04 Oct 2021	771	318,485	0.6
18 Oct 2022	750	278,347	0.6

Table S12. Estimated age-structured populations and mortality rates for rainbow trout and redside shiner in Diablo Lake. Age structured populations were based on 1,000 rainbow trout ≥ 200 mm FL (age 3+) and 1,000 redside shiner ≥ 70 mm FL (age 3+), as smaller fish were not effectively sampled by the hydroacoustics. Data was too limited in Diablo Lake, thus rainbow trout are reported as a unit population of 1,000. Redisde shiner population abundance was estimated from hydroacoustics surveys in October 2021 and annual survival rate was estimated from the size distribution observed in the hydroacoustics survey.

Species	Z	Annual survival (%)	Age	Abundance per 1,000 fish[a]	Estimated population size[b]	Age-specific abundance
Rainbow trout	1.315	26.8	1	10,944	1,000	10,944
			2	2,937		2,937
			3	788		788
			4	212		212
Redside shiner	0.288	75.0	1	583	11,000	6,413
			2	437		4,807
			3	328		3,608
			4	246		2,706
			5	184		2,024
			6	138		1,518
			7	104		1,144

[a] For salmonids, age-structured populations were based on 1,000 fish ≥ 200 mm FL (age 3+); for redside shiner, this was based on 1,000 fish ≥ 70 mm FL (age 3+) in Diablo Lake, as smaller fish were not effectively sampled by the hydroacoustics

[b] Data was too limited in Diablo Lake, thus salmonid species are reported as a unit population of 1,000. For redside shiner, we used estimates of population abundance from hydroacoustics surveys.

Table 13. Mean thermal experience for rainbow trout and redside shiner during each month in Diablo Lake.

	Temperature °C	
Month	RBT	RSS
Jan	5.0	5.0
Feb	5.0	5.0
Mar	5.7	5.7
Apr	7.5	7.5
May	9.9	9.5
Jun	11.4	10.9
Jul	13.4	12.9
Aug	14.3	13.8
Sep	13.1	12.7
Oct	11.1	11.0
Nov	9.3	9.3
Dec	6.8	6.8

Table S14. Seasonal diet proportions (wet weight, g) for rainbow trout in Diablo Lakes from stomach content analysis. N: sample size of non-empty stomachs, RSS: redside shiner, Sal: salmonid, Unk-fish: unidentified fish, Daph: Daphnia, Lept: Leptodora, Zoop: other zooplankton, IM-insect: immature insect, AD-insect: adult insect.

Length	Season	N	RSS	Sal	Unk-fish	Amphibia	Daph	Lept	Zoop	Amphipod	Snail	Benthos	IM-insect	AD-insect	Other
Diablo Lake															
	Spring	1	0.000	0.000	0.095	0.000	0.877	0.000	0.000	0.000	0.000	0.000	0.000	0.000	0.028
	Summer	44	0.000	0.000	0.131	0.000	0.331	0.205	0.000	0.007	0.015	0.004	0.235	0.072	0.001
	Fall	23	0.000	0.000	0.036	0.000	0.257	0.001	0.005	0.041	0.172	0.003	0.019	0.467	0.001

Table S15. Seasonal diet proportions (wet weight) compared to stable isotope mixing model results (SIMM, 95% credible intervals) for broad prey categories for rainbow trout and redside shiner in Ross and Diablo Lakes. Redside shiner diet data was from previously published estimates of volumetric proportions (Welch 2012). Season refers to the season that the diet sample or tissue sample was collected. Sample size (N) is indicated for stomach contents and stable isotope samples

					Fish		Zooplankton		Benthos/insect/other	
Species	Length	Season	*N*: Diet	*N*: SIMM	Diet	SIMM	Diet	SIMM	Diet	SIMM
Diablo Lake										
RBT	all	Spring	1		0.095		0.877		0.028	
		Summer	44	29	0.131	0.281 (0.176-0.374)	0.536	0.258 (0.069-0.434)	0.334	0.461 (0.308-0.642)
		Fall	23		0.036		0.263		0.703	
RSS		Summer		19	-	0.361 (0.245-0.464)	-	0.274 (0.085-0.445)	-	0.364 (0.21-0.542)

Table S16. Rainbow trout and redside shiner seasonal diet proportions used as inputs into bioenergetics model simulations for Diablo Lake. Diets were assumed to be consistent across fish size for both rainbow trout and redside shiner in Diablo Lake. Sample size (N) of stomach content analysis is indicated for the seasons in which non-empty stomach contents were collected. Winter diets were set to be constant between day 245 and 336 (Jan 1- Apr 1). All diets were linearly interpolated between seasons. *Denotes seasons in which stable isotope mixing model results were used to modify these diet inputs for the bioenergetics simulations. RSS: redside shiner, Sal: salmonid, Unk-fish: unidentified fish, Daph: Daphnia, Lept: Leptodora, Zoop: other zooplankton, IM-insect: immature insect, AD-insect: adult insect.

				Diet proportions												
Length	Day	Season	*N*	RSS	Sal	Unk-fish	Amphibia	Daph	Lept	Zoop	Amphipod	Snail	Benthos	IM-insect	AD-insect	Other
Rainbow trout																
All	1	Spring*	1	0.000	0.000	0.281	0.000	0.258	0.000	0.000	0.000	0.000	0.461	0.000	0.000	0.000
	91	Summer*	-	0.000	0.000	0.281	0.000	0.258	0.000	0.000	0.000	0.000	0.461	0.000	0.000	0.000
	92	Summer	44	0.000	0.000	0.131	0.000	0.331	0.205	0.000	0.007	0.015	0.004	0.235	0.072	0.000
	154	Fall	23	0.000	0.000	0.036	0.000	0.257	0.001	0.005	0.041	0.172	0.002	0.019	0.467	0.000
	245	Winter	-	0.000	0.000	0.000	0.000	0.000	0.000	0.000	0.041	0.172	0.298	0.488	0.000	0.001
	336	Spring	-	0.000	0.000	0.000	0.000	0.000	0.000	0.000	0.041	0.172	0.298	0.488	0.000	0.001
Redside shiner																
All	1	Spring*	-	0.361	0.000	0.000	0.000	0.138	0.000	0.137	0.000	0.000	0.364	0.000	0.000	0.000
	92	Summer*	-	0.361	0.000	0.000	0.000	0.138	0.000	0.137	0.000	0.000	0.364	0.000	0.000	0.000
	154	Fall	-	0.000	0.000	0.000	0.000	0.279	0.000	0.131	0.000	0.000	0.094	0.248	0.248	0.000
	245	Winter	-	0.000	0.000	0.000	0.000	0.000	0.000	0.000	0.000	0.000	0.500	0.500	0.000	0.000
	336	Spring	-	0.000	0.000	0.000	0.000	0.000	0.000	0.000	0.000	0.000	0.500	0.500	0.000	0.000

Table S17. Bioenergetics simulation inputs and corresponding estimates of feeding rate (% C_{max}), annual per capita consumption (g), and growth efficiency (%). All simulations ran for 365 days (day 1= May 1). Energy density (ED, J/g) of the consumer was linearly interpolated during the simulation from the initial to final value reported. Sample sizes (*N*) are given for the number of individuals used in scale back-calculations for each annulus.

Species	Age	*N*	Spawn day	Spawn loss (%)	Initial FL (mm)	Initial W (g)	Final W (g)	Initial ED (J/g)	Final ED (J/g)	$\%C_{max}$	Growth (g)	Cons (g)	GE (%)	Daphnia cons (g)
Diablo Lake														
Rainbow trout	1	158		0.0	76	5.4	32.6	4,996	4,996	23	27.2	271.0	10.0	90.0
	2	130		0.0	137	32.6	91.2	4,996	4,996	26	58.6	716.0	8.0	254.0
	3	79	45	8.0	196	91.2	224.9	4,996	4,996	31	133.7	1,601.0	8.0	571.0
	4	28	45	8.0	274	224.9	395.2	4,996	4,996	33	170.3	2,719.0	6.0	999.0
Redside shiner	1	3		0.0	37	0.6	2.0	4,911	4,911	154	1.4	10.0	14.0	3.0
	2	3	61	11.0	54	2.0	3.7	4,911	4,911	150	1.7	14.0	12.0	5.0
	3	3	61	11.0	67	3.7	5.9	4,911	4,911	145	2.2	18.0	12.0	6.0
	4	3	61	11.0	78	5.9	8.7	4,911	4,911	142	2.8	22.0	13.0	7.0
	5	3	61	11.0	88	8.7	12.1	4,911	6,208	156	3.4	29.0	12.0	9.0
	6	3	61	11.0	98	12.1	15.8	6,208	6,208	155	3.6	33.0	11.0	11.0
	7	3	61	11.0	106	15.8	19.6	6,208	6,208	129	3.9	31.0	13.0	10.0

Figures

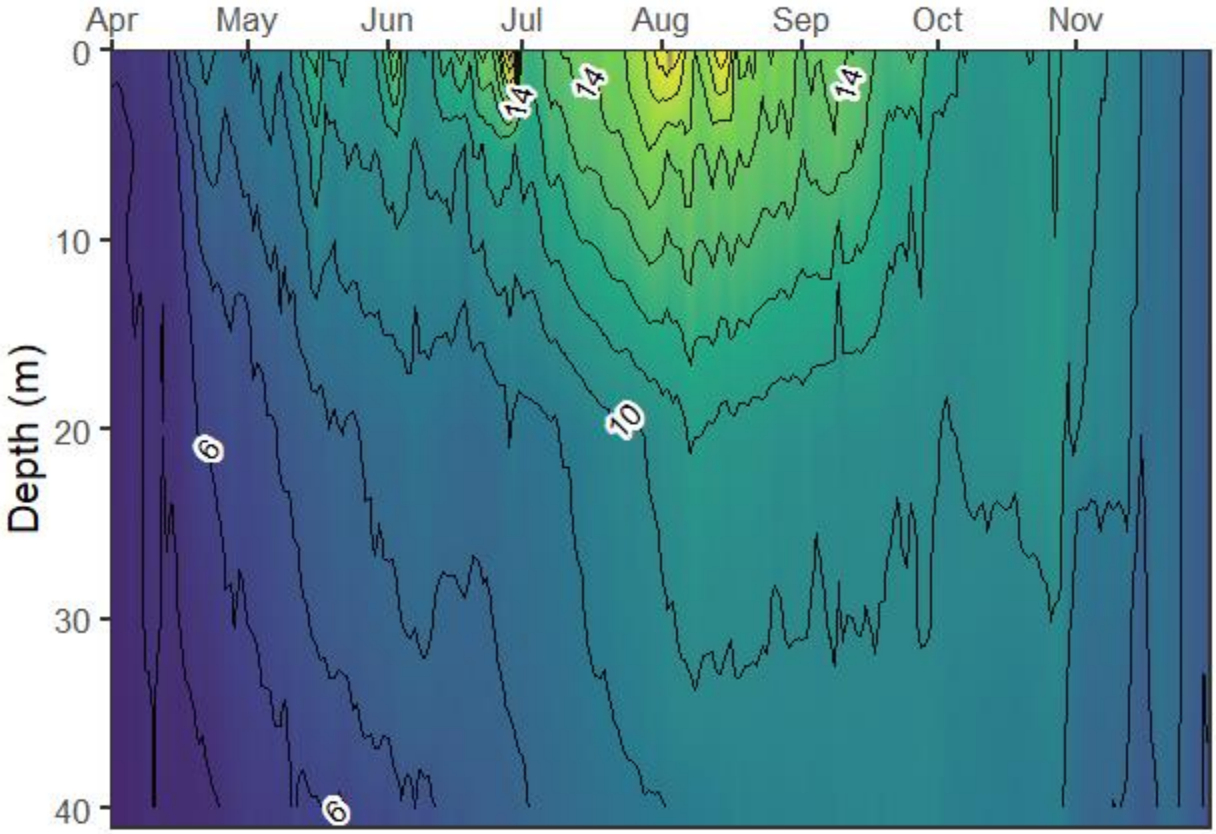

Figure S16. Isocline for Diablo Lake in 2021. Temperatures (°C) came from an array of sensors deployed every 5 m and taking readings four times per day.

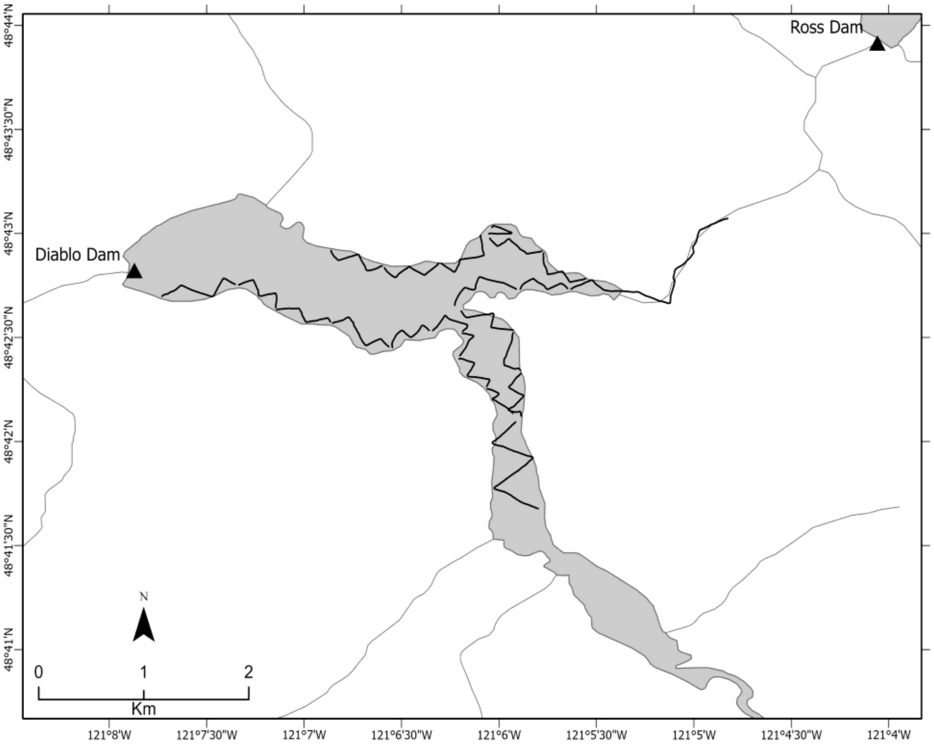

Figure S17. Map of Diablo Lake hydroacoustics transects surveyed at night in September 2021.

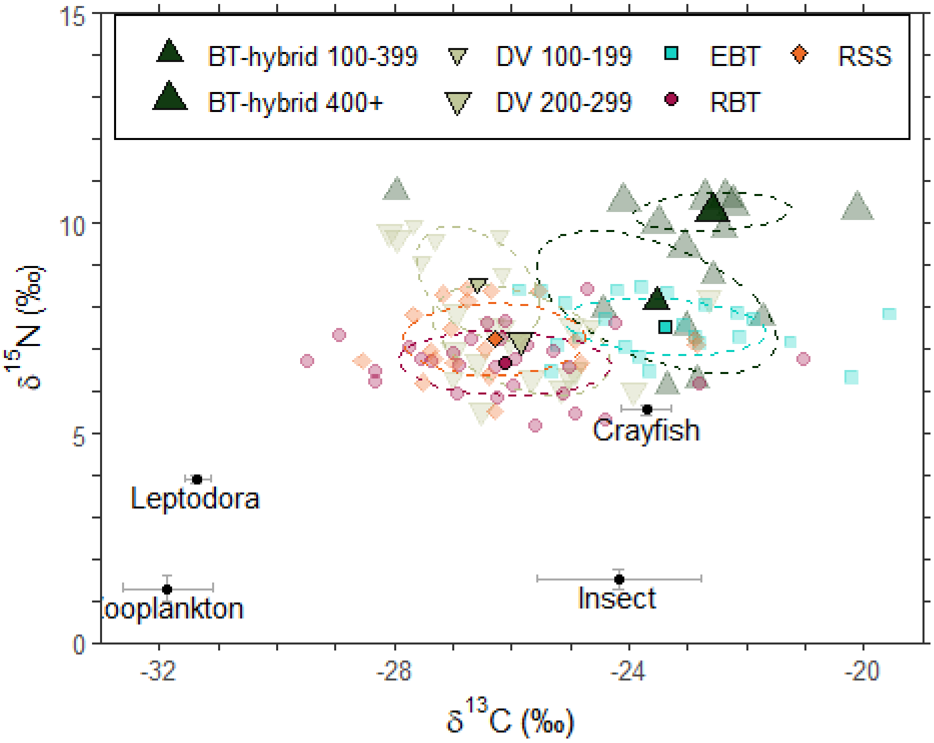

Figure S18. Stable isotope biplots of the Diablo Lake food web. Consumer species were separated by size classes if significant differences in stable isotope values were observed. The darker colored symbols represent the group centroids, while the lighter shaded symbols represent individual fish. BT-hybrid: bull trout and char hybrids, DV: Dolly Varden, EBT: brook trout, RBT: rainbow trout, RSS: redside shiner. Numbers following the species code represent the group's size bin, in mm FL. Ellipses contain 40% of the data for each consumer species/size group.

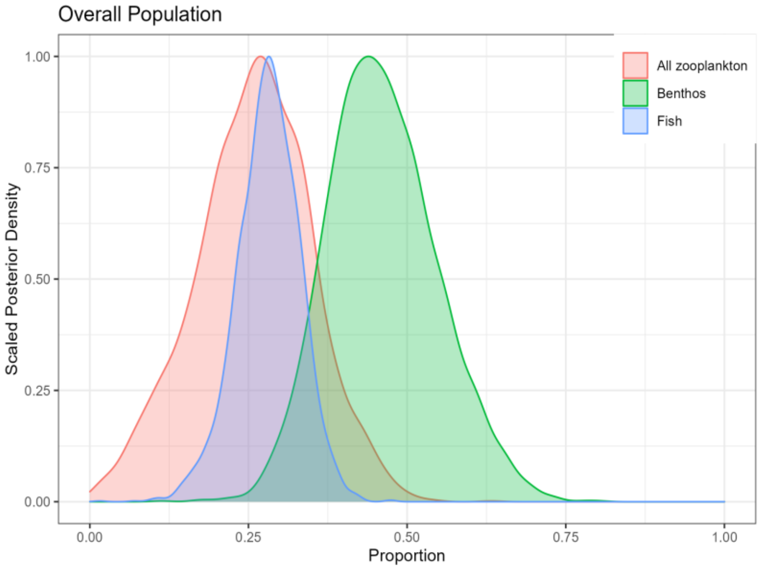

Figure S19. Stable isotope mixing model posterior densities for all rainbow trout in Diablo Lake sampled in the summer.

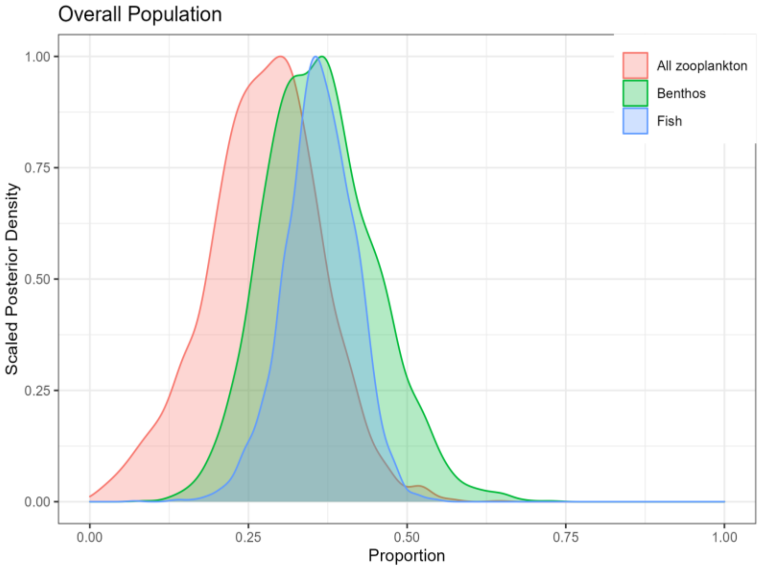

Figure S20. Stable isotope mixing model posterior densities for all redside shiner in Diablo Lake sampled in the summer.

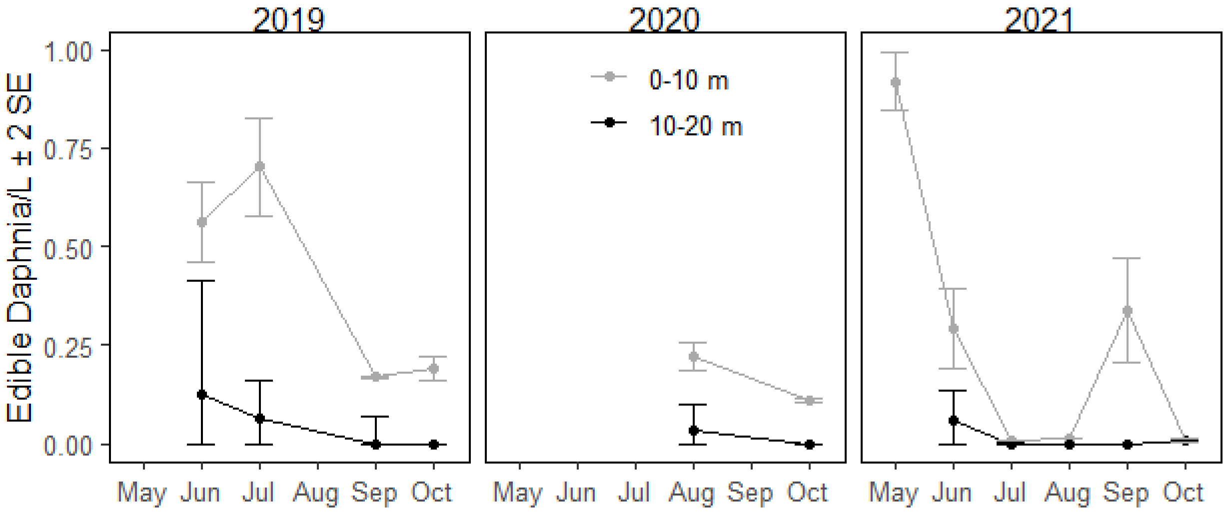

Figure S21. Average monthly densities for edible sized *Daphnia* (≥ 1 mm BL) in the epilimnion (0-10 m depth) and the metalimnion (10-20 m depth) in Diablo Lake during 2019-2021.

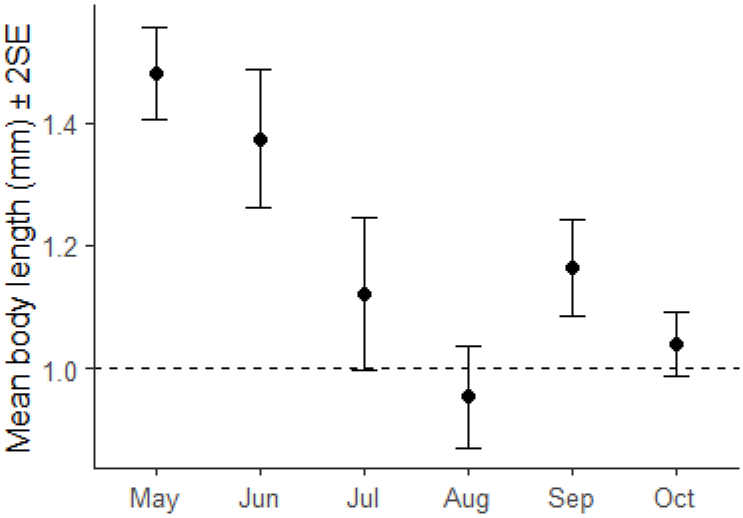

Figure S22. Monthly mean *Daphnia* body lengths (mm) in the 0-20 m samples in Diablo Lake in 2021. Dashed line at 1-mm represents minimum edible size for salmonids.

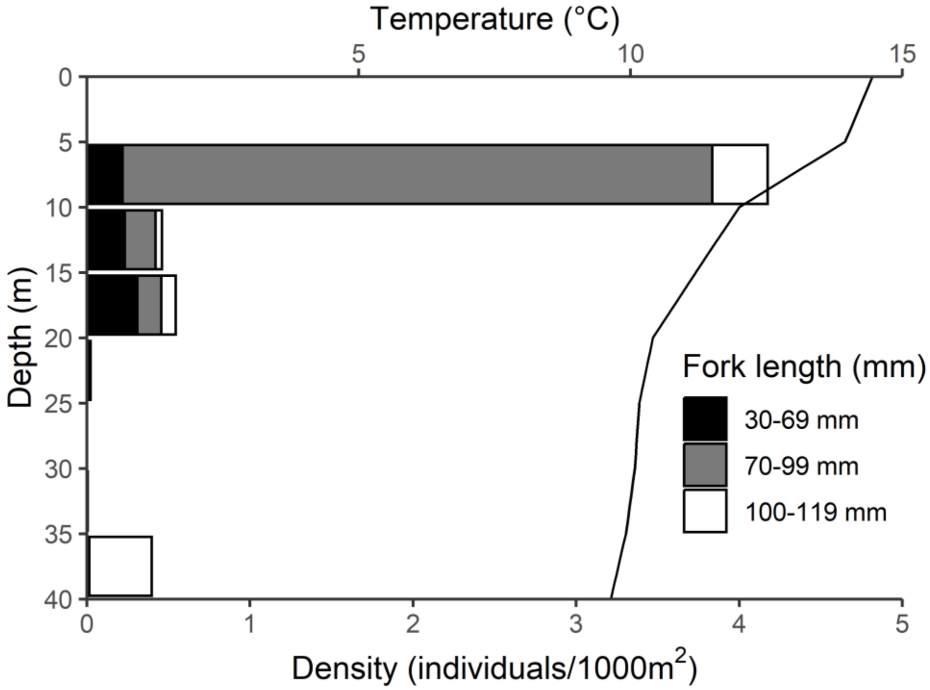

Figure S23. Depth distribution of redside shiner from hydroacoustics surveys and thermal structure in Diablo Lake in early September 2021. Densities represent the lake-wide average for each 5 m depth bin and reported size class.

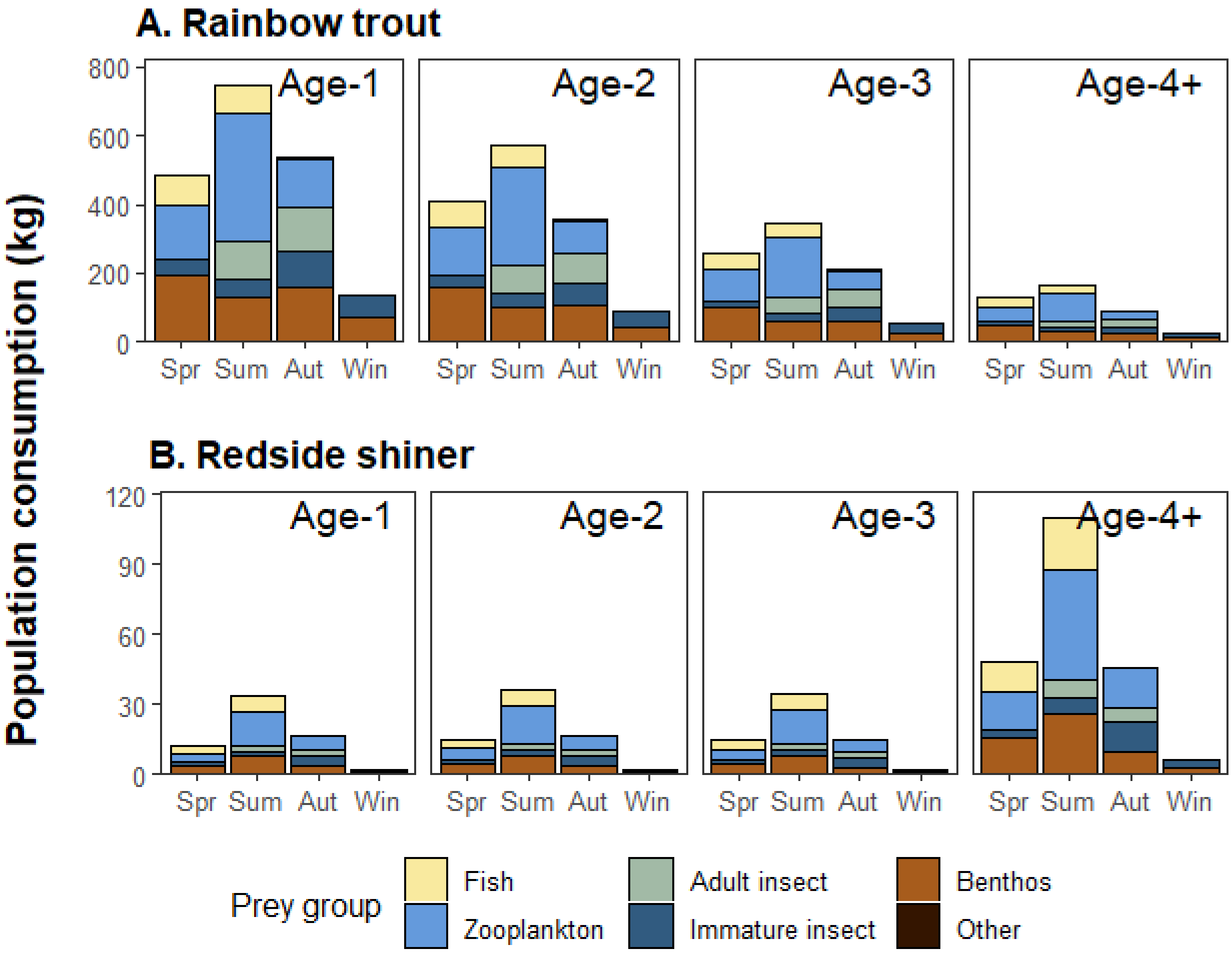

Figure S24. Seasonal consumption for a unit 1,000 size structured population of rainbow trout (A) and the estimated population of 20,000 redside shiner (B) in Diablo Lake. Note the different y-axis scales between A and B.

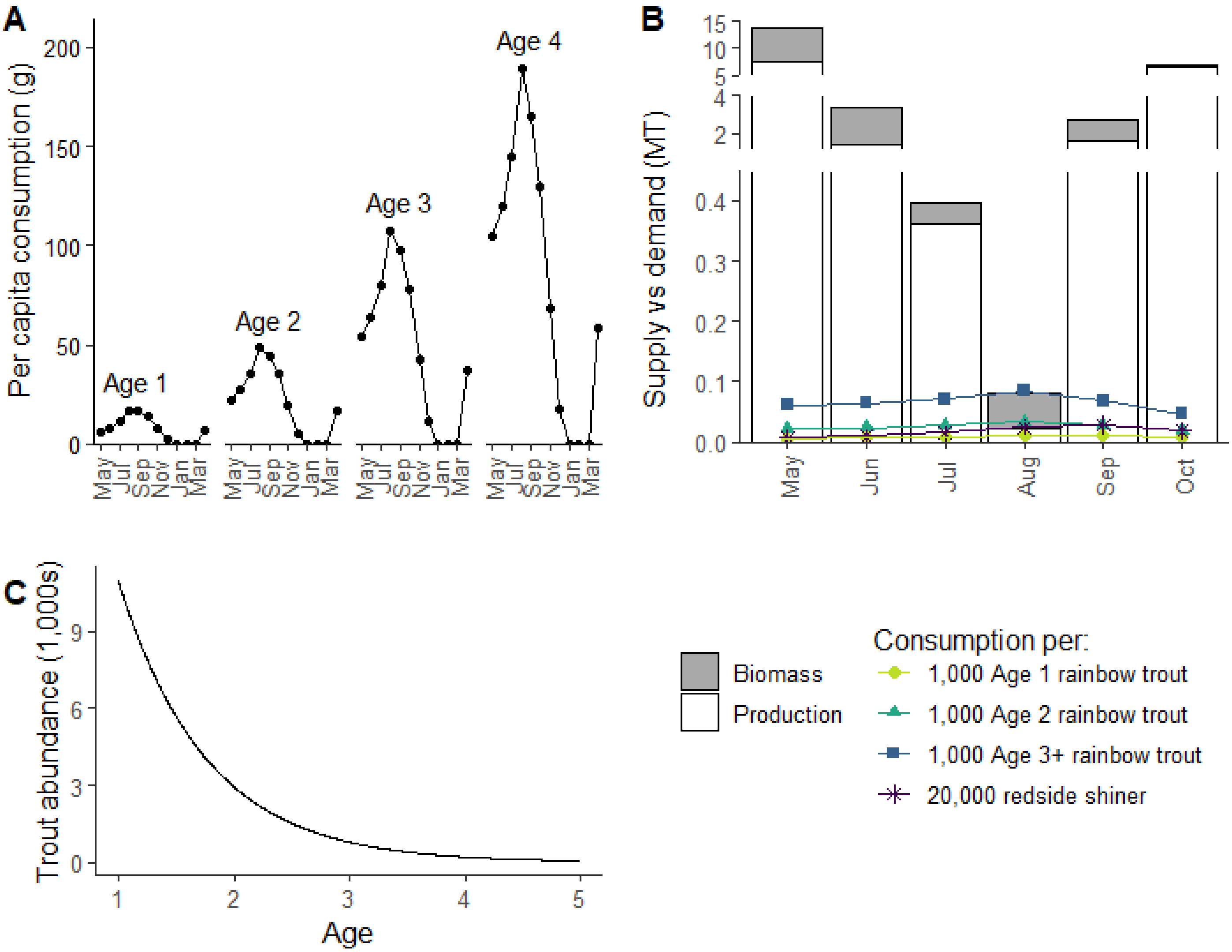

Figure S25. Consumption demand and prey supply for planktivorous fishes in Diablo Lake. (A) Per capita monthly consumption of *Daphnia* for each age-class of rainbow trout. (B) *Daphnia* biomass and production compared to consumption demand per 1,000 rainbow trout in each age class and the estimated redside shiner population of 20,000. Note the axis breaks on the y axis. (C) Rainbow trout abundance through time for a unit population of 1,000 fish ≥ 200 mm FL.

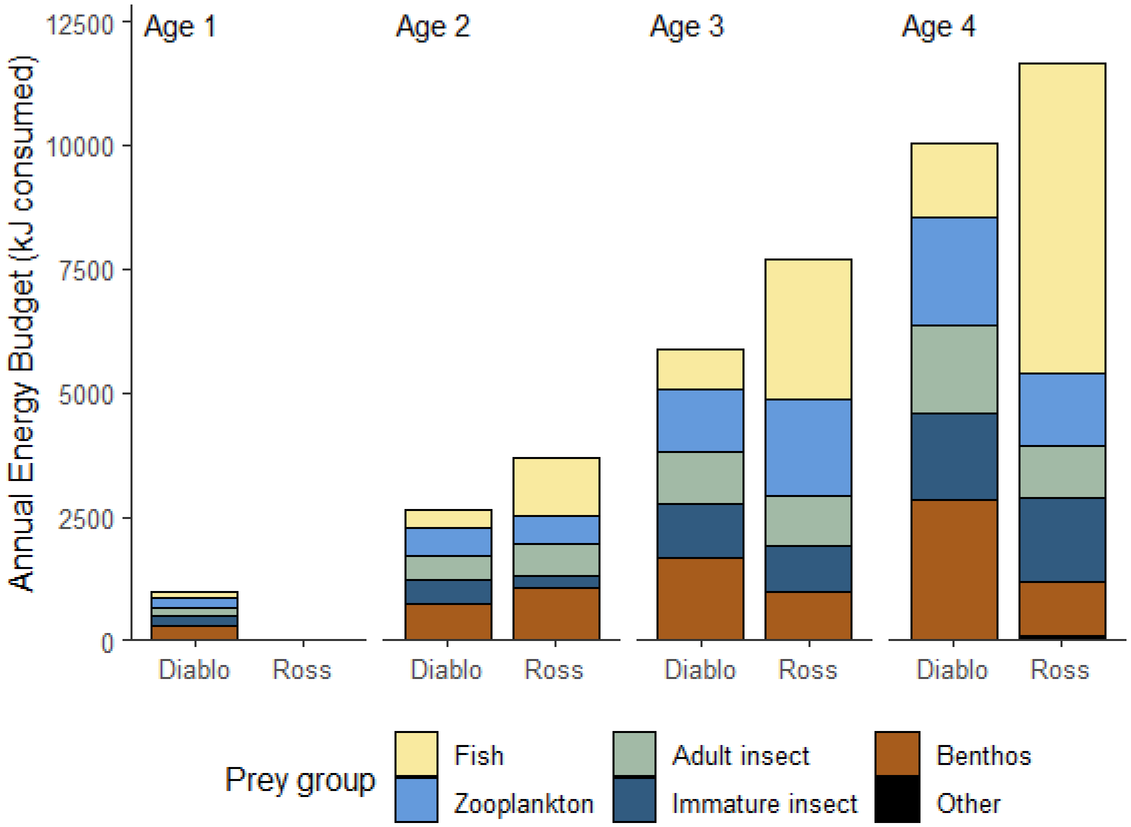

Figure S26. Annual energy budgets of rainbow trout in Ross Lake compared to Diablo Lake.

Chapter 3: Shift in piscivory following invasion of a minnow in a mid-elevation reservoir

Abstract

Predation can play an important role in structuring communities, and predator-prey dynamics can be altered when new species enter ecosystems. An unauthorized introduction of redside shiner (*Richardsonius balteatus*) into reservoirs in the Upper Skagit River, Washington created concern that a consequent shift in predator-prey dynamics in the reservoirs could reduce recruitment and production of rainbow trout (*Oncorhynchus mykiss*) and the other native salmonids in the basin. We quantified predation mortality in Ross Lake on nonnative redside shiner and juvenile native salmonids to evaluate the potential role of predation in regulating these populations and limiting survival of native species of concern. We used bioenergetics modeling and stable isotope analysis combined with directed field measurements of growth, seasonal diet, and thermal experience of piscivorous salmonids to quantify their consumption demand on prey fish species to evaluate the relative magnitude of predation mortality on invasive redside shiners and native salmonids. While redside shiner are the dominant prey species in Ross Lake, the modest biomass of native salmonids consumed translated into substantial mortality, the magnitude of which depended on the size at which prey fishes were eaten. This information provides important context for how nonnative species (redside shiners) may indirectly impact native species (salmonids) through shared predation (apparent competition) and is necessary to support management decisions surrounding nonnative species control, sustainability of native salmonids, and introductions of anadromous fishes.

Introduction

Invasive species can alter aquatic ecosystems in various ways, often disrupting trophic relationships via multiple direct and indirect pathways (Jackson et al. 2017). Invaders can become significant predators, competitors, or prey within the host food web. Invasive species that operate at intermediate trophic levels can serve multiple roles and exert ambiguous effects on different species. Such invaders might compete for similar foods with other mid-trophic level species while also serving as an important alternative prey source for predators that either buffers existing prey from predation or amplifies predation mortality by supporting larger populations of shared predators (apparent competition: Holt 1977). The structure and function of food webs influence diversity and productivity of ecosystems; thus, understanding how species invasions alter trophic dynamics is critical to protect ecosystem services and conserve threatened species (McCann 2007). Reservoirs are particularly susceptible to species invasions (Havel et al. 2015) and often have a unique set of management challenges associated with their "hybrid" or novel food webs, necessitating adaptive management frameworks that incorporate food web monitoring and research (Naiman et al. 2012).

Introduced prey species can reduce the equilibrium abundance of native prey species by supporting the increase in abundance of a shared predator – an indirect interaction often termed "apparent competition," because the impacts of the invader on an existing prey species is often mistakenly attributed to competition rather than an asymmetric increase in predation mortality imposed on the existing prey species (Holt 1977). Native species are particularly vulnerable to impacts of apparent competition when they express life history traits that leave them more vulnerable to predation than the novel prey (Holt 1977). The population-level response of native prey species to such indirect interactions thus depends on vital rates of all prey species, as well as spatial and temporal overlap of predators and prey (Holt 1984; Holt and Kotler 1987). Changes to the predation-risk landscape can also influence changes in behavior or distribution by prey fish in response to trade-offs between foraging and predation risk (Dill et al. 2003). Such behaviorally-mediated effects can result in negative responses such as reduced growth or reproductive rates even when direct predation is absent, and these non-consumptive effects can be larger than direct effects of predation (Creel and Christianson 2008).

Redside shiner *Richardsonius balteatus*, a small-bodied minnow, has established nonnative populations in Arizona, Colorado, Montana, Utah, Washington, and Wyoming, USA (Nico and Fuller 2020), and in British Columbia, Canada (Larkin and Smith 1954). These introductions have commonly been associated with declining growth rate and production of rainbow trout *Oncorhynchus mykiss*, and competition for food has been proposed as the causal link between redside shiner and rainbow trout (Lindsey 1950; Larkin and Smith 1954; Johannes and Larkin 1961; Smith et al. 2021). However, redside shiner can also be a major contributor to the energy budget of trout in lakes where they coexist (Lindsey 1950), especially for larger rainbow trout (Larkin and Smith 1954). Despite the increased growth rates of piscivorous rainbow trout, decreased catch rates of smaller fish led to the hypothesis that competition with redside shiner reduced the growth rates of juvenile rainbow trout, thereby exposing them to one or more years of additions mortality before they recruited to the fishery (Larkin and Smith 1954). Mortality at the extended juvenile stage for salmonids could also be exacerbated by increased levels of predation by larger piscivorous rainbow trout, although this process of apparent competition has not been evaluated in any lakes where redside shiner have been introduced.

An unauthorized introduction of redside shiner in Ross Lake in the early 2000s sparked management concerns regarding trends of decreasing recruitment of rainbow trout, which were the most abundant fish in the lake basin, and the other native salmonids ESA-listed bull trout *Salvelinus confluentus* and Dolly Varden *S. malma*. Redside shiner is now the primary prey species for bull trout in Ross Lake (Eckmann et al. 2018), and are also eaten by rainbow trout (Downen 2014). In this study we characterize the food web response to a mid-trophic level invasive species and its relative impact as a direct competitor, versus an apparent competitor, using redside shiner in Ross Lake as a case study. We previously demonstrated depressed growth by rainbow trout and a reduced forage base of *Daphnia* under current conditions in Ross Lake, compared to years prior to invasion (Chapter 2). Depressed growth from direct competition would increase mortality by extending the period of time that juveniles are vulnerable to predation (i.e., before they can outgrow predators). Increased predation pressure due to increased abundance of piscivorous fishes could amplify these impacts. The goal of this study was thus to evaluate predation as a limitation to production of prey species in Ross Lake. To accomplish this, we applied bioenergetics modeling to field data to address two specific objectives: 1) quantify consumption demand on redside shiner and juvenile salmonids, and 2) compare annual predation to the estimated abundance of prey species. We hypothesized that predation in Ross Lake is capable of regulating native salmonid and nonnative redside shiner populations. We discuss these predator-prey interactions within the context of seasonal thermal constraints on habitat use and prey availability.

Methods

Study system

Ross Lake is the uppermost of three reservoirs impounded by hydroelectric projects in the Upper Skagit River, WA (Fig. 1). Ross Lake is the largest and deepest of these reservoirs (elevation at full pool = 489 m above sea level, storage at full pool = 1.78 km^3, max depth = 116 m, mean depth = 37 m), extending northward from Ross Dam for approximately 37 km to the border with British Columbia at full pool. Ross Lake is oligotrophic and has strong thermal stratification from around June until October when it deepens and begins to mix, with peak summer surface temperatures between 18-22°C, depending on the year and region of the lake (Fig. 2). Ross Lake is drawn down between 16-25 m every year during the fall and winter before refilling in the spring, and drawdowns in recent years have reached 40 m (Fig. S1).

Ross Lake has native rainbow trout, bull trout, and Dolly Varden *S. malma*, nonnative eastern brook trout *S. fontinalis* (introduced in the early 1900s), cutthroat trout *O. clarkii* (introduced in the early or mid-1900s), and redside shiner *Richardonius balteatus*, which have proliferated since their unauthorized introduction ca. 2000. Hybridization has been documented between rainbow trout and cutthroat trout, as well as Dolly Varden, bull trout, and brook trout. Rainbow trout spawn in tributaries in the spring (May-June), emerge in the late summer, and most recruit to Ross Lake around age 2-3. *Salvelinus* spp. spawn in the tributaries in the fall (beginning in October) and presumably rear for 1-2 years before migrating to the reservoir, though habitat occupancy and migration during this stage are largely unstudied.

Fish collection

Potential predators were collected in spring, summer, and fall in 2019-2021, using sinking multi-mesh gill nets set approximately in three distinct depth strata corresponding to the epilimnion (0-10 m), metalimnion (10-20 m), and hypolimnion (20-30 m). Limitations to fish sampling in 2019 and 2020 from permitting and COVID-19 restrictions resulted in low or missing sample sizes for some species/size class/season bins, so data were pooled across all years. Angling was conducted opportunistically to increase sample sizes while minimizing mortality risk to bull trout which were listed as threatened under the Endangered Species Act.

All fish were measured for fork length (mm) and weight (0.1 g), fin tissue (for genetic and stable isotope analyses), and scale samples (plus otoliths from mortalities). Bull trout, Dolly Varden, and hybrids that were healthy enough to be released were held in a live well with aerators, anesthetized with buffered MS-222 prior to processing, and then recovered in the live well before releasing. Stomach contents from fish were collected using gastric lavage, with contents filtered into a 500-ug sieve and immediately placed on ice. Fish were identified to species in the field; however, due to difficulties in distinguishing bull trout, Dolly Varden, and their hybrids, native char tissue samples were identified at the Washington State Department of Fish and Wildlife Genetics Lab for final species assignment as either bull trout, Dolly Varden, or hybrids (including all potential crosses between native char and brook trout).

Size structure, abundance, mortality

We created age-structured populations based on a unit population of 1,000 fish > 200 mm FL for each species using annual survival rates S (Beauchamp et al. 2007). To estimate S, we used weighted catch curve analysis (Miranda and Bettoli 2007) on gillnet monitoring data from 2006-2018 (collected and maintained by North Cascades National Park) for the salmonids to estimate annual survival rates (S) and instantaneous mortality rates (Z) for each species (Table 1; Miranda and Bettoli 2007). Daily age class abundance was then estimated by applying daily instantaneous mortality rates ($Z/365$) to the initial age-class abundance.

Little is known about the actual population abundance of the salmonid species in this system; however, annual snorkel surveys for bull trout in the Upper Skagit River (British Columbia) provide limited abundance index data for the Ross Lake basin (Foster 2020). Previous telemetry studies on bull trout in the Upper Skagit have concluded that the vast majority of the population migrates between Ross Lake and the Skagit River for at least some portion of the year (Nelson 2006), supporting our use of these surveys to estimate the Ross Lake population. These surveys (1998, 2009-2017, and 2020) were conducted during early September and covered mainstem reaches starting at the Chittenden Bridge immediately upstream of the Ross Lake reservoir to the confluence with the Sumallo River (31.3 river km upstream). Importantly, these surveys occur about a month before the presumptive spawning period. Abundance of the Upper Skagit bull trout population was estimated at ca. 4,800 adults in 2011 using these snorkel counts, assuming the study area represented around 40% of the high-quality spawning habitat accessible to Ross Lake (Seattle City Light 2012). Updating this estimate with counts from surveys in 2017 and 2020 (1,241 and 1,070 individuals, respectively), we estimated 3,000 bull trout > 200 mm FL in Ross Lake. From the population of bull trout, we used relative frequencies from the gillnet catch in 2018-2021 to expand to the other salmonid species.

Stable isotope analysis

Stable isotope analysis was conducted on fish fin tissue and whole bodies of zooplankton and assorted benthic invertebrates (tissue removed from shells) to map each lake's food web and complement stomach content analysis. We aimed to analyze fin tissue from 5-10 fish of each species in each size class (100 mm FL intervals for salmonids, 50 mm FL intervals for redside shiners) for each lake during the summer; however, samples from other years and seasons were analyzed if sample sizes were not sufficient. In Diablo Lake, most fish samples came from 2019 and a frozen archive in 2017 (samples collected and maintained by North Cascades National Park) and all invertebrates were collected in 2019. In Ross Lake, most fish and zooplankton samples were collected in 2019, and all other invertebrate samples were collected in the fall of 2021. Other invertebrate herbivores and omnivores were collected for stable isotope analysis to provide representative end-members for primary pelagic and benthic consumers in the food web.

All of the fish consumer and invertebrate samples were measured for $\delta^{15}N$ and $\delta^{13}C$ by the University of Washington IsoLab using a ThermoFinnigan MAT253 isotope ratio mass spectrometer and Costech elemental analyzer or by the University of Washington Facility for Compound-Specific Isotope Analysis of Environmental Samples using a Thermo Scientific Delta V isotope ratio mass spectrometer and a CE elemental analyzer. Both labs referenced samples to 2 glutamic acid standards and Bristol Bay Sockeye Salmon. Stable isotope ratios are reported using delta (δ) notation in permil units (‰) compared to Vienna Pee Dee Belemite for C and air for N. Isotopic values of fish consumers were compared among size classes within each lake using non-parametric Kruskal-Wallis and Dunn's multiple comparison test to evaluate ontogenetic differences in diet and guide how we pooled isotope and diet data across size classes within a species.

Bioenergetic model inputs

Diet composition

Stomach contents were identified using a dissecting microscope and sorted into taxonomic groups at varying levels. Blotted wet weights (0.0001 g) were recorded for each taxonomic group identified and pooled across key prey functional groups (Table S1). For fish prey, fork length (mm) was measured for each individual if possible. Where fish were too digested, standard length or spinal length were measured to the nearest mm and then converted to fork length using linear regressions developed from our fish samples. Fish prey were identified using diagnostic bones where available; additional fish prey were identified genetically using PCR if adequate tissue was available; otherwise it remained as unidentified fish prey. Wet weights were converted into proportions, which were then averaged within species, size-class, and season sampling blocks. Diet data were pooled across size-classes when stable isotope values were not significantly different (Tables S2-3). Prey energy densities were taken from the literature or measured directly in this study (Table S1).

We used Bayesian stable isotope mixing models (SIMMs) with the MixSIAR package in R (Stock et al. 2018) to estimate diet proportions from stable isotope signatures for comparison to the seasonal stomach content data. These estimates of diet proportions integrated over longer periods and thus complement the finer-scale taxonomic resolution and short-term (e.g., within the previous ~24 h) diet proportions estimated from stomach content analysis. We fit the mixing models using raw source data with prey sources grouped into three broad categories (fish, zooplankton, insects/other benthic invertebrates; details available in the Supplementary Methods). In the absence of predator and prey-specific trophic discrimination factors (TDF), we used mean TDFs (± SD) of $\delta^{15}N = 3.4‰ \pm 1.0‰$ and $\delta^{13}C = 0.4‰ \pm 1.3‰$ (Post 2002). This is consistent with much of the literature in similar fisheries studies (e.g., Rubenson et al. 2020; Hansen et al. 2021), but TDFs can vary among species, prey items, and tissue types (Bond and Diamond 2011; Canseco et al. 2022). Details regarding how stomach contents (Table S4) and stable isotope mixing models (Table S5, Figs. S2-S8) were combined with general ecological knowledge to construct seasonal diet inputs for the simulations (Tables S6-S7) are available in the Supplementary Methods.

Thermal experience

Vertical temperature data were collected at two sites during sampling (Fig. 1) and combined with data from Seattle City Light and North Cascades National Park to estimate thermal experience for salmonids in Ross Lake. For simplicity in bioenergetics simulations, we only used temperature data from the southern site to estimate thermal experience. Thermal experience was determined using patterns in depth distribution observed from gillnet catch data in 2021, the only year we had complete depth-temperature arrays of gillnets in all seasons (Fig. 3). Thermal experience was assigned by temperature-based rules developed from these depth distribution patterns and general knowledge about the species thermal requirements. If the mean temperature in the epilimnion was ≤ 18°C, we assumed rainbow trout would occupy this layer, and the average epilimnion temperature was used. If the mean temperature in the epilimnion was > 18°C, we assumed 75% of rainbow trout occupied the metalimnion with 25% in the epilimnion.

If the mean temperature in the epilimnion was ≤ 18°C, we assumed brook trout occupied the epilimnion, and the average temperature in this layer was used. Otherwise, brook trout occupied the metalimnion. We assumed that bull trout and Dolly Varden selected temperatures from 11-15 °C and avoided temperatures > 15 °C (Gutowsky et al. 2017). If the mean epilimnion temperature was < 15 °C, we assumed that they were equally distributed throughout the water column from 0-30 m. If the mean epilimnitic temperature was > 15 °C and the mean metalimnion was < 15 °C, we assumed that they were equally distributed throughout the meta- and hypolimnion from 10-30 m. If both the epi- and metalimnion were > 15 °C, we assumed that they would be restricted to the hypolimnion between 20-30 m. During the colder isothermal conditions, we used average surface temperatures from the Ross Lake Forebay site (data collected by Seattle City Light) for all species' thermal experience in Jan-Apr and Nov-Dec. Daily temperatures were averaged across each layer and weighted-average temperatures calculated based on proportion of fish assumed to occupy each depth layer (Table S8).

Age, growth, predator energy

Size at age and annual growth increments were estimated from scale back-calculations. For each species, scales were imaged, measuring circuli and annuli using Image Pro Premier software (Media Cybernetics Inc, version 10). Where necessary, we corroborated scale-based ages and annuli markings with otoliths if available. Geometric mean regression (GMR) was used to evaluate the relationship between fish fork length (FL) and scale radius (SR) to avoid biased estimates from either of the ordinary regressions of FL~SR or SR~FL (Ricker 1992). Scale data were pooled across sites within each species in each reservoir. For char species, fish sampled in tributaries were included in the scale radius regression to increase sample size and expand the range of lengths represented to improve the intercept correction for the back-calculation and to avoid inflated estimates of back-calculated age. The Fraser-Lee proportional method (Fraser 1916, Lee 1920, Ricker 1992) was used to back-calculate fish FL at each annulus using the following equation:

$$FL_i = \frac{SR_i}{SR_{cap}} \times (FL_{cap} - a) + a \qquad (1)$$

where FL_i is the back-calculated fork length (mm) at a given annulus, SR_i is the scale radius at that annulus, SR_{cap} is the scale radius (mm) at capture, FL_{cap} is the fork length (mm) at capture, and a is the intercept from the GMR lines (Table 2). Back-calculated FLs were converted to wet weight using wet weight-FL regressions for salmonids in each reservoir basin (Table 3).

Energy density (J/g wet weight) of consumers was estimated using bomb calorimetry (Parr model 6725 semi-micro bomb calorimeter) for a subset of whole bodies collected across seasons in Ross Lake (Rainbow trout: *N* = 27, FL = 148-492 mm, W = 33-989 g; bull trout and hybrids: *N* = 42, FL = 184-577 mm, W = 70-2238 g; Dolly Varden: *N* = 2, FL = 174-180 mm, W = 58-58 g; brook trout: *N* = 16, FL = 200-405 mm, W = 89-731 g). We evaluated the relationship between energy density and consumer body weight within each species and set energy density inputs for the bioenergetics simulations depending on the initial and final weights for each age-class (Table 4). Due to limited sample size, Dolly Varden, bull trout, and their hybrids were pooled for this analysis.

Spawning losses for bull trout and brook trout were taken from the literature (Magnan et al. 2005; Lowery and Beauchamp 2015) and all char spawning was set for Oct 9 (day 161 of the simulation). The oldest Dolly Varden sampled in either reservoir was 4 years old. Given this, we set spawning for Dolly Varden to occur at age 3 and set spawning loss to 9.8%. Spawning losses for rainbow trout were set at 8% body weight for ages 3+ (Juncos et al. 2013) which occurred in mid-June (day 45 of the simulation). In the simulations, spawning was represented as a loss in weight occurring on a single day.

Predation mortality

We ran simulations of the Wisconsin-style bioenergetics model using Fish Bioenergetics 4.0 (Deslauriers et al. 2017) parameterized for rainbow trout (Rand et al. 1993), bull trout/Dolly Varden (Mesa et al. 2013), and brook trout (Hartman and Sweka 2001; Hartman and Cox 2008). We fit the model to annual growth using average back-calculated weight at annulus as the initial and final weights (g) to generate an estimate of $\%C_{max}$ across the entire simulation and per capita consumption of each prey group. We started simulations on May 1, the average date of annulus formation in Ross Lake rainbow trout (Woodin 1974), assuming this to be an appropriate estimation for time of annulus formation for the other salmonid species. *Daphnia* weigh about 50% less in diet samples than they do fresh (Luecke and Brandt 1993; Stockwell et al. 1999), therefore simulated consumption of *Daphnia* (g) was multiplied by 2 to estimate the fresh weight consumed for direct comparison to biomass and production estimates. Daily abundance for each age class was estimated by applying Z_{day} to the initial starting population, and each day thereafter. Per capita consumption for each age-class of each consumer was expanded to the population level by multiplying individual consumption by the daily age-class abundance.

Annual consumption of fish prey biomass was translated into numerical predation potential by dividing the estimated consumption by the weight of prey fish at the presumptive time of consumption. We had no data on the size or age distribution of salmonids consumed, thus we projected predation potential for a range of sizes of vulnerable prey. Consumption estimates on different age classes of prey species were adjusted daily to account for prey growth and gape limitation of the predators, assuming that fish could consume prey up to 50% of their length (Beauchamp and Van Tassell 2001; Juanes et al. 2002; Beauchamp et al. 2007; Winters and Budy 2015). The age-specific daily weights of predators and prey fish from bioenergetics simulations were converted to daily FL estimates using their length-weight relationships (Table 3), allowing fish to maintain their FL during simulated periods of weight loss. This estimated consumption on each native salmonid prey species and age class assumed they were 100% of the total salmonid fraction of consumption. These estimates were expanded to measure predation potential across various predation scenarios, assuming each prey species and age class accounted for a range (from 1% to 100%) of the total estimated consumption on salmonids. We simulated consumption estimates for redside shiner using the same methods, accounting for a range of the total estimated consumption on redside shiner.

Results

Stable isotopes and diet composition

In Ross Lake, rainbow trout exhibited ontogenetic shifts in trophic position associated with the onset of piscivory at larger size classes, whereas trophic positions for char species showed some variation, but no trend with size (Fig. 4; Supplement Tables S2-3). Centroids for smaller rainbow trout < 300 mm FL showed a mixed reliance on pelagic and benthic resources, and trophic position increased through a transition size of 300-399 mm FL, progressively shifting to more benthic signals, before stabilizing at a higher trophic position at FL ≥ 400 mm (Fig. 5). All char were positioned in a high trophic level like rainbow trout ≥ 400 mm FL, with Dolly Varden slightly more pelagic than bull trout, char hybrids, and brook trout (Fig. 4). The trophic niche space of redside shiner overlapped with rainbow trout 100-199 mm FL, was slightly more benthic than rainbow trout 200-299 mm FL, and were a full trophic level below native char (δN^{15} difference: bull trout = 3.0‰; Dolly Varden = 3.2‰), and a partial trophic level below brook trout (δN^{15} difference = 2.4‰) and rainbow trout 300-399 mm FL (δN^{15} difference = 2.0‰). Rainbow trout 200-299 mm FL were just less than a trophic level below native char (δN^{15} difference: bull trout = 2.5‰; Dolly Varden = 2.7‰) and were a partial trophic level below brook trout (δ^{15} difference = 1.9‰) and rainbow trout 300-399 mm FL (δN^{15} difference = 1.5‰).

Stomach contents and stable isotope analyses using SIMMs indicated high levels of piscivory for all bull trout/hybrids, Dolly Varden, brook trout, and larger (400+ mm FL) rainbow trout in Ross Lake (Table S5). For these species, fish prey were generally a higher proportion of diets in the spring and summer than in fall. Rainbow trout 300-399 mm FL consumed moderate proportions of fish, especially in the summer. Diet proportions estimated from SIMMs tended to estimate higher contributions of fish by smaller rainbow trout (<300 mm FL) in Ross Lake which we attributed to consumption of redside shiner eggs, larvae, and small juveniles, as these life stages are more digestible and hence less detectable in diet samples (Legler et al. 2010). Salmonids rarely occurred in diet samples in Ross Lake (Table S9), thus we pooled the proportions of salmonids in the diet inputs for bioenergetics simulations to due uncertainty in the estimates. Salmonids were observed in diets across all seasons, and all salmonid species were observed in at least one diet (Table S9). Rainbow trout were observed in diets more frequently than char species and contributed the most to diets during the fall.

Depth distribution and thermal experience

Depth distributions of salmonids observed in Ross Lake gillnet surveys aligned with current information on thermal preferences for salmonid species (Fig. 3). Rainbow trout predominantly occupied the epilimnion during spring and summer in the southern region of Ross Lake with fewer fish in 10-20 m depths, whereas more rainbow trout shifted into the 10-20 m and a few into even deeper depths during destratification in fall. The mean temperature in the epilimnion at the time of summer sampling at this site was < 18°C, which is commonly considered within the maximum thermal preference for rainbow trout feeding at naturally occurring ration levels that are typically well below satiation (e.g., Rand et al. 1993; McCarthy et al. 2009; Armstrong and Schindler 2011). By contrast, rainbow trout at the warmer northern site primarily occupied the metalimnion with only about 30% caught in the epilimnion during the summer, where temperatures approached 20°C. At the southern site, brook trout were observed exclusively in the epilimnion, while at the northern site, most brook trout were caught in the metalimnion, with a small fraction in the hypolimnion, and none observed in the epilimnion. Bull trout and char hybrids were evenly distributed throughout the water column during the spring, and across the top 20 m during the fall at the southern site. During summer stratification, they were primarily occupying the cooler meta- and hypolimnion where mean temperatures were at or below 15°C. At the warmer north site during the summer, bull trout were primarily occupying the hypolimnion, when mean temperature in the metalimnion exceeded 15°C.

Predation mortality

Predators in Ross Lake consumed fish < 32% of their body lengths, and there were no clear trends between prey length and predator length (Fig. 6). Brook trout consumed smaller fish on average (mean = 50, 23-85 mm FL) than rainbow trout (mean = 61, 23-111 mm FL) or bull trout (mean = 62, 35-114 mm FL), but this reflects, in part, differences in predator size distribution (mean prey length as % of consumer length; brook trout = 17 %; rainbow trout = 17 %; bull trout = 15 %). Size distribution of fish prey in diets corresponded closely with the size distribution of redside shiner. The overall mean size of fish observed in stomach contents was 60 mm FL, which corresponds to approximately 2.5 g wet weight for redside shiner or rainbow trout.

Bioenergetics simulations indicated that redside shiner accounted for the majority of fish biomass consumed by salmonids, totaling 5917 kg annually by the total piscivore population indexed to 3,000 bull trout > 200 mm FL. Annual per capita fish consumption varied by species and age-class, with the highest rate by rainbow trout age 6 and the lowest by rainbow trout age 2 (Table 4). However, due to differences in abundance, the rainbow trout population consumed the most redside shiner (3928 kg), followed by bull trout (1597 kg), brook trout (352 kg), and Dolly Varden (40 kg). This total biomass of fish prey consumed corresponds to approximately 2,367,000 fish annually at the average size of 2.5 g (approximately 20% of the estimated 12 million). Predation could contribute to a substantial fraction of annual mortality, depending on the relative contributions of each age class to predator diets (Fig. S10).

The diets of piscivores included minor contributions of salmonid fish prey (Table S4), but this still translated into substantial biomass consumed and mortality. The estimated population of piscivores consumed 309 kg of salmonids over the year, with bull trout consuming the most (205 kg), followed by rainbow trout (76 kg), brook trout (17 kg), and Dolly Varden (10 kg). This total biomass consumed corresponds to approximately 124,000 salmonids annually at 2.5 g, the average size of fish observed in stomach contents.

Mortality rate (in terms of numbers consumed annually) depends largely on habitat occupancy and growth of prey fish. Most rainbow trout in the reservoir were presumed to migrate from the tributaries during age 2 or 3 (7-44 g, Jensen et al. in review). As juvenile rainbow trout grow, predation rates would decline due to two mechanisms: 1) as prey weight increases, the number of individual fish needed to fulfill the consumption demand (biomass) of predators declines, and 2) as prey length increases, the number of predators able to successfully capture them declines. Thus, rainbow trout would be less vulnerable to predation if they recruit to the reservoir at a larger size (Fig. 7). After accounting for gape limitation of consumers and growth of prey, predation could account for up to 18,197 age 1 or 1,521 age 2 rainbow trout if 100% of predation on salmonid prey was devoted exclusively to either age class (Fig. S11). Due to the presumably low abundance of Dolly Varden in the reservoir, even low levels of predation (1-10% of the salmonid fraction of the diets) could account for 6-55% of the back-calculated abundance of age 2 Dolly Varden (Fig. S11).

Another 2313 kg of unidentifiable fish were consumed, corresponding to approximately 925,000 fish annually at the average size of 2.5 g. Predatory rainbow trout age 2-3 consumed more than half of this unidentified fish biomass (1267 kg; 507,000 individuals at 2.5 g), which were most likely redside shiner due to the small size at these ages.

Discussion

Our quantitative food web study indicated that nonnative redside shiner are the dominant prey for piscivorous salmonids in Ross Lake. Despite the relatively low proportion of observed piscivory directed toward salmonids as prey, bioenergetic simulations indicated that this level of predation could translate into significant mortality on juvenile salmonids depending on their age and size when recruiting to the lake and subsequent growth rates. Notably, piscivory was not observed in any size class of rainbow trout in the decades prior to the redside shiner invasion (Seattle City Light 1972). Historically, only large bull trout were piscivorous prior to the redside shiner invasion. With the currently large population of redside shiners, all species of native and non-native salmonids have become highly piscivorous. Redside shiners have provided a year-round supply of small-bodied forage fish. Collectively, this behavioral shift in foraging mode by the salmonids in the reservoir appears to have increased predation mortality on the native salmonids and could be limiting recruitment for these adfluvial populations. The magnitude of this recent predation impact will depend on environmental conditions that influence the spatial-temporal overlap of piscivores, redside shiners, and juvenile salmonids, and the relative sizes of predators and prey when encountered.

Most salmonids recruiting to Ross Lake at age 2-3 (85-160 mm FL, 17-44 g, Jensen et al. in review) experience lower predation risk owing to the reduced number of effective predators that are at least twice their body length, and because fewer heavier prey are required to satisfy required consumption of predators. Limited observations of salmonids in diet samples prevented us from quantifying species- and stage-specific predation rates. Predation on salmonids will likely be focused on the species and life-stages that are most abundant and accessible, which is supported by the higher proportion of rainbow trout observed in diet samples. Most adfluvial rainbow trout recruited to the reservoir at age 2 or 3, but the proportion of younger juveniles migrating to the reservoir prior to this age is unknown, and predation mortality could remove many of them. Previous reports have documented downstream migration of newly emerged fry and observations of age 0 rainbow trout along the shoreline in Ross Lake in August and October (Seattle City Light 1973, 1974; Johnston 1989), presuming that large numbers of rainbow trout migrate to the lake during their first summer, in addition to life histories that rear in the tributaries for 1-2 years (Downen 2014). Migration at younger ages could be induced by low productivity or by a lack of seasonably suitable rearing habitat in the tributaries (Slaney and Northcote 1974; Olsson et al. 2006), or an innate behavior (e.g., Knight et al. 1999); however, slow growth also commonly results in greater age at migration. Additional directed field sampling of diets and juvenile migration timing would be required to quantify the effect of predation on survival and recruitment rates of the juvenile salmonids.

Access to fish prey depends on spatial overlap between predators and prey, which during the growing season is largely driven by thermal structure and species-specific physiological requirements. Bull trout were the most constrained by temperatures during the summer, isolating them from the epilimnetic depths primarily occupied by redside shiner. Nevertheless, redside shiner remained a dominant prey during this season. Telemetry work in Ross Lake showed that some bull trout exhibit diel vertical migrations during the summer (Eckmann et al. 2018). High redside shiner densities in the epilimnion could represent a tradeoff for foraging bull trout, where capture efficiency is high enough to compensate for the increased thermal exposure. Though bull trout overlap more with rainbow trout and other native salmonids during the summer, typically occupying the metalimnion at least partially, encounter rates would probably be low. Bull trout in Ross Lake exhibit poor body condition (i.e., lower weight at a given length) compared to the standard equation (Hyatt and Hubert 2000), and some lakes and reservoirs where thermal conditions might not limit access to more prey fishes (e.g., Lake Billy Chinook, Chilko Lake, Kachess Lake; Fig. S12), indicating that constrained access to prey fish may impact growth. Increased epilimnetic temperatures associated with climate change or dam operations could further constrain bull trout access to redside shiner, which could further limit growth rates or direct more predation on native salmonids, highlighting an important area of research to inform management under future conditions.

Food web structure (including thermally driven species interactions) can play an important role in driving the impacts of introduced species. In some reservoir systems with more diverse assemblages of prey fish, bull trout feed on a variety of species, potentially buffering the predation impacts on any one species (Beauchamp and Van Tassell 2001; Wainright et al. 2021).

Limited availability of potential fish prey in this simple food web likely prevents this buffering effect, thereby increasing direct impacts of predation on native salmonids (Warnock et al. 2022). This also has implications for the proposed introduction of anadromous salmonids above these dams, which could be exposed to substantial levels of predation mortality depending on how consumption shifts to newly available species. Evaluating these food web interactions in the presence of nonnative species thus provides the necessary information to manage such novel food webs in the face of future environmental change to support robust ecosystems.

Acknowledgments

Funding and support for this study was provided by Seattle City Light - in particular, we thank Jeff Fisher, Erin Lowery, and the Diablo Lake boat house crew for critical support provided during our field operations. We would like to thank North Cascades National Park and Ross Lake Resort for their assistance with field sampling logistics. We also want to thank Tom Barnett in particular for his support, angling efforts, and knowledge of the Ross Lake fishery. Lisa Wetzel, Ella Wagner, Nancy Elder, and Jeff Duda assisted in the field and laboratory. Tom Quinn and Julian Olden provided valuable editorial comments that improved the quality of this manuscript. Handling of vertebrates was conducted under the auspices of the Institutional Animal Care and Use Committee of the U.S. Geological Survey, Western Fisheries Research Center IACUC protocols #2008-57.

References

Armstrong, J. B., and D. E. Schindler. 2011. Excess digestive capacity in predators reflects a life of feast and famine. Nature 476:84–88.

Beauchamp, D. A., A. D. Cross, J. L. Armstrong, K. W. Myers, J. H. H. Moss, J. L. Boldt, and L. J. Haldorson. 2007. Bioenergetic responses by Pacific salmon to climate and ecosystem variation. North Pacific Anadromous Fish Commission Bulletin 4:257–269.

Beauchamp, D. A., and J. J. Van Tassell. 2001. Modeling seasonal trophic interactions of adfluvial bull trout in Lake Billy Chinook, Oregon. Transactions of the American Fisheries Society 130:204–216.

Bond, A. L., and A. W. Diamond. 2011. Recent Bayesian stable-isotope mixing models are highly sensitive to variation in discrimination factors. Ecological Applications 21:1017–1023.

Canseco, J. A., E. J. Niklitschek, and C. Harrod. 2022. Variability in δ 13C and δ 15N trophic discrimination factors for teleost fishes: A meta-analysis of temperature and dietary effects. Reviews in Fish Biology and Fisheries 32:313–329.

Creel, S., and D. Christianson. 2008. Relationships between direct predation and risk effects. Trends in Ecology & Evolution 23:194–201.

Deslauriers, D., S. R. Chipps, J. E. Breck, J. A. Rice, and C. P. Madenjian. 2017. Fish Bioenergetics 4.0: An R-based modeling application. Fisheries 42:586–596.

Dill, L. M., M. R. Heithaus, and C. J. Walters. 2003. Behaviorally mediated indirect interactions in marine communities and their conservation implications. Ecology 84:1151–1157.

Downen, M. R. 2014. Final report: Ross Lake rainbow broodstock program, Upper Skagit reservoir fish community surveys and management plan (FPT 14-09). Washington Department of Fish & Wildlife.

Eckmann, M., J. Dunham, E. J. Connor, and C. A. Welch. 2018. Bioenergetic evaluation of diel vertical migration by bull trout (*Salvelinus confluentus*) in a thermally stratified reservoir. Ecology of Freshwater Fish 27:30–43.

Foster, J. 2020. 2020 Skagit River snorkel survey report. Triton Environmental Consultants Ltd.

Gutowsky, L. F. G., P. M. Harrison, E. G. Martins, A. Leake, D. A. Patterson, D. Z. Zhu, M. Power, and S. J. Cooke. 2017. Daily temperature experience and selection by adfluvial bull trout (*Salvelinus confluentus*). Environmental Biology of Fishes 100:1167–1180.

Hansen, A. G., J. R. Gardner, K. A. Connelly, M. Polacek, and D. A. Beauchamp. 2021. Resource use among top-level piscivores in a temperate reservoir: Implications for a threatened coldwater specialist. Ecology of Freshwater Fish:1–23.

Hartman, K. J., and M. K. Cox. 2008. Refinement and testing of a brook trout bioenergetics model. Transactions of the American Fisheries Society 137:357–363.

Hartman, K., and J. Sweka. 2001. Development of a bioenergetics model for Appalachian brook trout. Proceedings of the Annual Conference of the Southeastern Association of Fish and Wildlife Agencies 55:38–51.

Havel, J. E., K. E. Kovalenko, S. M. Thomaz, S. Amalfitano, and L. B. Kats. 2015. Aquatic invasive species: Challenges for the future. Hydrobiologia 750:147–170.

Holt, R. D. 1977. Predation, apparent competition, and the structure of prey communities. Theoretical Population Biology 12:197–229.

Holt, R. D. 1984. Spatial heterogeneity, indirect interactions, and the coexistence of prey species. The American Naturalist 124:377–406.

Holt, R. D., and B. P. Kotler. 1987. Short-term apparent competition. American Naturalist 130:412–430.

Hyatt, M. H., and W. A. Hubert. 2000. Proposed standard-weight (Ws) equations for kokanee, golden trout and bull trout. Journal of Freshwater Ecology 15:559–563.

Jackson, M. C., R. J. Wasserman, J. Grey, A. Ricciardi, J. T. A. Dick, and M. E. Alexander. 2017. Novel and disrupted trophic links following invasion in freshwater ecosystems. Pages 55–97 *in* D. Bohan, A. Dumbrell, and F. Massol, editors. Networks of Invasion: Empirical Evidence and Case Studies. Academic Press.

Jensen, B. L., R. C. Johnson, J. J. Duda, C. O. Ostberg, T. J. Code, J. H. Mclean, K. D. Stenberg, K. A. Larsen, M. S. Hoy, and D. A. Beauchamp. in review. Growth performance of rainbow trout in reservoir tributaries and implications for steelhead growth potential above Skagit River dams. North American Journal of Fisheries Management.

Johannes, R. E., and P. A. Larkin. 1961. Competition for food between redside shiners (*Richardsonius balteatus*) and rainbow trout (*Salmo gairdneri*) in two British Columbia lakes. Journal of the Fisheries Research Board of Canada 18:203–220.

Johnston, J. M. 1989. Ross Lake: The fish and fisheries (Report No. 89-6). Washington Department of Wildlife.

Juanes, F., J. A. Buckel, and S. S. Frederick. 2002. Feeding ecology of piscivorous fishes. Pages 267–283 *in* P. J. B. Hart and J. D. Reynolds, editors. Handbook of Fish Biology and Fisheries. Blackwell Science Ltd.

Juncos, R., D. A. Beauchamp, and P. H. Vigliano. 2013. Modeling prey consumption by native and nonnative piscivorous fishes: Implications for competition and impacts on shared prey in an ultraoligotrophic lake in Patagonia. Transactions of the American Fisheries Society 142:268–281.

Knight, C. A., R. W. Orme, and D. A. Beauchamp. 1999. Growth, survival, and migration patterns of juvenile adfluvial Bonneville cutthroat trout in tributaries of Strawberry Reservoir, Utah. Transactions of the American Fisheries Society 128:553–563.

Larkin, P. A., and S. B. Smith. 1954. Some effects of introduction of the redside shiner on the Kamloops trout in Paul Lake, British Columbia. Transactions of the American Fisheries Society 83:161–175.

Legler, N. D., T. B. Johnson, D. D. Heath, and S. A. Ludsin. 2010. Water temperature and prey size effects on the rate of digestion of larval and early juvenile fish. Transactions of the American Fisheries Society 139:868–875.

Lindsey, C. C. 1950. The relation of the redside shiner to production of trout in British Columbia. B.C. Game Commission, Scientific Report.

Lowery, E. D., and D. A. Beauchamp. 2015. Trophic ontogeny of fluvial bull trout and seasonal predation on Pacific salmon in a riverine food web. Transactions of the American Fisheries Society 144:724–741.

Luecke, C., and D. Brandt. 1993. Notes: Estimating the energy density of Daphnid prey for use with rainbow trout bioenergetics models. Transactions of the American Fisheries Society 122:386–389.

Magnan, P., R. Proulx, and M. Plante. 2005. Integrating the effects of fish exploitation and interspecific competition into current life history theories: An example with lacustrine brook trout (*Salvelinus fontinalis*) populations. Canadian Journal of Fisheries and Aquatic Sciences 62:747–757.

McCann, K. 2007. Protecting biostructure. Nature 446:29.

McCarthy, S. G., J. J. Duda, J. M. Emlen, G. R. Hodgson, and D. A. Beauchamp. 2009. Linking habitat quality with trophic performance of steelhead along forest gradients in the South Fork Trinity River watershed, California. Transactions of the American Fisheries Society 138:506–521.

Mesa, M. G., L. K. Weiland, H. E. Christiansen, S. T. Sauter, and D. A. Beauchamp. 2013. Development and evaluation of a bioenergetics model for bull trout. Transactions of the American Fisheries Society 142:41–49.

Miranda, L. E., and P. W. Bettoli. 2007. Mortality. Pages 229–277 *in* C. S. Guy and M. L. Brown, editors. Analysis and interpretation of freshwater fisheries data. American Fisheries Society.

Naiman, R. J., J. R. Alldredge, D. A. Beauchamp, P. A. Bisson, J. Congleton, C. J. Henny, N. Huntly, R. Lamberson, C. Levings, E. N. Merrill, W. G. Pearcy, B. E. Rieman, G. T. Ruggerone, D. Scarnecchia, P. E. Smouse, and C. C. Wood. 2012. Developing a broader scientific foundation for river restoration: Columbia River food webs. Proceedings of the National Academy of Sciences of the United States of America 109:21201–21207.

Nelson, T. C. 2006. Final Report: Upper Skagit watershed native char project 2001-2004. LGL Limited Environmental Research Associates.

Nico, L., and P. Fuller. 2020. *Richardsonius balteatus* (Richardson, 1836): U.S. Geological Survey, Nonindigenous Aquatic Species Database. Available: https://nas.er.usgs.gov/queries/FactSheet.aspx?SpeciesID=644.

Olsson, I. C., L. A. Greenberg, E. Bergman, and K. Wysujack. 2006. Environmentally induced migration: The importance of food. Ecology Letters 9:645–651.

Post, D. M. 2002. Using stable isotopes to estimate trophic position: Models, methods, and assumptions. Ecology 83:703–718.

Rand, P. S., D. J. Stewart, P. W. Seelbach, M. L. Jones, and L. R. Wedge. 1993. Modeling steelhead population energetics in Lakes Michigan and Ontario. Transactions of the American Fisheries Society 122:977–1001.

Rubenson, E. S., D. J. Lawrence, and J. D. Olden. 2020. Threats to rearing juvenile Chinook salmon from nonnative smallmouth bass inferred from stable isotope and fatty acid biomarkers. Transactions of the American Fisheries Society 149:350–363.

Seattle City Light. 1972. The aquatic environment, fishes and fishery: Ross Lake and the Canadian Skagit River (Interim report No. 1 Volume 1). City of Seattle.

Seattle City Light. 1973. The aquatic environment, fishes and fishery: Ross Lake and the Canadian Skagit River (Interim report No. 2 Volume 1). City of Seattle.

Seattle City Light. 1974. The aquatic environment, fishes and fishery: Ross Lake and the Canadian Skagit River (Interim report No. 3 Volume 1). City of Seattle.

Seattle City Light. 2012. Biological Evaluation - supplement: Impacts of entrainment of bull trout. Skagit River Hydroelectric Project License (FERC no. 553) amendment: addition of a second power tunnel at the Gorge Development.

Slaney, P. A., and T. G. Northcote. 1974. Effects of prey abundance on density and territorial behavior of young rainbow trout (*Salmo gairdneri*) in laboratory stream channels. Journal of the Fisheries Research Board of Canada 31:1201–1209.

Smith, C. D., J. M. Plumb, N. S. Adams, and G. J. Wyatt. 2021. Predator and prey events at the entrance of a surface-oriented fish collector at North Fork Dam, Oregon. Fisheries Management and Ecology 28:172–182.

Stock, B. C., A. L. Jackson, E. J. Ward, A. C. Parnell, D. L. Phillips, and B. X. Semmens. 2018. Analyzing mixing systems using a new generation of Bayesian tracer mixing models. PeerJ 6:e5096.

Stockwell, J. D., K. L. Bonfantine, and B. M. Johnson. 1999. Kokanee foraging: A *Daphnia* in the stomach is worth two in the lake. Transactions of the American Fisheries Society 128:169–174.

Wainright, C. A., C. C. Muhlfeld, J. J. Elser, S. L. Bourret, and S. P. Devlin. 2021. Species invasion progressively disrupts the trophic structure of native food webs. Proceedings of the National Academy of Sciences 118:1–5.

Warnock, W. G., J. L. Thorley, S. K. Arndt, T. J. Weir, M. D. Neufeld, J. A. Burrows, and G. F. Andrusak. 2022. Kootenay Lake kokanee (*Oncorhynchus nerka*) collapse into a predator pit. Canadian Journal of Fisheries and Aquatic Sciences 79:234–248.

Winters, L. K., and P. Budy. 2015. Exploring crowded trophic niche space in a novel reservoir fish assemblage: How many is too many? Transactions of the American Fisheries Society 144:1117–1128.

Woodin, R. M. 1974. Age, growth, survival, and mortality of rainbow trout (*Salmo gairdneri gairdneri*, Richardson) from Ross Lake drainage. Master’s thesis. University of Washington.

Tables

Table 1. Estimated age-structured populations and mortality rates for salmonid species in Ross Lake.

Species	Z	Annual survival (%)	Age	Abundance per 1,000 fish[a]	Relative species frequency[b]	Estimated population size[c]	Age-specific abundance
Brook trout	1.273	28.0	2	2,790	0.286	858	2,394
			3	781			670
			4	219			188
Bull trout/hybrids	0.552	57.6	2	827	1.000	3,000	2,481
			3	476			1,428
			4	274			822
			5	158			474
			6	91			273
Dolly Varden	0.552	57.6	2	1,736	0.126	378	656
			3	1,000			378
Rainbow trout	1.011	36.4	2	890	2.430	7,290	6,484
			3	647			4,717
			4	236			1,720
			5	86			627
			6	31			226

[a] For salmonids, age-structured populations were based on 1,000 fish ≥ 200 mm FL (age 3+). Earlier age classes were back-calculated using the same survival rate.

[b] Population adjustments for salmonids in Ross Lake were made based on species frequencies relative to bull trout/hybrids from NOCA gillnet catch data from 2010-2019.

[c] Ross Lake salmonid populations are based on an estimated 3,000 bull trout/hybrids ≥ 200 mm FL.

Table 2. Model coefficients and R^2 for geometric mean regressions on scale radius (SR, mm) and fork length (FL, mm) relationship for fish sampled in Ross Lake and its tributaries. Equation is in the form FL = a + b*SR.

Species	*N*	R^2	a	b
Bull trout/hybrids	218	0.905	-17.587	407.309
Dolly Varden	86	0.840	27.563	305.876
Brook trout	67	0.648	-24.380	450.481
Rainbow trout	393	0.774	42.894	155.501

Table 3. Length-weight regressions for salmonids in Ross Lake. Equations are in the exponential form $W = a \times FL^{b}$.

Species	*N*	*P*	R^2	a	b
Bull trout/hybrids	336	< 0.001	0.997	1.12×10^{-5}	2.974
Dolly Varden	175	< 0.001	0.994	8.26×10^{-6}	3.048
Brook trout	130	< 0.001	0.985	7.79×10^{-6}	3.076
Rainbow trout	1,917	< 0.001	0.996	1.27×10^{-5}	2.961

Table 4. Bioenergetics simulation inputs and corresponding estimates of feeding rate (% C_{max}), annual per capita consumption (g), and growth efficiency (%) for salmonids in Ross Lake. All simulations ran for 365 days (day 1= May 1). Energy density (J/g) of the consumer was linearly interpolated during the simulation from the initial to final value reported. Sample sizes (*N*) are given for the number of individuals used in scale back-calculations for each annulus.

Species	Age	*N*	Spawn day	Spawn loss (%)	Initial FL (mm)	Initial W (g)	Final W (g)	Initial ED (J/g)	Final ED (J/g)	%C_{max}	Growth (g)	Cons (g)	GE (%)	Salmonid cons (g)	Total fish cons (g)
Brook trout	3	55	161	8.0	189	95.3	299.6	5,110	5,474	66	204.2	1,634.0	12.0	23.0	592.0
	4	28	161	8.0	285	299.6	531.1	5,474	5,887	64	231.5	2,796.0	8.0	41.0	1,059.0
Bull trout/hybrids	3	163		0.0	205	99.1	310.4	5,441	5,609	31	211.3	791.0	27.0	50.0	551.0
	4	120		0.0	309	310.4	643.3	5,609	5,874	27	332.9	1,492.0	22.0	92.0	1,045.0
	5	83	161	10.0	401	643.3	1,003.5	5,874	6,161	25	360.2	2,302.0	16.0	139.0	1,620.0
	6	25	161	12.0	468	1,003.5	1,390.9	6,161	6,469	25	387.4	3,087.0	13.0	185.0	2,178.0
Dolly Varden	3	10	161	10.0	178	64.9	131.5	5,414	5,467	26	66.6	383.0	17.0	33.0	242.0
Rainbow trout	2	391		0.0	117	20.7	117.9	4,996	4,996	32	97.2	983.0	10.0	0.0	229.0
	3	355	45	8.0	210	117.9	268.5	4,996	4,996	32	150.6	1,926.0	8.0	19.0	571.0
	4	280	45	8.0	292	268.5	403.9	4,996	4,996	31	135.4	2,756.0	5.0	11.0	1,249.0
	5	112	45	8.0	338	403.9	554.8	4,996	6,672	36	150.9	4,197.0	4.0	17.0	1,904.0
	6	21	45	8.0	374	554.8	877.9	6,672	6,672	36	323.1	5,301.0	6.0	0.0	3,293.0

Figures

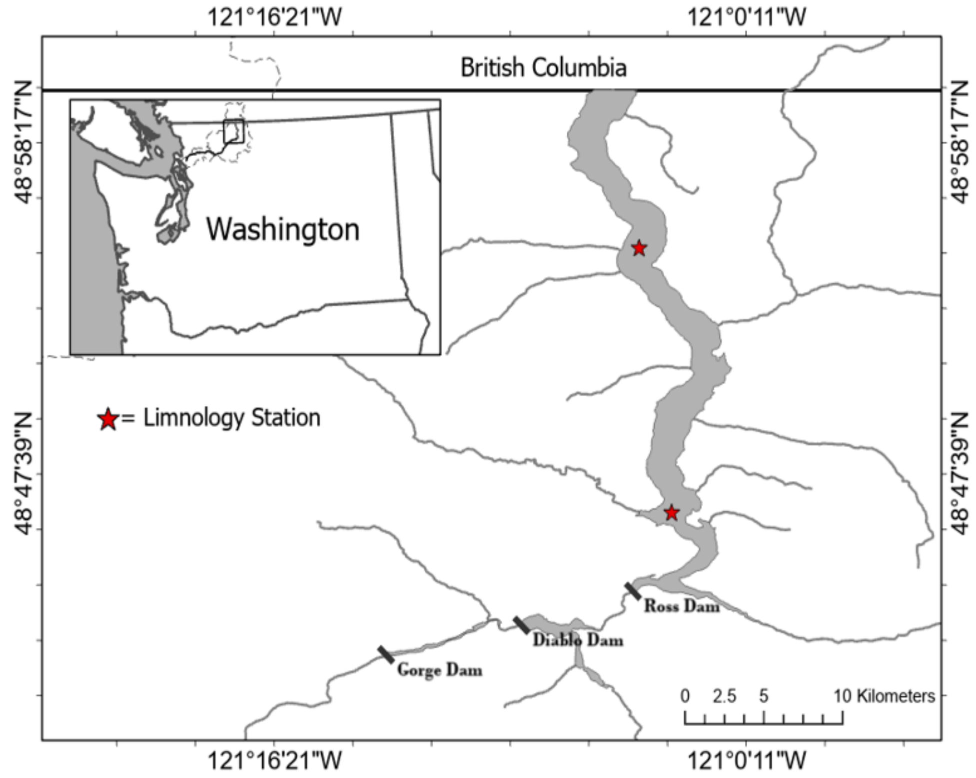

Figure 1. Map of the study system.

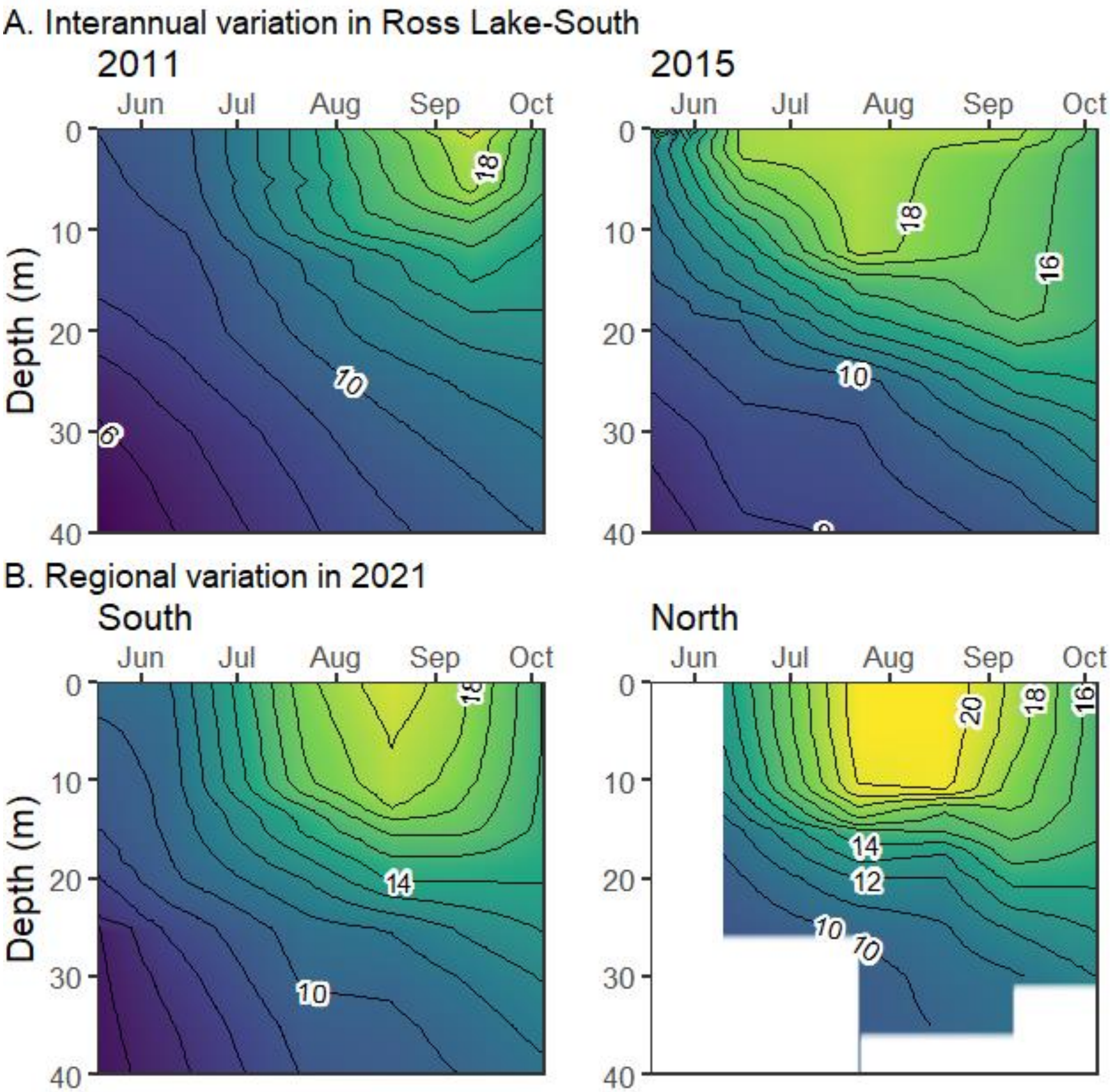

Figure 2. Isoclines for Ross Lake showing variation in thermal structure (°C) by year (A) and region (B). Data prior to 2019 was collected by the NPS. The Ross Lake South site is located mid-lake in the pelagic zone near the confluence with Big Beaver Creek, and the North site was located mid-lake in the pelagic zone near the confluence with Little Beaver Creek.

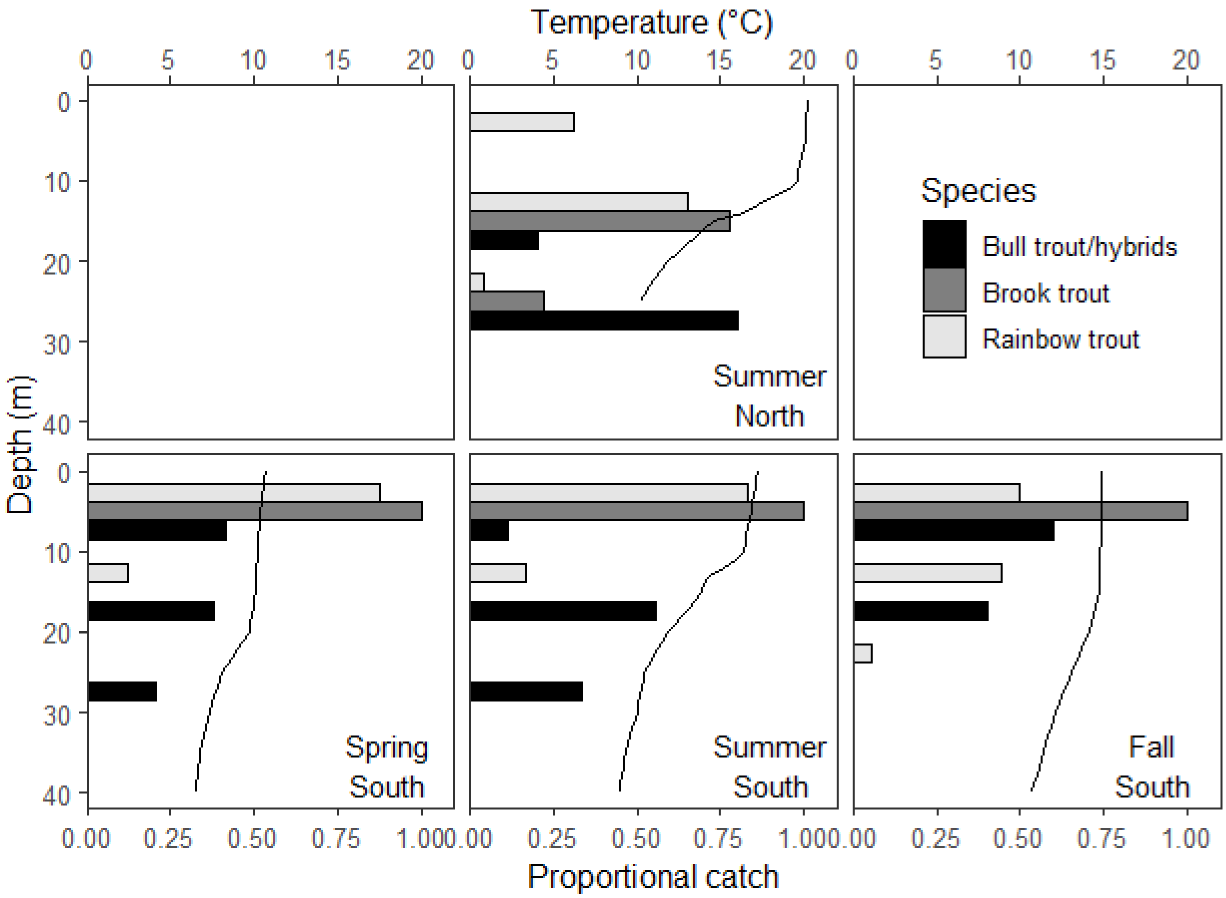

Figure 3. Depth distribution of salmonids as inferred through proportional catch rates in a full set of gillnet arrays in Ross Lake in 2021.

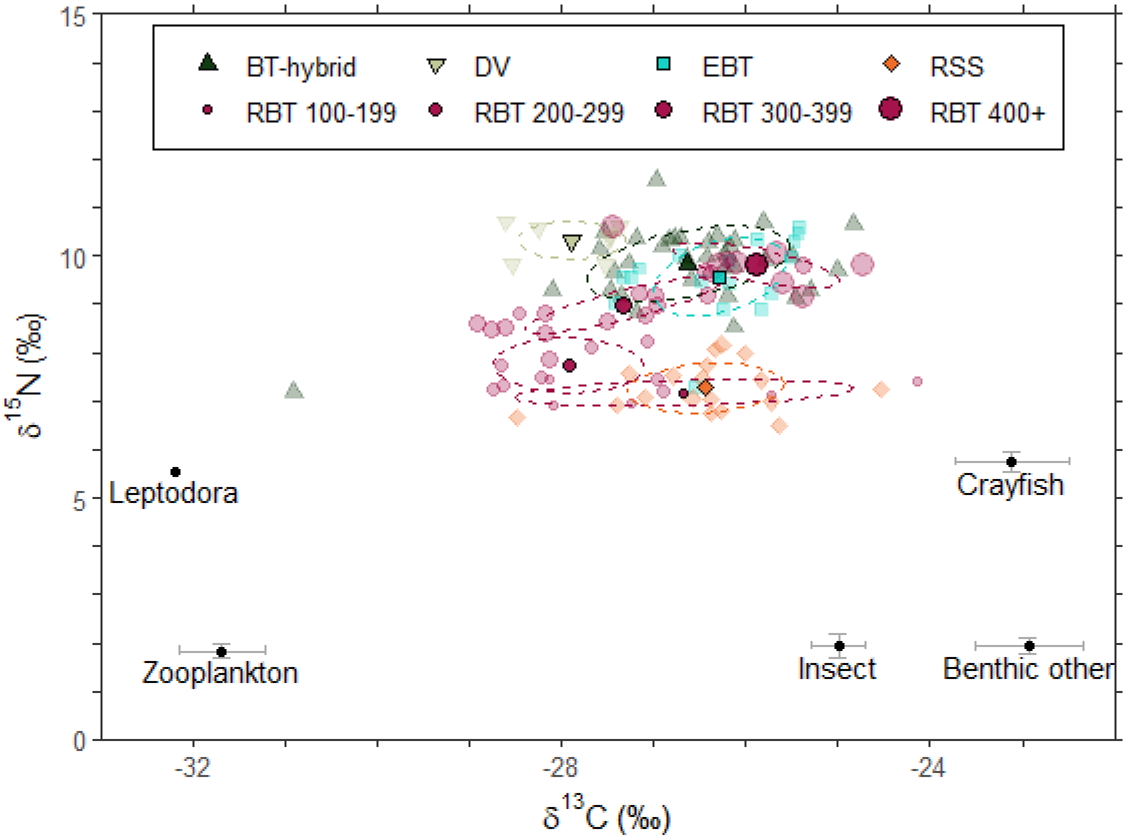

Figure 4. Stable isotope biplots of the Ross Lake food web. Consumer species were separated by size classes if significant differences in stable isotope values were observed. The darker colored symbols represent the group centroids, while the lighter shaded symbols represent individual fish. BT-hybrid: bull trout and char hybrids, DV: Dolly Varden, EBT: brook trout, RBT: rainbow trout, RSS: redside shiner. Numbers following the species code represent the group's size bin, in mm FL. Ellipses contain 40% of the data for each consumer species/size group.

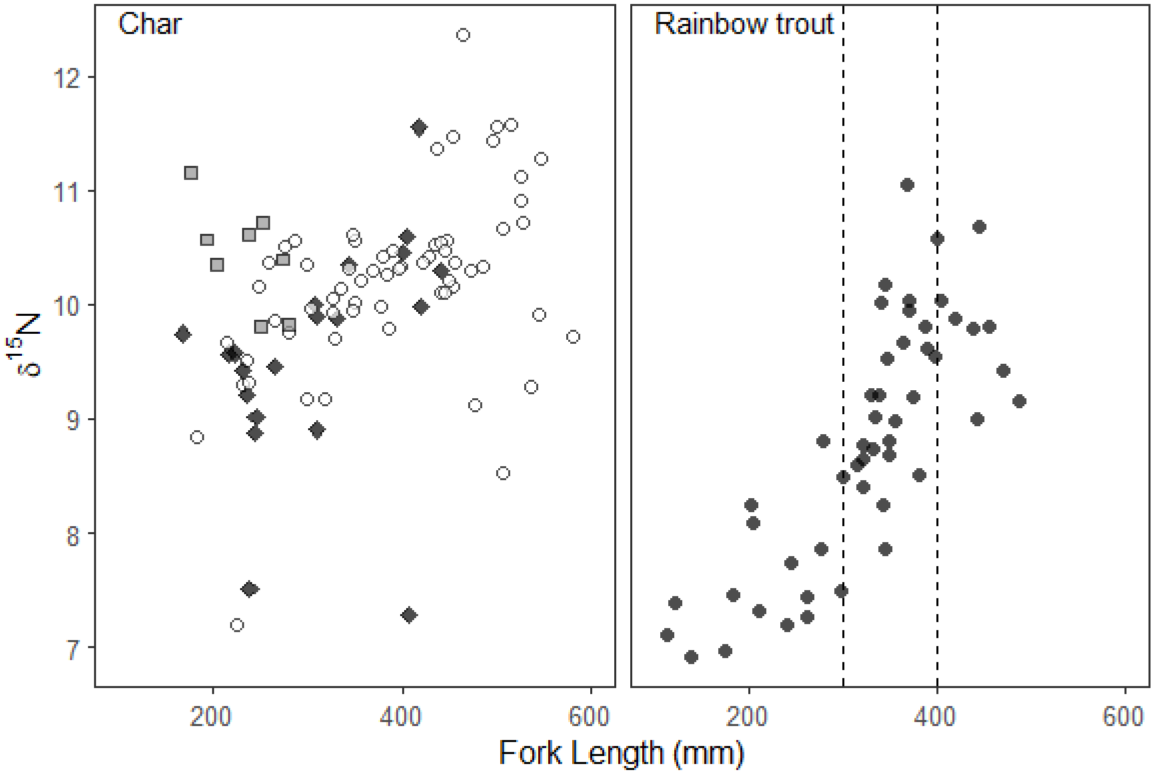

Figure 5. Stable isotope δ^{15}N as a function of fork length (mm) for rainbow trout and char species (bull trout/hybrids: open circles, Dolly Varden: grey squares, brook trout: filled diamonds) in Ross Lake. Dotted lines show the ontogenetic transition to piscivory for rainbow trout.

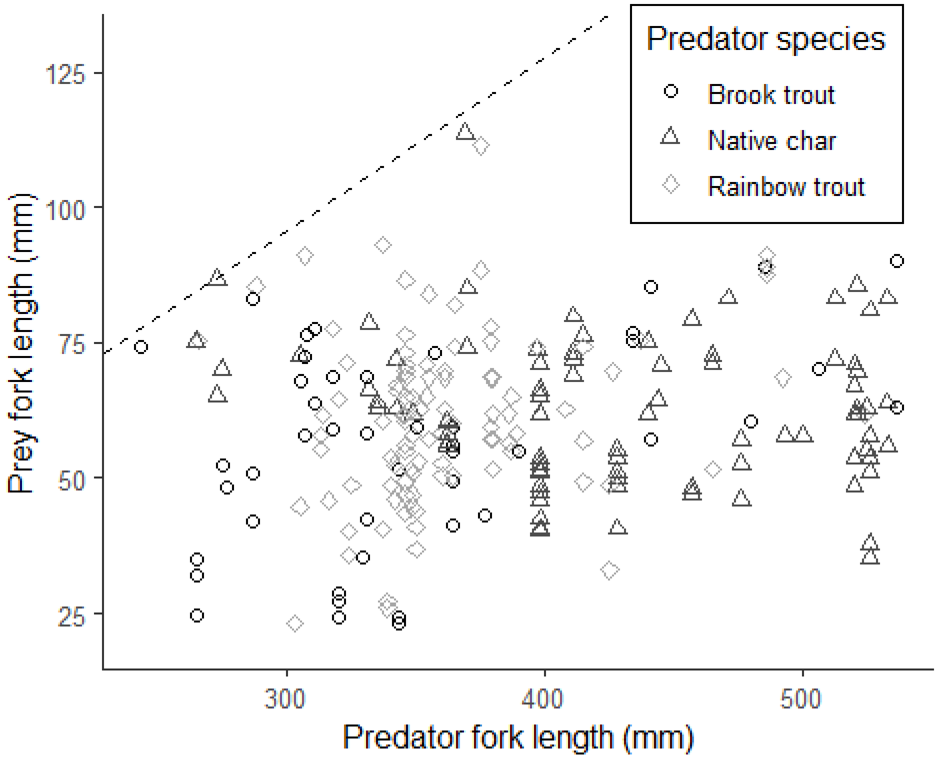

Figure 6. Redside shiner fork length compared to predator fork length for all predator species in Ross Lake. All prey fish observed were < 32% of predator fork length, represented by the dashed line.

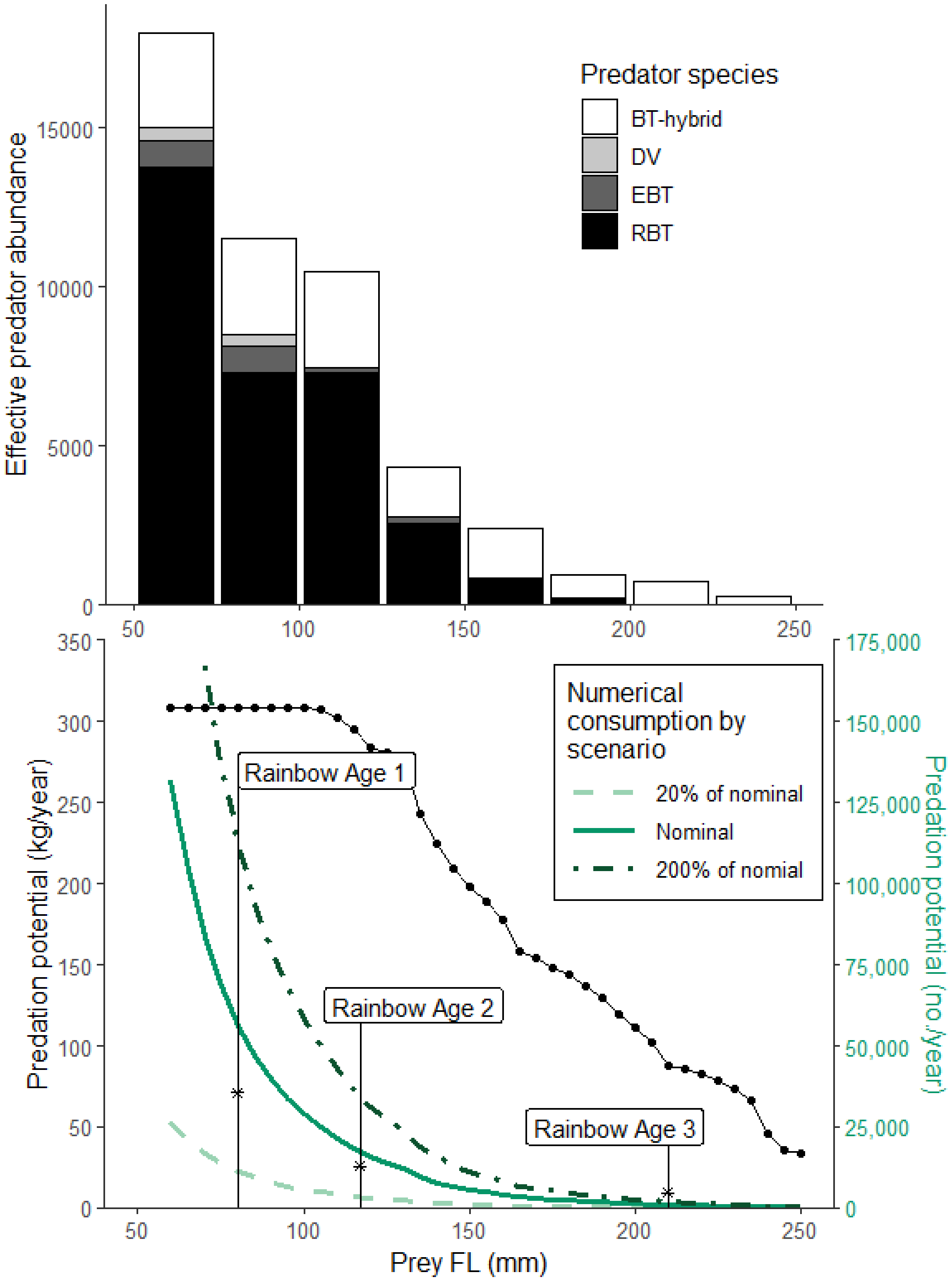
Effective predator abundance
0
5000
10000
15000
50
100
150
200
250
Predator species
BT-hybrid
DV
EBT
RBT
Predation potential (kg/year)
0
50
100
150
200
250
300
350
Predation potential (no./year)
0
25,000
50,000
75,000
100,000
125,000
150,000
175,000
Rainbow Age 1
Rainbow Age 2
Rainbow Age 3
Numerical consumption by scenario
20% of nominal
Nominal
200% of nomial
Prey FL (mm)

Figure 7. Predation potential on salmonids in Ross Lake as a function of prey size and predator abundance. Abundance of effective predators for each 50 mm size class of prey (top panel) is based on the age-structured population abundance and mean fork length at annulus for each predator species. Annual predation potential (bottom panel) in biomass (black line and points, left axis) and fish numbers (green lines, right axis) represents the maximum predation (solid green line) that could occur for any given prey size assuming that 100% of the estimated predation on salmonids was directed at that size of fish. Alternate scenarios are also presented to indicate predation potential 1) at 20% of the maximum and 2) if predation on salmonids was twice as much as we estimated. Fork length at annulus is indicated for rainbow trout age 1-3, and the asterisks indicate the estimated age-class abundance corresponding to the axis on the right.

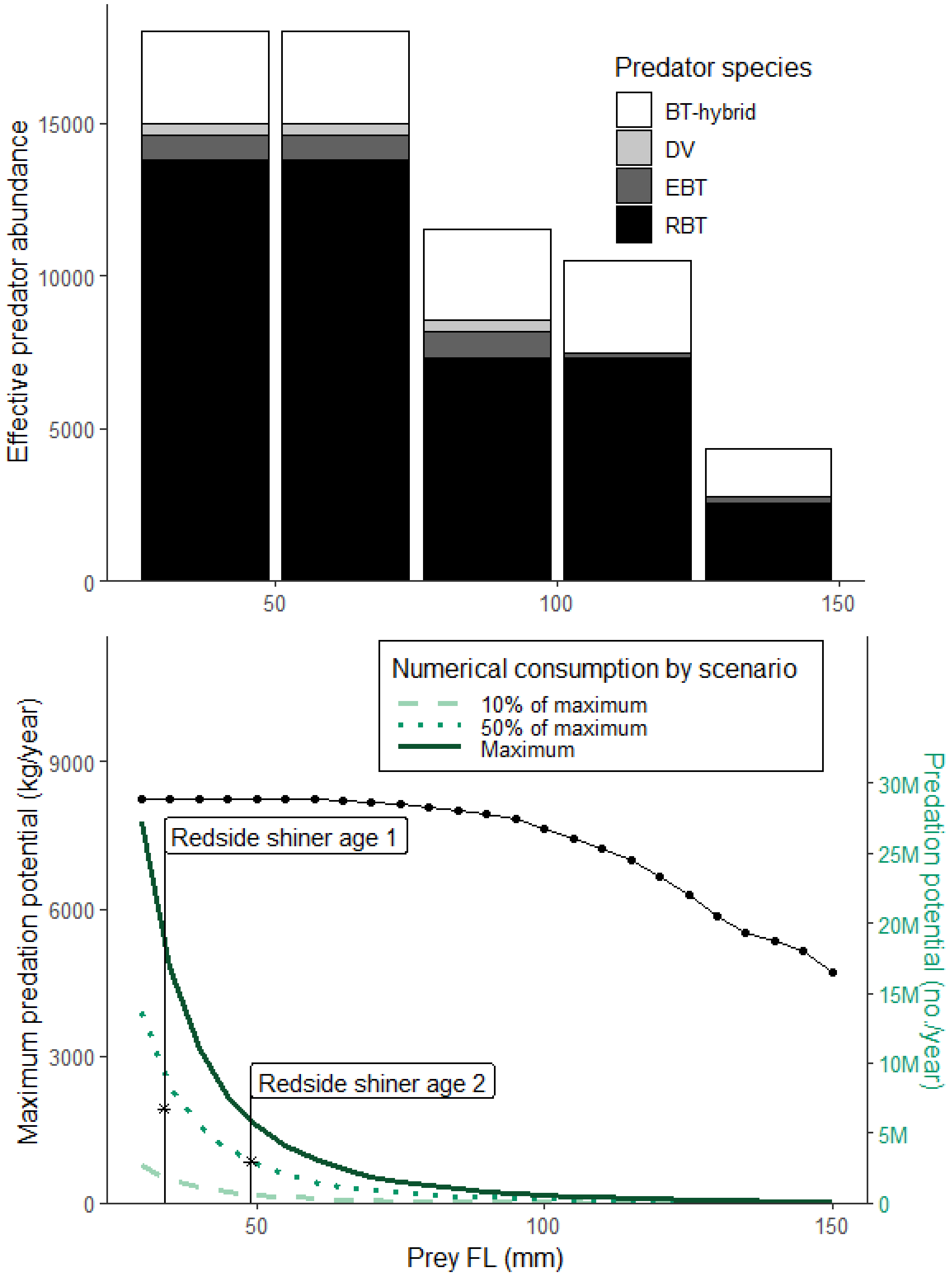
Predator species
BT-hybrid
DV
EBT
RBT
Effective predator abundance
0
5000
10000
15000
50
100
150
Numerical consumption by scenario
10% of maximum
50% of maximum
Maximum
Redside shiner age 1
Redside shiner age 2
Maximum predation potential (kg/year)
0
3000
6000
9000
Predation potential (no./year)
0
5M
10M
15M
20M
25M
30M
50
100
150
Prey FL (mm)

Figure 8. Predation potential on redside shiner in Ross Lake as a function of prey size and predator abundance. Abundance of effective predators for each 50 mm size class of prey (top panel) is based on the age-structured population abundance and mean fork length at annulus for each predator species. Annual predation potential (bottom panel) in biomass (black line and points, left axis) and fish numbers (green lines, right axis) represents the maximum predation (solid green line) that could occur for any given prey size assuming that 100% of the estimated predation on redside shiner and unidentified fish was directed at that size of fish. Alternate scenarios are also presented that show 50% and 10% of the maximum predation potential. Fork length at annulus is indicated for age 1 and 2, and the asterisks indicate the estimated age-class abundance corresponding to the axis on the right.

Chapter 3: Supplementary Materials - Ross Lake

Methods

Bayesian stable isotope mixing models (SIMMs)

Inclusion of specific prey items in the model was partially based on diet analysis and dependent on species and size class. Potential fish prey for rainbow trout 100-199 and 200-299 mm FL included redside shiner and the smallest rainbow trout, while potential fish prey for 300+ mm FL rainbow trout also included rainbow trout 200-299 mm. For all char species, potential fish prey included all fish < 300 mm FL. Prey sources for all consumers also included all zooplankton (mixed zooplankton sample and *Leptodora*) and benthic invertebrates/insects (variety of taxa).

Diet inputs and seasonal consumption

Details regarding how stomach contents (Table S6) and stable isotope mixing models (Table S5, Figs. S2-S8) were combined with general ecological knowledge to construct seasonal diet inputs for the simulations (Tables S6-S7) are described below:

Mixing models predicted a larger contribution of fish than stomach content analysis for small rainbow trout (100-199 and 200-299 mm), therefore we incorporated mixing model results into the spring-summer diet inputs. We assumed stable isotope signatures were incorporated over the previous 1-3 months, and therefore assigned summer SIMM proportions to be constant from simulation day 1 (May 1) to approximate timing of summer sampling (Aug 1, day 92). We did not have stable isotope samples from the fall, so we used proportions from diet analysis for both summer and fall. We assumed zero consumption of fish or zooplankton by this size class in the winter and set this winter diet to end on day 336 (Apr 1) after which it linearly increases to spring levels.

Mixing model results aligned well with stomach contents for larger rainbow trout 300+ mm (comparing stable isotope data to the previous season's stomach contents). The one exception was the predicted contribution of zooplankton versus benthos/insects in the spring for 300-399 mm fish, where the diet samples showed a heavy reliance on benthos (mainly immature insects) and the mixing model showed a reliance on zooplankton instead. We used stomach contents as the seasonal diet inputs for this size class. Due to low diet sample size, we used SIMMs proportions to inform spring-summer diets for rainbow trout 400+. Stomach contents were used for inputs for all other seasons for 300-399 and 400+ mm rainbow trout. For winter diets, we used fall stomach contents and brought zooplankton and adult insects down to zero, replacing them with benthos. As above, we set winter to end on day 336 (Apr 1) at which point diet proportions linearly change to spring levels.

Bull trout SIMM proportions in Ross Lake corresponded fairly well to diet samples, though predicted slightly lower fish consumption than diets in spring or summer. Brook trout stable isotopes also corresponded well, though with slightly higher zooplankton predicted during spring/summer. We therefore used proportions from stomach contents for bull trout/hybrids and brook trout, as sample sizes were robust. For winter, we zeroed out zooplankton if necessary (replacing with benthos). Small samples for Dolly Varden required us to use SIMM proportions for spring-summer, diet samples for summer, and we assumed summer diet proportions were constant through the winter.

References

Beauchamp, D. A., and J. J. Van Tassell. 2001. Modeling seasonal trophic interactions of adfluvial bull trout in Lake Billy Chinook, Oregon. Transactions of the American Fisheries Society 130:204–216.

Furey, N. B., and S. G. Hinch. 2017. Bull trout movements match the life history of sockeye salmon: Consumers can exploit seasonally distinct resource pulses. Transactions of the American Fisheries Society 146:450–461.

Tables

Table S1. Prey energy densities used in bioenergetics simulations. Note that the energy density for Daphnia reflects their compressed form in the gut and is approximately 2x higher in J/g than 'fresh' Daphnia.

Prey group	Energy density (J/g wet weight)	Source
RSS	5,000	this study
Salmonid	4,000	this study
Unid. Fish	5,000	this study
Amphibia	3,980	Crump 1979
Daphnia	3,860	Luecke & Brandt 1993
Leptodora	3,860	Luecke & Brandt 1993
Zooplankton other	2,260	Luecke & Brandt 1993
Amphipod	4,316	James et al. 2012
Snail	2,789	McCarthy et al. 2009
Benthic other	2,789	McCarthy et al. 2009
Immature insect	3,365	McCarthy et al. 2009
Adult insect	5,000	McCarthy et al. 2009
Other	3,500	

Table S2. Significance of size class as a predictor of stable isotope values for δ13C and δ15N from fish sampled in Ross Lake in the summer. Column headings represent the isotope used as a response variable and values represent p value of the nonparametric Kruskal-Wallis with size class as a predictor variable. Significant p values are reported in bold (α=0.05).

	Species	n	δ13C	δ15N
Ross Lake	BT-hybrid	34	**0.004**	0.17
	DV	7	0.617	0.617
	EBT	17	0.06	0.182
	RBT	37	**0.009**	**< 0.001**

Table S3. Pairwise comparisons of difference in isotopic signatures between size classes from nonparametric Dunn test. Pairwise comparisons were only included for those isotopes and species identified as significantly different with the Kruskal-Wallis test. Significantly different comparisons (p < 0.05) are indicated in bold.

Lake	Species	Isotope	Comparison	P
Ross Lake	BT-hybrid	d13C	100-199 : 200-299	1
		d13C	100-199 : 300-399	1
		d13C	200-299 : 300-399	0.179
		d13C	100-199 : 400+	1
		d13C	**200-299 : 400+**	**0.003**
		d13C	300-399 : 400+	1
	RBT	d13C	100-199 : 200-299	0.627
		d13C	100-199 : 300-399	1
		d13C	200-299 : 300-399	1
		d13C	100-199 : 400+	1
		d13C	**200-299 : 400+**	**0.006**
		d13C	300-399 : 400+	0.063
		d15N	100-199 : 200-299	1
		d15N	**100-199 : 300-399**	**0.005**
		d15N	**200-299 : 300-399**	**0.03**
		d15N	**100-199 : 400+**	**< 0.001**
		d15N	**200-299 : 400+**	**< 0.001**
		d15N	300-399 : 400+	0.402

Table S4. Seasonal diet proportions (wet weight, g) for salmonids in Ross Lake from stomach content analysis. Size-classes were pooled for bull trout, Dolly Varden, and brook trout, where ontogenetic differences in diet (based on stable isotope signatures) were not observed. N: sample size of non-empty stomachs, RSS: redside shiner, Sal: salmonid, Unk-fish: unidentified fish, Daph: Daphnia, Lept: Leptodora, Zoop: other zooplankton, IM-insect: immature insect, AD-insect: adult insect.

Length	Season	N	RSS	Sal	Unk-fish	Amphibia	Daph	Lept	Zoop	Amphipod	Snail	Benthos	IM-insect	AD-insect	Other
Bull trout/hybrids															
	Spring	43	0.708	0.023	0.052	0.023	0.010	0.000	0.000	0.073	0.000	0.000	0.108	0.003	0.000
	Summer	51	0.585	0.039	0.133	0.000	0.045	0.075	0.000	0.093	0.000	0.000	0.017	0.000	0.012
	Fall	37	0.336	0.081	0.240	0.027	0.008	0.007	0.028	0.070	0.000	0.017	0.141	0.046	0.000
Dolly Varden															
	Spring	2	0.000	0.000	0.000	0.000	0.000	0.000	0.000	0.582	0.000	0.000	0.418	0.000	0.000
	Summer	4	0.500	0.250	0.000	0.000	0.000	0.000	0.000	0.000	0.000	0.000	0.250	0.000	0.000
	Fall		-	-	-	-	-	-	-	-	-	-	-	-	-
Brook trout															
	Spring	17	0.538	0.001	0.069	0.000	0.000	0.001	0.000	0.028	0.073	0.105	0.134	0.004	0.048
	Summer	40	0.600	0.050	0.107	0.008	0.002	0.014	0.000	0.001	0.000	0.002	0.135	0.082	0.000
	Fall	5	0.101	0.000	0.000	0.000	0.000	0.000	0.000	0.000	0.130	0.000	0.386	0.327	0.056
Rainbow trout															
100-199	Spring	4	0.000	0.000	0.000	0.000	0.243	0.087	0.000	0.249	0.012	0.000	0.251	0.157	0.000
	Summer	29	0.019	0.000	0.040	0.000	0.181	0.049	0.019	0.002	0.012	0.000	0.225	0.419	0.035
	Fall	2	0.000	0.000	0.500	0.000	0.000	0.000	0.273	0.000	0.000	0.000	0.031	0.196	0.000
200-299	Spring	17	0.004	0.000	0.000	0.000	0.196	0.093	0.057	0.000	0.000	0.000	0.472	0.178	0.000
	Summer	28	0.098	0.000	0.060	0.000	0.258	0.294	0.058	0.000	0.000	0.000	0.080	0.132	0.019
	Fall	13	0.077	0.035	0.190	0.000	0.225	0.033	0.002	0.000	0.000	0.000	0.162	0.268	0.008
300-399	Spring	64	0.324	0.005	0.025	0.004	0.026	0.020	0.000	0.004	0.012	0.037	0.479	0.056	0.007
	Summer	68	0.503	0.000	0.124	0.000	0.138	0.115	0.000	0.016	0.000	0.012	0.001	0.087	0.004
	Fall	77	0.346	0.006	0.043	0.000	0.185	0.039	0.001	0.000	0.017	0.007	0.191	0.150	0.016
400+	Spring	4	0.671	0.000	0.000	0.000	0.000	0.000	0.000	0.000	0.000	0.000	0.215	0.114	0.000
	Summer	12	0.894	0.000	0.083	0.000	0.005	0.001	0.000	0.004	0.000	0.006	0.001	0.001	0.005
	Fall	7	0.475	0.000	0.016	0.000	0.022	0.000	0.001	0.000	0.141	0.075	0.270	0.000	0.000

Table S5. Seasonal diet proportions (wet weight) compared to stable isotope mixing model results (SIMM, 95% credible intervals) for broad prey categories for salmonids in Ross Lake. Season refers to the season that the diet sample or tissue sample was collected.

					Fish		Zooplankton		Benthos/insect/other	
Species	Length	Season	*N*: Diet	*N*: SIMM	Diet	SIMM	Diet	SIMM	Diet	SIMM
BT-hybrid	all	Spring	43		0.783		0.010		0.207	
		Summer	51	34	0.757	0.636 (0.377-0.749)	0.120	0.187 (0.083-0.414)	0.122	0.177 (0.06-0.296)
		Fall	37		0.657		0.043		0.301	
DV		Spring	2		0.000		0.000		1.000	
		Summer	4	7	0.750	0.671 (0.488-0.786)	0.000	0.275 (0.152-0.416)	0.250	0.054 (0.002-0.167)
		Fall			-		-		-	
EBT		Spring	17		0.608		0.001		0.392	
		Summer	40	17	0.757	0.63 (0.507-0.728)	0.016	0.124 (0.051-0.218)	0.228	0.246 (0.15-0.343)
		Fall	5		0.101		0.000		0.899	
RBT	100-199	Spring	4		0.000		0.330		0.669	
		Summer	29	5	0.059	0.304 (0.111-0.496)	0.249	0.336 (0.08-0.636)	0.693	0.359 (0.088-0.607)
		Fall	2		0.500		0.273		0.227	
	200-299	Spring	17		0.004		0.346		0.650	
		Summer	28	9	0.158	0.377 (0.182-0.542)	0.610	0.434 (0.317-0.558)	0.231	0.188 (0.043-0.346)
		Fall	13		0.302		0.260		0.438	
	300-399	Spring	64		0.354		0.046		0.599	
		Summer	68	21	0.627	0.406 (0.181-0.586)	0.253	0.511 (0.3-0.75)	0.120	0.083 (0.008-0.202)
		Fall	77	10	0.395	0.607 (0.418-0.734)	0.225	0.254 (0.114-0.462)	0.381	0.138 (0.031-0.242)
	400+	Spring	4		0.671		0.000		0.329	
		Summer	12	7	0.977	0.71 (0.59-0.812)	0.006	0.076 (0.005-0.202)	0.017	0.214 (0.085-0.329)
		Fall	7		0.491		0.023		0.486	

Table S6. Rainbow trout seasonal diet proportions for each length bin (mm FL) used as inputs into bioenergetics model simulations. Sample size (N)) of stomach content analysis is indicated for the seasons in which non-empty stomach contents were collected. Winter diets were set to be constant between day 245 and 336 (Jan 1- Apr 1). All diets were linearly interpolated between seasons. *Denotes seasons in which stable isotope mixing model results were used to modify these diet inputs for the bioenergetics simulations. RSS: redside shiner, Sal: salmonid, Unk-fish: unidentified fish, Daph: Daphnia, Lept: Leptodora, Zoop: other zooplankton, IM-insect: immature insect, AD-insect: adult insect.

				Diet proportions												
Length	Day	Season	*N*	RSS	Sal	Unk-fish	Amphibia	Daph	Lept	Zoop	Amphipod	Snail	Benthos	IM-insect	AD-insect	Other
100-199	1	Spring*	4	0.304	0.000	0.000	0.000	0.243	0.087	0.007	0.134	0.006	0.000	0.135	0.084	0.000
	91	Summer*	-	0.304	0.000	0.000	0.000	0.243	0.087	0.007	0.134	0.006	0.000	0.135	0.084	0.000
	92	Summer	29	0.019	0.000	0.040	0.000	0.181	0.049	0.019	0.002	0.012	0.000	0.225	0.419	0.034
	154	Fall	2	0.000	0.000	0.500	0.000	0.000	0.000	0.273	0.000	0.000	0.000	0.031	0.196	0.000
	245	Winter	-	0.000	0.000	0.000	0.000	0.000	0.000	0.000	0.000	0.000	1.000	0.000	0.000	0.000
	336	Spring	-	0.000	0.000	0.000	0.000	0.000	0.000	0.000	0.000	0.000	1.000	0.000	0.000	0.000
200-299	1	Spring*	17	0.377	0.000	0.000	0.000	0.246	0.117	0.071	0.000	0.000	0.000	0.137	0.052	0.000
	91	Summer*	-	0.377	0.000	0.000	0.000	0.246	0.117	0.071	0.000	0.000	0.000	0.137	0.052	0.000
	92	Summer	28	0.098	0.000	0.060	0.000	0.258	0.294	0.058	0.000	0.000	0.000	0.080	0.132	0.020
	154	Fall	13	0.077	0.035	0.190	0.000	0.225	0.033	0.002	0.000	0.000	0.000	0.162	0.268	0.008
	245	Winter	-	0.077	0.000	0.190	0.000	0.000	0.000	0.000	0.000	0.000	0.571	0.162	0.000	0.000
	336	Spring	-	0.077	0.000	0.190	0.000	0.000	0.000	0.000	0.000	0.000	0.571	0.162	0.000	0.000
300-399	1	Spring	64	0.324	0.005	0.025	0.005	0.026	0.020	0.000	0.004	0.012	0.037	0.479	0.056	0.007
	92	Summer	68	0.503	0.000	0.124	0.000	0.138	0.115	0.000	0.016	0.000	0.012	0.001	0.087	0.004
	154	Fall	77	0.346	0.006	0.043	0.000	0.185	0.039	0.001	0.000	0.017	0.007	0.191	0.150	0.015
	245	Winter	-	0.346	0.006	0.043	0.000	0.000	0.000	0.000	0.000	0.017	0.381	0.191	0.000	0.016
	336	Spring	-	0.346	0.006	0.043	0.000	0.000	0.000	0.000	0.000	0.017	0.381	0.191	0.000	0.016
400+	1	Spring*	4	0.671	0.000	0.039	0.000	0.076	0.000	0.000	0.000	0.000	0.000	0.140	0.074	0.000
	91	Summer*	-	0.671	0.000	0.039	0.000	0.076	0.000	0.000	0.000	0.000	0.000	0.140	0.074	0.000
	92	Summer	12	0.894	0.000	0.083	0.000	0.005	0.001	0.000	0.004	0.000	0.006	0.001	0.001	0.005
	154	Fall	7	0.475	0.000	0.016	0.000	0.022	0.000	0.001	0.000	0.141	0.075	0.270	0.000	0.000
	245	Winter	-	0.475	0.000	0.016	0.000	0.000	0.000	0.000	0.000	0.141	0.098	0.270	0.000	0.000
	336	Spring	-	0.475	0.000	0.016	0.000	0.000	0.000	0.000	0.000	0.141	0.098	0.270	0.000	0.000

Table S7. Seasonal diet proportions used as inputs into bioenergetics model simulations for char species in Ross Lake. No ontogenetic shifts in stable isotope signature were observed, thus diet inputs were pooled across length bins. Sample size (N) of stomach content analysis is indicated for the seasons in which non-empty stomach contents were collected. Winter diets were set to be constant between day 245 and 336 (Jan 1- Apr 1). All diets were linearly interpolated between seasons. *Denotes seasons in which stable isotope mixing model results were used to modify these diet inputs for the bioenergetics simulations. RSS: redside shiner, Sal: salmonid, Unk-fish: unidentified fish, Daph: Daphnia, Lept: Leptodora, Zoop: other zooplankton, IM-insect: immature insect, AD-insect: adult insect.

					Diet proportions											
Length	Day	Season	N	*RSS*	Sal	Unk-fish	Amphibia	Daph	Lept	Zoop	Amphipod	Snail	Benthos	IM-insect	AD-insect	Other
Bull trout/hybrids																
All	1	Spring	43	0.708	0.023	0.052	0.023	0.010	0.000	0.000	0.073	0.000	0.000	0.108	0.003	0.000
	92	Summer	51	0.585	0.039	0.133	0.000	0.045	0.075	0.000	0.093	0.000	0.000	0.017	0.000	0.013
	154	Fall	37	0.336	0.081	0.240	0.027	0.008	0.007	0.028	0.070	0.000	0.016	0.141	0.046	0.000
	245	Winter	-	0.336	0.081	0.240	0.027	0.000	0.000	0.000	0.070	0.000	0.059	0.141	0.046	0.000
	336	Spring	-	0.336	0.081	0.240	0.027	0.000	0.000	0.000	0.070	0.000	0.059	0.141	0.046	0.000
Dolly Varden																
All	1	Spring*	2	0.000	0.000	0.671	0.000	0.275	0.000	0.000	0.027	0.000	0.000	0.027	0.000	0.000
	91	Sumer*	-	0.000	0.000	0.671	0.000	0.275	0.000	0.000	0.027	0.000	0.000	0.027	0.000	0.000
	92	Summer	4	0.500	0.250	0.000	0.000	0.000	0.000	0.000	0.000	0.000	0.000	0.250	0.000	0.000
	245	Winter	-	0.500	0.000	0.000	0.000	0.000	0.000	0.000	0.000	0.000	0.250	0.250	0.000	0.000
	336	Spring	-	0.500	0.000	0.000	0.000	0.000	0.000	0.000	0.000	0.000	0.250	0.250	0.000	0.000
Brook trout																
All	1	Spring	17	0.538	0.001	0.069	0.000	0.000	0.001	0.000	0.028	0.073	0.105	0.134	0.004	0.047
	92	Summer	40	0.600	0.050	0.107	0.008	0.002	0.014	0.000	0.001	0.000	0.001	0.135	0.082	0.000
	154	Fall	5	0.101	0.000	0.000	0.000	0.000	0.000	0.000	0.000	0.130	0.000	0.386	0.327	0.056
	245	Winter	-	0.101	0.000	0.000	0.000	0.000	0.000	0.000	0.000	0.130	0.000	0.386	0.327	0.056
	336	Spring	-	0.101	0.000	0.000	0.000	0.000	0.000	0.000	0.000	0.130	0.000	0.386	0.327	0.056

Table S8. Average monthly thermal experience for bull trout/Dolly Varden (BT), brook trout (EBT), and rainbow trout (RBT) in Ross Lake.

	Temperature °C		
Month	BT	EBT	RBT
Jan	5.1	5.1	5.1
Feb	4.2	4.2	4.2
Mar	4.6	4.6	4.6
Apr	6.3	6.3	6.3
May	8.4	9.8	9.8
Jun	10.6	12.5	12.5
Jul	11.9	15.8	15.8
Aug	12.5	16.1	16.6
Sep	12.8	17.2	17.2
Oct	13.3	14.1	14.1
Nov	10.4	10.4	10.4
Dec	7.1	7.1	7.1

Table S9. Percentage contribution by weight of Salmonid species to seasonal diets in Ross Lake. Column labels correspond to the following species of prey fish: NC = native char, RBT = rainbow trout, EBT = brook trout, WCT = cutthroat trout.

Consumer species	FL (mm)	Season	Total diets	Diets with salmonids	NC	RBT	EBT	WCT	Unid. Sal
Bull trout/hybrids		Spring	43	1	0.66%	0.00%	0.00%	0.00%	1.66%
		Summer	51	2	0.00%	1.96%	1.96%	0.00%	0.00%
		Fall	37	3	0.00%	8.11%	0.00%	0.00%	0.00%
Dolly Varden		Spring	2	0	0.00%	0.00%	0.00%	0.00%	0.00%
		Summer	4	1	0.00%	0.00%	25.00%	0.00%	0.00%
Brook trout		Spring	17	1	0.00%	0.06%	0.00%	0.00%	0.00%
		Summer	40	2	2.50%	2.50%	0.00%	0.00%	0.00%
		Fall	5	0	0.00%	0.00%	0.00%	0.00%	0.00%
Rainbow trout	100-199	Spring	4	0	0.00%	0.00%	0.00%	0.00%	0.00%
		Summer	29	0	0.00%	0.00%	0.00%	0.00%	0.00%
		Fall	2	0	0.00%	0.00%	0.00%	0.00%	0.00%
	200-299	Spring	17	1	0.00%	0.00%	0.00%	0.00%	0.03%
		Summer	28	0	0.00%	0.00%	0.00%	0.00%	0.00%
		Fall	13	1	0.00%	3.45%	0.00%	0.00%	0.00%
	300-399	Spring	64	1	0.00%	0.54%	0.00%	0.00%	0.00%
		Summer	68	0	0.00%	0.00%	0.00%	0.00%	0.00%
		Fall	77	1	0.00%	0.00%	0.00%	0.62%	0.00%
	400	Spring	4	0	0.00%	0.00%	0.00%	0.00%	0.00%
		Summer	12	0	0.00%	0.00%	0.00%	0.00%	0.00%
		Fall	7	0	0.00%	0.00%	0.00%	0.00%	0.00%

Figures

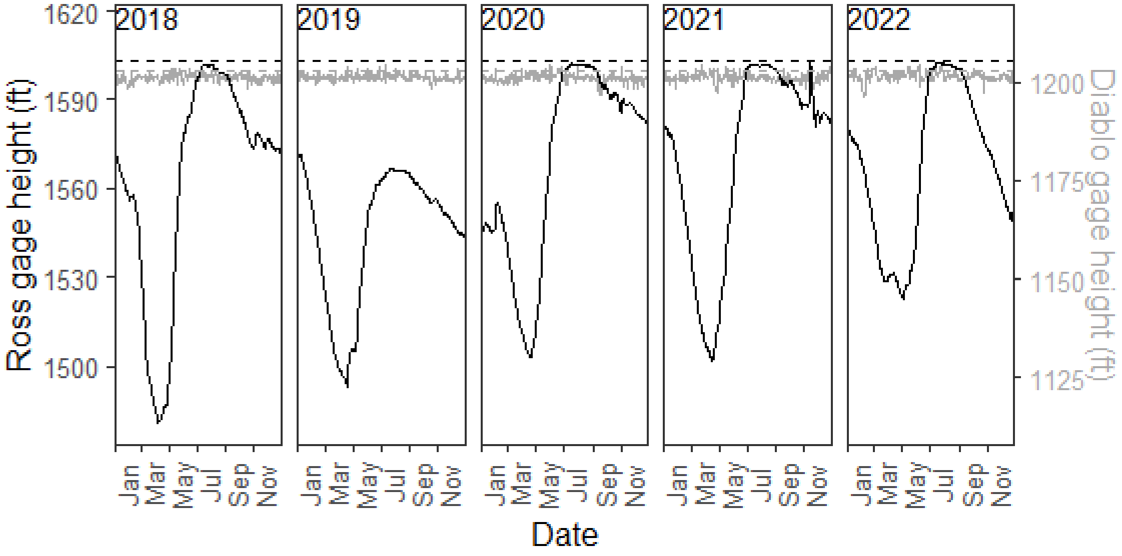

Figure S1. Reservoir surface elevation (ft) for Ross (black) and Diablo (grey) lakes in 2018-2022. Data retreived from USGS Water Data using the 'dataRetrieval' package. Dotted lines represent elevation at each respective reservoirs normal 'full pool' operation.

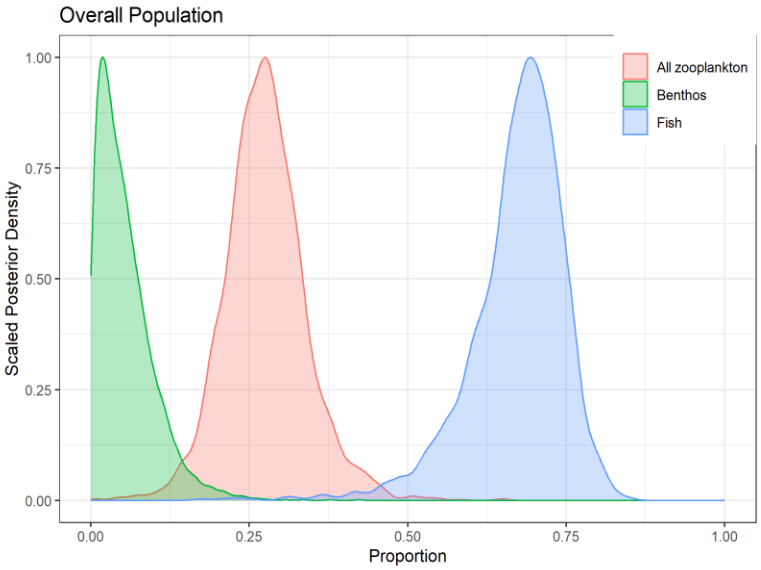

Figure S2. Stable isotope mixing model posterior densities for all Dolly Varden in Ross Lake sampled in the summer.

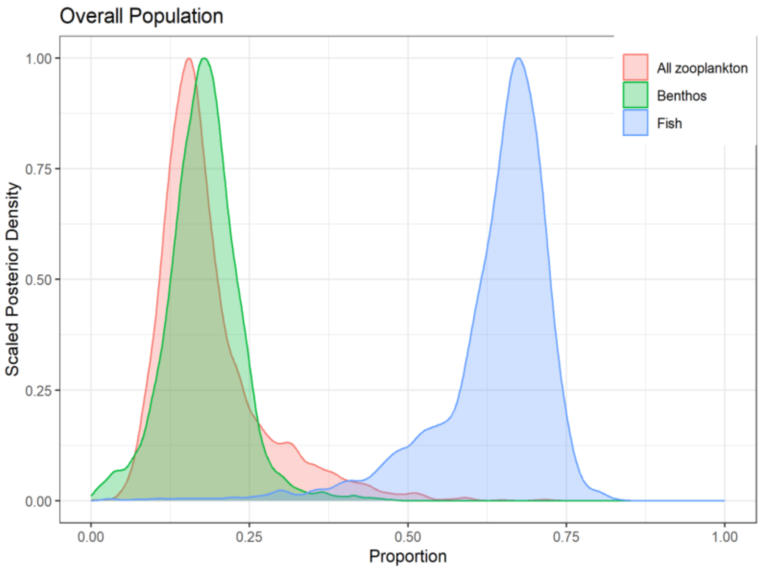

Figure S3. Stable isotope mixing model posterior densities for all bull trout/hybrids in Ross Lake sampled in the summer.

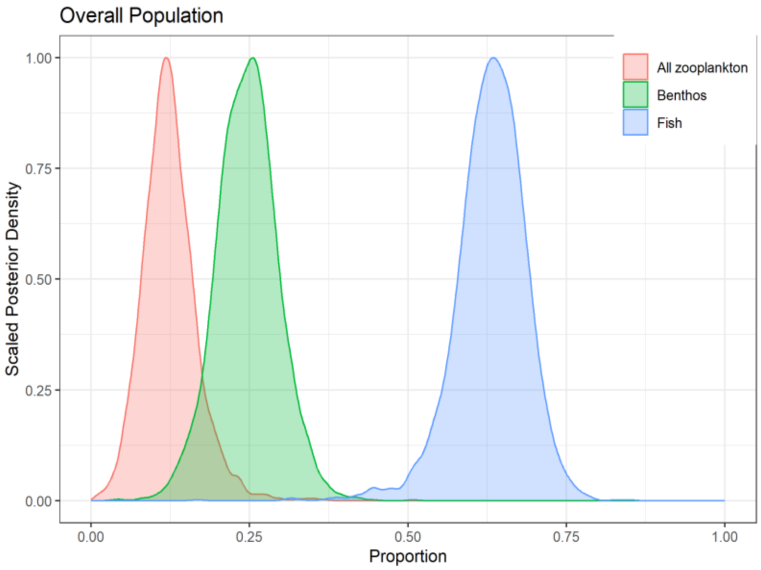

Figure S4. Stable isotope mixing model posterior densities for all brook trout in Ross Lake sampled in the summer.

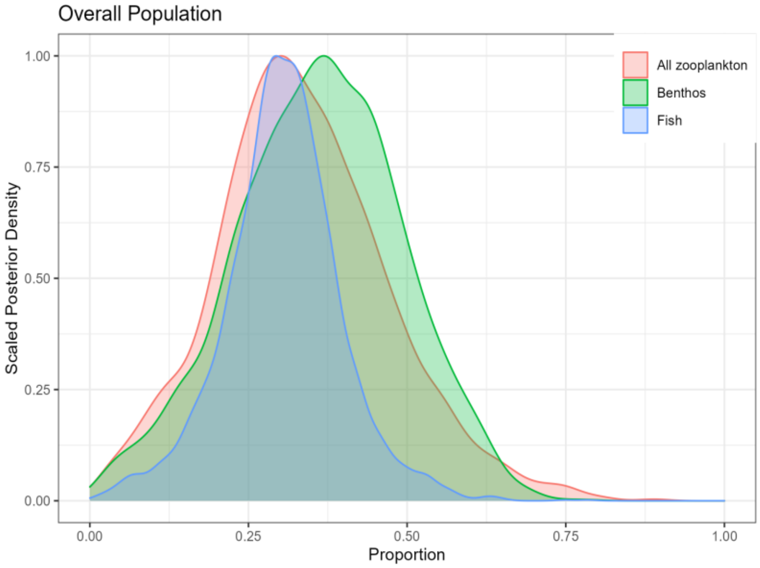

Figure S5. Stable isotope mixing model posterior densities for rainbow trout 100-199 mm FL in Ross Lake sampled in the summer.

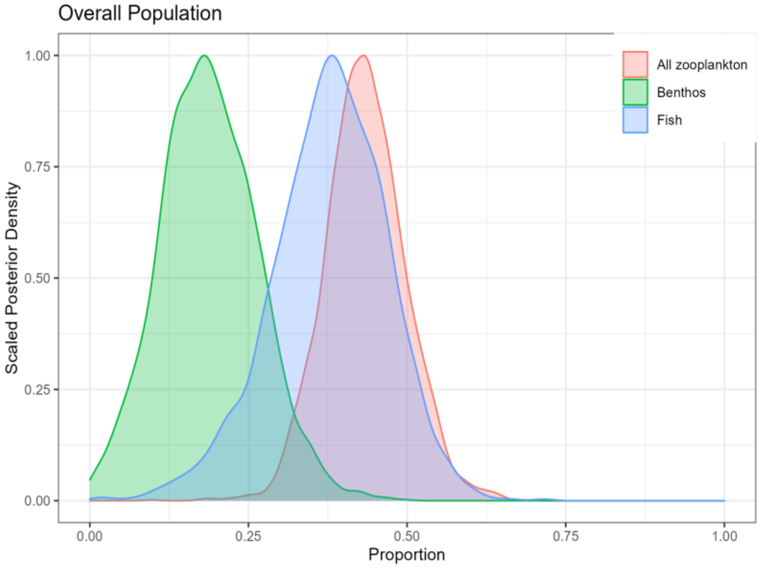

Figure S6. Stable isotope mixing model posterior densities for rainbow trout 200-299 mm FL in Ross Lake sampled in the summer.

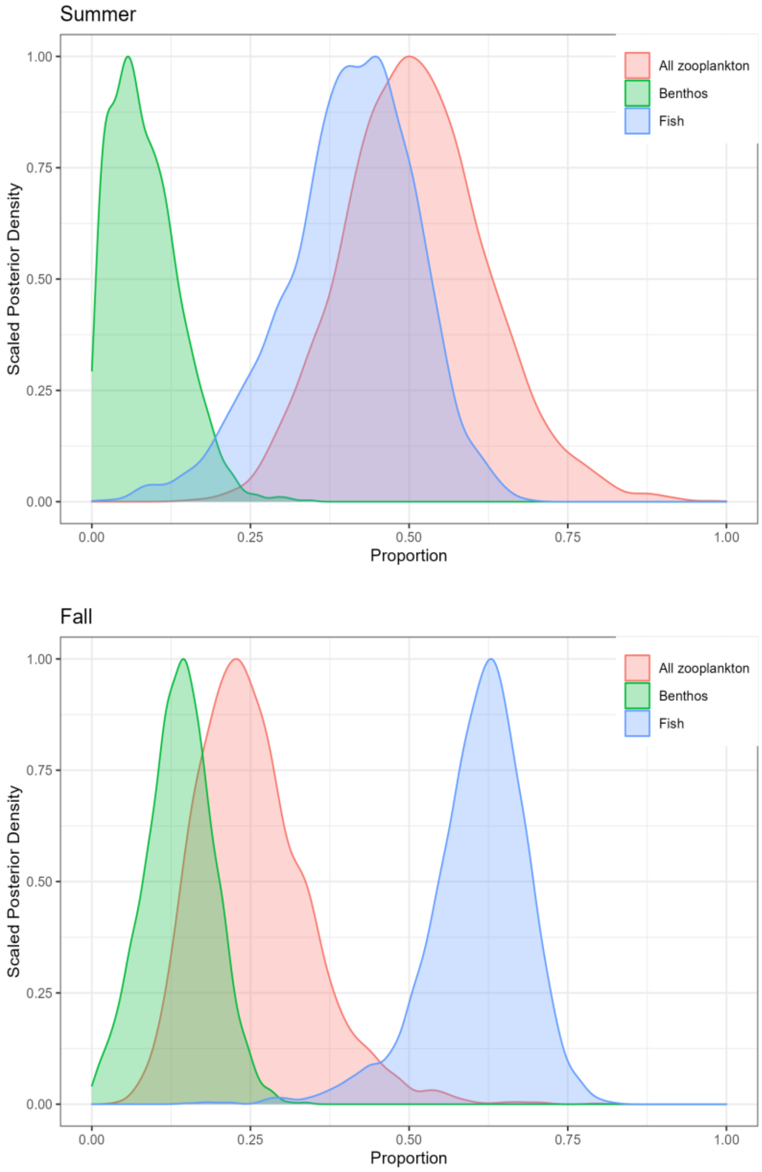

Figure S7. Stable isotope mixing model posterior densities for rainbow trout 300-399 mm FL in Ross Lake sampled in the summer and fall.

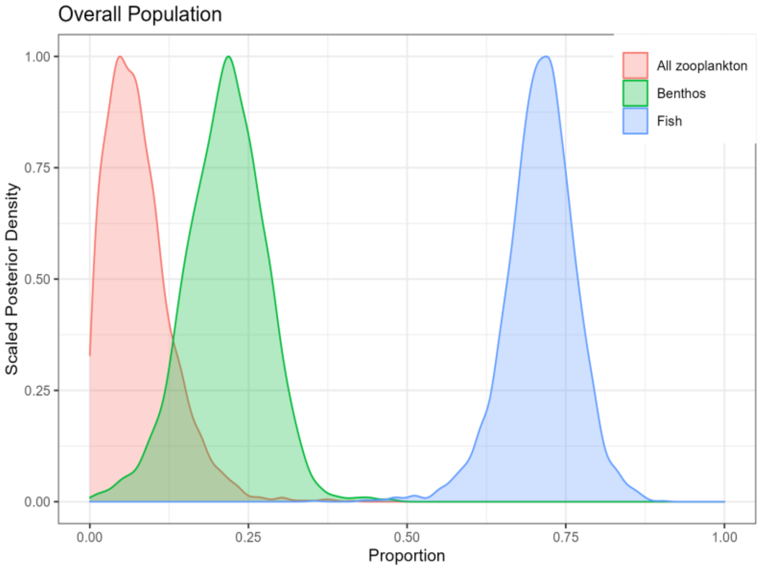

Figure S8. Stable isotope mixing model posterior densities for rainbow trout 400+ mm FL in Ross Lake sampled in the summer.

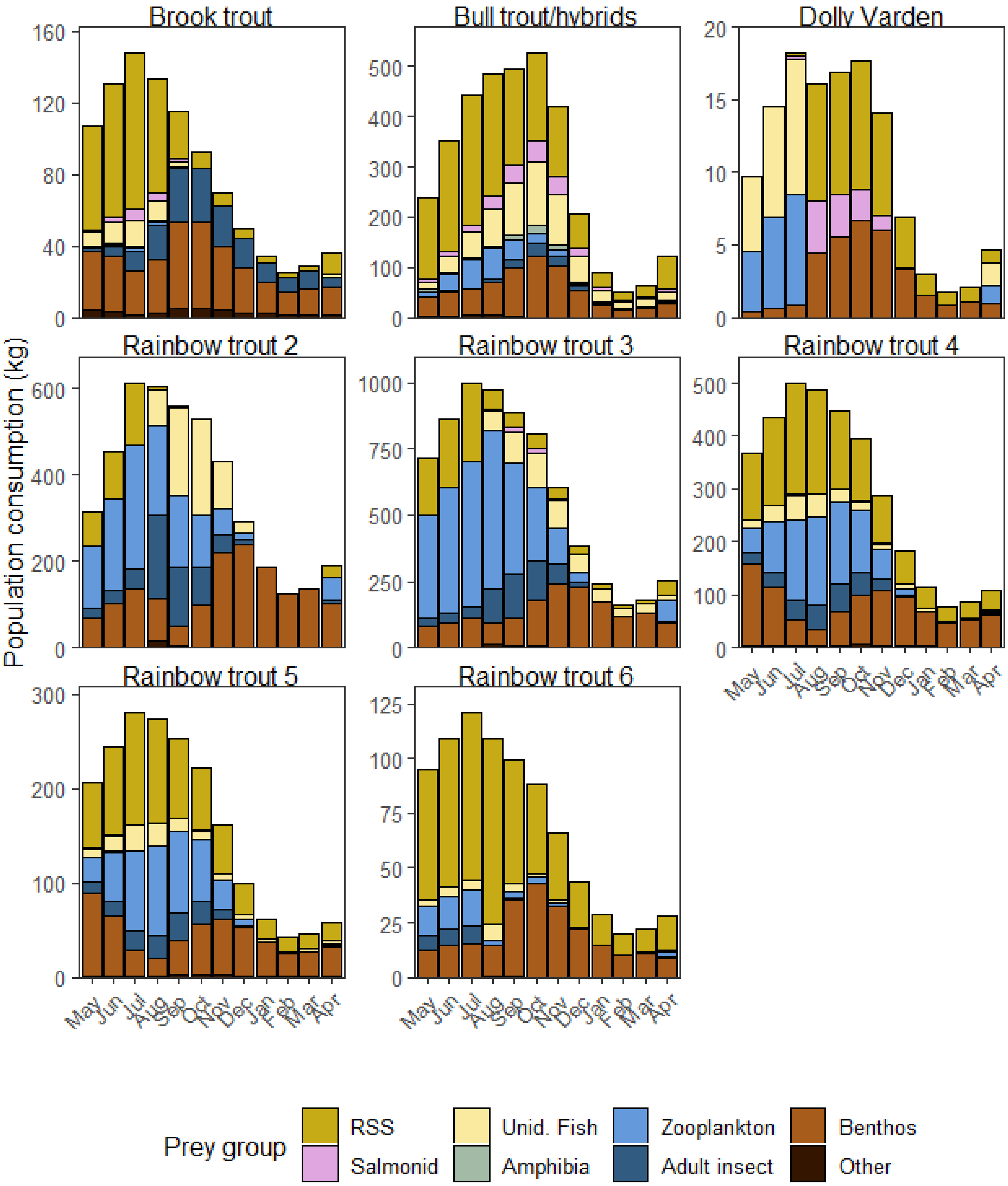

Figure S9. Simulated monthly population consumption for each salmonid species in Ross Lake. Rainbow trout are separated by age class. Note the different y-axis scales.

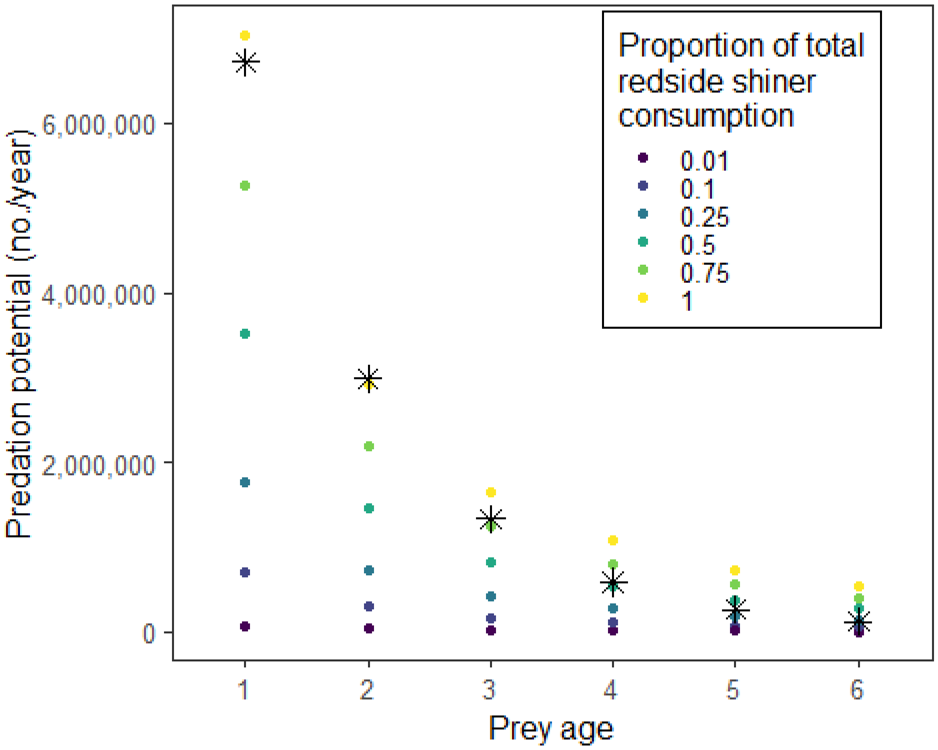

Figure S10. Simulated annual predation potential on each age class of redside shiner in Ross Lake after accounting for daily fish growth and gape limitation (assuming predators can consume fish up to 50% of their length). Annual predation (individual fish) is modeled for a range of proportional allocation to the redside shiner component of the diets. Asterisks indicate the estimated age-class abundance of redside shiner in October.

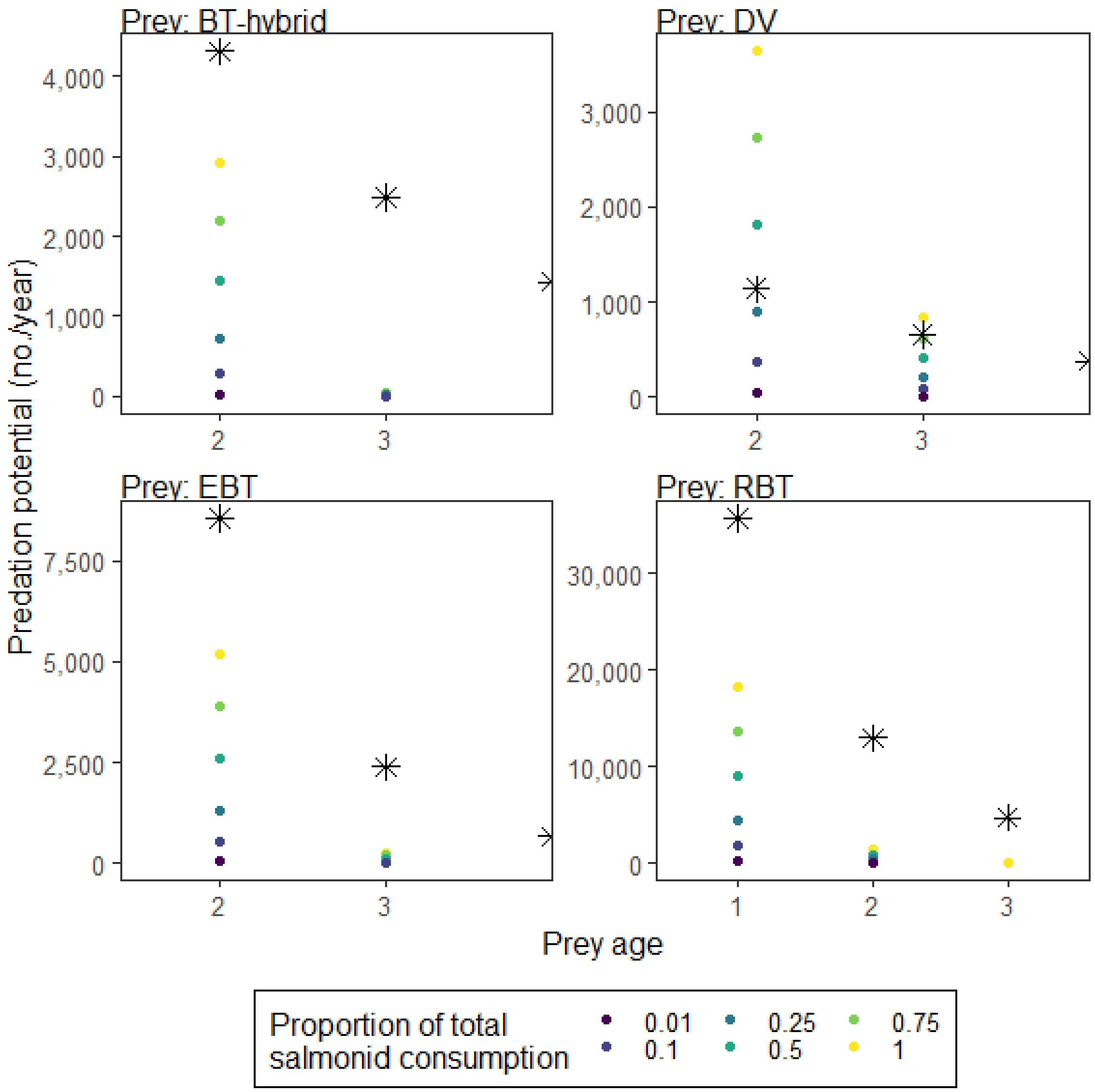

Figure S11. Simulated annual predation potential on each age class of salmonids (BT-hybrid: bull trout and hybrids, DV: Dolly Varden, EBT: brook trout, RBT: rainbow trout) after accounting for daily fish growth and gape limitation (assuming predators can consume fish up to 50% of their length). Annual predation (individual fish) is modeled for a range of proportional allocation to the salmonid component of the diets. Asterisks indicate the estimated age-class abundance of the prey species.

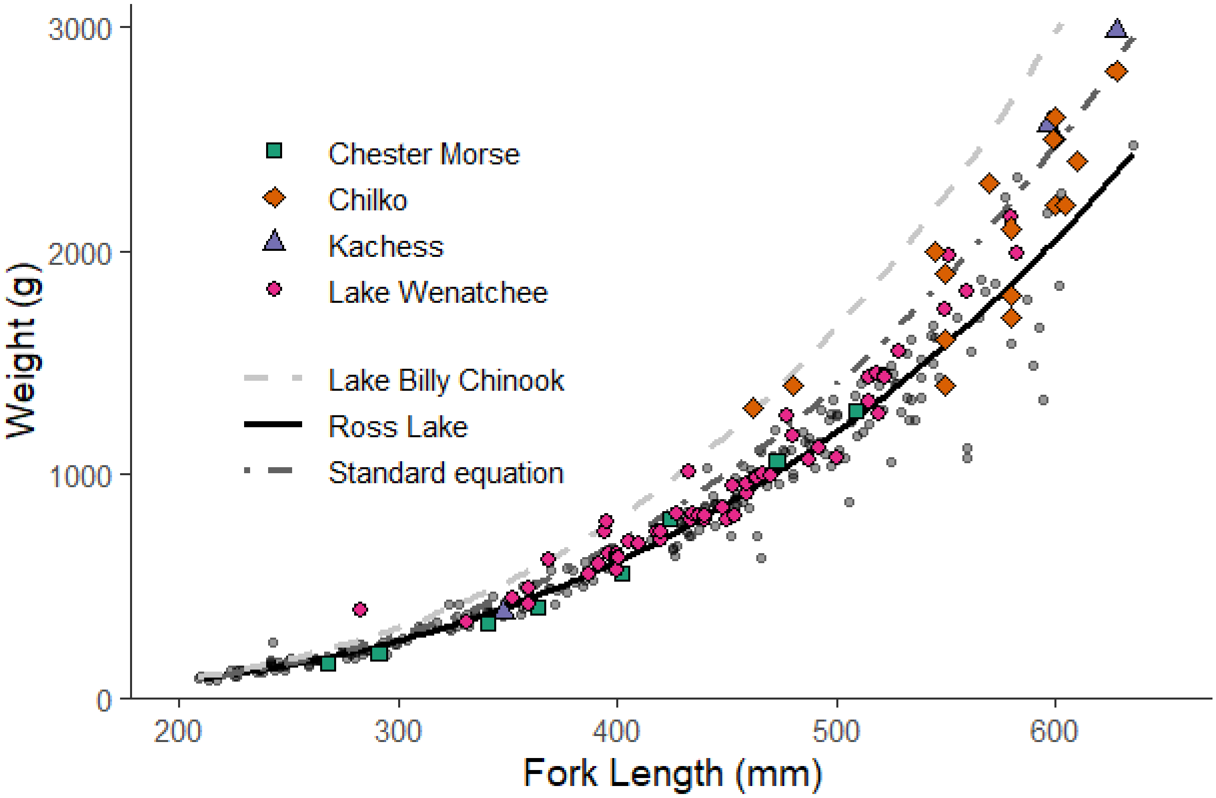

Figure S12. Length-weight relationship for bull trout/hybrids in Ross Lake (small grey points), compared to the standard equation (Hyatt & Hubert 2000), the reported equation from Lake Billy Chinook (Beauchamp and Van Tassel 2001), bull trout in Chilko Lake (data from Furey and Hinch 2017), and some bull trout sampled in Kachess Lake, Chester Morse Lake, and Lake Wenatchee (internal data).

Chapter 3: Supplementary Materials - Diablo Lake

Methods

Study system

Diablo Lake is downstream of Ross Lake, also oligotrophic, and much smaller (elevation at full pool = 368 m, storage at full pool = 0.112 km^3, max depth = 98 m, mean depth = 35 m). Due to the hypolimnetic withdrawal from Ross Lake and inflows from glacial streams, Diablo Lake is colder, weakly stratified, has lower water transparency, and lake level fluctuates within ± 1.5 m throughout the year (Fig. S16; Fig. S1). The fish species assemblage is the same in Diablo Lake as in Ross Lake. Redside shiners presumably spread to Diablo Lake after their introduction to Ross Lake, but the population has not yet proliferated in Diablo Lake as it has in Ross Lake. Diablo Lake has low levels of natural fish production and is regularly stocked with rainbow trout from the Marblemount Hatchery, originated from Ross Lake broodstock (Table S11). In recent years, only fry have been stocked in the lake during fall.

Fish collection

Fish collection methods followed those described for Ross Lake. Fish sampling in Diablo Lake was particularly constrained due to concerns about bull trout and limited samples were available to analyze.

Size structure, abundance, mortality

Age-structured populations were created following the same methods as in Ross Lake. Due to severe data limitations in Diablo Lake, no abundance estimates were possible, so we evaluated consumption for age-structured unit populations of 1,000 rainbow trout, 100 bull trout, 100 brook trout, and 100 Dolly Varden > 200 mm FL (Table S12). This approach accounts for the variability associated with varying diets, per capita consumption rates, and relative abundance among age classes of consumers and allows managers to easily scale up or down the resulting consumption estimates to evaluate different predation scenarios based on alternative population estimates and uncertainty (Beauchamp et al. 2007).

Stable isotope analysis

Stable isotope analysis followed the same methods as described for Ross Lake.

Bioenergetic model inputs

Diet composition – Diet composition and inputs for bioenergetic simulations were determined using a combination of stomach content analysis and stable isotope mixing models (SIMMs), following the same methods as described for Ross Lake. Species were pooled across length bins if significant differences in stable isotope signatures were not detected using non-parametric Kruskal-Wallis and Dunn’s multiple comparison test (Tables S12 and S13). Diet proportions from stomach content analysis are reported in Table S14, comparisons between proportions estimated from SIMMs (Figs. S14-S19) and stomach contents are in Table S15, and diet proportions used as inputs into the bioenergetics simulations in Tables S16 and S17.

Low diet sample sizes for char in Diablo lake required us to rely mainly on SIMMs. We assumed SIMMs from summer samples characterized average diet contributions across the previous 3 months, thus set diets as SIMMs proportions from day 1 (May 1) to day 92 (Aug 1) of the simulation. We used fall diets, and then zeroed out fish, zooplankton, and adult insects over winter, replacing with benthos and immature insects. For bull trout 100-399 mm FL, we used

SIMM proportions for the spring/summer, and interpolated proportions linearly from mid summer to fall stomach content proportions, on Oct 1 (day 154). We set winter diets to be the same as fall, zeroing out the minor contribution of zooplankton. For bull trout/hybrids 400+ mm FL, we used SIMM proportions from spring through fall (day 1-154), and zeroed out zooplankton for the winter. For Dolly Varden 100-199 mm FL, we used SIMM proportions from day 1-91, then used stomach contents from summer samples, linearly interpolating from summer to fall stomach contents, and then holding fall diet constant through the end of winter (day 336). For Dolly Varden 200-299 mm FL, we used SIMM proportions for spring-summer, and used stomach contents from summer and assumed these proportions were constant until the end of winter. These diet proportions correspond to piscivory by Dolly Varden only during the spring and summer, which would align with timing of rainbow trout (spring) and redside shiner (summer) spawning. As with other species, summer SIMM proportions for brook trout were used from spring to summer (day 1-92), then summer stomach contents were set for day 93, linearly interpolated to fall diets, and then zooplankton were zeroed out for winter.

Thermal experience – Vertical temperature data were collected continuously at a single site in the main basin of Diablo Lake using a vertical array of Hobo temperature loggers (Onset Computer Corporation) collecting temperatures every 5 m from the surface to 40 m depth once every 6 hours. Daily mean temperature at each depth was computed and linearly interpolated at 1-m intervals to compute mean temperatures across layers (epi-, meta-, and hypolimnion) and through time. Any missing data were linearly interpolated through time. Permitting restrictions to gillnetting in Diablo Lake prevented us from analyzing seasonal depth distribution for salmonids, thus we relied on observations from Ross Lake. We assigned thermal experience to each species using the same rules as described for Ross Lake (Table 13).

Age, growth, and predator energy – Age and growth analysis for Diablo Lake fish followed the methods described for Ross Lake. Scale radius-FL regressions and FL-weight regressions were computed for each species separately from fish in Ross Lake (Tables 19 and 20). Predator energy density and spawning losses used in the simulation were the same as described for Ross Lake (Table 17).

Predation mortality

Predation mortality by the age-structured unit populations was estimated following the same methods as described for Ross Lake.

Results

Stable isotopes and diet composition

Stable isotope signatures within species groupings varied more in Diablo Lake than in Ross Lake (Fig. S18). The largest bull trout/hybrids 400+ mm FL had the highest trophic position and their diets were benthically oriented. Smaller bull trout/hybrids 100-399 mm FL and brook trout were similarly benthic but at a lower trophic position. The diets of Dolly Varden, rainbow trout, and redside shiner were all more pelagic than those of bull trout and brook trout. No ontogenetic shift towards piscivory was observed in rainbow trout in Diablo Lake (Fig. S21). Trophic niche space of redside shiner overlapped with rainbow trout and Dolly Varden 200-299 mm FL, and they were half a trophic level below Dolly Varden 100-199 mm FL (δN^{15} difference = 1.6‰). Redside shiner were positioned more pelagically than brook trout and bull trout , and were half a trophic level below smaller bull trout 100-399 mm FL (δN^{15} difference = 1.6‰) and a full trophic level below bull trout $\geq$ 400 mm FL (δN^{15} difference =3.2‰).

Seasonal diet patterns in Diablo Lake were difficult to infer due to low sample sizes, however SIMMs were helpful in discerning patterns in dominant prey during the bulk of the growing season (Table S15). SIMMs indicated that fish and benthos/insects were important prey items for bull trout/hybrids 100-399 mm FL and brook trout during spring and summer; larger bull trout were primarily piscivorous. SIMMs predicted a moderate contribution of fish prey to Dolly Varden diets in spring and summer; however, no fish were observed in diets during these seasons. Rainbow trout were the least reliant on fish prey in Diablo Lake, but as in Ross Lake, SIMMs predicted higher contributions of fish to diets than observed in stomach contents. Contribution of fish prey in the diets of rainbow trout declined in the fall, likely in response to decreased access and availability of redside shiner eggs and larvae.

Predation mortality

No fish in Diablo stomach contents were positively identified to species, nor were in adequate condition to obtain body length, obscuring our ability to characterize size-specific predation on juvenile salmonids versus redside shiner. Therefore, all results are presented for total fish predation potential. Per capita consumption of fish by bull trout in Diablo Lake was lower than in Ross Lake but orders of magnitude higher than rainbow trout or brook trout (Table S17). However, due to the extremely low abundance of bull trout, the unit population of 1,000 rainbow trout 200+ mm FL consumed more fish (139 kg; 56,000 individuals at 2.5 g) than the unit population of 100 bull trout (95 kg; 38,000 individuals at 2.5 g), or brook trout (11 kg; 4,000 individuals at 2.5 g). While estimated predation demand in Diablo was substantially lower than in Ross Lake, this could still represent a critical limitation to survival for juvenile native salmonids in the reservoir due to their low abundance, depending on how predation is allocated to the different species and age classes (Fig. S23). For example, if age 2 bull trout were just 1% of the fish consumed (by weight) by the unit population of 100 bull trout, this would still account for around 23% of the estimated age 2 abundance.

Juvenile rainbow trout (age 1-2) may consume the most fish biomass due to their abundance, however gape limitation restricts their potential fish prey to redside shiner in the growing season. Uncertainty in survival of hatchery fry and thus abundance of these juvenile age classes makes it difficult to quantify their potential predation impact on the redside shiner population. The back-calculated population of 10,944 age 1 rainbow trout was estimated to consume 179 kg of fish. At this size, the rainbow trout would be limited to consuming fish < 80 mm FL (6.4 g), with most consumption during the growing season limited to fish < 60 mm FL (2.5 g). This level of consumption equates to 72,000 individuals annually at the average size of 2.5 g. The back-calculated population of 2,937 age 2 rainbow trout was estimated to consume 151 kg of fish which corresponds to 72,000 individuals at 2.5 g. Once adjusted for gape limitation, consumption by rainbow trout represented extreme levels of predation potential across age classes (Fig. S24). For example, even if age 1 redside shiner are only 5% by weight of the fish prey consumed by all rainbow trout, consumption by age 1, age 2, and age 3+ populations exceeds their estimated abundance. While we do not know how much of this consumption is targeted at fry or eggs, it is likely that this predation represents a severe limitation to survival in this population that was estimated at around 10,000 individuals ≥ 70 mm FL in September 2021.

Discussion

Our quantitative food web study indicated that the level of fish predation in Diablo Lake is expected to be substantially less than Ross Lake due to presumably smaller predator populations; however, this could still represent an important constraint on survival of juvenile salmonids in the lake because of their low abundance. Predation may also be an important mechanism constraining population size of nonnative redside shiner, particularly in Diablo Lake.

Predation mortality in Diablo Lake is even more difficult to discern compared to Ross Lake due to severe data limitations and zero positively identified fish prey in diet samples. Most of the fish predation in Diablo Lake is likely focused on small hatchery rainbow trout and redside shiner, as these are the most abundant fish prey. However, cannibalism by bull trout could be a severe limitation to this population, even if rates of cannibalism are relatively low, due to the low estimated population abundance. Cannibalism in adfluvial bull trout is rarely reported, though it has been identified as a potential limitation in other reservoirs such as Lake Billy Chinook, Oregon (Beauchamp and Van Tassell 2001). The benthic orientation of bull trout observed in the stable isotope signatures indicate that their fish predation may be more focused on smaller conspecifics or brook trout rather than redside shiner and rainbow trout. Notably, predation on brook trout may also be severe, presenting a possible mechanism limiting abundance of this nonnative species in Diablo Lake.

Despite low levels of piscivory by rainbow trout in Diablo Lake, total predation demand of the population (assumed to be primarily focused on redside shiner) far exceeded our estimates of redside shiner abundance from hydroacoustic surveys that occurred in September. This could be due to a few different factors. First, substantial predation from juvenile rainbow trout is likely directed toward redside shiner eggs and fry, of which we do not have any information on the abundance and production. Additionally, our abundance surveys occurred in September, near the end of the growing season, after the most significant levels of predation would have occurred.

Limited data on the rainbow trout population size and survival rates, particularly at early life stages, also introduces uncertainty to our predation estimates. However, simulated predation levels in Diablo suggest that predation could be a severe limitation to redside shiner population growth in this lake, and understanding the relative roles of predation vs other environmental variables (e.g., water temperature) in limiting this nonnative population is critical to fully assess threat of population expansion and further invasion.

References

Beauchamp, D. A., A. D. Cross, J. L. Armstrong, K. W. Myers, J. H. H. Moss, J. L. Boldt, and L. J. Haldorson. 2007. Bioenergetic responses by Pacific salmon to climate and ecosystem variation. North Pacific Anadromous Fish Commission Bulletin 4:257–269.

Beauchamp, D. A., and J. J. Van Tassell. 2001. Modeling seasonal trophic interactions of adfluvial bull trout in Lake Billy Chinook, Oregon. Transactions of the American Fisheries Society 130:204–216.

Tables

Table S10. Recent stocking reports for rainbow trout in Diablo Lake. Data acquired from the Washington Department of Fish and Wildlife (WDFW).

Release date	Fish per pound	Total release (kg)	Number released	Mean fish weight (g)
06 Oct 2015	1,200	65	172,213	0.4
18 Oct 2016	1,000	78	172,929	0.5
28 Oct 2016	1,000	22	48,700	0.5
28 Apr 2017	200	192	84,750	2.3
21 Sep 2017	1,200	64	170,000	0.4
04 Apr 2018	175	220	85,000	2.6
08 Oct 2018	984	128	276,600	0.5
02 Oct 2019	713	89	140,229	0.6
	994	37	80,662	0.5
06 Oct 2020	963	117	249,097	0.5
04 Oct 2021	771	187	318,485	0.6
18 Oct 2022	750	168	278,347	0.6

Table 11. Estimated age-structured populations and mortality rates for salmonid species in Diablo Lake.

Species	Z	Annual survival (%)	Age	Estimated population size[a]	Age-specific abundance
Brook trout	1.901	14.9	3	100	100
Bull trout/hybrids	0.611	54.3	3	100	48
			4		26
			5		14
			6		8
			7		4
Dolly Varden	0.611	54.3	3	100	100
Rainbow trout	1.315	26.8	1	1,000	10,944
			2		2,937
			3		788
			4		212

[a] Population data was too limited in Diablo Lake, thus char species are reported as a unit population of 100 and rainbow trout as 1,000 fish ≥ 200 mm FL (age 3+). Earlier age classes were back-calculted using the same survival rate.

Table S12. Significance of size class as a predictor of stable isotope values for δ13C and δ15N from fish sampled in Ross Lake in the summer. Column headings represent the isotope used as a response variable and values represent p value of the nonparametric Kruskal-Wallis with size class as a predictor variable. Significant p values are reported in bold (α=0.05).

	Species	n	δ13C	δ15N
Diablo Lake	BT-hybrid	15	0.578	0.058
	DV	23	0.245	**0.039**
	EBT	23	0.884	0.062
	RBT	29	0.115	0.185

Table S13. Pairwise comparisons of difference in isotopic signatures between size classes from nonparametric Dunn test. Pairwise comparisons are only included for species and isotopes that were significant in the Kruskal-Wallis test. Significantly different comparisons ($p < 0.05$) are indicated in bold.

Lake	Species	Isotope	Comparison	P
Diablo Lake	**DV**	**d15N**	**100-199 : 200-299**	**0.039**

Table S14. Seasonal diet proportions (wet weight, g) for salmonids in Diablo Lake from stomach content analysis. Size-classes were pooled for rainbow trout and brook trout, where ontogenetic differences in diet (based on stable isotope signatures) were not observed. RSS: redside shiner, Sal: salmonid, Unk-fish: unidentified fish, Daph: Daphnia, Lept: Leptodora, Zoop: other zooplankton, IM-insect: immature insect, AD-insect: adult insect.

Length	Season	N	RSS	Sal	Unk-fish	Amphibia	Daph	Lept	Zoop	Amphipod	Snail	Benthos	IM-insect	AD-insect	Other
Bull trout/hybrids															
100-399	Spring		-	-	-	-	-	-	-	-	-	-	-	-	-
	Summer	3	0.000	0.000	0.000	0.000	0.000	0.000	0.000	0.223	0.000	0.000	0.777	0.000	0.000
	Fall	6	0.000	0.000	0.185	0.000	0.001	0.000	0.000	0.522	0.085	0.000	0.036	0.170	0.000
400+	Spring	1	0.000	0.993	0.000	0.000	0.000	0.000	0.000	0.002	0.000	0.000	0.000	0.005	0.000
	Summer	1	0.000	0.000	0.000	0.000	0.000	0.000	0.000	0.000	0.000	0.000	0.960	0.040	0.000
	Fall		-	-	-	-	-	-	-	-	-	-	-	-	-
Dolly Varden															
100-199	Spring		-	-	-	-	-	-	-	-	-	-	-	-	-
	Summer	6	0.000	0.000	0.000	0.000	0.000	0.000	0.000	0.587	0.000	0.007	0.237	0.169	0.000
	Fall	2	0.000	0.000	0.043	0.000	0.000	0.000	0.000	0.916	0.000	0.000	0.040	0.001	0.000
200-299	Spring	1	0.000	0.000	0.000	0.000	0.000	0.000	0.000	1.000	0.000	0.000	0.000	0.000	0.000
	Summer	2	0.000	0.000	0.000	0.000	0.000	0.000	0.000	0.362	0.000	0.101	0.537	0.000	0.000
	Fall		-	-	-	-	-	-	-	-	-	-	-	-	-
Brook trout															
	Spring	1	0.000	0.000	0.000	0.000	0.000	0.000	0.000	0.007	0.116	0.000	0.853	0.024	0.000
	Summer	7	0.000	0.000	0.000	0.000	0.029	0.000	0.000	0.094	0.220	0.000	0.288	0.311	0.058
	Fall	8	0.000	0.000	0.219	0.000	0.010	0.000	0.001	0.165	0.033	0.006	0.004	0.562	0.000
Rainbow trout															
	Spring	1	0.000	0.000	0.095	0.000	0.877	0.000	0.000	0.000	0.000	0.000	0.000	0.000	0.028
	Summer	44	0.000	0.000	0.131	0.000	0.331	0.205	0.000	0.007	0.015	0.004	0.235	0.072	0.001
	Fall	23	0.000	0.000	0.036	0.000	0.257	0.001	0.005	0.041	0.172	0.003	0.019	0.467	0.001

Table S15. Seasonal diet proportions (wet weight) compared to stable isotope mixing model results (SIMM, 95% credible intervals) for broad prey categories for rainbow trout and redside shiner in Ross and Diablo Lakes. Redside shiner diet data was from previously published estimates of volumetric proportions (Welch 2012). Season refers to the season that the diet sample or tissue sample was collected.

					Fish		Zooplankton		Benthos/insect/other	
Species	Length	Season	*N*: Diet	*N*: SIMM	Diet	SIMM	Diet	SIMM	Diet	SIMM
BT-hybrid	100-399	Spring			-		-		-	
		Summer	3	8	0.000	0.493 (0.239-0.717)	0.000	0.109 (0.004-0.338)	1.000	0.398 (0.145-0.652)
		Fall	6		0.185		0.001		0.813	
	400+	Spring	1		0.993		0.000		0.007	
		Summer	1	7	0.000	0.863 (0.714-0.95)	0.000	0.05 (0.002-0.154)	1.000	0.087 (0.006-0.223)
		Fall			-		-		-	
DV	100-199	Spring			-		-		-	
		Summer	6	8	0.000	0.524 (0.308-0.692)	0.000	0.29 (0.105-0.444)	1.000	0.187 (0.019-0.425)
		Fall	2		0.043		0.000		0.957	
	200-299	Spring	1		0.000		0.000		1.000	
		Summer	2	15	0.000	0.348 (0.206-0.485)	0.000	0.227 (0.043-0.41)	1.000	0.425 (0.236-0.635)
		Fall			-		-		-	
EBT	all	Spring	1		0.000		0.000		1.000	
		Summer	7	23	0.000	0.433 (0.343-0.512)	0.029	0.065 (0.002-0.211)	0.971	0.502 (0.361-0.613)
		Fall	8		0.219		0.011		0.770	
RBT		Spring	1		0.095		0.877		0.028	
		Summer	44	29	0.131	0.281 (0.176-0.374)	0.536	0.258 (0.069-0.434)	0.334	0.461 (0.308-0.642)
		Fall	23		0.036		0.263		0.703	

Table S16. Rainbow trout seasonal diet proportions used as inputs into bioenergetics model simulations for Diablo Lake. Ontogenetic shifts in stable isotope signatures were not observed in Diablo Lake, thus diet proportions were pooled across length bins. Sample size (N) of stomach content analysis is indicated for the seasons in which non-empty stomach contents were collected. Winter diets were set to be constant between day 245 and 336 (Jan 1- Apr 1). All diets were linearly interpolated between seasons. *Denotes seasons in which stable isotope mixing model results were used to modify these diet inputs for the bioenergetics simulations. RSS: redside shiner, Sal: salmonid, Unk-fish: unidentified fish, Daph: Daphnia, Lept: Leptodora, Zoop: other zooplankton, IM-insect: immature insect, AD-insect: adult insect.

				Diet proportions												
Length		Season	*N*	RSS	Sal	Unk-fish	Amphibia	Daph	Lept	Zoop	Amphipod	Snail	Benthos	IM-insect	AD-insect	Other
All	1	Spring*	1	0.000	0.000	0.281	0.000	0.258	0.000	0.000	0.000	0.000	0.461	0.000	0.000	0.000
	91	Summer*	-	0.000	0.000	0.281	0.000	0.258	0.000	0.000	0.000	0.000	0.461	0.000	0.000	0.000
	92	Summer	44	0.000	0.000	0.131	0.000	0.331	0.205	0.000	0.007	0.015	0.004	0.235	0.072	0.000
	154	Fall	23	0.000	0.000	0.036	0.000	0.257	0.001	0.005	0.041	0.172	0.002	0.019	0.467	0.000
	245	Winter	-	0.000	0.000	0.000	0.000	0.000	0.000	0.000	0.041	0.172	0.298	0.488	0.000	0.001
	336	Spring	-	0.000	0.000	0.000	0.000	0.000	0.000	0.000	0.041	0.172	0.298	0.488	0.000	0.001

Table S17. Seasonal diet proportions used as inputs into bioenergetics model simulations for char species in Diablo Lake. Length bins (mm FL) are indicated for species where ontogenetic differences in stable isotope signatures were observed. Sample size (N) of stomach content analysis is indicated for the seasons in which non-empty stomach contents were collected. Winter diets were set to be constant between day 245 and 336 (Jan 1- Apr 1). All diets were linearly interpolated between seasons. *Denotes seasons in which stable isotope mixing model results were used to modify these diet inputs for the bioenergetics simulations. RSS: redside shiner, Sal: salmonid, Unk-fish: unidentified fish, Daph: Daphnia, Lept: Leptodora, Zoop: other zooplankton, IM-insect: immature insect, AD-insect: adult insect.

					Diet proportions											
Length		Season	N	*RSS*	Sal	Unk-fish	Amphibia	Daph	Lept	Zoop	Amphipod	Snail	Benthos	IM-insect	AD-insect	Other
Bull trout/hybrids																
100-399	1	Spring*	-	0.000	0.000	0.493	0.000	0.109	0.000	0.000	0.136	0.000	0.000	0.262	0.000	0.000
	92	Summer*	3	0.000	0.000	0.493	0.000	0.109	0.000	0.000	0.136	0.000	0.000	0.262	0.000	0.000
	154	Fall	6	0.000	0.000	0.186	0.000	0.001	0.000	0.000	0.522	0.085	0.000	0.036	0.170	0.000
	245	Winter	-	0.000	0.000	0.187	0.000	0.000	0.000	0.000	0.522	0.085	0.000	0.036	0.170	0.000
	336	Spring	-	0.000	0.000	0.187	0.000	0.000	0.000	0.000	0.522	0.085	0.000	0.036	0.170	0.000
400+	1	Spring*	-	0.000	0.000	0.863	0.000	0.050	0.000	0.000	0.000	0.000	0.087	0.000	0.000	0.000
	154	Fall*	-	0.000	0.000	0.863	0.000	0.050	0.000	0.000	0.000	0.000	0.087	0.000	0.000	0.000
	245	Winter	-	0.000	0.000	0.863	0.000	0.000	0.000	0.000	0.000	0.000	0.137	0.000	0.000	0.000
	336	Spring	-	0.000	0.000	0.863	0.000	0.000	0.000	0.000	0.000	0.000	0.137	0.000	0.000	0.000
Dolly Varden																
100-199	1	Spring*	-	0.000	0.000	0.524	0.000	0.290	0.000	0.000	0.000	0.000	0.186	0.000	0.000	0.000
	91	Summer*	-	0.000	0.000	0.524	0.000	0.290	0.000	0.000	0.000	0.000	0.186	0.000	0.000	0.000
	92	Summer	6	0.000	0.000	0.000	0.000	0.000	0.000	0.000	0.587	0.000	0.007	0.237	0.169	0.000
	154	Fall	2	0.000	0.000	0.043	0.000	0.000	0.000	0.000	0.916	0.000	0.000	0.040	0.001	0.000
	336	Spring	-	0.000	0.000	0.043	0.000	0.000	0.000	0.000	0.916	0.000	0.000	0.040	0.001	0.000
200-299	1	Spring*	-	0.000	0.000	0.348	0.000	0.227	0.000	0.000	-	0.000	0.425	0.000	0.000	0.000
	91	Summer*	-	0.000	0.000	0.348	0.000	0.227	0.000	0.000	-	0.000	0.425	0.000	0.000	0.000
	92	Summer	2	0.000	0.000	0.000	0.000	0.000	0.000	0.000	0.362	0.000	0.101	0.537	0.000	0.000
	336	Spring	-	0.000	0.000	0.000	0.000	0.000	0.000	0.000	0.362	0.000	0.101	0.537	0.000	0.000
Brook trout																
All	1	Spring*	-	0.000	0.000	0.433	0.000	0.065	0.000	0.000	0.004	0.057	0.000	0.429	0.012	0.000
	91	Summer*	-	0.000	0.000	0.433	0.000	0.065	0.000	0.000	0.004	0.057	0.000	0.429	0.012	0.000
	92	Summer	7	0.000	0.000	0.000	0.000	0.029	0.000	0.000	0.094	0.220	0.000	0.288	0.311	0.058
	154	Fall	8	0.000	0.000	0.219	0.000	0.010	0.000	0.001	0.165	0.033	0.006	0.004	0.562	0.000
	245	Winter	-	0.000	0.000	0.219	0.000	0.000	0.000	0.000	0.165	0.033	0.017	0.004	0.562	0.000
	336	Spring	-	0.000	0.000	0.219	0.000	0.000	0.000	0.000	0.165	0.033	0.017	0.004	0.562	0.000

Table 18. Average monthly thermal experience for bull trout/Dolly Varden (BT), brook trout (EBT), and rainbow trout (RBT) in Diablo Lake.

	Temperature °C		
Month	BT	EBT	RBT
Jan	5.0	5.0	5.0
Feb	5.0	5.0	5.0
Mar	5.7	5.7	5.7
Apr	7.5	7.5	7.5
May	8.4	9.9	9.9
Jun	9.4	11.4	11.4
Jul	11.2	13.4	13.4
Aug	12.3	14.3	14.3
Sep	11.7	13.1	13.1
Oct	10.7	11.1	11.1
Nov	9.3	9.3	9.3
Dec	6.8	6.8	6.8

Table 19. Model coefficients and R^2 for geometric mean regressions on scale radius (SR, mm) and fork length (FL, mm) relationship for fish sampled in Diablo Lake and its tributaries. Equation is in the form FL = a + b*SR.

Species	*N*	R^2	a	b
Bull trout/hybrids	16	0.920	-32.977	444.815
Dolly Varden	34	0.837	42.914	271.715
Brook trout	74	0.835	-0.349	411.305
Rainbow trout	158	0.862	39.885	162.110

Table 20. Length-weight regressions for salmonids in Diablo Lake. Equations are in the exponential form $W = a \times FL^b$.

Species	*N*	*P*	R^2	a	b
Bull trout/hybrids	66	< 0.001	0.995	1.27×10^{-5}	2.964
Dolly Varden	124	< 0.001	0.997	8.29×10^{-6}	3.052
Brook trout	337	< 0.001	0.996	9.10×10^{-6}	3.049
Rainbow trout	547	< 0.001	0.992	1.84×10^{-5}	2.899

Table S21. Bioenergetics simulation inputs and corresponding estimates of feeding rate (% C_{max}), annual per capita consumption (g), and growth efficiency (%) for salmonids in Diablo Lake. All simulations ran for 365 days (day 1= May 1). Energy density (J/g) of the consumer was linearly interpolated during the simulation from the initial to final value reported. Sample sizes (*N*) are given for the number of individuals used in scale back-calculations for each annulus.

Species	Age	*N*	Spawn day	Spawn loss (%)	Initial FL (mm)	Initial W (g)	Final W (g)	Initial ED (J/g)	Final ED (J/g)	%C_{max}	Growth (g)	Cons (g)	GE (%)	Salmonid cons (g)	Total fish cons (g)
Brook trout	3	17	161	8.0	198	94.2	174.4	5,108	5,250	43	80.2	772.0	10.0	0.0	207.0
Bull trout/hybrids	3	11		0.0	192	87.7	318.9	5,432	5,616	37	231.2	868.0	27.0	0.0	260.0
	4	7		0.0	306	318.9	577.1	5,616	5,822	27	258.2	1,350.0	19.0	0.0	428.0
	5	6	161	10.0	374	577.1	1,067.2	5,822	6,212	28	490.1	2,400.0	20.0	0.0	2,071.0
	6	4	161	12.0	465	1,067.2	2,153.4	6,212	7,076	36	1,086.2	5,397.0	20.0	0.0	4,657.0
	7	2	161	14.0	595	2,153.4	3,590.2	7,076	8,220	37	1,436.8	9,350.0	15.0	0.0	8,069.0
Rainbow trout	1	158		0.0	76	5.4	32.6	4,996	4,996	23	27.2	271.0	10.0	0.0	24.0
	2	130		0.0	137	32.6	91.2	4,996	4,996	26	58.6	716.0	8.0	0.0	72.0
	3	79	45	8.0	196	91.2	224.9	4,996	4,996	31	133.7	1,601.0	8.0	0.0	164.0
	4	28	45	8.0	274	224.9	395.2	4,996	4,996	33	170.3	2,719.0	6.0	0.0	296.0

Figures

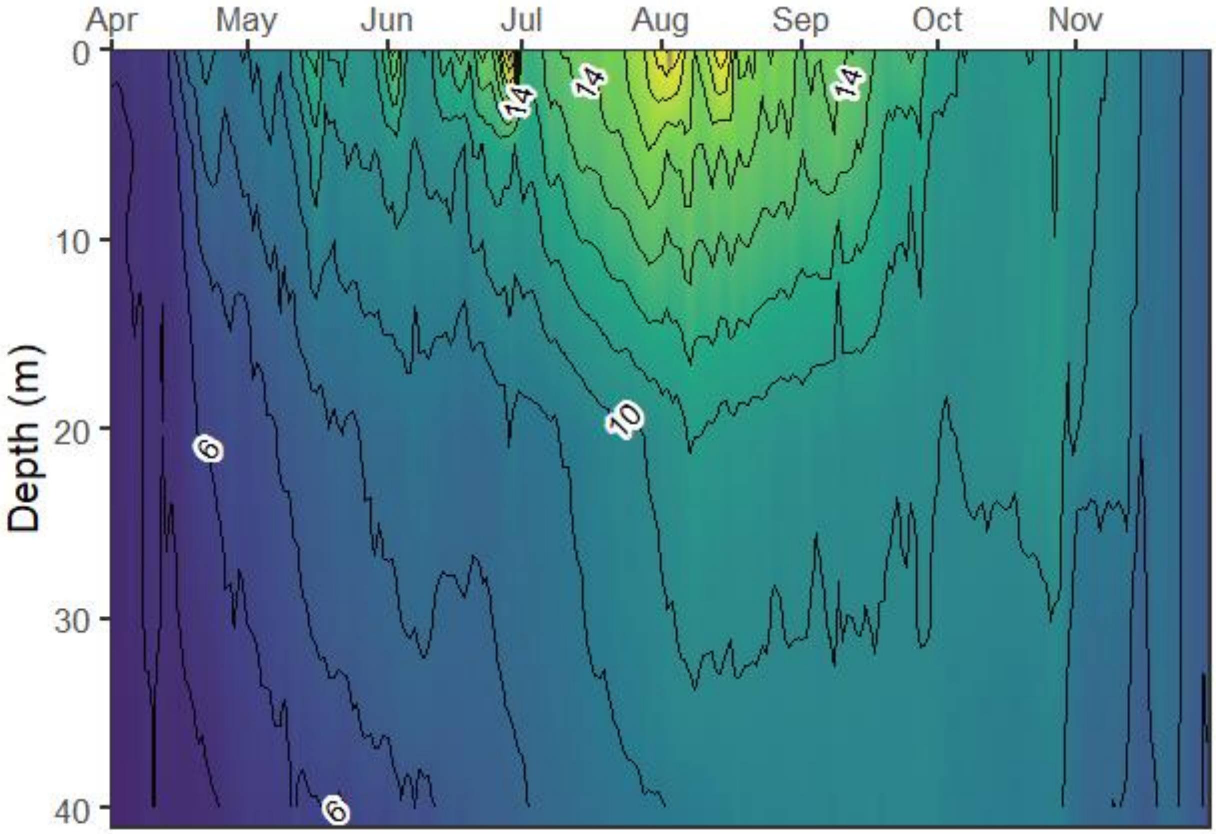

Figure S13. Isocline for Diablo Lake in 2021. Temperatures (°C) came from an array of sensors deployed every 5 m and taking readings four times per day.

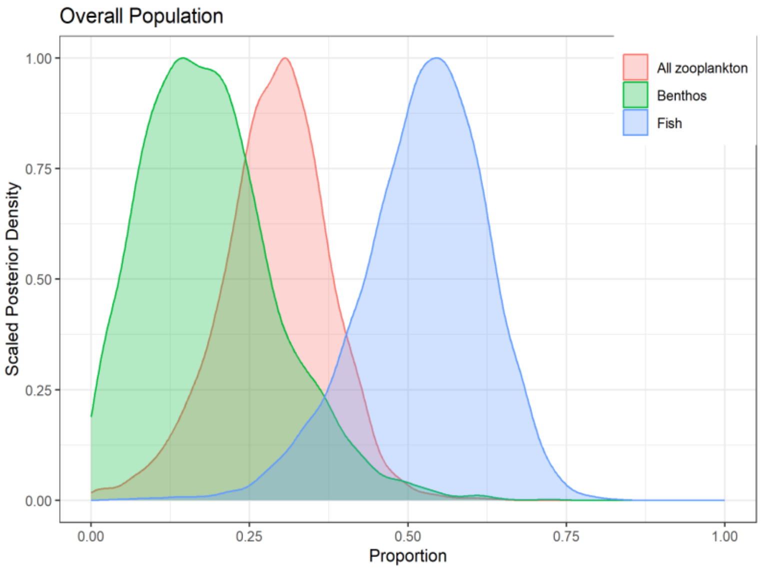

Figure S14. Stable isotope mixing model posterior densities for Dolly Varden 100-199 mm FL in Diablo Lake sampled in the summer.

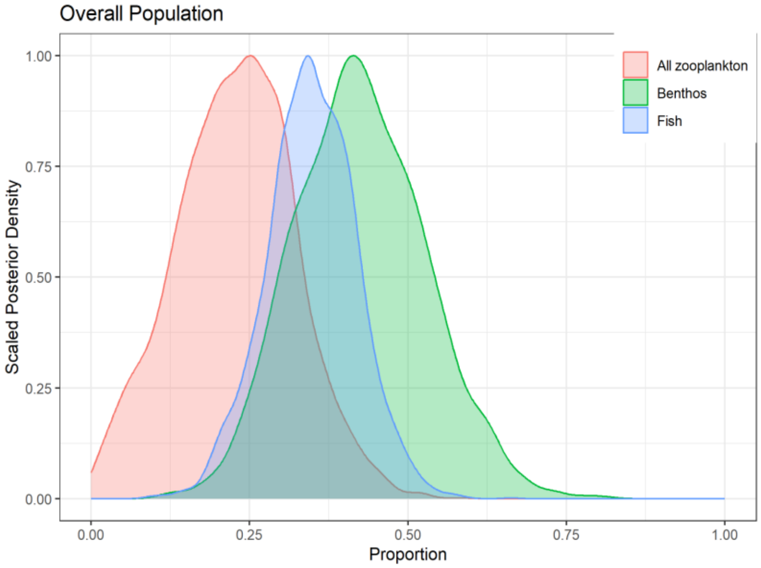

Figure S15. Stable isotope mixing model posterior densities for Dolly Varden 200-299 mm FL in Diablo Lake sampled in the summer.

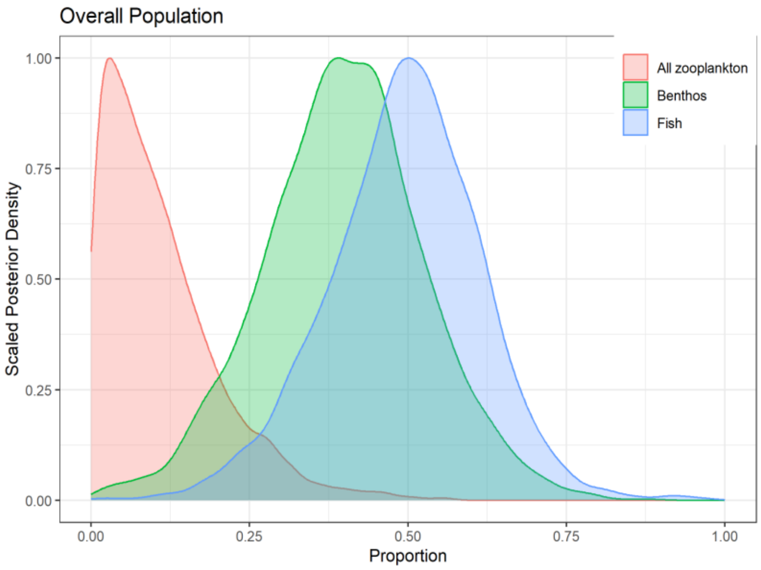

Figure S16. Stable isotope mixing model posterior densities for bull trout/hyrbids < 400 mm FL in Diablo Lake sampled in the summer.

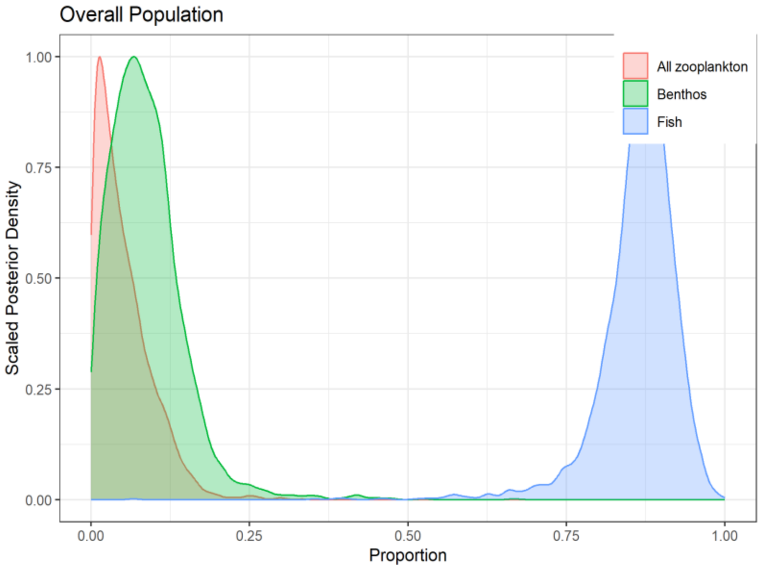

Figure S17. Stable isotope mixing model posterior densities for bull trout/hyrbids ≥ 400 mm FL in Diablo Lake sampled in the summer.

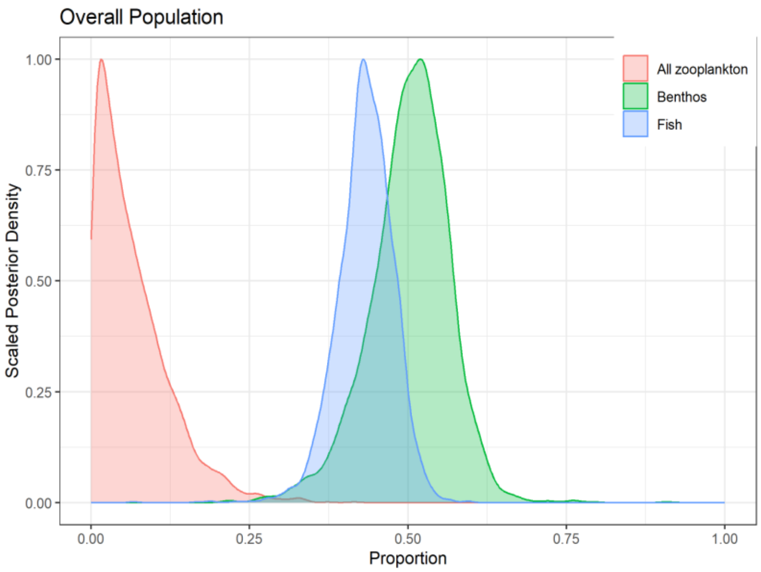

Figure S18. Stable isotope mixing model posterior densities for all brook trout in Diablo Lake sampled in the summer.

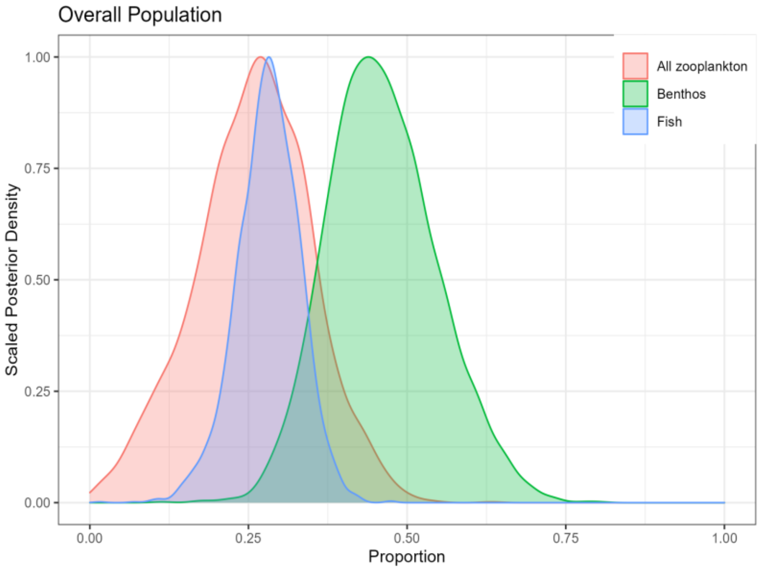

Figure S19. Stable isotope mixing model posterior densities for all rainbow trout in Diablo Lake sampled in the summer.

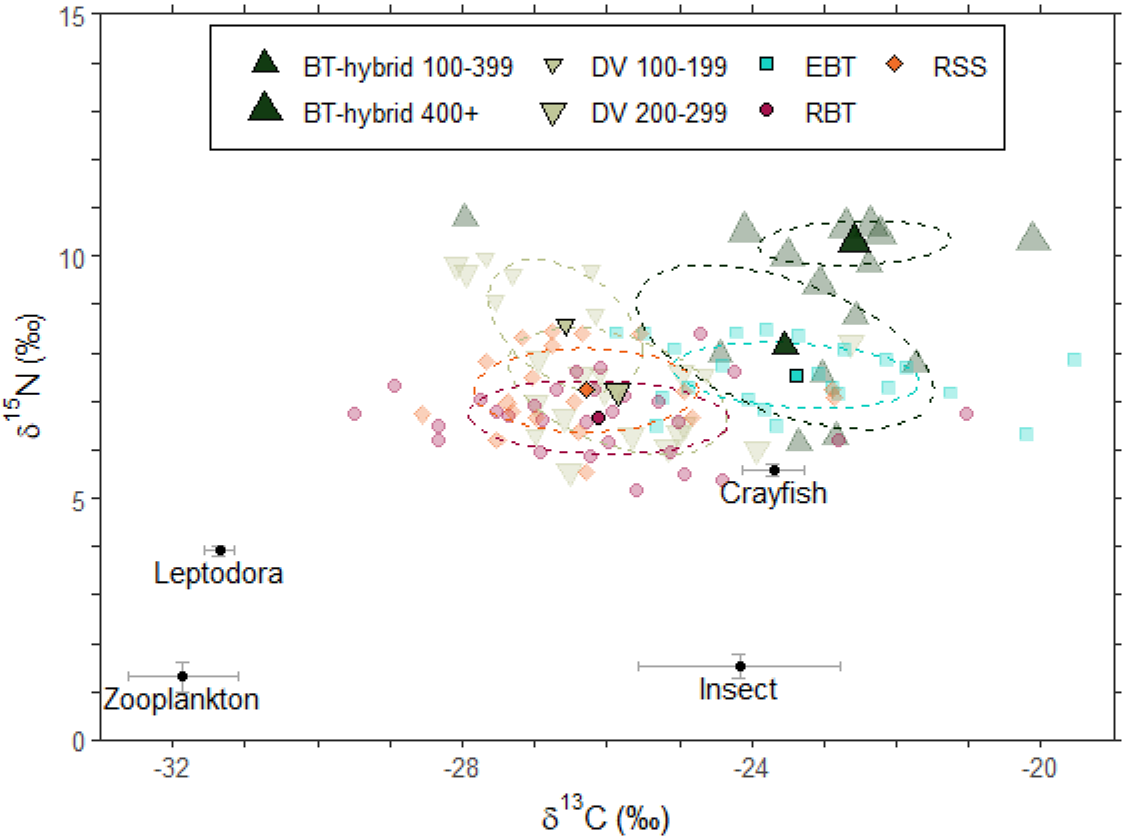

Figure S20. Stable isotope biplots of the Diablo Lake food web. Consumer species were separated by size classes if significant differences in stable isotope values were observed. The darker colored symbols represent the group centroids, while the lighter shaded symbols represent individual fish. BT-hybrid: bull trout and char hybrids, DV: Dolly Varden, EBT: brook trout, RBT: rainbow trout, RSS: redside shiner. Numbers following the species code represent the group's size bin, in mm FL. Ellipses contain 40% of the data for each consumer species/size group.

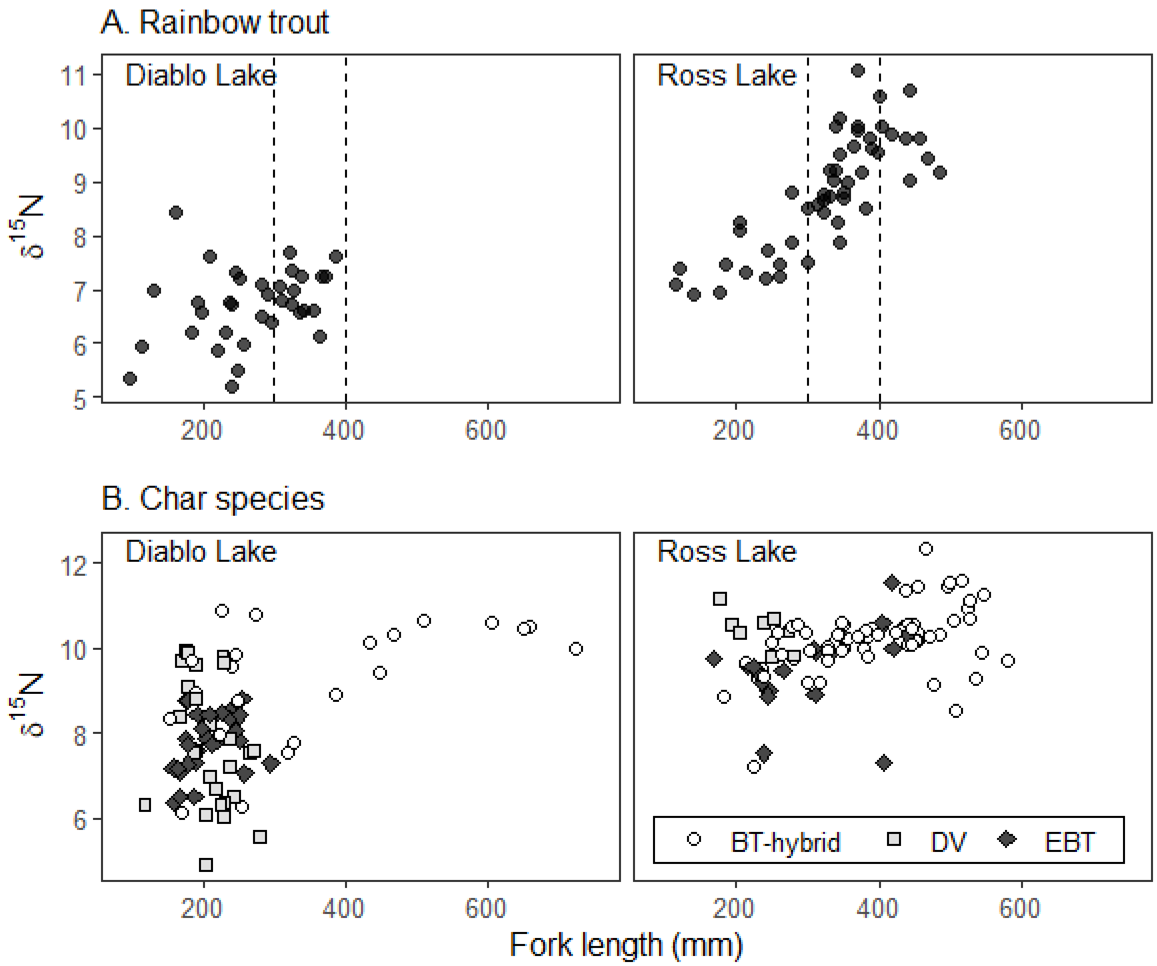

Figure S21. Stable isotope $\delta^{15}N$ as a function of fork length (mm) for rainbow trout (A) and char species (B) in Ross and Diablo Lakes. BT-hybrids = bull trout and hybrids, DV = Dolly Varden, and EBT = brook trout. Dotted lines in (A) show the ontogenetic transition to piscivory in Ross Lake.

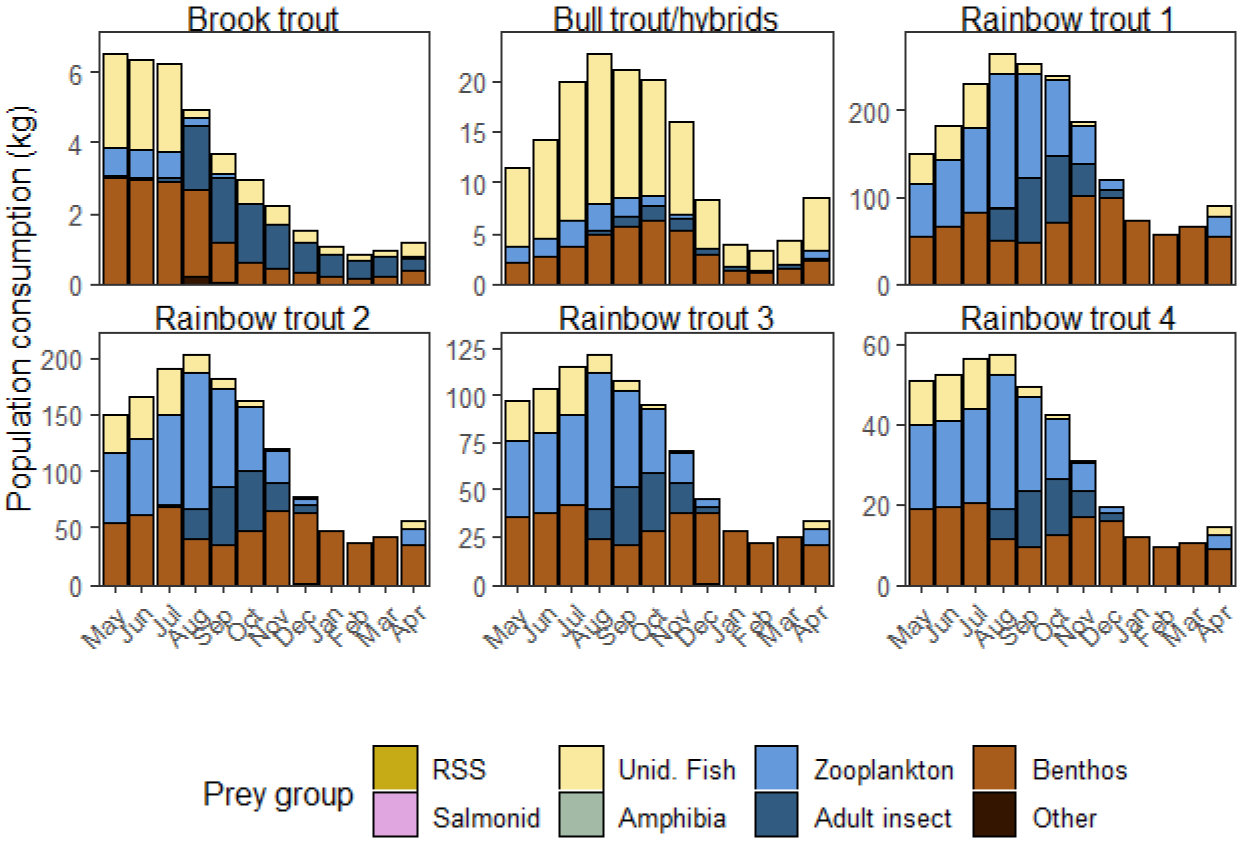

Figure S22. Simulated monthly population consumption for each salmonid species in Diablo Lake. Rainbow trout are separated by age class. Note the different y-axis scales.

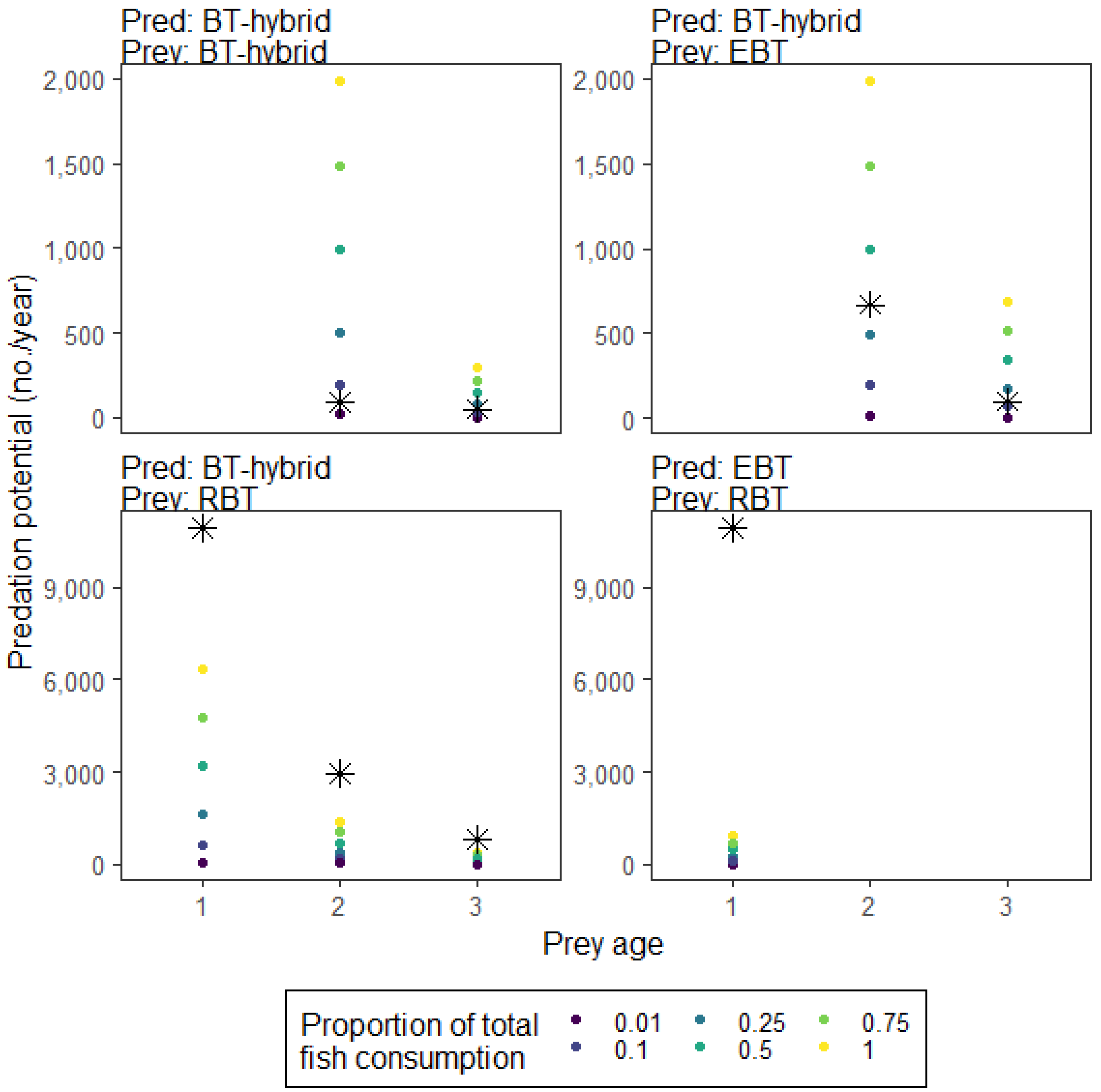

Figure S23. Simulated annual predation potential by each predator species on each prey-specific age class of vulnerable salmonids in Diablo Lake after accounting for daily fish growth and gape limitation (assuming predators can consume fish up to 50% of their length). Annual predation (individual fish) is modeled for a range of proportional allocation to the total fish component of the diets. Asterisks indicate the estimated age-class abundance of the prey species based on our age-structured unit populations (1,000 rainbow trout > 200 mm FL, 100 brook trout > 200 mm FL, 100 bull trout > 200 mm FL). BT-hybrid = bull trout and hybrids, EBT = brook trout, RBT= rainbow trout.

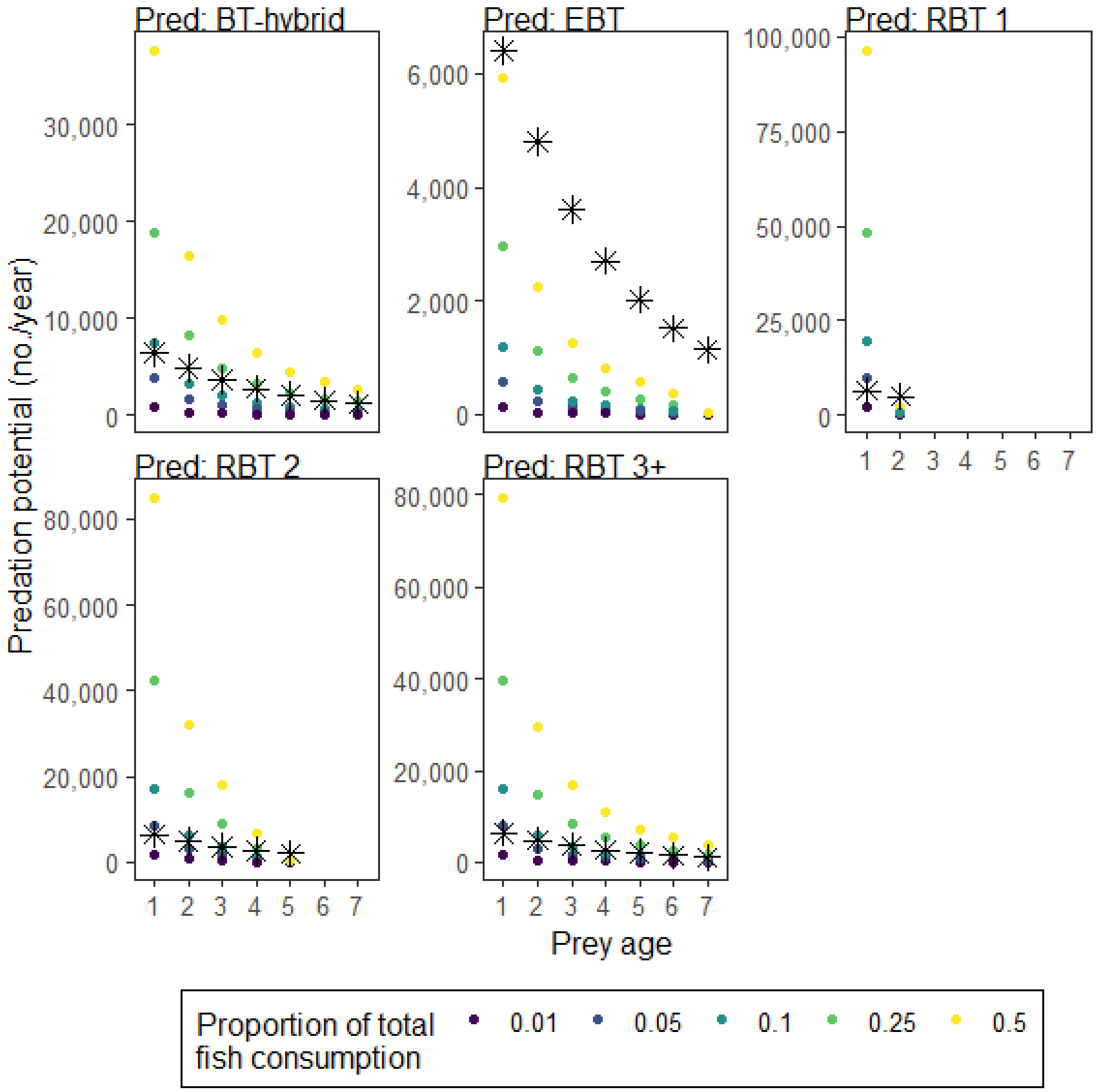

Figure S24. Simulated annual predation potential on each age class of vulnerable redside shiner in Diablo Lake after accounting for daily fish growth and gape limitation (assuming predators can consume fish up to 50% of their length). Annual predation potential (individual fish) is modeled for a range of proportional allocation to the total fish component of the diets. Asterisks indicate the estimated age-class abundance of redside shiner in September. BT-hybrid = bull trout and hybrids, EBT = brook trout, RBT= rainbow trout. Note the different scales on the y axis.

Chapter 4: Prey availability and predation as potential limitations to feasibility of anadromous salmonid introductions in a mid-elevation reservoir

Abstract

Introducing anadromous fish upstream of migration barriers has frequently been proposed as a conservation strategy, but existing conditions and future changes to these ecosystems (e.g., invasive species, climate change, water operations) influence the capacity to support such introductions. In the Upper Skagit River, Washington, USA, introduction of anadromous salmonids above three high-head dams has been proposed; however, the proliferation of invasive redside shiner from an unauthorized introduction approximately 20 years ago in Ross Lake fundamentally altered food web interactions, presenting challenges for growth and production of introduced anadromous salmonids like sockeye *Oncorhynchus nerka*, Chinook *O. tshawytscha*, or coho salmon *O. kisutch* and steelhead *O. mykiss* in Ross Lake. By combining empirical measurements of zooplankton availability and temporal patterns in thermal structure of the reservoir with bioenergetics model simulations to quantify the rearing capacity of Ross Lake, we estimated that the lake could support an initial abundance of 1.7 to 3.9 million sockeye salmon fry entering in the spring after accounting for the temporal consumption demand by the existing planktivore population dominated by redside shiner. The initial number of salmon fry the lake could support was based on conservative estimates of food supply during the most limiting month. The initial fry estimates varied with the expected fry-to-smolt survival rate, and whether or not salmonids would be thermally restricted from prey in the epilimnion, but translated to estimates of 212,000 to 332,000 smolts leaving the following spring, and 8,700 to 13,600 returning adults, using mean fry-to-smolt and smolt-to-adult survival rates from sockeye salmon in nearby Baker Lake, in the Skagit River system. We estimated that predation potential could represent substantial mortality for lake-rearing sockeye or Chinook salmon. Predation is expected to play a lesser role in limiting survival of species that migrate through the reservoir compared to species feeding there for all or most of their lives in freshwater. These results provide a case study and framework for examining bottom up and top down processes in the food web that influence growth and survival of introduced anadromous salmonids in reservoir habitats, thus guiding the direction of future feasibility studies in Ross Lake and other regulated rivers where introduction programs are considered.

Introduction

Species reintroductions are becoming an increasingly popular and important tool to conserve biodiversity considering ongoing rapid ecological change (Seddon et al. 2007; Swan et al. 2018; Bubac et al. 2019). The goal is to re-establish viable populations of at-risk species throughout their native range after extirpation. Despite its popularity, decades of failed reintroductions prompted researchers and the IUCN to develop guidelines for reintroduction programs to help mitigate risk, increase chance of success, and improve our understanding of factors driving reintroduction success (Armstrong and Seddon 2008; IUCN 2013). Reintroduction can aid in freshwater fish conservation, as many species face extreme range contraction (He et al. 2019); however, many of these programs have been unsuccessful (Cochran-Biederman et al. 2015). Two key factors correlated with reintroduction success for freshwater fishes are 1) adequately addressing the initial cause for decline, and 2) thoroughly assessing habitat availability and quality in the reintroduction area (Cochran-Biederman et al. 2015). These factors are reflected in the various guidelines provided for managing reintroduction programs (e.g., Dunham et al. 2011; IUCN 2013; Anderson et al. 2014).

Introducing anadromous salmonids above impassable dams is gaining traction as a method of restoring populations restricted from historical spawning and rearing habitat (Anderson et al. 2014) or as conservation introductions into new habitats. Trap and haul programs are one of the only methods available to reintroduce anadromous salmonids to historical spawning habitat upstream of high head dams (i.e., those not suitable for volitional passage structures such as ladders) and are currently being used and proposed in regulated systems throughout the Pacific Northwest (reviewed in Kock et al. 2021). Many of these programs are in their infancy or have scant monitoring data reported, limiting our ability to evaluate factors driving success or failure of reintroduction efforts into reservoir habitats. Kock et al. (2021) reported considerable variation in the effectiveness of the programs reviewed, but also noted that success is context dependent and defined by different management objectives of stakeholders. Limitations to success of reintroduction into reservoirs are varied (Kock et al. 2021) and can include migration delays and handling stress leading to high mortality rates for adults, differences in stock-specific production rates of the donor populations (Matala et al. 2019), differential fitness of hatchery fish and impacts of interbreeding (Sard et al. 2015; Evans et al. 2016), high juvenile mortality rates associated with predation in the reservoirs (Kock et al. 2019), and other challenges for downstream migrating juveniles (e.g., mismatch between water operations and migration timing, collection efficiency of the smolt traps, handling stress during collection; Flagg and Ruehle 2000; Keefer et al. 2012).

Reservoirs present a suite of challenges to anadromous fishes due to new and intensified biotic interactions operating in novel food webs (Naiman et al. 2012). Reservoirs tend to harbor more nonnative species compared to natural habitats (Johnson et al. 2008), which can affect growth and survival of juvenile salmonids through direct and indirect pathways associated with temporal food supply, predation or competition. Extreme seasonal drawdowns in high head reservoirs can also alter food webs and prey availability by limiting benthic production (Hansen et al. 2018) and can also challenge upstream and downstream migrations. However, drawdowns can limit invasive competitors/predators and improve downstream migration success of smolts (Murphy et al. 2019b). While predation in reservoir habitats can limit the survival of juvenile salmonids, these habitats can also provide better growing conditions and larger sizes that confer higher survival as migrants contend with strong size-selective mortality processes through downstream migration and ocean residency (Koehler et al. 2006; Monzyk et al. 2014; Bourret et al. 2014; Murphy et al. 2019a). Additionally, cold water available in deep thermally stratified reservoirs provide important thermal refuge for adult fish on their spawning migration (Naughton et al. 2018).

The feasibility and success of anadromous introductions will depend on numerous physical and ecological risks and constraints (Anderson et al. 2014; Kock et al. 2021) – an important component of which is evaluating the food web constraints of the recipient habitats. Understanding carrying capacity for nearly obligate lake rearing species like sockeye salmon *Oncorhynchus nerka*, or Chinook salmon *O. tshawytscha* that facultatively use lakes as primary juvenile rearing habitats (Koehler et al. 2006; Arostegui and Quinn 2019), is critical to evaluate whether reservoirs can support enough smolt production to achieve goals of an introduction program. Adequate zooplankton supply is required to support the minimum growth and body size required to reduce predation risk in reservoirs as well as survive outmigration and the first year in the ocean. Availability of zooplankton is directly related to juvenile growth and smolt production potential (Koenings and Kyle 1997; Edmundson and Mazumder 2001). Overstocking could reduce zooplankton, induce density-dependent growth suppression, and inhibit subsequent survival, which would undermine success of an introduction (Koenings and Kyle 1997). While such bottom-up controls are central to the models of many sockeye salmon stocking and enhancement programs, the importance of predation in limiting survival and smolt production has also been acknowledged (Foerster and Ricker 1941; Cartwright et al. 1998; Sorel et al. 2016b).

In the Skagit River, Washington, the re-licensing of three high-head hydropower dams with the Federal Energy Regulatory Commission has prompted requests by the licensing participants to study fish passage and introductions of anadromous salmonids above these dams. In response, a fish passage program has been proposed with the goal to “meaningfully contribute to recovering self-sustaining, harvestable salmon runs in the Skagit River watershed without negatively impacting native Skagit Basin fish populations and the Skagit River watershed ecosystem” (Seattle City Light 2023). The number of returning adults that could be produced from this currently inaccessible habitat will be determined by the spawning capacity in the mainstem Skagit River and the tributaries above the dams in addition to survival rates during successive life stages – freshwater rearing, downstream smolt migration, marine residency, and upstream adult migration. Habitat capacity in the mainstem and tributaries above the dams may be limited – intrinsic potential (IP) modeling estimates that most of this habitat is of low or medium IP for Chinook salmon and coho salmon *O. kisutch*, and while more high IP habitat exists for steelhead *O. mykiss* (anadromous rainbow trout), bioenergetic analysis of native rainbow trout growth suggests that low growth potential in these habitats could limit survival of steelhead smolts (Duda and Hardiman in review; Jensen et al. in review). The reservoirs may offer better growth for freshwater rearing life histories; however, proliferation of invasive redside shiner *Richardsonius balteatus* in Ross Lake in the early 2000s could limit zooplankton supply for reservoir rearing fish. Additionally, predation pressure by multiple species of piscivorous salmonids could also impact juvenile survival, and thus smolt production.

Building on a quantitative analysis of the reservoirs under current conditions (Chapters 2 and 3), we evaluated the Ross Lake food web in the context of anadromous salmonid introductions to determine the suitability of this habitat for smolt production. Our primary objectives were to 1) estimate the resource capacity in Ross Lake and the number of lake-rearing juveniles that could be supported using bioenergetics modeling, and 2) estimate predation potential and evaluate the impact on survival and smolt production of lake rearing fish as well as those migrating through the reservoir. Our analysis focused specifically on limitations within the reservoir habitat. We did not consider spawning potential in the tributaries, and assumed it was not limited; thus we address the question as, assuming that spawning and incubation habitats are not limiting, what level of smolt production could be supported by reservoir-rearing juveniles. Coupled with studies evaluating constraints throughout the remainder of the life cycle, this study contributes to a broader understanding of the feasibility of introducing anadromous salmonids above these dams.

Methods

Study system

The Skagit River flows from headwaters in southwestern British Columbia approximately 240 km through northwestern Washington before draining into Puget Sound. The Upper Skagit River is impounded by three hydroelectric dams that were completed in 1924 (Gorge Dam), 1930 (Diablo Dam), and 1953 (Ross Dam) and are integrated for electricity production for Seattle City Light. Ross Lake is the largest (storage at full pool = 1.78 km^3) and most upstream of the three reservoirs, with water surface at 489 m elevation and extending 37 km at full pool, which is approximately 1.6 km past the border with British Columbia. Ross Lake is typically drawn down 16-25 m during the winter, although drawdowns have extended to 40 m in recent years, and thermally stratifies from around June through October with peak surface temperatures from 18-22 °C and hypolimnetic temperatures around 8-12 °C (Fig. 1).

Downstream of the dams, the Skagit River supports some of the largest populations of ESA-listed Chinook salmon, steelhead, and bull trout *Salvelinus confluentus* (resident, fluvial, and anadromous) in the Puget Sound region. In addition, the river also supports large populations of coho salmon, pink salmon *O. gorbuscha*, and chum salmon *O. keta*. This habitat also includes a suite of other native species including daces *Rhinichthys* spp., threespine stickleback *Gasterosteus aculeatus*, suckers *Catostomus* spp., lampreys *Lampetra* spp., sculpins *Cottus* spp., mountain whitefish *Prosopium williamsoni*, white sturgeon *Acipenser transmontanus*, resident rainbow trout, and resident and anadromous coastal cutthroat trout *O. clarkii clarkii*. Above the dams, the reservoirs, tributaries, and Skagit River mainstem have stream resident and adfluvial populations of native rainbow trout, as well as bull trout and Dolly Varden *S. malma* which are genetically distinct from populations below the dams (Smith 2010). Nonnative species above the dams include brook trout *S. fontinalis*, presumed to have adfluvial and resident life histories, and redside shiner which occupy exclusively lentic habitat and have become very abundant since their unauthorized introduction around 20 years ago.

Candidate anadromous species and life histories

The potential limitations to growth and survival of introduced anadromous salmonids in the reservoirs is dependent upon the timing of and size at migration to the reservoir, and temporal occupancy of this habitat. These traits vary among species and life history types within species; therefore, we must evaluate these limitations for each species and life history. The following section reviews candidate species for introduction and their observed life history traits related to juvenile size and migration in the Skagit River below the dams.

Chinook salmon – Chinook salmon in the Skagit River below the dams exhibit three general juvenile migration life histories: fry migrants, parr migrants, and yearling migrants (WDFW and SRSC 2005; Zimmerman et al. 2015). Fry migrants quickly migrate downstream following emergence and rear in estuarine habitats for several months before migrating into marine nearshore or pelagic habitats. The migrant fry arrive in the estuary at an average size of 39 mm FL, usually in “February or March. Parr migrants rear for a few months in freshwater habitat, reaching an average size of 75 mm FL, before migrating to marine habitats usually in late May or June. Yearling migrants rear for over a year in freshwater habitats until an average size of 120 mm FL, before migrating to the Salish Sea typically from late March through May. Utilization of lakes and reservoirs by juvenile Chinook salmon is common, and the extent of occupancy in these habitats varies (Koehler et al. 2006; Monzyk et al. 2014; Arostegui and Quinn 2019). Reservoir rearing has been an advantageous life history strategy for rapid growth by Chinook salmon in Lake Washington (Koehler et al. 2006) and the regulated Willamette Basin, presumably due to higher growth potential in the lentic habitat (Monzyk et al. 2014; Bourret et al. 2014; Murphy et al. 2019a). Therefore, it is reasonable to assume that the yearling migrant life history could include reservoir rearing (emigrating to the reservoir as fry: Monzyk et al. 2014) if Chinook salmon are introduced above the dams, presuming an adequate growth environment is available.

Steelhead – Wild steelhead in the Skagit River below the dams typically rear in freshwater for 2-3 years before out migrating either as age 2 smolts (most common) at an average size of 161-172 mm FL, or as age 3+ smolts (less common) at an average size of 180-

191 mm FL (Thompson and Beauchamp 2014). Migration occurs from February-June, though it typically peaks from April-May (Thompson and Beauchamp 2014). Utilization of lake or reservoir habitat for rearing by juvenile steelhead is exceedingly rare for anadromous individuals of this species, with no occurrences reported in natural lakes or reservoirs (Lowery and Beauchamp 2010; Arostegui and Quinn 2019), except for a single instance in Lake Washington where out-migrating smolts were observed feeding on the spring *Daphnia* bloom in the lake for less than a month (Beauchamp 1995). Thus, it seems likely that if introduced above the dams, utilization of reservoir habitat by steelhead would be limited to a short duration during smolt out-migration.

Sockeye salmon – Sockeye salmon fry typically recruit to lakes soon after emergence in the spring and rear for 1-2 years before migrating to the ocean. Baker Lake provides the only population of sockeye salmon currently in the Skagit River basin. This population is primarily supported by hatchery fry released into the Upper and Lower Baker lakes each spring, with minimal natural production observed. Most sockeye salmon in Baker Lake spend one full year in the lake, migrating out to the ocean as age 1 smolts at an average size of 112 mm fork length and 13 g, though small fractions of the population also exhibit migration in their first year or at ages 2-3 (Overman 2022). Sockeye salmon and potentially Chinook salmon are therefore the most likely anadromous salmonids to utilize reservoirs as primary freshwater growth habitats.

Coho salmon –- Coho salmon in the Salish Sea typically rear in freshwater for a year, migrating to the ocean during the following spring (primarily in May) where they spend approximately 18 months before returning to freshwater in September-November (peak in October) to spawn at age 3 (Zimmerman et al. 2015; Quinn and Losee 2022). Lake habitat is not commonly used by coho salmon during their freshwater rearing in Washington or further south, in contrast to observations of lake rearing reported in British Columbia and Alaska (Arostegui and Quinn 2019). Further, coho salmon have not been observed using reservoir habitat for extended periods of rearing in the western United States, thus we expect that a lake-rearing life history for this species would be unlikely in Ross Lake.

Bioenergetics simulations

Bioenergetics simulations were run for a hypothetical sockeye salmon population in Ross Lake to estimate per capita consumption demand on *Daphnia* using Fish Bioenergetics 4.0 (Deslauriers et al. 2017) and the parameterized model for sockeye salmon (Beauchamp et al. 1989). Empirical measures from Upper Baker Lake sockeye salmon were used as surrogate rates for growth and mortality (Overman 2022). Initial weight (0.2 g) was estimated from mean size of Baker Lake hatchery releases during the spring and final weight (12.8 g) was estimated from the mean size of smolts captured the following year in the floating surface collector (FSC) during peak emigration in May, the peak month of emigration (Overman 2022). We ran the simulation for 365 d, beginning on May 1, to estimate daily per capita consumption by fitting to initial and final weight. Mean release timing of hatchery fry into the lake was actually closer to mid-April; however, we started the simulation on May 1 for convenience to align the end of the simulation with peak timing of smolt emigration from the lake.

Thermal experience was estimated using mean temperatures at depth from vertical temperature profiles collected in Ross Lake from May through November in 2010-2021, and surface temperatures in the forebay from November through April in 2009, 2010, and 2013 (data collected and maintained by Seattle City Light). We assumed that when the epilimnion was < 18°C, that sockeye salmon would be evenly distributed from 0-30 m. When the epilimnion was ≥

18°C, we assumed that sockeye salmon would be evenly distributed from 10-30 m. We then computed thermal experience as the mean temperature across all depths occupied (Table 1).

Sockeye tend to be heavily planktivorous in lakes and reservoirs, consuming high proportions of zooplankton (preferentially Daphnia when available) during the spring and summer across a range of zooplankton densities (Scheuerell et al. 2005; Sorel et al. 2016a; Hansen et al. 2017). Reflecting this, we used seasonal proportional diet data from kokanee in the Lewis River reservoirs (Sorel et al. 2016a) and energy densities from the literature (Luecke and Brandt 1993; McCarthy et al. 2009) to inform our diet inputs for the simulations (Table 2). *Daphnia* weigh about 50% less and contain about 50% less water when sampled from stomach contents of salmonids than when measured from fresh zooplankton samples (Luecke and Brandt 1993; Stockwell et al. 1999); therefore, simulated consumption of *Daphnia* (g) was multiplied by 2 to estimate the fresh weight consumed for direct comparison to available biomass and production.

Daphnia availability and sockeye salmon capacity in Ross Lake

We utilized published data on monthly *Daphnia* production (biomass produced/month), standing stock biomass, and consumption demand of the existing Ross Lake zooplanktivores (rainbow trout and redside shiner; Chapter 2) to quantify the remaining prey availability and evaluate resource capacity for sockeye salmon rearing in the lake. Current consumption demand versus *Daphnia* availability was evaluated for the whole sampled water column (0-20 m depth) in addition to a depth-use scenario to determine whether thermally driven behavior may limit access to food supplies, as behavioral thermoregulation in lentic habitats is well documented for sockeye salmon (Brett 1971) and Chinook salmon (Monzyk et al. 2014). For this depth-use scenario, consumption demand versus prey availability was evaluated separately for the epilimnion (0-10 m) and the metalimnion (10-20 m) during thermally stratified periods when warmer epilimnetic temperatures might inhibit access by salmonids. We assumed that salmonids would be restricted to the metalimnion during peak thermal stratification, whereas redside shiners would be able to use the entire available supply; thus, redside shiner consumption was evenly divided between the two layers, and rainbow trout consumption was restricted to the metalimnion. This depth-use scenario is a simplification to characterize depth-stratified consumption demand assuming salmonids are restricted from the epilimnion. We expect this to occur when epilimnetic temperatures exceed 18 °C. Depth-stratified gillnet sampling in Ross Lake showed that the majority of rainbow trout (around 70%) were occupying depths below the epilimnion when these temperatures exceeded 18 °C (Chapter 3). These assumptions are also consistent with bioenergetic-based estimates of temperature-dependent growth potential at observed (rainbow trout and redside shiner) or expected (sockeye salmon) feeding rates (Fig. S1).

We evaluated Ross Lake's rearing capacity for sockeye salmon on a monthly basis using two conservative estimates of carrying capacity: 1) based on a maximum exploitation rate of 50% of combined *Daphnia* production by the entire planktivorous fish community, assuming that the food available for sockeye salmon was what remained after consumption by the existing planktivores (e.g., Hansen et al. 2016; Sorel et al. 2016a), and 2) based on a maximum exploitation rate of 50% of combined *Daphnia* production + standing stock biomass. We evaluated monthly carrying capacity for the 0-20 m depth strata and the segregated depth use scenario described above. For this depth-use scenario, we assumed sockeye salmon could only access *Daphnia* below the epilimnion and therefore set the maximum exploitation rate to 50% of production + biomass in the metalimnion. We estimated rearing capacity in terms of the initial number of juvenile sockeye salmon that could be fed each month by dividing the monthly remaining *Daphnia* available (maximum exploitation rate - current consumption demand of existing rainbow trout and redside shiner) by the monthly per capita consumption rates from the sockeye salmon bioenergetics simulations described above.

For the two carrying capacity scenarios, we calculated the initial number of fry required to enter Ross Lake in May to fit our estimated carrying capacity in September (the most limiting month for prey supply in both scenarios) and the resulting number of smolts produced the following May, assuming survival rates were constant throughout the year. We calculated these figures across a range of annual in-lake fry-smolt survival rates including the range observed in Upper Baker Lake (min = 3.6%, mean = 8.5%, max = 14.3%; Overman 2022) and using a global average of 25% survival (Quinn 2005) as our maximum bound estimate. We then estimated how many adults would be expected to return under each scenario each scenario using the smolt-to-adult return rate from Upper Baker Lake sockeye salmon from recent years compared to the historical mean (2015-2021: 4.1%; 1999-2021: 6.3%; Overman 2022). We did not incorporate predation into the carrying capacity model, as we expect predation mortality to be dynamic and variable, and thus challenging to incorporate. Therefore, we evaluated the two processes separately. The impact of different predation rates on the abundance of fry and smolts can be inferred through the scenarios modeling various rates of fry-smolt survival.

Predation mortality

Predation potential was evaluated using simulated monthly consumption by the current piscivore populations in Ross Lake, based on an age-structured unit population of 1,000 bull trout > 200 mm FL and abundance of the other salmonid species expanded by using relative frequencies from gill net surveys. For every 1,000 bull trout > 200 mm FL, the relative abundances for other salmonids corresponded to 2,430 rainbow trout, 286 brook trout, and 126 Dolly Varden > 200 mm FL (Chapter 3). Daily consumption was simulated for each age class of each species using bioenergetics models, which were informed by predator growth rates (from scale analysis), seasonal and size-specific stomach content analysis and stable isotope mixing models for each species and size class of predator, and thermal experience estimated using empirical depth-distributions and monthly vertical temperature profiles (see Chapter 3 for detailed methods and analysis). Under current conditions, the primary fish prey in the lake is redside shiner; however, a measurable proportion of salmonid prey are also consumed and the proportion of salmonids in the diet could change following introduction of anadromous fishes depending on their densities and spatial/temporal availability. Thus, we quantified minimum predation potential as the current population consumption on resident salmonids, as well as across a range of higher proportional contributions of putative anadromous fish to piscivore diets to bound a reasonable range of possible predation mortality rates.

Simulated consumption of all fish prey was converted to numbers of lake-rearing sockeye and Chinook salmon by dividing the biomass consumed (g) by the daily simulated body weight (g) for sockeye salmon from the bioenergetic simulations described in the carrying capacity section above. Daily growth of lake-rearing Chinook salmon was simulated assuming they recruit to the lake as fry (Monzyk et al. 2014) in March and grow to the same size as the yearling life history below the dams (Initial size: 39 mm FL, 0.7 g; Final size: 120 mm FL, 19.7 g). Predation was adjusted for gape limitation of the predator population assuming that predators could consume fusiform prey up to 50% of their length (Baldwin et al. 2000; Beauchamp and Van Tassell 2001; Juanes et al. 2002; Beauchamp et al. 2007; Winters and Budy 2015). Daily fork lengths (mm) of each predator age class, juvenile sockeye salmon, and lake-rearing Chinook were estimated from the simulated weight using length-weight regressions developed for the resident populations (Table 3), Upper Baker Lake sockeye salmon 2010-2021 ($W = 2.61 \times 10^{-6} \times FL^{3.264}$, $R^2 = 0.938$, N=8301, FL range: 60-173 mm; Overman 2022), and Skagit River steelhead as a surrogate for Chinook ($W = 1.52 \times 10^{-5} \times FL^{2.94}$, $R^2 = 0.99$, N=628, FL range: 45-235 mm; Thompson and Beauchamp 2016). This was done for several scenarios, assuming that predation on juvenile sockeye and Chinook salmon would account for a range from 10-100% of the total fish portion of the diet. For species that would only be using the reservoir as a migration corridor, predation mortality was estimated using a similar approach but only during the month(s) of expected migration and size of expected migrants (detailed in the species descriptions section of the methods above).

Abundance of the salmonid piscivores is not well studied in this system; however, annual snorkel surveys in the Upper Skagit River (British Columbia) provide some abundance index data for bull trout in the Ross Lake basin (Foster 2020). Telemetry studies on bull trout in the Upper Skagit River have shown that most of the population migrates between Ross Lake and the Skagit River for at least some portion of the year (Nelson 2006), supporting our choice to use these surveys to estimate abundance of the Ross Lake population. These surveys (1998, 2009-2017, and 2020) were conducted during early September and covered only mainstem reaches starting at the Chittenden Bridge immediately upstream of the Ross Lake reservoir to the confluence with the Sumallo River (31.3 river km upstream). Notably, these surveys occur about a month before spawning is believed to begin, thus these counts may underestimate the actual spawning population (Nelson et al. 2004; Nelson 2006). Abundance of Upper Skagit River bull trout was estimated at ca. 4,800 adults in 2011 using counts from these surveys and assumed the survey area represents around 40% of the high quality spawning habitat accessible to Ross Lake

(Seattle City Light 2012). Updating this estimate with counts from surveys in 2017 and 2020 (1,241 and 1,070 individuals, respectively), we could estimate an adult bull trout population in Ross Lake from 2,700 to 3,100. Thus, for our analysis of predation potential on introduced anadromous salmonids, we also evaluated predation by the piscivore population relative to an estimated abundance of 3,000 bull trout > 200 mm FL in Ross Lake, which upon the expansion described above corresponds to 7,290 rainbow trout, 858 brook trout, and 378 Dolly Varden.

Results

Daphnia availability and sockeye salmon capacity

Daphnia densities in Ross Lake were low across all months, years, and regions sampled, with < 1 individual/L observed except during June 2019 (Fig. 2). Densities were typically, but not always, lower in the metalimnion compared to the epilimnion, and these densities were consistently lower than the threshold at which sockeye will switch from feeding exclusively on *Daphnia* (0.4 individuals/L, Scheuerell et al. 2005). Supply (in terms of biomass and production) was lowest in May and continually increased to a peak in August before declining substantially in September (Fig. 3). However, consumption demand by the dominant planktivores in the lake (redside shiner and rainbow trout) was lowest in May and highest in September, indicating that prey were most limited in late summer.

Bioenergetic simulations estimated that juvenile sockeye salmon in Ross Lake would annually consume 74.2 g *Daphnia* (fresh weight) per capita. The monthly initial abundance of juvenile sockeye salmon that could be supported by the *Daphnia* supply in Ross Lake varied by nearly fortyfold depending on the month, thermal restriction scenario evaluated, and the carrying capacity definition used (Table 4). Using the more conservative capacity definition (maximum consumption demand of 50% of *Daphnia* production by the existing planktivore community plus introduced sockeye salmon), we estimated that Ross Lake could not support any additional planktivores in June if they are thermally restricted to the metalimnion, whereas around 5,140,000 could be supported if not restricted. September was the most limiting month assuming no thermal restriction and could support around 54,000 juveniles, which corresponded to initial fry abundances (assuming entry on May 1) of 87,000 if annual fry-smolt survival is 25% or 125,000 if annual fry-smolt survival is 8.5%.

Capacity estimates were considerably higher when using the more liberal capacity definition – maximum consumption demand of 50% of *Daphnia* production + biomass by the existing planktivore community plus introduced sockeye salmon (Table 4). Under this constraint September was still the most limiting month, and we estimated capacity to support around 1,460,000 juveniles during this month if sockeye salmon are not restricted from the epilimnion, which corresponded to initial fry abundances of 2,330,000 if annual fry-smolt survival is 25% or 3,352,000 if annual fry-smolt survival is 8.5%. These capacity estimates were 51% higher than in the scenario of thermal restriction from the epilimnion. The month of June could support the highest number of juveniles under the scenario of no thermal restriction (10,356,000), which corresponded to initial fry abundances of 11,650,000 or 12,768,000 assuming annual fry-smolt survival of 25% or 8%, respectively.

Using the constraint of a maximum consumption demand of 50% of *Daphnia* biomass + production by the existing planktivore community plus introduced sockeye salmon in the most limiting month of September as the nominal scenario, we estimated potential smolt production in the following spring from 120,058 smolts under a scenario of thermal restriction and low fry-smolt survival (3.6%) to 679,087 smolts under a scenario of no thermal restriction and high fry-smolt survival (25%; Table 5). The potential number of returning adults varies with the capacity estimate as well as survival at the fry-to-smolt and smolt-to-adult stages (Table 5), with a low estimate of 4,922 adults (thermal restriction during the most limiting month, fry-smolt survival = 3.6%, and smolt-adult survival = 4.1%) and a high estimate of 42,782 (no thermal restriction during the most limiting month, fry-smolt survival = 25%, and smolt-adult survival = 6.3%). Using the mean fry-smolt survival rate from Upper Baker Lake sockeye salmon (8.5%) and their contemporary mean smolt-to-adult survival (4.1%), we estimated adult returns from 8,701 to 13,617, under capacity scenarios of thermal restriction and no thermal restriction in the most limiting month, respectively.

Predation mortality

The unit population of piscivores (bull trout, rainbow trout, brook trout, Dolly Varden, relative to 1,000 bull trout > 200 mm FL) in Ross Lake consumed an estimated 2846 kg of fish annually, with most composed of nonnative redside shiner (1972 kg) and unidentified fish (771 kg) and a smaller portion of salmonids (103 kg). Fish consumption was highest during the growing season, peaking during July, and was lowest during Dec-Apr (Fig. 4). Current predation on salmonids was lowest in spring and increased through summer and fall. Simulated consumption during winter was very low, and consumption of salmonid prey, based on diet interpolations between fall and spring, was extremely low.

We assumed that the current predation demand on native salmonids would represent the minimum expected predation potential on introduced salmonids. Thus, to estimate a minimum level of predation in terms of numbers of fish, assuming that 100% of predation on native salmonids would be replaced by anadromous salmonids, we divided monthly biomass of salmonids consumed by the average monthly body weight of sockeye salmon from bioenergetics simulations. This resulted in an estimated 59,293 juveniles consumed annually by a unit predator population referenced to 1,000 bull trout > 200 mm FL. Chinook that migrated directly to the reservoir for rearing until achieving smolt size the following year would be subjected to an estimated loss of 16,748 juveniles during the 12 months of simulated reservoir rearing (beginning on March 1). This translates into considerably lower mortality for the species migrating through the reservoir compared to species or life history types that reared predominantly in the reservoir (Table 6). The fry-migrant life history of Chinook would be the smallest fish migrating through the reservoir and are thus the most vulnerable; however, the overall impact of predation would be buffered because metabolically-regulated consumption rates are lower during their expected migration during March.

Current consumption rates of salmonids in Ross Lake may not reflect diets following introduction of anadromous salmonids, due to the expected higher densities of anadromous juveniles compared to the resident salmonid population, and easier access by predatory salmonids to them compared to redside shiner during thermal stratification. Therefore, we also evaluated predation potential across a range of proportions of diet switching to anadromous juveniles. Predation potential for sockeye salmon was highest during the spring, when predator consumption was low but increasing and the newly recruited sockeye salmon were small; however, predation would be heavily influenced by the portion of total fish consumption that shifted to lake-rearing sockeye or Chinook salmon (Fig. 5). Predation in spring and early summer by the unit population relative to 1,000 bull trout could be substantial in May alone, for example ranging from around 96,000 sockeye salmon if they comprised 10% of total fish consumption, to 771,000 if they became 80% of the total fish consumption. This could compound into considerable annual mortality in the lake, from 273,000 individuals if sockeye salmon were 10% of the fish prey consumed across the year, to 2,453,000 individuals if they were 90% of the fish prey consumed. Due to the larger size of yearling smolts and earlier emigration to the lake compared to sockeye salmon, we estimated lower predation potential on Chinook salmon (Fig. 5). We estimated comparable annual mortality during their first 12 months of reservoir rearing from 66,000 individuals if lake-rearing Chinook were 10% of the fish prey consumed across the year, to 594,000 individuals if they were 90% of the fish prey consumed.

Fish simply migrating through the reservoir would be exposed to less predation pressure in the reservoir, and the impact would be dependent on their size and timing of migration and the response of the predators to a predictable annual pulse of prey (Fig. 6). Despite their small size, the fry-migrant life history of Chinook salmon may be less vulnerable to predation as their expected window of migration occurs when predator consumption rates are relatively low. This would still translate to a maximum predation potential of 72,067 fry across the migration window, assuming 100% of fish consumption by the unit predator population was targeted at migrating Chinook fry. Predation potential decreases as size/age at migration increases, with age 3 steelhead smolts exhibiting the lowest numeric maximum predation potential.

Expanding from the predation impact by a unit population of 1,000 bull trout > 200 mm FL and the corresponding abundances of the other predatory salmonids to our best estimate of the actual predator population abundance (all piscivores relative to 3,000 bull trout > 200 mm FL) has the largest implications for fry-smolt survival rates of lake-rearing sockeye and Chinook salmon. This could translate into annual predation losses from 818,000 juvenile sockeye salmon if they were 10% of the fish fraction of annual consumption, to 7,358,000 individuals if they were 90% of the fish prey consumed. Estimates of predation potential on juvenile Chinook salmon in their first 12 months of reservoir rearing are considerably lower compared to sockeye salmon and range from 198,000 individuals if they were 10% of the fish prey consumed across the year, to 1,783,000 individuals if they were 90% of the fish prey consumed.

Discussion

Our study indicated that modest resource capacity may be available to support lake rearing for pelagic anadromous salmonids in Ross Lake; however, predation could limit juvenile survival, and thus smolt production, of lake rearing species. Predation would also affect smolts migrating through the reservoir, but to a lesser extent. The levels of mortality would depend on the size of the juveniles, timing and duration of reservoir occupancy, and the proportion of piscivore diets that would shift to anadromous salmonids. The relative role of predation in driving overall fry-smolt survival rates of any introduced populations will depend on the number of migrants, and thus can only be evaluated in the context of the estimated production potential of the tributaries.

Our evaluation of both carrying capacity and predation potential on lake-rearing sockeye salmon is strongly influenced by their expected growth rate and the potential effects of size-selective mortality. We used growth data from Upper Baker Lake sockeye salmon as a surrogate for what could happen in Ross Lake. They are stocked from the hatchery into the lake in the spring as fed fry, and age 1 smolts (mean: 112 mm FL) are larger than what is typical for the species (mode of age-1 smolt lengths: 60-90 mm, Quinn 2005). Sockeye salmon growth in lakes is closely linked to zooplankton density (mg/m^2) and water temperature (Hyatt and Stockner 1985; Edmundson and Mazumder 2001), thus low zooplankton biomass in Ross Lake may result in lower-than-expected growth. Although the lake could theoretically support additional slower growing fish (because their individual consumption demand is lower), this would likely present a tradeoff with increased mortality. Slower growing juveniles would be more vulnerable to predation during reservoir rearing and this could result in lower fry-smolt survival rates. Smaller smolt size could also result in lower marine survival rates (Henderson and Cass 1991).

Uncertainty in how effectively sockeye salmon would be able to feed on the low zooplankton densities observed in Ross Lake limit our ability to predict how these various tradeoffs may play out in Ross Lake. Our analysis of zooplankton production was limited to *Daphnia*, but densities were most often at or below the threshold where sockeye salmon feed exclusively on *Daphnia* (0.4 individuals/L, Scheuerell et al. 2005), thus it may be important to expand zooplankton analysis to include other prey species such as copepods. Notably though, *Daphnia* were the dominant zooplankton taxa consumed by rainbow trout in Ross Lake, with larger bodied *Leptodora* also contributing substantially in some seasons, but we observed minimal proportions of copepods or *Bosmina* in rainbow trout diets, and copepod densities were similarly low from May-October (< 0.5/L; Chapter 2). Further, kokanee exhibit around 70% lower capture success on copepods compared to *Daphnia* (30% success compared to 100% success; Hyatt 1980), thus switching to copepods would likely result in lower foraging efficiency and growth rate for sockeye juveniles. Functional response experiments would improve our understanding of the relationship between zooplankton density and sockeye salmon consumption/growth rates. Such experiments have been done with kokanee; however, the experimental prey densities used previously (minimum of 3 *Daphnia*/L, Koski and Johnson 2002) were not representative of the low *Daphnia* density observed in Ross Lake.

We identified that predation potential on lake rearing juveniles may be a substantial limitation to survival and corresponding smolt production in Ross Lake; however, uncertainty in how fish predation would shift towards introduced anadromous species corresponds to a large range of potential effect size. In Kachess Lake, Washington — a reservoir where bull trout cooccur with pelagic kokanee, non-pelagic salmonids, redside shiner, and other littoral/benthic prey fish — stable isotope mixing models estimated that pelagic salmonids contributed 76% of bull trout diets (Hansen et al. 2021). Kokanee are also the dominant prey for larger bull trout, rainbow trout, and cutthroat trout in Pend Oreille Lake, Idaho (Clarke et al. 2005). During periods of stratification when the epilimnion is too warm for most salmonids, pelagic species such as sockeye salmon may be more available to piscivorous salmonids than redside shiner because of their overlapping thermal preferences and depth-use. Under current conditions lacking anadromous salmonid introductions, diel vertical migration to feed on redside shiner in the epilimnion may be the most efficient foraging strategy due to their high densities (Eckmann et al. 2018); however, we would expect this to change as densities of salmonids increase in deeper water following proposed introductions. Further, predation on juvenile sockeye salmon can determine fry survival in lakes and has been a barrier to success for some enhancement/stocking programs (Foerster and Ricker 1941; Beauchamp et al. 1995; Cartwright et al. 1998). We expect that predation pressure will vary as predator populations are likely to change over time; however, by using the unit population approach, predation impacts can be easily updated by multiplying across our estimated size-structured consumption rates, which incorporate seasonal variability in diet, consumption rates, and relative abundance among species and size/age classes of predators.

Bull trout and rainbow trout in Ross Lake are currently feeding at relatively low or average proportions of their theoretical maximum consumption rates (%C_{max}; bull trout: 25-31%; rainbow trout: 31-36%; Chapter 3). One possible explanation for this is that warm temperatures in the epilimnion limit foraging opportunities for these predators during the summer, preventing them from fully exploiting these resources. Alternatively, if bull trout can remain in contact with high densities of redside shiners and maintain higher than average feeding rates in the epilimnion, some fraction of these predators might adopt this strategy as long as prey densities remain high and predictable, and epilimnetic temperatures do not increase. If densities of introduced salmonids are high enough, this could increase consumption rates by the predators beyond what we estimated in our simulations. Bull trout are also known to binge feed (i.e., temporary episodes when $\%C_{max} > 100\%$) while tracking pulses of salmon migrations, so predation rates on migrating smolts could also exceed our predictions (Furey et al. 2016; Furey and Hinch 2017). Recent studies tracking predator-prey behaviors at floating smolt collectors have reported bull trout tracking pulses of smolt migrations at these structures, as they do in lake outlets of natural systems (Smith et al. 2021, 2022).

Introduced anadromous salmonids will need to navigate the tradeoffs between growth potential and survival in tributary habitats versus predation risk in the reservoirs. Given the high levels of predation in Ross Lake under current conditions, life history expressions that migrate at larger sizes/older ages may be advantageous for introduced anadromous salmonids in this system. Production of such life histories will thus be limited by growth and production potential in the tributaries. Intrinsic potential (IP) modeling of the Skagit River mainstem and other tributaries above the dams indicated that these habitats are of predominantly low or medium IP for Chinook and coho salmon (Duda and Hardiman in review), suggesting potential habitat limitations for these species. The IP modeling indicated that high IP habitat is more prevalent for steelhead; however, bioenergetic analyses of rainbow trout growth in Ross Lake tributaries have estimated low scope for growth for this species (Jensen et al. in review). That study determined that age-2 rainbow trout did not attain adequate growth rates to reach the size of successful age-2 or age-3 steelhead smolts downstream of the dams without extending the duration of stream rearing and incurring further mortality. This initial analysis indicates that potential production of these late-migrant life histories may be limited in tributaries of Ross Lake.

Our analysis was limited to scenarios of single species introductions; evaluating the food web capacity for introductions of multiple species simultaneously would become increasingly complex. The rearing capacity of the reservoir could support one or a mix of juvenile salmonid species, but the finite availability of zooplankton would need to be shared among species and life history types. Introducing multiple species might buffer predation on any one species, but this would depend on differential spatial-temporal overlap with piscivores and their relative abundance. It may also be important to consider any cascading effects to redside shiner survival and abundance that may be associated with decreased zooplankton availability (resource competition with sockeye salmon) or decreased predation pressure if piscivore diets shift to consuming more salmonids and fewer redside shiner. These food web interactions will play out within the physical context of the reservoir hydrology as driven by water operations, thus highlighting the importance of evaluating seasonal flow management in relation to juvenile migration timing and the corresponding effects on migration rates through the reservoir and vulnerability to predation. Exploration of these more complex responses is beyond the scope of this study, but nonetheless important to consider for further feasibility evaluations. If experimental introductions are to occur, an adaptive management and research program would be critical to address these concerns and adequately monitor food web changes and factors driving introduction success. A successful introduction program will rely on adult returns that exceed replacement enough to support harvest and sufficient spawner escapement, which could be a challenge in this system given the limitations to growth and survival that have been identified thus far. Future feasibility studies would therefore benefit from focusing on these potential challenges identified for the juvenile life stage.

Acknowledgments

Funding and support for this study was provided by Seattle City Light - in particular, we thank Jeff Fisher, Erin Lowery, and the Diablo Lake boat house crew for critical support provided during our field operations. We would like to thank North Cascades National Park and Ross Lake Resort for their assistance with field sampling logistics. We also want to thank Tom Barnett in particular for his support, angling efforts, and knowledge of the Ross Lake fishery. We are grateful for Lisa Wetzel, Ella Wagner, Nancy Elder, and Jeff Duda for assistance in the field and laboratory, and Tom Quinn, Julian Olden, and Jeff Duda for providing valuable editorial comments that improved the quality of this manuscript. Handling of vertebrates was conducted under the auspices of the Institutional Animal Care and Use Committee of the U.S. Geological Survey, Western Fisheries Research Center IACUC protocols #2008-57.

References

Anderson, J. H., G. R. Pess, R. W. Carmichael, M. J. Ford, T. D. Cooney, C. M. Baldwin, and M. M. McClure. 2014. Planning pacific salmon and steelhead reintroductions aimed at long-term viability and recovery. North American Journal of Fisheries Management 34:72–93.

Armstrong, D. P., and P. J. Seddon. 2008. Directions in reintroduction biology. Trends in Ecology and Evolution 23:20–25.

Arostegui, M. C., and T. P. Quinn. 2019. Reliance on lakes by salmon, trout and charr (*Oncorhynchus*, *Salmo* and *Salvelinus*): An evaluation of spawning habitats, rearing strategies and trophic polymorphisms. Fish and Fisheries 20:775–794.

Baldwin, C. M., D. A. Beauchamp, and J. J. V. Tassell. 2000. Bioenergetic assessment of temporal food supply and consumption demand by salmonids in the Strawberry Reservoir food web. Transactions of the American Fisheries Society 129:429–450.

Beauchamp, D. A. 1995. Riverine predation on sockeye salmon fry migrating to Lake Washington. North American Journal of Fisheries Management 15:358–365.

Beauchamp, D. A., A. D. Cross, J. L. Armstrong, K. W. Myers, J. H. H. Moss, J. L. Boldt, and L. J. Haldorson. 2007. Bioenergetic responses by Pacific salmon to climate and ecosystem variation. North Pacific Anadromous Fish Commission Bulletin 4:257–269.

Beauchamp, D. A., M. G. Lariviere, and G. L. Thomas. 1995. Evaluation of competition and predation as limits to juvenile kokanee and sockeye salmon production in Lake Ozette, Washington. North American Journal of Fisheries Management 15:193–207.

Beauchamp, D. A., D. J. Stewart, and G. L. Thomas. 1989. Corroboration of a bioenergetics model for sockeye salmon. Transactions of the American Fisheries Society 118:597–607.

Beauchamp, D. A., and J. J. Van Tassell. 2001. Modeling seasonal trophic interactions of adfluvial bull trout in Lake Billy Chinook, Oregon. Transactions of the American Fisheries Society 130:204–216.

Bourret, S. L., B. P. Kennedy, C. C. Caudill, and P. M. Chittaro. 2014. Using otolith chemical and structural analysis to investigate reservoir habitat use by juvenile Chinook salmon *Oncorhynchus tshawytscha*. Journal of Fish Biology 85:1507–1525.

Brett, J. R. 1971. Energetic responses of salmon to temperature: A study of some thermal relations in the physiology and freshwater ecology of sockeye salmon (*Oncorhynchus nerka*). American Zoologist 11:99–113.

Bubac, C. M., A. C. Johnson, J. A. Fox, and C. I. Cullingham. 2019. Conservation translocations and post-release monitoring: Identifying trends in failures, biases, and challenges from around the world. Biological Conservation 238:108239.

Cartwright, M. A., D. A. Beauchamp, and M. D. Bryant. 1998. Quantifying cutthroat trout (*Oncorhynchus clarki*) predation on sockeye salmon (*Oncorhynchus nerka*) fry using a bioenergetics approach. Canadian Journal of Fisheries and Aquatic Sciences 55:1285–1295.

Clarke, L. R., D. T. Vidergar, and D. H. Bennett. 2005. Stable isotopes and gut content show diet overlap among native and introduced piscivores in a large oligotrophic lake. Ecology of Freshwater Fish 14:267–277.

Cochran-Biederman, J. L., K. E. Wyman, W. E. French, and G. L. Loppnow. 2015. Identifying correlates of success and failure of native freshwater fish reintroductions. Conservation Biology 29:175–186.

Deslauriers, D., S. R. Chipps, J. E. Breck, J. A. Rice, and C. P. Madenjian. 2017. Fish Bioenergetics 4.0: An R-based modeling application. Fisheries 42:586–596.

Duda, J. J., and J. M. Hardiman. in review. Applying intrinsic potential models to evaluate salmon introduction into mainstem and tributary habitats upstream of the Skagit River Hydroelectric Project: U.S. Geological Survey Open-File Report.

Dunham, J., K. Gallo, D. Shively, C. Allen, and B. Goehring. 2011. Assessing the feasibility of native fish reintroductions: A framework applied to threatened bull trout. North American Journal of Fisheries Management 31:106–115.

Eckmann, M., J. Dunham, E. J. Connor, and C. A. Welch. 2018. Bioenergetic evaluation of diel vertical migration by bull trout (*Salvelinus confluentus*) in a thermally stratified reservoir. Ecology of Freshwater Fish 27:30–43.

Edmundson, J. A., and A. Mazumder. 2001. Linking growth of juvenile sockeye salmon to habitat temperature in Alaskan Lakes. Transactions of the American Fisheries Society 130:644–662.

Evans, M. L., M. A. Johnson, D. Jacobson, J. Wang, M. Hogansen, and K. G. O'Malley. 2016. Evaluating a multi-generational reintroduction program for threatened salmon using genetic parentage analysis. Canadian Journal of Fisheries and Aquatic Sciences 73:844–852.

Flagg, T. A., and T. E. Ruehle. 2000. Cle Elum Lake anadromous salmon restoration feasibility study: Summary of research, 2000 final report to Bonneville Power Administration (BPA Report DOE/BP-64840-4). Bonneville Power Administration - Environment, Fish and Wildlife Division.

Foerster, R. E., and W. E. Ricker. 1941. The effect of reduction of predaceous fish on survival of young sockeye salmon at Cultus Lake. Journal of the Fisheries Research Board of Canada 5:315–336.

Foster, J. 2020. 2020 Skagit River snorkel survey report. Triton Environmental Consultants Ltd.

Furey, N. B., and S. G. Hinch. 2017. Bull trout movements match the life history of sockeye salmon: Consumers can exploit seasonally distinct resource pulses. Transactions of the American Fisheries Society 146:450–461.

Furey, N. B., S. G. Hinch, M. G. Mesa, and D. A. Beauchamp. 2016. Piscivorous fish exhibit temperature-influenced binge feeding during an annual prey pulse. Journal of Animal Ecology 85:1307–1317.

Hansen, A. G., J. R. Gardner, D. A. Beauchamp, R. Paradis, and T. P. Quinn. 2016. Recovery of sockeye salmon in the Elwha River, Washington, after dam removal: Dependence of smolt production on the resumption of anadromy by landlocked kokanee. Transactions of the American Fisheries Society 145:1303–1317.

Hansen, A. G., J. R. Gardner, K. A. Connelly, M. Polacek, and D. A. Beauchamp. 2018. Trophic compression of lake food webs under hydrologic disturbance. Ecosphere 9:1–11.

Hansen, A. G., J. R. Gardner, K. A. Connelly, M. Polacek, and D. A. Beauchamp. 2021. Resource use among top-level piscivores in a temperate reservoir: Implications for a threatened coldwater specialist. Ecology of Freshwater Fish:1–23.

Hansen, A. G., M. Polacek, K. A. Connelly, J. R. Gardner, and D. A. Beauchamp. 2017. Food web interactions in Kachess and Keechelus Reservoirs, Washington: Implications for threatened adfluvial bull trout and management of water storage - Final Report. Washington Cooperative Fish and Wildlife Research Unit.

He, F., C. Zarfl, V. Bremerich, J. N. W. David, Z. Hogan, G. Kalinkat, K. Tockner, and S. C. Jähnig. 2019. The global decline of freshwater megafauna. Global Change Biology 25:3883–3892.

Henderson, M. A., and A. I. Cass. 1991. Effect of smolt size on smolt-to-adult survival for Chilko Lake sockeye salmon. Canadian Journal of Fisheries and Aquatic Sciences 48:988–994.

Hyatt, K. D., and J. G. Stockner. 1985. Responses of sockeye salmon (*Oncorhynchus nerka*) to fertilization of British Columbia coastal lakes. Canadian Journal of Fisheries and Aquatic Sciences 42:320–331.

IUCN. 2013. Guidelines for reintroductions and other conservation translocations. Version 1.0. Gland, Switzerland: IUCN Species Survival Commission.

Jensen, B. L., R. C. Johnson, J. J. Duda, C. O. Ostberg, T. J. Code, J. H. Mclean, K. D. Stenberg, K. A. Larsen, M. S. Hoy, and D. A. Beauchamp. in review. Growth performance of rainbow trout in reservoir tributaries and implications for steelhead growth potential above Skagit River dams. North American Journal of Fisheries Management.

Johnson, P. T. J., J. D. Olden, and M. J. V. Zanden. 2008. Dam invaders: Impoundments facilitate biological invasions into freshwaters. Frontiers in Ecology and the Environment 6:357–363.

Juanes, F., J. A. Buckel, and S. S. Frederick. 2002. Feeding ecology of piscivorous fishes. Pages 267–283 *in* P. J. B. Hart and J. D. Reynolds, editors. Handbook of Fish Biology and Fisheries. Blackwell Science Ltd.

Keefer, M. L., G. A. Taylor, D. F. Garletts, C. K. Helms, G. A. Gauthier, T. M. Pierce, and C. C. Caudill. 2012. Reservoir entrapment and dam passage mortality of juvenile Chinook salmon in the Middle Fork Willamette River. Ecology of Freshwater Fish 21:222–234.

Kock, T. J., J. W. Ferguson, M. L. Keefer, and C. B. Schreck. 2021. Review of trap-and-haul for managing Pacific salmonids (*Oncorhynchus* spp.) In impounded river systems. Reviews in Fish Biology and Fisheries 31:53–94.

Kock, T., R. Perry, G. Hansen, P. Haner, A. Pope, J. Plumb, K. Cogliati, and A. Hansen. 2019. Evaluation of Chinook salmon fry survival in Lookout Point Reservoir, Western Oregon, 2017. U.S. Geological Survey Open-File Report 2019-1011.

Koehler, M. E., K. L. Fresh, D. A. Beauchamp, J. R. Cordell, C. A. Simenstad, and D. E. Seiler. 2006. Diet and bioenergetics of lake-rearing juvenile Chinook salmon in Lake Washington. Transactions of the American Fisheries Society 135:1580–1591.

Koenings, J. P., and G. B. Kyle. 1997. Consequences to juvenile sockeye salmon and the zooplankton community resulting from intense predation. Alaska Fishery Research Bulletin 4:120–135.

Koski, M. L., and B. M. Johnson. 2002. Functional response of kokanee salmon (*Oncorhynchus nerka*) to *Daphnia* at different light levels. Canadian Journal of Fisheries and Aquatic Sciences 59:707–716.

Lowery, E. D., and D. A. Beauchamp. 2010. Baseline food web assessment of the Upper Clackamas River basin prior to reintroduction of bull trout. Report # WACFWRU-010-02. US Geological Survey, Washington Cooperative Fish and Wildlife Research Unit.

Luecke, C., and D. Brandt. 1993. Notes: Estimating the energy density of Daphnid prey for use with rainbow trout bioenergetics models. Transactions of the American Fisheries Society 122:386–389.

Matala, A. P., S. R. Narum, B. P. Saluskin, M. V. Johnston, J. E. Newell, D. E. Fast, and P. F. Galbreath. 2019. Early observations from monitoring a reintroduction program: Return of sockeye salmon to a nursery lake of historical importance. Transactions of the American Fisheries Society 148:271–288.

McCarthy, S. G., J. J. Duda, J. M. Emlen, G. R. Hodgson, and D. A. Beauchamp. 2009. Linking habitat quality with trophic performance of steelhead along forest gradients in the South Fork Trinity River watershed, California. Transactions of the American Fisheries Society 138:506–521.

Monzyk, F. R., R. Emig, J. D. Romer, and T. A. Friesen. 2014. Life-history characteristics of juvenile spring Chinook salmon rearing in Willamette Valley reservoirs [online]. Oregon Department of Fish and Wildlife - Upper Willamette Research, Monitoring and Evaluation Program.

Murphy, C. A., C. S. Lee, B. Johnson, I. Arismendi, and S. L. Johnson. 2019a. GrowChinook: An optimized multimodel and graphic user interface for predicting juvenile Chinook salmon growth in lentic ecosystems. Canadian Journal of Fisheries and Aquatic Sciences 12:1–12.

Murphy, C. A., G. Taylor, T. Pierce, I. Arismendi, and S. L. Johnson. 2019b. Short-term reservoir draining to streambed for juvenile salmon passage and non-native fish removal. Ecohydrology 12:1–9.

Naiman, R. J., J. R. Alldredge, D. A. Beauchamp, P. A. Bisson, J. Congleton, C. J. Henny, N. Huntly, R. Lamberson, C. Levings, E. N. Merrill, W. G. Pearcy, B. E. Rieman, G. T. Ruggerone, D. Scarnecchia, P. E. Smouse, and C. C. Wood. 2012. Developing a broader scientific foundation for river restoration: Columbia River food webs. Proceedings of the National Academy of Sciences of the United States of America 109:21201–21207.

Naughton, G. P., M. L. Keefer, T. S. Clabough, M. J. Knoff, T. J. Blubaugh, C. Sharpe, and C. C. Caudill. 2018. Reservoir provides cool-water refuge for adult Chinook salmon in a trap-and-haul reintroduction program. Marine and Freshwater Research 69:1995–2007.

Nelson, T. C. 2006. Final Report: Upper Skagit watershed native char project 2001-2004. LGL Limited Environmental Research Associates.

Nelson, T. C., C. E. J. Mussell, and J. Rissling. 2004. Progress report 2003: Upper Skagit watershed native char project. LGL Limited Environmental Research Associates.

Overman, N. C. 2022. Baker River Juvenile Sockeye Population Analysis [unpublished data]. Washington Department of Fish & Wildlife.

Quinn, T. P. 2005. The Behavior and Ecology of Pacific Salmon and Trout, 1st edition. University of Washington Press.

Quinn, T. P., and J. P. Losee. 2022. Diverse and changing use of the Salish Sea by Pacific salmon, trout, and char. Canadian Journal of Fisheries and Aquatic Sciences 79:1003–1021.

Sard, N. M., K. G. O’Malley, D. P. Jacobson, M. J. Hogansen, M. A. Johnson, and M. A. Banks. 2015. Factors influencing spawner success in a spring Chinook salmon (*Oncorhynchus tshawytscha*) reintroduction program. Canadian Journal of Fisheries and Aquatic Sciences 72:1390–1397.

Scheuerell, J. M., D. E. Schindler, M. D. Scheuerell, K. L. Fresh, T. H. Sibley, A. H. Litt, and J. H. Shepherd. 2005. Temporal dynamics in foraging behavior of a pelagic predator. Canadian Journal of Fisheries and Aquatic Sciences 62:2494–2501.

Seattle City Light. 2012. Biological Evaluation - supplement: Impacts of entrainment of bull trout. Skagit River Hydroelectric Project License (FERC no. 553) amendment: addition of a second power tunnel at the Gorge Development.

Seattle City Light. 2023. Final License Application to the Federal Energy Regulatory Committee. Exhibit E - Appendix G: Skagit project upstream and downstream fish passage program. Available at: https://www.seattle.gov/light/skagit/Relicensing/default.htm.

Seddon, P. J., D. P. Armstrong, and R. F. Maloney. 2007. Developing the science of reintroduction biology. Conservation Biology 21:303–312.

Smith, C. D., T. W. Hatton, and N. S. Adams. 2022. Monitoring fish abundance and behavior, using multi-beam acoustic imaging sonar, at a selective water withdrawal structure in Lake Billy Chinook, Deschutes River, Oregon, 2020. US Geological Survey Open-File Report 2022-1038:1–31.

Smith, C. D., J. M. Plumb, N. S. Adams, and G. J. Wyatt. 2021. Predator and prey events at the entrance of a surface-oriented fish collector at North Fork Dam, Oregon. Fisheries Management and Ecology 28:172–182.

Smith, M. J. 2010. Final Report: Population structure and genetic assignment of bull trout (*Salvelinus confluentus*) in the Skagit River basin. University of Washington.

Sorel, M. H., A. G. Hansen, K. A. Connelly, and D. A. Beauchamp. 2016a. Trophic feasibility of reintroducing anadromous salmonids in three reservoirs on the North Fork Lewis River, Washington: Prey supply and consumption demand of resident fishes. Transactions of the American Fisheries Society 145:1331–1347.

Sorel, M. H., A. G. Hansen, K. A. Connelly, A. C. Wilson, E. D. Lowery, and D. A. Beauchamp. 2016b. Predation by northern pikeminnow and tiger muskellunge on juvenile salmonids in a high-head reservoir: Implications for anadromous fish reintroductions. Transactions of the American Fisheries Society 145:521–536.

Stockwell, J. D., K. L. Bonfantine, and B. M. Johnson. 1999. Kokanee foraging: A *Daphnia* in the stomach is worth two in the lake. Transactions of the American Fisheries Society 128:169–174.

Swan, K. D., N. A. Lloyd, and A. Moehrenschlager. 2018. Projecting further increases in conservation translocations: A Canadian case study. Biological Conservation 228:175–182.

Thompson, J. N., and D. A. Beauchamp. 2014. Size-selective mortality of steelhead during freshwater and marine life stages related to freshwater growth in the Skagit River, Washington. Transactions of the American Fisheries Society 143:910–925.

Thompson, J. N., and D. A. Beauchamp. 2016. Growth of juvenile steelhead *Oncorhynchus mykiss* under size-selective pressure limited by seasonal bioenergetic and environmental constraints. Journal of Fish Biology 89:1720–1739.

WDFW, and SRSC. 2005. Skagit Chinook recovery plan. Washington Department of Fish and Wildlife (WDFW) & Skagit River System Cooperative (SRSC).

Winters, L. K., and P. Budy. 2015. Exploring crowded trophic niche space in a novel reservoir fish assemblage: How many is too many? Transactions of the American Fisheries Society 144:1117–1128.

Zimmerman, M. S., J. R. Irvine, M. O’Neill, J. H. Anderson, C. M. Greene, J. Weinheimer, M. Trudel, and K. Rawson. 2015. Spatial and temporal patterns in smolt survival of wild and hatchery coho salmon in the Salish Sea. Marine and Coastal Fisheries 7:116–134.

Tables

Table 1. Mean, minimum, and maximum daily thermal experience in each month used for simulated sockeye salmon in Ross Lake.

	Temperature °C		
Month	Min	Mean	Max
May	7.4	8.5	9.5
Jun	9.6	10.6	11.8
Jul	11.8	13.0	14.0
Aug	13.1	13.8	14.7
Sep	13.9	15.2	15.5
Oct	12.0	13.5	14.7
Nov	8.8	10.4	12.1
Dec	5.8	7.1	8.7
Jan	4.6	5.1	5.7
Feb	4.1	4.2	4.6
Mar	4.1	4.6	5.1
Apr	5.2	6.3	7.6

Table 2. Diet proportions and energy densities (J/g wet weight) used for sockeye salmon bioenergetics simulations. These data were borrowed from kokanee in Yale Reservoir, WA (Sorel et. al 2016a). Winter diet was assumed to contain minimal *Daphnia* due to lower availability. Diet proportions were linearly interpolated through time in the simulation. Energy densities for zooplankton are sourced from Luecke & Brandt (1993), and insects from McCarthy et al. (2009). Note that the energy density for *Daphnia* reflects their compressed form in the gut and is approximately 2x higher in J/g than 'fresh' *Daphnia*.

		Daphnia	Zooplankton other	Immature insect	Adult insect
Simulation day	Season	3860 J/g	2260 J/g	3365 J/g	5000 J/g
1	Spring	0.684	0.084	0.189	0.043
62	Summer	0.755	0.162	0.083	0.000
154	Fall	0.879	0.062	0.000	0.059
274	Winter	0.200	0.400	0.400	0.000
365	Spring	0.684	0.084	0.189	0.043

Table 3. Length-weight regressions for salmonids in Ross Lake. Equations are in the exponential form $W = a \times FL^{b}$.

Species	*N*	*P*	R^2	a	b
Bull trout/hybrids	336	< 0.001	0.997	1.12×10^{-5}	2.974
Dolly Varden	175	< 0.001	0.994	8.26×10^{-6}	3.048
Brook trout	130	< 0.001	0.985	7.79×10^{-6}	3.076
Rainbow trout	1,917	< 0.001	0.996	1.27×10^{-5}	2.961

Table 4. Monthly estimates of sockeye salmon capacity (#s of juveniles) and the corresponding number of fry entering the lake in May assuming annual fry survival (S) is 8.5% (mean fry-smolt survival in Upper Baker Lake, Overmann 2022) or 25% (global average, Quinn 2005). Capacity estimates are given for two depth-use scenarios: 1) salmonids have full access to the water column (0-20 m) or 2) salmonids are thermally restricted from the epilimnion (10-20 m) during stratification. The thermal restriction scenario is not included for May or October because we would not expect thermal exclusion of salmonids in these months. For each depth-use scenario, estimates are shown based on 1) a conservative carrying capacity definition for total consumption not to exceed 50% of production and 2) a more liberal definition of consumption not to exceed 50% of production + biomass. Capacity estimates for the most limiting month of September are in bold.

		No thermal restriction (0-20 m)			Thermal restriction (10-20 m)		
Capacity definition	Month	Capacity	Initial fry abundance (S=8.5%)	Initial fry abundance (S=25%)	Capacity	Initial fry abundance (S=8.5%)	Initial fry abundance (S=25%)
50% biomass + production	May	10,046,618	10,046,618	10,046,618	-	-	-
	Jun	10,355,767	12,767,573	11,649,737	2,193,357	2,704,179	2,467,421
	Jul	8,127,822	12,271,375	10,246,898	2,986,596	4,509,159	3,765,258
	Aug	6,170,447	11,485,812	8,751,223	3,399,799	6,328,464	4,821,757
	Sep	**1,460,625**	**3,352,045**	**2,330,369**	**968,018**	**2,221,542**	**1,544,434**
	Oct	2,093,817	5,884,409	3,743,769	-	-	-
50% production	Jun	5,135,605	6,331,661	5,777,307	0	0	0
	Jul	5,780,337	8,727,145	7,287,380	2,380,058	3,593,408	3,000,584
	Aug	3,553,515	6,614,595	5,039,765	2,760,415	5,138,300	3,914,952
	Sep	**54,338**	**124,702**	**86,694**	**150,563**	**345,533**	**240,217**
	Oct	553,376	1,555,194	989,443	-	-	-

Table 5. Hypothetical population estimates of smolt production and adult returns based on two different juvenile carrying capacity scenarios. Scenario 1: juvenile carrying capacity is based on a maximum exploitation rate of 50% Daphnia production + biomass in the most limiting month of September, assuming juveniles are thermally excluded from the epilimnion. Scenario 2: juveniles carrying capacity is based on maximum exploitation rate of 50% Daphnia production + biomass in the most limiting month of September, assuming juveniles are not thermally excluded from the epilimnion. Fry survival rates represent in-lake survival estimates for age-1 smolts from Upper Baker Lake from the time of hatchery release to collection at the floating surface collector (2009-2021). Historical smolt-adult return rate (SAR) of 6.3% is an average from Baker Lake in 1999-2021 and the recent SAR of 4.1% is an average from 2015-2021.

				Adult returns	
Scenario	Fry-smolt survival (%)	Initial fry abundance in lake	Smolt abundance	SAR: 4.1 %	SAR: 6.3 %
1	3.6	3,334,950	120,058	4,922	7,564
	8.5	2,496,630	212,214	8,701	13,369
	25.0	1,735,677	433,919	17,791	27,337
2	3.6	5,219,221	187,892	7,704	11,837
	8.5	3,907,244	332,116	13,617	20,923
	25.0	2,716,348	679,087	27,843	42,782

Table 6. Estimated predation potential on introduced anadromous salmonids migrating through Ross Lake assuming that 100% of current salmonid consumption switches to each of these migrant expressions. Potential numbers consumed are reported for the size-structured predator population relative to 1,000 bull trout (including 2,430 rainbow trout, 286 brook trout, and 126 Dolly Varden), and the population relative to the estimated abundance of 3,000 bull trout (including 7,290 rainbow trout, 858 brook trout, and 378 Dolly Varden).

				Predation potential (individuals)		
Species/life-history	FL (mm)	Weight (g)	Population estimate	Mar	May	Jun
Chinook fry-migrant	39	0.72	1,000 BT	2,745	-	-
			3,000 BT	8,237	-	-
Chinook parr-migrant	75	4.90	1,000 BT	-	-	1,062
			3,000 BT	-	-	3,185
Chinook yearling	120	19.70	1,000 BT	-	158	-
			3,000 BT	-	474	-
Steelhead age-2 smolt	130	24.90	1,000 BT	-	125	-
			3,000 BT	-	375	-
Steelhead age-3 smolt	165	50.30	1,000 BT	-	62	-
			3,000 BT	-	186	-

Figures

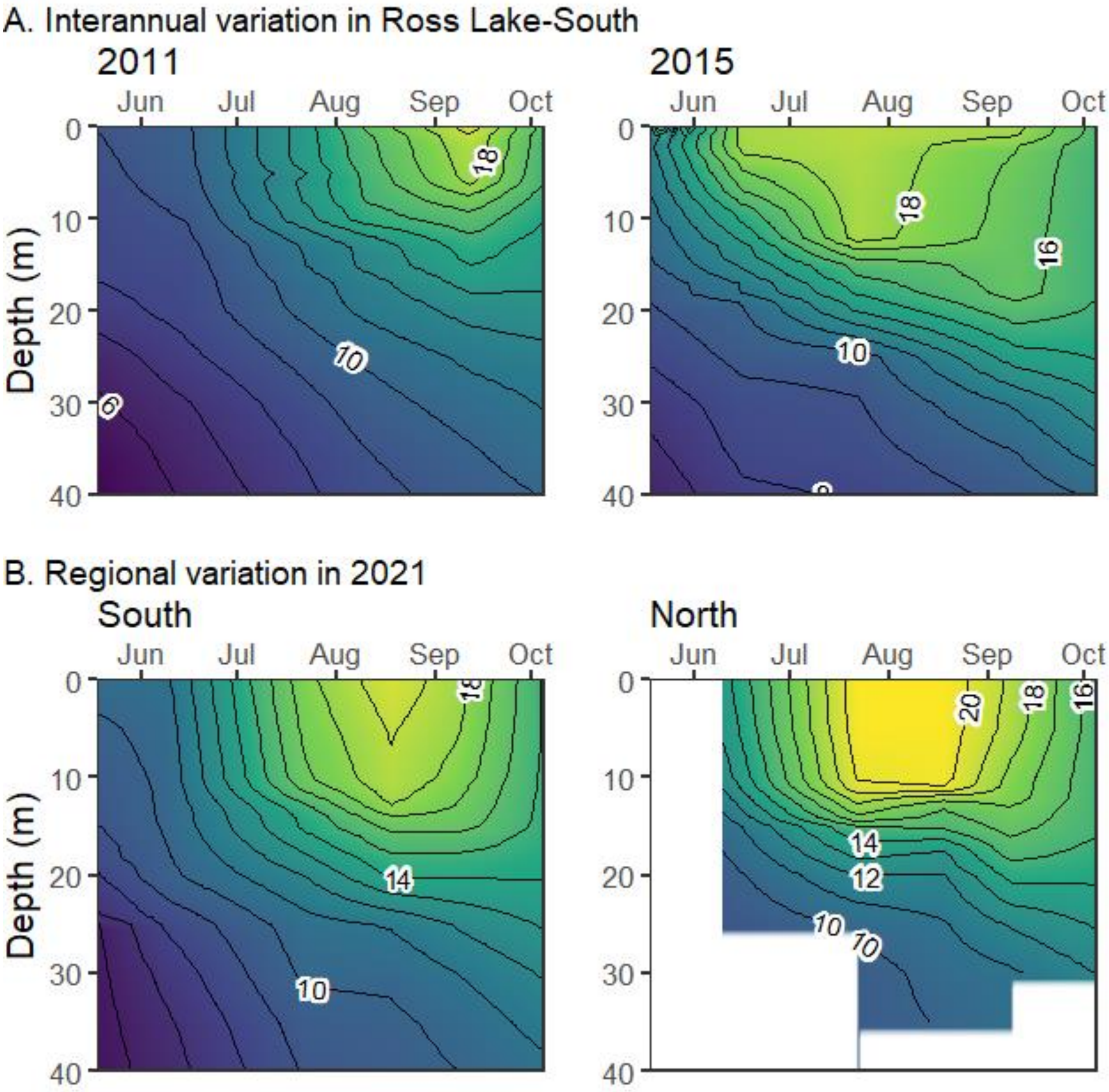

Figure 1. Temperature (°C) isoclines for Ross Lake showing variation in thermal structure by year (A) and region (B). Data prior to 2019 was collected by the NPS. The Ross Lake South site is located mid-lake in the pelagic zone near the confluence with Big Beaver Creek, and the North site was located mid-lake in the pelagic zone near the confluence with Little Beaver Creek.

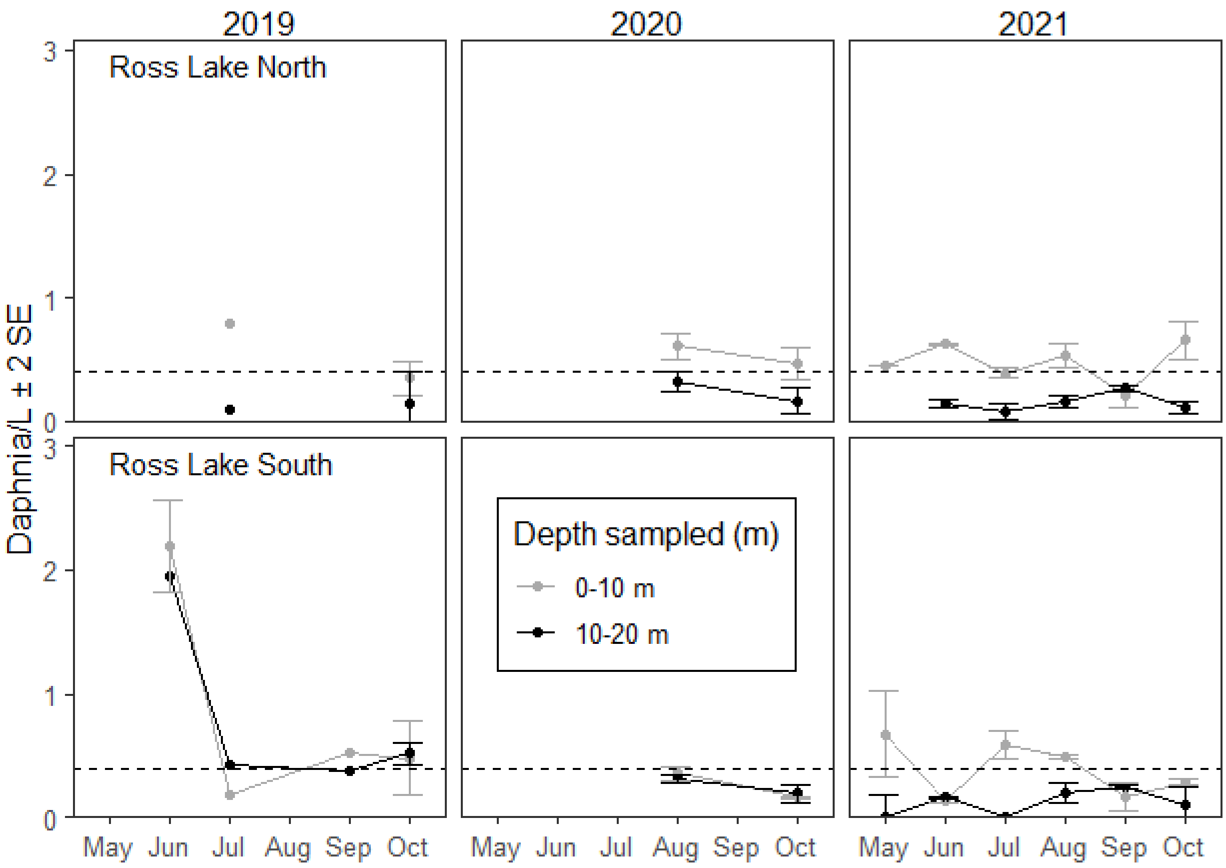

Figure 2. Average monthly densities for *Daphnia* in Ross and Diablo Lakes 2019-2021. Dashed line represents the threshold density (0.4/L) at which sockeye salmon begin to feed exclusively on *Daphnia* (Scheuerell et al. 2005).

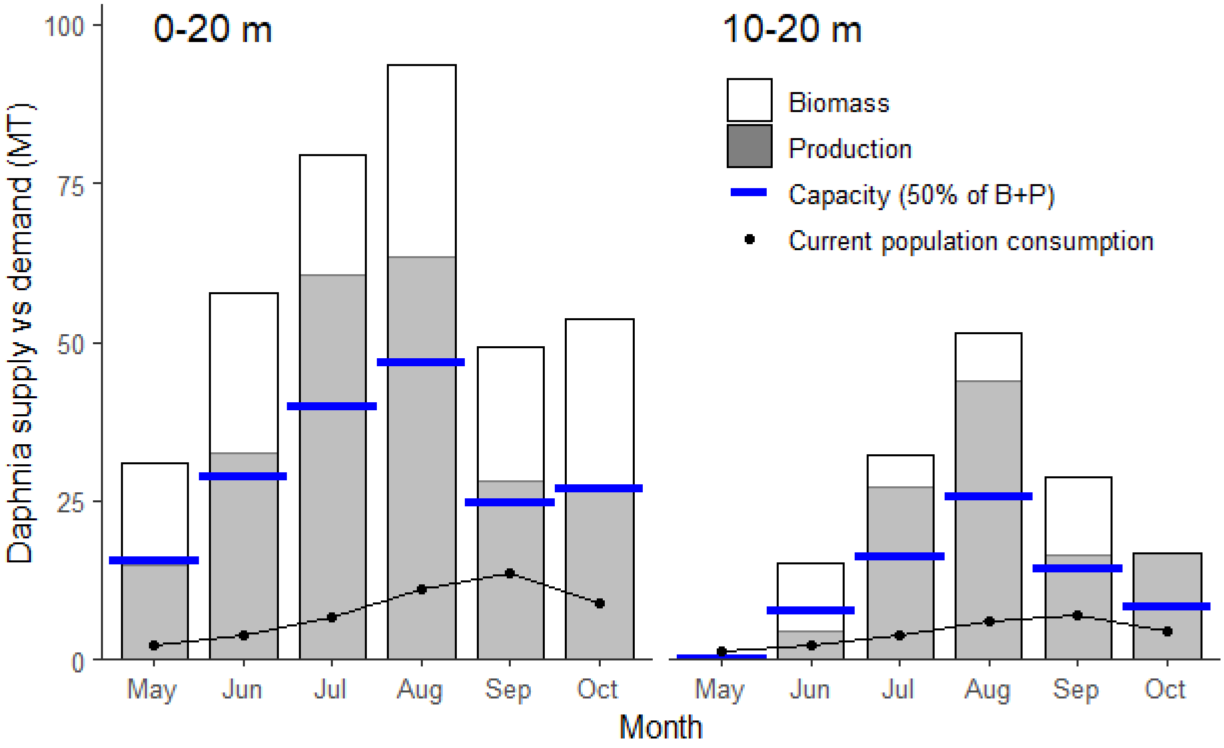

Figure 3. *Daphnia* supply versus demand for the combined epi- and metalimnion (0-20 m depth) and the metalimnion (0-10 m depth) in Ross Lake. Current population consumption demand includes redside shiner and rainbow trout. Carrying capacity of the resource, indicated for each month (blue bars), is defined as 50% of total biomass + production.

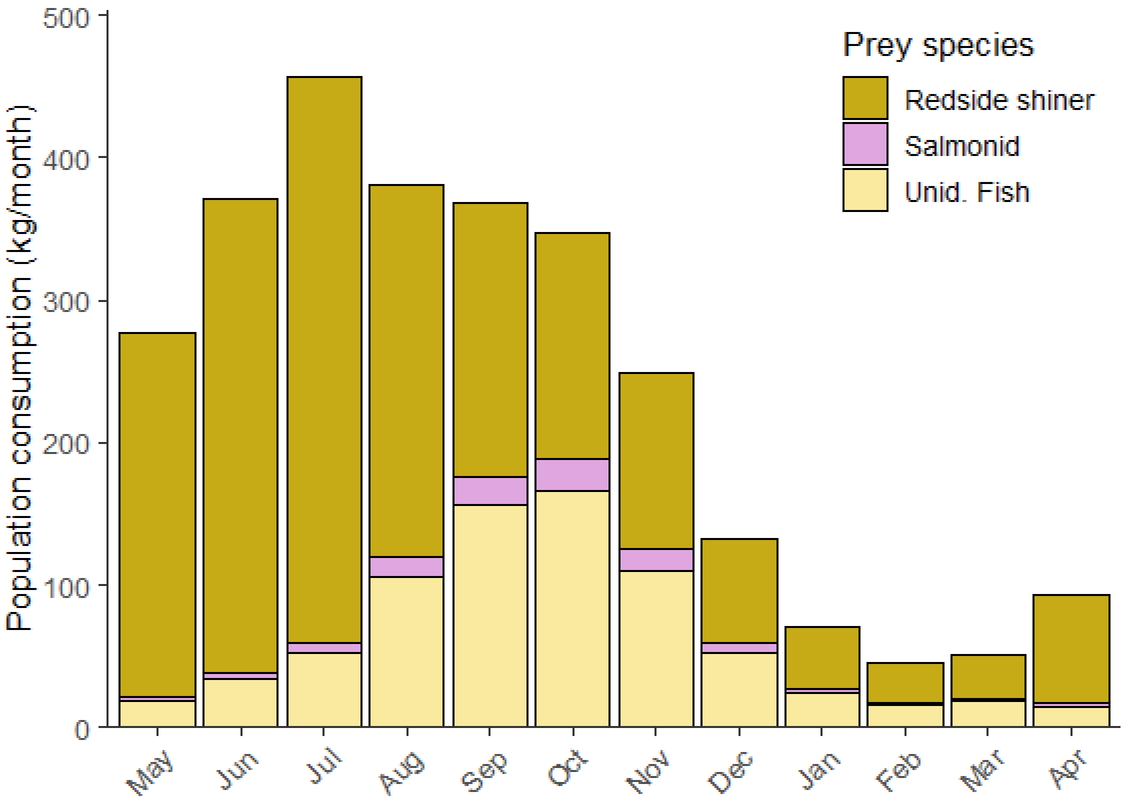

Figure 4. Monthly consumption demand by on fish prey in Ross Lake under current conditions by the unit predator population (1,000 bull trout, 2,430 rainbow trout, 286 brook trout, and 126 Dolly Varden > 200 mm FL).

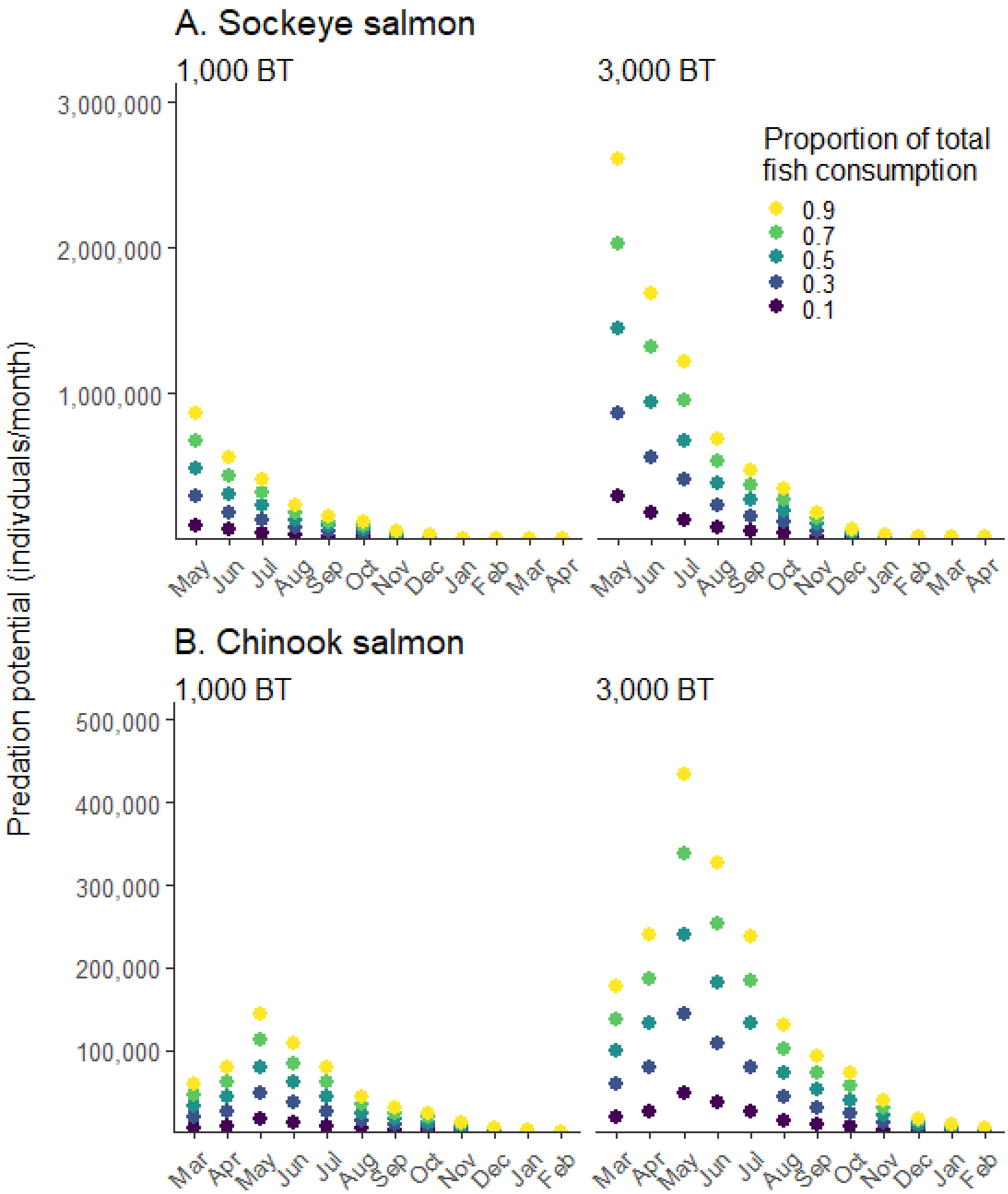

Figure 5. Monthly predation potential on sockeye and Chinook salmon juveniles rearing in Ross Lake as a function of the proportion of current predator fish consumption (from 10% to 90%) that switch to introduced sockeye salmon. Predation potential is shown for the unit predator population (i.e., all piscivores relative to 1,000 bull trout > 200 mm FL) and abundance of 3,000 bull trout > 200 mm FL that reflects the best existing data on bull trout population size in the Upper Skagit basin. Note the different x-axes between A and B panels - months in each panel are ordered to begin with the expected timing of recruitment to the lake.

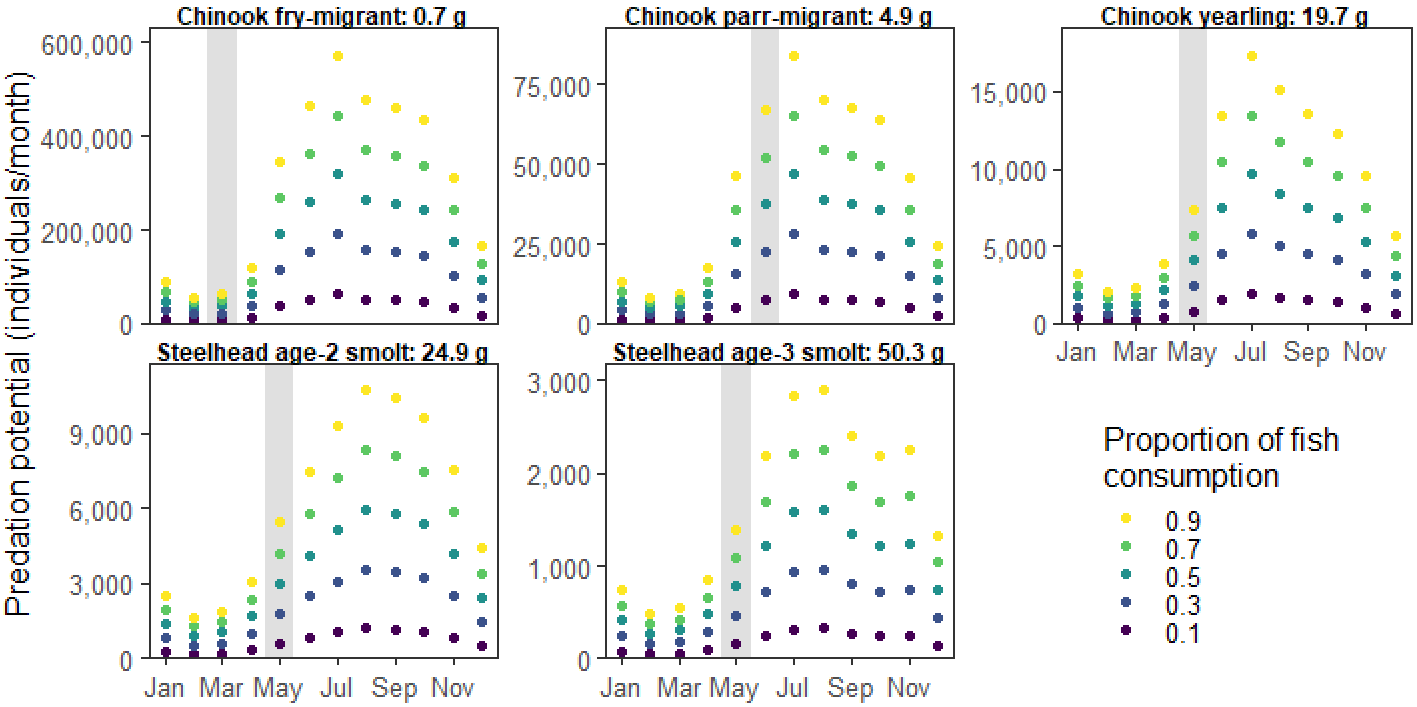

Figure 6. Predation potential of various anadromous species and migrant expressions in Ross Lake for the unit predator population (i.e., all piscivores relative to 1,000 BT > 200 mm FL). Panel labels include the expected size at migration for each species and life history type (see text for citations). Each point represents the estimated predation assuming a different fraction of the predator fish consumption (10-90%) switches to each species/life history. Shaded panel indicates the expected month of migration.

Chapter 4: Supplementary Materials - Ross Lake

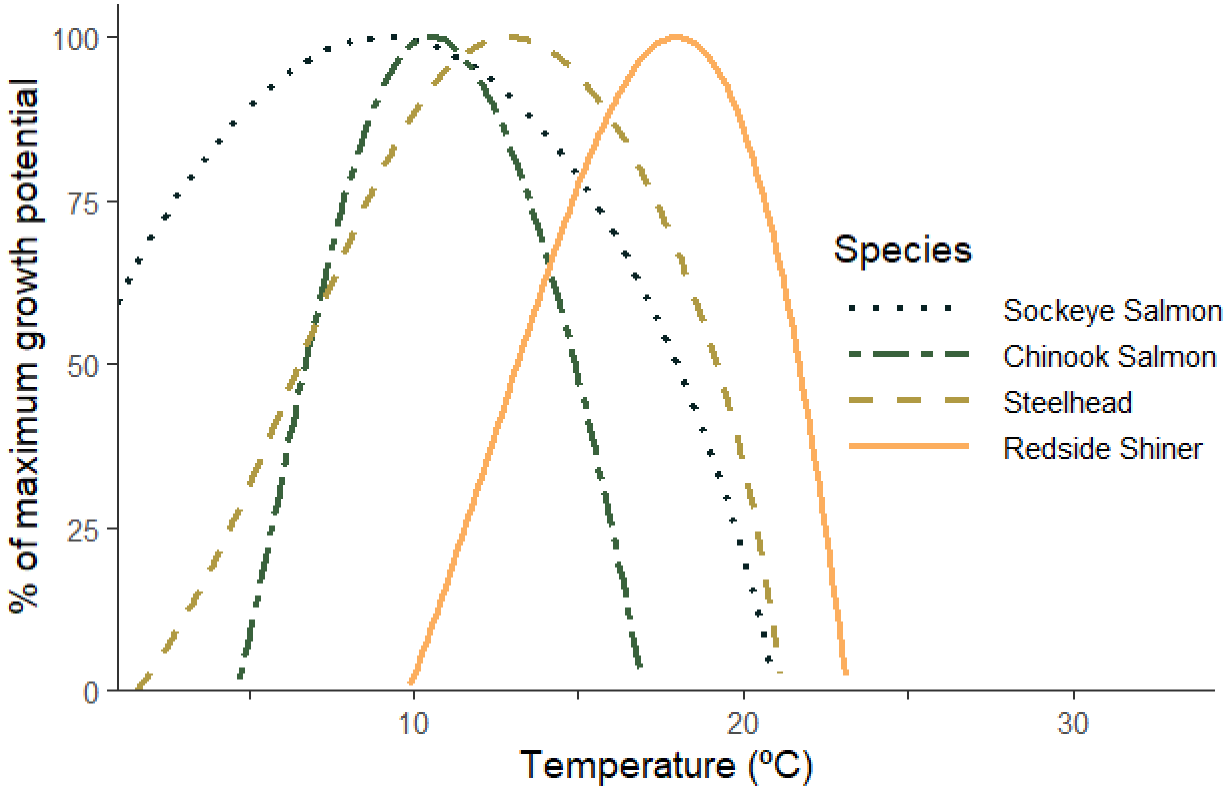

Figure S1. Growth potential as a function of temperature for existing planktivores and anadromous salmonids proposed for introduction into Ross Lake. Species were modeled for their expected body size and %Cmax during stratification in August as follows: sockeye salmon (%Cmax = 40, weight = 1.5 g), Chinook salmon (%Cmax = 40, weight = 8 g), rainbow trout (%Cmax = 40, weight = 20 g), redside shiner (%Cmax = 100, weight = 3 g). Rainbow trout weight was based on the typical size of age 2 fish in the tributaries during the summer - the age at which they might begin recruiting to the lake.

Chapter 4: Supplementary Materials - Diablo Lake

Methods

Methods for Diablo Lake follow those described in Ross Lake. Only predation mortality was evaluated for Diablo Lake, as zooplankton analysis indicated this lake is likely at its resource capacity (Chapter 2). Therefore, we only quantified predation potential for stream-rearing species and life histories. See Chapter 3 Supplementary Materials for details regarding the analysis methods and data limitations of assessing predation demand in Diablo Lake.

Results

Predation mortality in Diablo Lake

We assumed there was no excess capacity to support lake-rearing fish in Diablo Lake, thus we only evaluated predation mortality for migrating juveniles. Fish consumption in Diablo Lake was substantially lower than Ross due to low estimated predator abundances. We estimated that the unit population of 1,000 rainbow trout > 200 mm FL consumed 139 kg, 100 bull trout > 200 mm FL consumed 95 kg, and 100 brook trout > 200 mm FL consumed 11 kg of fish annually. Due to their large size at migration, age 3 steelhead smolts would experience the lowest maximum predation potential at 116 individuals, and Chinook parr migrants would be the most vulnerable with a maximum predation potential of 17,176 individuals during their migration window (Table SS1). High vulnerability of Chinook parr migrants is a result of multiple factors including their small size, larger number of effective predators (including age 2 RBT), and migration timing during the middle of the growing season when piscivore consumption rates are highest.

Table S1. Maximum predation potential in Diablo Lake for each species and migrant life history assuming 100% of predator fish consumption is targeting each species throughout their migration window. Numbers consumed are reported for each unit population of predator: BT-hybrid = 100 bull trout/hybrids > 200 mm FL, EBT = 100 brook trout > 200 mm FL, RBT 2 = back-calculated abundance of 2,937 rainbow trout age 2, RBT 3+ = 1,000 rainbow trout ≥ age 3.

		Size at migration		Numbers consumed by predator				
Species/life-history	Migration window	FL (mm)	Weight (g)	BT-hybrid	EBT	RBT 2	RBT 3+	Total
Chinook fry-migrant	Mar - Mar	39	0.72	3,307	295	0	0	3,602
Chinook parr-migrant	Jun - Jun	75	4.90	1,959	527	7,580	7,110	17,176
Chinook yearling	May - May	120	19.70	349	0	0	580	929
Steelhead age-2 smolt	May - May	130	24.90	276	0	0	459	735
Steelhead age-3 smolt	May - May	165	50.30	116	0	0	0	116

Summary and conclusion

These studies highlight the various ways reservoir food web interactions can influence growth and survival of native fish species, and how these interactions can be driven by emerging challenges in reservoirs such as invasive species, climate change, and water operations. This food web context is important for assessing the feasibility of introducing anadromous salmonids above impassable dams in regulated river systems, as the available prey supply and predation pressure can both limit success of such efforts. In Ross Lake, we observed how an invasive omnivore can influence prey availability for native species and alter energy flows through the food web by both bottom-up (as a resource competitor) and top-down (as a food source) controls. For anadromous introductions above these dams to be successful, these introduced habitats (both tributary and reservoir) must have the capacity to support adequate growth and production of additional fish. Invasive redside shiner influence the carrying capacity and production rate for introduced anadromous salmonids in Ross Lake by driving zooplankton supply (which controls fish density and growth rates) and supporting a robust predator population (which can control survival rates and smolt production). As climate change continues to alter seasonal temperatures, hydrology, and thermal structure in lentic habitats (Woolway and Merchant 2019; Miranda et al. 2020), habitat availability and growth potential for fish will also change, underscoring the need to incorporate these food web dynamics with predictions of habitat under future climate and water operations scenarios. While the data presented in these chapters focus on the Ross Lake food web under current conditions, it sets the stage for analyses to explicitly link future environmental conditions to these food web dynamics. I have summarized the major findings for each chapter below.

Chapter 1

- I parameterized a Wisconsin-style bioenergetics model for the nonnative redside shiner and evaluated its performance. This model can be integrated into Fish Bioenergetics 4.0 (Deslauriers et al. 2017) and will aid efforts to evaluate the ecological impact of this species where it has invaded and inform management objectives and strategies for control.

- I found that redside shiner have a higher thermal optima than many salmonid species with which it coexists, suggesting that population growth and performance of this species, and thus their ecological impact, may increase as the climate warms. However, scope for growth in this species is limited to a relatively narrow band of optimum temperatures, with poor performance at low temperatures.

- This model serves as a foundation to explore how consumption and growth relates to temperature, providing valuable information to identify habitats vulnerable to invasion or population expansion and evaluate how their ecological impact may change through time and space.

Chapter 2

- Nonnative redside shiner and smaller rainbow trout (< 300 mm FL) in Ross Lake overlap in diet, both relying on a mixture of zooplankton, insects, and other benthic organisms. Though redside shiner have a much lower per capita consumption demand on *Daphnia*, they are the dominant consumers due to their large population abundance (approx. 12 million individuals > 40 mm FL).

- Current consumption demand by both populations never exceeds 50% of monthly *Daphnia* production and standing stock biomass, and is often much lower, suggesting excess *Daphnia* supply exists. Additionally, redside shiner are feeding at their maximum consumption rates, and thus prey supply does not appear to be limiting this population.

- Rainbow trout are growing slower and consuming less energy than in the 1970s, suggesting they are not feeding as effectively as they used to. *Daphnia* densities were lower in the current study compared to the 1970s, and I hypothesize that these current densities are limiting the consumption rate of the smaller rainbow trout.

Chapter 3

- Redside shiner are the dominant prey fish consumed in Ross Lake, consumed by all salmonid species including rainbow trout, signifying a shift in predator-prey dynamics following their introduction.

- The minor proportion of salmonids consumed may still translate to high predation mortality for these native species, depending on their size, growth, and timing of migration to the lake. Predation is therefore a potential limitation to the survival and production of native salmonids in Ross Lake.

- This increased predation pressure on native salmonids could be amplifying the impacts of direct competition between redside shiner and rainbow trout. The depressed growth rates of rainbow trout (Chapter 2) could be increasing predation mortality for this species by extending the period over which they are vulnerable to predation (i.e., before they outgrow predators).

Chapter 4

- There is surplus *Daphnia* supply in Ross Lake to support some lake-rearing sockeye salmon proposed for introduction above these dams; however, predation mortality may impose a substantial limitation to juvenile survival and smolt production.
- While redside shiner are currently the dominant prey fish for salmonid predators in Ross Lake, this is not typical in other lakes and reservoirs where they coexist with populations of pelagic salmonids (i.e., kokanee and sockeye salmon). Therefore, predator diets may shift, the extent of which would depend on the density of introduced salmonids and overlap with predators in time and space. This remains a substantial data gap in our ability to quantify the impact of predation on introduced anadromous salmonids.
- Paired with information on the intrinsic potential and growth environment in the tributaries, this research suggests low production and survival of introduced anadromous salmonids in Ross Lake and associated tributaries. A successful introduction program will rely on adult returns that exceed replacement enough to support harvest and sufficient spawner escapement, which may be challenging in this system. Future feasibility studies, if they are to occur, would benefit from focusing on these expected challenges during the juvenile life stage.

Conclusion

These emerging challenges are not exclusive to the Upper Skagit River, and as such, this research provides important insights on the complex dynamics driving lentic food web structure that will help inform management and operations of these regulated ecosystems across the region to conserve key native species into the future. As trap and haul programs are increasingly used as a conservation strategy for (re)-introducing anadromous salmonids above impassable dams (Kock et al. 2021), this research highlights the importance of considering food web responses to anadromous introductions and provides a framework to address these issues in other regulated river systems. Results from this project will pave the way for future analyses that couple food web patterns with hydrodynamic models to predict climate change alterations to lake thermal structure (e.g., see Winslow et al. 2017) and identify how water management strategies could mitigate climate change stressors on lake ecosystems. For example, in systems where stratification is restricting native fish production and favoring the spread of invasive species, reservoirs could be de-stratified by altering the timing, depth and rate at which water is withdrawn. These water management strategies directly impact local communities that rely on hydropower, flood control, agricultural irrigation, potable and other water needs. Having a better understanding of and capability to predict ecosystem responses to altered thermal structure in lakes will help managers determine optimal water-use strategies to minimize detrimental impacts to aquatic communities within and downstream of dams and reservoirs while maintaining the necessary services that these systems provide.

References

Deslauriers, D., S. R. Chipps, J. E. Breck, J. A. Rice, and C. P. Madenjian. 2017. Fish Bioenergetics 4.0: An R-based modeling application. Fisheries 42:586–596.

Kock, T. J., J. W. Ferguson, M. L. Keefer, and C. B. Schreck. 2021. Review of trap-and-haul for managing Pacific salmonids (*Oncorhynchus* spp.) In impounded river systems. Reviews in Fish Biology and Fisheries 31:53–94.

Miranda, L. E., G. Coppola, and J. Boxrucker. 2020. Reservoir fish habitats: A perspective on coping with climate change. Reviews in Fisheries Science and Aquaculture 28:478–498.

Winslow, L. A., G. J. A. Hansen, J. S. Read, and M. Notaro. 2017. Large-scale modeled contemporary and future water temperature estimates for 10774 Midwestern U.S. lakes. Scientific Data 4:1–11.

Woolway, R. I., and C. J. Merchant. 2019. Worldwide alteration of lake mixing regimes in response to climate change. Nature Geoscience 12:271–276.